Functional Characterisation

of the Spindle Pole Body Component

Bbp1p

Carolin Schramm

A thesis submitted for the degree of Doctor of Philosophy

University of Glasgow

Faculty of Medicine

&

Beatson Institute for Cancer Research

Glasgow

January 2001

FÜR INGE, KARL UND DORA

Contents

List of Tables

Materials and Methods:

Results:

List of Figures

Introduction:

Results:

List of Publications

1. Schramm, C., Elliott, S., Shevchenko, A., Shevchenko, A. and Schiebel E. (2000) The Bbp1p-Mps2p complex connects the SPB to the nuclear envelope and is essential for SPB duplication. *EMBO J.*, **19**(3), 421-33.

2. Janke, C., Ortiz, J., Lechner, J., Shevchenko, A., Shevchenko, A., Magiera, M., Schramm, C. and Schiebel, E. (2001) The budding yeast Spc24p and Spc25p interact with Ndc80p and Nuf2p at the kinetochore and are important for kinetochore clustering and checkpoint control. *EMBO J.*, **20**(4), 777-791.

3. Schramm, C., Janke, C. and Schiebel E. (2001) Molecular dissection of yeast spindle pole bodies by two-hybrid approaches, immunoprecipitation and *in vitro* binding. In: *Centrosomes and spindle pole bodies. Methods in Cell Biology*. **67**, *in press*.

Abbreviations

Ade	adenine
Amp	Ampicillin
BBP1	Bfr1p binding protein 1
BFR1	Brefeldin A resistance 1
Bis-Tris	2-bis(2-hydroxyethyl)amino-2-(hydroxymethyl)-1,3-propanediol
bp	base pair
BSA	Bovine serum albumin
CNBr	Cyanogen bromide
D	Dalton
DAPI	4', 6-diamidino-2-phenylindole
dATP	deoxy adenosine triphosphate
dCTP	deoxy cytidine triphosphate
dGTP	deoxy guanosine triphosphate
DMSO	dimethyl sulfoxide
DNA	deoxyribonucleic acid
DNAse	deoxyribonuclease
DTT	Dithiothreitol
dTTP	deoxy thymidine triphosphate
EDTA	Ethylenediaminetetraacetic acid
EGTA	Ethylene gycol-bis(β-aminoethyl ether)-tetraacetic acid
EM	electron microscopy
et al.	*et alii*
FACS	fluorescence assisted cell sorting/flow analysis cytometry system
5-FOA	5'-Fluoroorotic acid
g	gravity
GFP	green fluorescent protein
GST	glutathione-S-transferase
h	hour
HA	hamagglutinin
HCCA	4-hydroxy-alpha-cyanocinnamic acid
HEPES	N-2-hydroxyethylpiperazine-N'-2-ethansulfonic acid
HRP	horse radish peroxidase
HU	hydroxy urea
IgG	immunoglobulin class G
IPTG	isopropyl-β-D-thiogalactopyranoside
KV	kilo Volt
l	litre
LB	Libroth
LiPEG	Lithium acetate polyethylene glycol
M	Molar
mA	milli Ampere
MALDI-MS	matrix assisted laser desorption ionisation mass spectronomy
mg	milli gram
min	minute
ml	milli litre

mM	milli Molar
MPS2	monopolar spindle 2
MTOC	microtubule organising centre
m/z	mass per charge
n_D	refractive index
ng	nano gram
nm	nano meter
OD	optical density
ORF	open reading frame
p	plasmid designation
PAGE	polyacrylamide gel electrophoresis
PBS	phosphate-buffered saline
PCR	polymerase chain reaction
PMSF	phenylmethylsulfonyl fluoride
ppm	parts per million
PVP	polyvinylpyrrolidone
rcf	relative centrifugal force
RNAse	ribonuclease
rpm	rotations per minute
RT	room temperature
SC	synthetic complete
SDS	sodium dodecyl sulfate
sec	second
SMY2	suppresser of myosin 2
SPB	spindle pole body
SPC	spindle pole body component
SPO	sporulation
TAE	Tris/acetate EDTA
Taq	*Thermus aquaticus*
TBS	Tris-buffered saline
TCA	trichloroacetic acid
Tris	tris(hydroxymethyl)-aminomethane
TST	tris sodium tween
TY	tryptone yeast
U	unit
Ura	uracil
V	Volt
(v/v)	volume per volume
(w/v)	weight per volume
X-Gal	5-bromo-4-chloro-3-indol-β-D-galactopyranoside
Y	yeast designation
YPAD	yeast peptone adenine dextrose
YPD	yeast peptone dextrose
YEp	yeast episomal plasmid
%	percent
µg	micro gram

µl	micro litre
µM	micro Molar
µm	micro meter

Symbols for amino acids

The following abbreviations for amino acids were used in this thesis:

D	Asp	aspartate
E	Glu	glutamine
F	Phe	phenylalanine
G	Gly	glycine
H	His	histidine
I	Ile	isoleucine
K	Lys	lysine
L	Leu	leucine
M	Met	methionine
N	Asn	asparagine
P	Pro	proline
R	Arg	arginine
S	Ser	serine
T	Thr	threonine
V	Val	valine
W	Trp	tryptophan
Y	Tyr	tyrosine

Yeast nomenclature

The yeast nomenclature was adopted from Demerec *et al.* (1966). Gene names are written in italics and consist of a three letter code plus a number. Wild type alleles are written in capitals and recessive alleles (mostly mutated) in small letters. A complete or partial deletion of a gene is indicated by 'Δ' and an insertion by '::'. Protein names consist of the gene name with only the first letter in capitals followed by 'p' at the end.

Summary

In budding yeast the microtubule organising centre (MTOC) is represented by a multi-layered structure called the spindle pole body (SPB) which stays embedded in the nuclear envelope throughout the cell cycle (Byers and Goetsch, 1975). The outer and inner plaque of the SPB are involved in the attachment of nuclear and cytoplasmic microtubules, a function provided by the γ-tubulin complex. The central plaque anchors the SPB in the nuclear envelope and extends into the half-bridge. The half-bridge is a specialised structure of the nuclear envelope which is essential for the cell cycle dependent duplication of the SPB (Byers and Goetsch, 1975). In early G_1-phase of the cell cycle a precursor of the new SPB, the so-called satellite, develops at the distal end of the half-bridge (Byers and Goetsch, 1975). It mainly consists of components of the central/outer plaque (Adams and Kilmartin, 1999). After 'Start' of the cell cycle, the satellite enlarges into a duplication plaque which is inserted into the nuclear envelope (Adams and Kilmartin, 1999; Byers and Goetsch, 1975). The inner plaque is most likely to be assembled onto the inserted duplication plaque from the nuclear side by attachment of the inner plaque component Spc110p to the central plaque component Spc29p (Adams and Kilmartin, 1999; Elliott *et al.*, 1999; Pereira *et al.*, 1998). Proper duplication of the SPB is a prerequisite for the formation of a functional mitotic spindle, and therefore the segregation of chromosomes and successful mitosis.

In this study, Bbp1p is described as a novel SPB component. *BBP1* was first identified as a high gene dosage suppresser of mutants in *SPC29* (S. Elliott, *published in* Schramm *et al.*, 2000), a gene coding for a component of the central plaque. Bbp1p was shown to localise to the SPB by fluorescence microscopy. In more detail, Bbp1p is present at the central plaque periphery as revealed by immunolabelling microscopy. Here, Bbp1p interacts with Spc29p as further indicated by two-hybrid experiments and *in vitro* binding (S. Elliott, *published in* Schramm *et al.*, 2000). In addition, Bbp1p interacts with the half-bridge component Kar1p in the yeast two-hybrid system. Via these interactions, Bbp1p may connect the central plaque to the half-bridge. High gene dosage of *SPC34*, coding for a SPB component of unknown function, and *SPC42*,

coding for a component of the central plaque rescued specific mutant alleles of *BBP1*, indicating further interactions of Bbp1p with SPB components. The known two-hybrid interaction between Bbp1p and Bfr1p (Xue *et al.*, 1996) was tested and repeated, but a direct interaction between the two proteins could not be established. Bfr1p is localised in the cytoplasm and might be enriched at the nuclear envelope, indicating a local proximity of Bfr1p to Bbp1p. Recent studies showed, that Bfr1p might be part of the Scp160p/Pab1p complex which is found at polyribosomes (Lang and Fridovich-Keil, 2000).

Furthermore, Bbp1p was shown to form a complex with Mps2p. Mps2p was identified by MALDI-MS in the affinity precipitate of Bbp1p-ProA. Mps2p co-precipitates with Bbp1p-3HA by immunoprecipitation and *vice versa*, Bbp1p co-precipitates with Mps2p-3HA. Both proteins also interact in the yeast two-hybrid system. High gene dosage of *MPS2* can suppress all known mutant alleles of *BBP1*. However, *BBP1* is a high gene dosage suppresser of *mps2-2* and *mps2-42*, but not *mps2-1*. Like Bbp1p, Mps2p is a component of the SPB which is localised at the central plaque periphery as shown by fluorescence microscopy and immunolabelling electron microscopy. Analysis of mutants in *BBP1* at the restrictive temperature revealed that they are defective in late steps of SPB duplication, like the proper insertion of the duplication plaque and the subsequent formation of the inner plaque. Failure in SPB duplication resulted in spindle formation and chromosome segregation defects. *Bbp1-1* cells displayed a typical G_2 arrest. An almost identical phenotype was observed before for mutants in *MPS2* (Winey *et al.*, 1991). The functional similarity of Bbp1p and Mps2p led to the hypothesis that the Bbp1p/Mps2p complex functions in SPB duplication. In addition, the growth defect of *bbp1* and *mps2* cells can be rescued by the deletion of *POM152*, a gene coding for a nuclear pore component. Interestingly, deletion of *POM152* rescues mutants in *NDC1* (Chial *et al.*, 1998), which are also defective in the insertion of the duplication plaque (Winey *et al.*, 1993).

BBP1 is an essential gene (Xue *et al.*, 1996; this study), but cells lacking *MPS2* are partially viable and can grow very slowly (Munoz-Centeno *et al.*, 1999; this study). Cells lacking *MPS2* display various abnormal phenotypes including multiple bud formation, unsuccessful chromosome segregation and abnormal SPB content. In a

suppresser screen *SMY2* was identified as unique high gene dosage suppresser of Δ*mps2* cells. *SMY2* is the homologue of the fission yeast *MPD2* which is a high gene dosage suppresser of *CDC7* (Cullen *et al.*, 2000), the budding yeast homologue of *CDC15*. In budding yeast high gene dosage of *SMY2* is known to rescue mutants in *MYO2* (Lillie and Brown, 1994), coding for the yeast class V unconventional myosin 2. In addition, the *mps2-42* allele is rescued by high gene dosage of *HSC82* coding for one of the two budding yeast *HSP90* chaperones. Hsp90p was shown to be a core component of the *drosophila* centrosome and it is required at different stages in the centrosome cycle (Lange *et al.*, 2000).

In addition to the Bbp1p/Mps2p complex another novel complex consisting of Spc24p, Spc25p and Ndc80p was isolated (Janke *et al.*, *in press*). Spc24p was enriched in precipitates of Ndc80p-6HA and Ndc80p co-precipitated with Spc24p-3HA. Furthermore, Spc24p co-precipitated with Spc25p-3HA. The direct interaction of the proteins was supported by the earlier finding that *SPC24* interacts with *SPC25* and *NDC80* in in the yeast two-hybrid system (Cho *et al.*, 1998). Recent studies in our laboratory showed that Spc24p, Spc25p and Ndc80p are part of a larger complex which associates with kinetochores (Janke *et al.*, *in press*).

1. Introduction

1.1 Events in the S. cerevsiae cell cycle

Saccharomyces cerevisiae also called budding yeast or baker's yeast, is an organism mainly specialised on proliferation. The single cell organism propagates through budding of daughter cells from the body of mother cells. The high proliferation rate of budding yeast is a welcome feature for the food industry, which utilises the yeast metabolism, as well as for researchers studying budding yeast as a model system for eukaryotic cells. For proliferation, the cell and its constituents have to be duplicated and duplicated organelles and chromosomes have to be separated before the completion of cell division. The set of processes required for the duplication and segregation of cell constituents and for the division into mother and daughter cells is called the cell cycle. The cell cycle can be divided into four different periods, G_1- (Gap 1), S- (synthesis), G_2- (Gap 2) and M-phase (mitosis) (Alberts *et al.*, 1994) (Figure 1). In early G_1, environmental conditions, mainly growth conditions, are critical for the commitment of budding yeast cells to the cell cycle. If nutrient conditions are sufficient, cells proceed through the cell cycle. However, if nutrients are limited, cells enter a quiescent state (haploid cells) or form spores (diploid cells) and persevere until conditions improve. In addition, haploid cells exposed to mating pheromone arrest in G_1, differentiate and finally mate (Lew *et al.*, 1997; Pringle and Hartwell, 1981). Cells, which have proceeded past a decision point or period called 'Start' do not have any alternative but continue through the cell cycle (Pringle and Hartwell, 1981). At the G_1/S transition several processes are initiated nearly simultaneously (Figure 2). The duplication of the spindle pole body (SPB), the yeast microtubule organising centre (MTOC) starts. The process of bud formation begins at the designated bud site. Furthermore, DNA replication is initiated, although this process might be slightly delayed in comparison to the other two. G_2- and M-phase are not clearly divided in the budding yeast cell cycle (Lew *et al.*, 1997). The nuclear envelope does not breakdown as observed in higher eukaryotes. Condensation of chromosomes occurs but single chromosomes cannot be observed by light microscopy (Gordon, 1977).

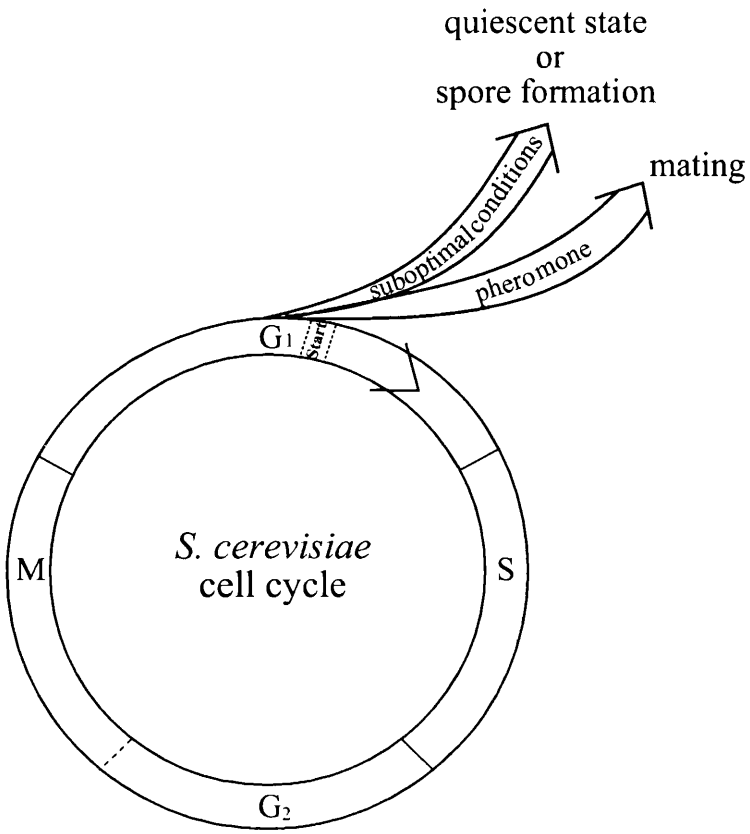

Figure 1: The *S. cerevisiae* cell cycle. The budding yeast cell cycle is divided in four phases termed G_1 (Gap 1), S (Synthesis), G_2 (Gap 2) and M (Mitosis; Alberts *et al.*, 1994). During a period in G_1 defined as 'Start' cells commit to the cell cycle (Pringle and Hartwell, 1981). In early G_1, prior to 'Start', cells enter into a quiescent state or start sporulation if nutrients are limited. If haploid cells are exposed to mating pheromone in early G_1 they initiate the mating program. The transition from G_2 to M is not well defined in budding yeast. Cytokinesis takes place after mitosis. The duration of the budding yeast cell cycle is approximately 2 h.

It is assumed that DNA replication is completed before the assembly of the short bipolar spindle (Byers and Goetsch, 1975; Kilmartin and Adams, 1984). In mitosis the spindle is positioned in the mother bud axis. The chromosomes are being separated in anaphase and in late anaphase each cell contains one SPB and a set of chromosomes. The cell cycle is completed by cell division (cytokinesis) and a new cycle can start.

1.2 Cell cycle regulation and cell cycle checkpoints in S. cerevisiae

The various processes involved in cell duplication are initiated at certain time points throughout the cell cycle in an exact order. Proper co-ordination of processes is monitored so that for example, chromosome segregation can not occur before completion of chromosome replication. While the cell cycle timing is provided by cyclins and cyclin dependent kinases (CDKs), the cell cycle progression is monitored by various checkpoints.

CDKs are inactive as monomers and require complex formation with regulatory proteins called cyclins for their activation (Morgan, 1995). CDK/cyclin complexes can regulate processes by phosphorylation including regulation of the CDK/cyclin complexes themselves by auto-regulatory feed back loops. The main CDK in *S. cerevisiae* is Cdc28p (Nasmyth, 1993; Reed, 1992). Cdc28p levels are constant throughout the cell cycle (Wittenberg and Reed, 1988) but levels of almost all cyclins fluctuate, thereby regulating Cdc28p activity. Cyclin fluctuation is achieved by transcriptional regulation (Epstein and Cross, 1992; Schwob and Nasmyth, 1993; Wittenberg *et al.*, 1990) and degradation (Seufert *et al.*, 1995; Willems *et al.*, 1996). In addition, kinase activity is regulated by activation/inactivation of CDK inhibitors. The degradation of cyclins and CDK inhibitors is initiated by ubiquitination by the anaphase promoting complex (APC) (Page and Hieter, 1999) or by the Skp1p-cullin-F-box (SCF) (Feldman *et al.*, 1997; Skowyra *et al.*, 1997). The ubiquitin label is recognised by the proteasome which is responsible for the degradation of poly-ubiquitinated proteins (Voges *et al.*, 1999; Zwickl *et al.*, 1999).

Most conditional lethal *cdc28* alleles cause an arrest of the cell cycle at 'Start' in G_1 (Reed, 1980) before DNA replication or bud initiation. Other mutants block nuclear division and cytokinesis (Piggott *et al.*, 1982) or show a mixed arrest in G_1 and G_2 (Zarzov *et al.*, 1997). According to their function throughout the cell cycle, cyclins can be divided in G_1 (Cln1p, Cln2p, Cln3p), S-phase (Clb5p, Clb6p) and mitotic cyclins (Clb1p, Clb2p, Clb3p, Clb4p). G_1 cyclin/Cdc28p complexes trigger DNA replication and bud formation in G_1 (Figure 2A) (Dirick *et al.*, 1995; Stuart and Wittenberg, 1995). G_1 cyclin/Cdc28p complexes are also necessary for SPB duplication to continue but early stages of duplication like the formation of the satellite are independent of Cdc28p activity since some mutants in *CDC28* arrest in the cell cycle with a single SPB already containing a satellite. The signal to initiate SPB duplication is therefore active before the Cdc28p/Start point. The S-phase cyclin/Cdc28p complexes are probably also involved in initiating DNA replication and in addition, in sustaining DNA replication in S-phase (Figure 2A) (Schwob and Nasmyth, 1993). The mitotic or B-type cyclins (Clb1p-Clb4p) form complexes with Cdc28p to promote various processes (Figure 2A). Clb3p and Clb4p cyclins are responsible for promoting SPB separation (Fitch *et al.*, 1992; Richardson *et al.*, 1992). Clb1p and Clb2p are essential for anaphase onset (Richardson *et al.*, 1992; Surana *et al.*, 1991). In complex with Cdc28p they trigger the reorganisation of the actin cytoskeleton leading to the isotropic switch in bud growth (see 1.3.2) (Lew and Reed, 1993). If cells lack Clb1p and Clb2p the isotropic switch does not occur and cells form elongated tubular buds. Destruction of the mitotic cyclins is necessary for events that lead to exit from mitosis (King *et al.*, 1996).

Completion of events triggered by cyclin/Cdc28p complexes is monitored by so called checkpoints. Checkpoints are signalling pathways that act to delay cell cycle progression when perturbations prevent the completion of certain cell cycle events (Hartwell and Weinert, 1989). So far, checkpoint pathways have been found to control DNA replication, DNA damage, spindle assembly/positioning and cell morphogenesis. The spindle checkpoint is the most relevant to this study and it will be discussed in more detail.

Figure 2: Key events in the *S. cerevisiae* cell cycle. (**A**) Cell cycle regulation by cyclins and the cyclin dependent kinase Cdc28p. Complex formation between cyclins and Cdc28p initiates steps of the cell cycle. Arrows indicate initiation. T-bar indicates inhibition. (**B**) The chromosomes in the cell cylce. In late G_1 after 'Start' chromosomes are being replicated. Sister chromatids are separated during mitosis. (**C**) The SPB and the microtubule cytoskeleton in the cell cycle. In early G_1, cells contain one SPB (square) nucleating nuclear and cytoplasmic microtubules (lines). The satellite (circle) forms at the end of the half-bridge in G_1 (Byers and Goetsch, 1975; Vallen *et al.*, 1992; Donaldson and Kilmartin, 1996). At this time point cytoplasmic microtubules attach to the half-bridge (Pereira *et al.*, 1999). When a small bud has formed, SPBs are duplicated and the nuclear microtubules of both SPBs interdigitate at sharp angles (O'Toole *et al.*, 1999). SPB separation is initiated by Clb3/4p-Cdc28p. A short spindle is formed in G_2. Spindle positioning is mediated by the cytoplasmic microtubules respectively (Jacobs *et al.*, 1988). Elongation of spindle microtubules indicates mitosis. SPBs are pushed (Hoyt *et al.*, 1992; Roof *et al.*, 1992) and pulled (Eshel *et al.*, 1993; Li *et al.*, 1993) apart by motor proteins acting on microtubules. (**D**) The actin cytoskeleton in the cell cycle. The actin cytoskeleton transports the secretory vesicles to sites of growth (arrows). Changes in the localisation of actin cables (lines) and cortical actin patches (circles) during bud formation and cytokinesis are indicated. The isotropic switch in bud growth occurs at S/G_2. (**E**) The cell cycle time scale. See Figure 1 for more detailed description.

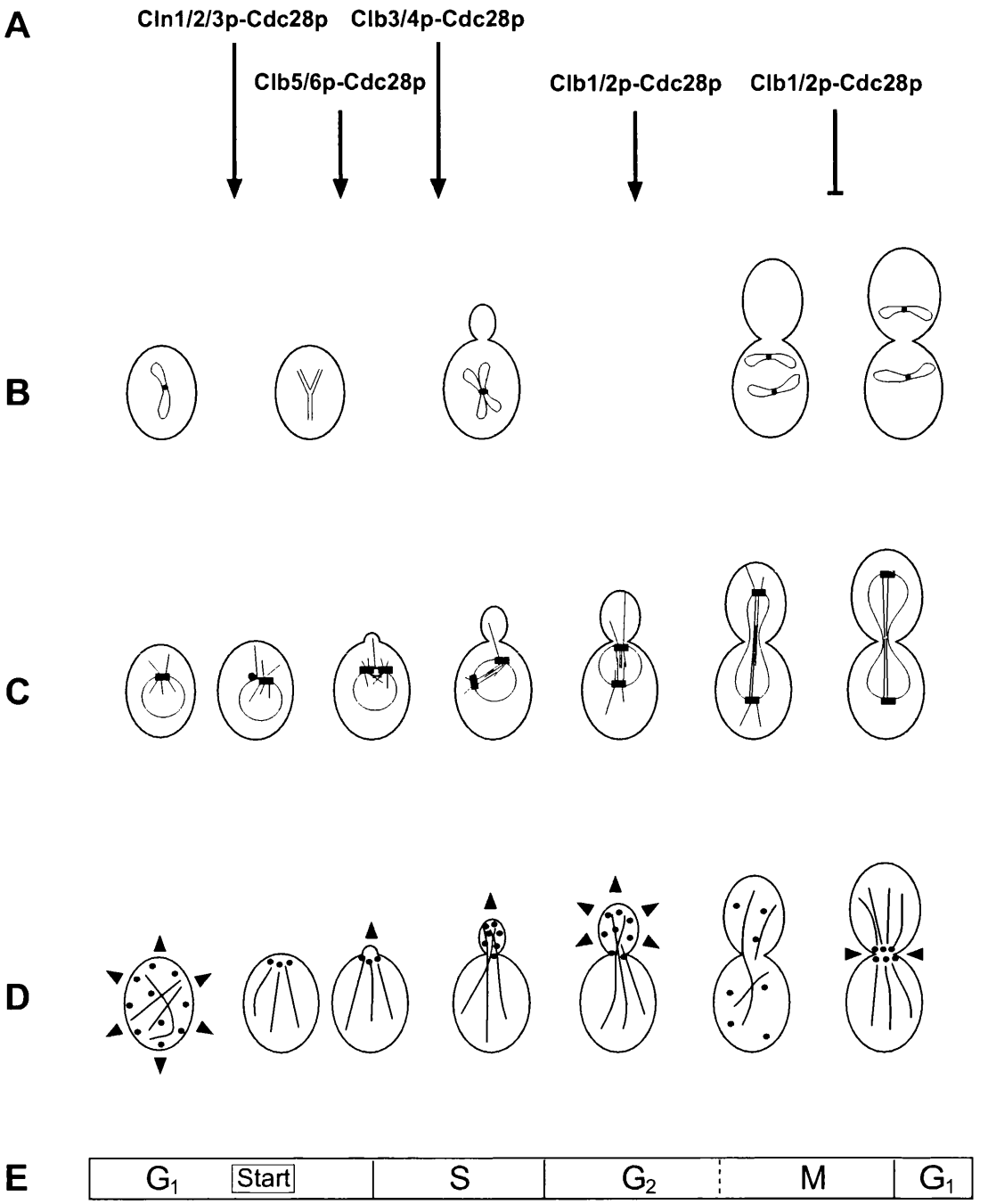

Figure 2: See facing page for figure legend.

The spindle checkpoint was first defined in budding yeast. Seven genes were identified whose deletion resulted in failure of cells to arrest in the cell cycle after microtubule depolymerisation (Hoyt *et al.*, 1991; Li and Murray, 1991; Weiss and Winey, 1996). The majority of these genes (*MAD1*, *MAD2*, *MAD3*, *BUB1*, *BUB3* and *MPS1*) codes for proteins which function in the spindle assembly checkpoint that senses failure of kinetochore microtubule attachment (Pangilinan and Spencer, 1996; Weiss and Winey, 1996). The other gene identified, *BUB2*, encodes a protein involved in the spindle checkpoint that monitors spindle positioning (Bloecher *et al.*, 2000; Pereira *et al.*, 2000; Wang *et al.*, 2000).

The spindle assembly checkpoint (Figure 3A) is activated by kinetochores which are not attached to spindle microtubules. Two theories exist for the generation of a signal activating the checkpoint (Li and Nicklas, 1995; Li and Nicklas, 1997). Firstly, unattached kinetochores *per se* could trigger the checkpoint. Secondly, the absence of tension at unattached kinetochores could be transformed into a chemical signal resulting in checkpoint activation. This yet unknown signal triggers a signalling cascade involving Mps1p, Bub1p, Bub3p and the Mad proteins. The complex signalling cascade is only partially understood. It is known that Mps1p phosphorylates Mad1p in a *BUB1*, *BUB3* and *MAD2* dependent manner (Farr and Hoyt, 1998). Furthermore, Bub1p can also activate the checkpoint but it does not function through phosphorylation of Mad1p. The target of the cascade is most likely the APC/C^{Cdc20p} complex. Cdc20p is the activator of the APC (Visintin *et al.*, 1997), a mulitsubunit ubiquitin ligase, which ubiquitinates Pds1p (securin) and thereby targets it for destruction by the proteasome (Cohen-Fix *et al.*, 1996). Before anaphase, Pds1p forms a complex with Eps1p (separin) keeping Eps1p in an inactive form (Ciosk *et al.*, 1998). Degradation of Pds1p results in activation of Esp1p which induces cleavage of Scc1p (cohesin) (Uhlmann and Nasmyth, 1998), a protein required for cohesion between sister chromatids during S phase (Michaelis *et al.*, 1997). As consequence, sister chromatid separation can occur. Binding of the Mad1p, Mad2p, Mad3p proteins to Cdc20p was shown *in vivo* (Hwang *et al.*, 1998). Furthermore, binding of Mad2p to Cdc20p-APC inhibits its ubiquitination activity (Fang *et al.*, 1998). The current model is that after checkpoint activation Mad1p, Mad2p, Mad3p form a complex with

Cdc20p-APC, thereby inhibiting the ubiquitination activity of the APC and therefore degradation of Pds1p and sister chromatid separation.

The spindle positioning checkpoint (Figure 3B) monitors spindle alignment in the mother bud axis. Bub2p and Bfa1p both localise to the cytoplasmic side of the SPB and form a two component GAP (GTPase-activating protein) (Pereira *et al.*, 2000). Here Tem1p interacts with these two proteins in early mitosis (Pereira *et al.*, 2000). If one SPB enters the bud, Tem1p comes in contact with its putative GEF (GDP/GTP exchange factor), Lte1p which is localised in the bud cortex (Bardin *et al.*, 2000; Pereira *et al.*, 2000). Tem1p is converted into its GTP-bound form which activates the mitotic exit network (MEN). The components of the MEN (Cdc5p, Cdc15p, Dbf2p, Dbf20p, Mob1p) trigger the destruction of B-type cyclins via the release of Cdc14p from the nucleolus (Shou *et al.*, 1999; Visintin *et al.*, 1999). Cdc14p promotes exit from mitosis in two ways. Firstly, it dephosphorylates Hct1p/Cdh1p which activates the APC, the ubiquitin-ligase responsible for destruction of Clb2p (Jaspersen *et al.*, 1999). Secondly, Cdc14p promotes the accumulation of the cyclin dependent kinase inhibitor Sic1p by activation of the transcription factor Swi5p and by preventing Sic1p degradation through Sic1p dephosphorylation (Visintin *et al.*, 1998). Thus, proper spindle alignment allows exit from mitosis due to destruction of Clb2p. If the SPB does not enter the bud as a result of failure in spindle alignment, the signalling cascade is not activated and exit from mitosis does not take place.

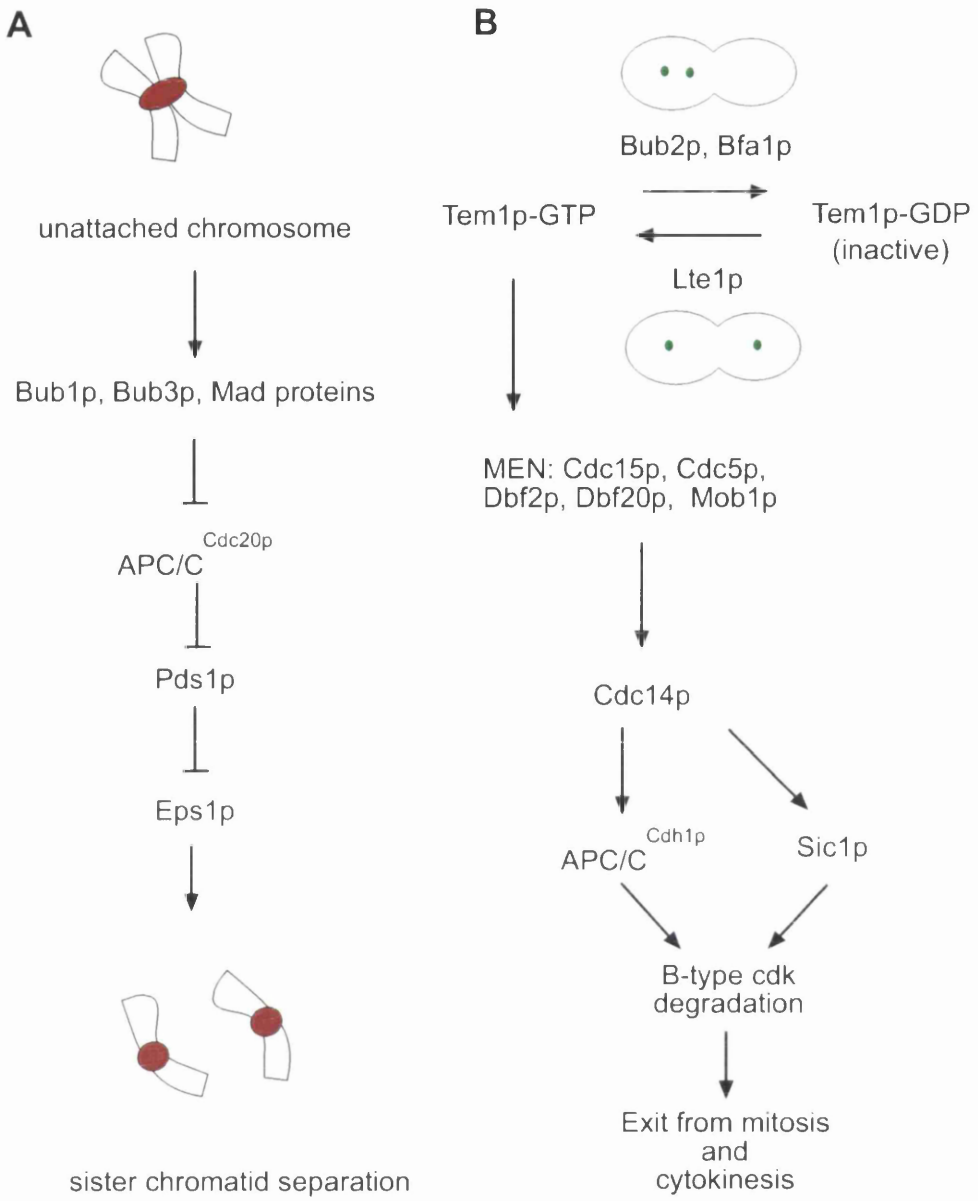

Figure 3: The spindle checkpoints. (**A**) The spindle assembly checkpoint. Unattached chromosomes activate the spindle checkpoint and delay the onset of anaphase. The checkpoint prevents the activation of the APC and therefore, the ubiquitination of Pds1p. As consequence, Eps1p remains inactive and sister chromatids are not separated. (**B**) The spindle positioning checkpoint and signalling leading to exit from mitosis. When the mitotic spindle is properly positioned, one SPB (green) can enter the bud and Tem1p can get in contact with its putative GEF (Lte1p) resulting in the active GTP-bound form of Tem1p. Tem1p-GTP initiates the indicated signalling cascade for exit from mitosis. Abnormal spindle positioning prevents contact of Tem1p with Lte1p and Tem1p remains inactive.

1.3 Functions of the cytoskeleton throughout the cell cycle

The cytoskeleton is a dynamic network of fibres, which fulfils functions throughout the cell cycle. It can be divided into microfilaments, microtubules and intermediate filaments. The morphology and function of microfilaments and microtubules will be discussed here for the budding yeast *S. cerevisiae* only, thus excluding functions of the cytoskeleton observed in higher eukaryotes like cell motility and intercellular contacts. Functions of the cytoskeleton in meiosis are omitted and the specialised microtubules of the centrosome of higher eukaryotes are mentioned in paragraph 1.4.1.

1.3.1 The microtubule cytoskeleton in the cell cycle

Microtubules are hollow cylinders of 25 nm in diameter which are made out of protofilaments consisting of hetero-dimers of α- and β-tubulin. The organisation of protofilaments and their arrangement in a cylinder result in the polarised structure of microtubules. The microtubule minus-end is formed by α-tubulin and the plus-end by β-tubulin. It has been shown for higher eukaryotes that microtubules nucleate at the MTOC with the minus-end and attach to chromosomes with the plus-end (Kellogg *et al.*, 1994). In budding yeast, nuclear microtubules nucleate at the inner plaque and cytoplasmic microtubules at the outer plaque (see 1.4.2 and 1.4.4) and at the half-bridge of the SPB (see 1.4.2.2.5) (Byers, 1981a; Pereira *et al.*, 1999; Snyder, 1994; Winey and Byers, 1993) which is a one-sided extension of the SPB (see 1.4.2). In budding yeast, the nuclear microtubules stay attached to the 16 chromosomes (haploid cell) throughout the cell cycle (O'Toole *et al.*, 1999).

In early G_1 of the cell cycle, cells contain one SPB and attached nuclear and cytoplasmic microtubules show an aster like distribution (Figure 2C). Cytoplasmic microtubules can also be seen attached to the bridge structure in G_1 and when bud formation has started, they are orientated into the bud (Figure 2C). After SPB duplication, both SPBs are still connected with each other via the bridge structure. At this stage, nuclear microtubules from both SPBs interdigitate at sharp angles (O'Toole *et al.*, 1999) (Figure 2C). After cleavage of the bridge, the SPBs move to opposite sites of the nuclear envelope and a bipolar spindle is formed (Figure 2C). The spindle

consists of a core of long microtubules and various short microtubules (O'Toole *et al.*, 1999). The cytoplasmic microtubules are essential for the positioning of the spindle within the cell along the mother bud axis (Jacobs *et al.*, 1988). Since the nuclear envelope does not break down in yeast during mitosis the entire nucleus moves during the positioning of the spindle (nuclear migration) mediated by microtubules. Proper spindle positioning ensures the separation of chromosomes into the daughter cell. During spindle and nuclear positioning in the mother bud neck, the spindle stays relatively short. Afterwards the spindle elongates and this event determines anaphase. The chromosomes are being separated in anaphase and spindle breakdown probably coincides with cytokinesis.

Microtubules function together with various motor proteins. In *S. cerevisiae* the kinesin–related gene products (Cin8p, Kip1-3p and Kar3p) and the dynein Dyn1p assist with spindle function (Carminati and Stearns, 1997; Cottingham and Hoyt, 1997; DeZwaan *et al.*, 1997; Li *et al.*, 1993). For example, Cin8p and Kip1p promote sliding of nuclear microtubules to push SPBs apart while dynein functions on cytoplasmic microtubules to create pulling forces. Taken together, microtubules are responsible for the movement of chromosomes and nuclear migration.

1.3.2 The actin cytoskeleton in the cell cycle

Microfilaments are actin polymers (filamentous actin, F-actin) which interact with actin-binding proteins to form a functional actin cytoskeleton. In budding yeast polymerised actin has been visualised by fluorescence microscopy and immunoelectron microscopy as actin fibres and as cortical actin patches (Adams and Pringle, 1984; Kilmartin and Adams, 1984; Mulholland *et al.*, 1994; Pringle *et al.*, 1989). Cortical actin patches are bundles of actin fibres associated with invaginations of the plasma membrane (Mulholland *et al.*, 1994). They are highly mobile but appear to be limited in their movement to the area in which they are found (Doyle and Botstein, 1996; Waddle *et al.*, 1996). The rate-limiting step in the polymerisation of filamentous actin from globular actin (G-actin) is the actin trimer formation (Cooper *et al.*, 1983; Tobacman and Korn, 1983). Polymerisation of monomeric actin into filaments is not energy dependent but ATP-bound actin can polymerise faster than ADP-bound actin

(Engel *et al.*, 1977). The actin nucleator might be the Arp2/3-complex which is conserved in eukaryotes (Kelleher *et al.*, 1995; Machesky *et al.*, 1994; Welch *et al.*, 1997a, b). The Arp2/3p hetero-dimer interacts with actin (Kelleher *et al.*, 1995) and the complex stimulates filament nucleation (Mullins *et al.*, 1998).

In *S. cerevisiae*, the actin cytoskeleton is involved in various aspects of bud formation. Bud formation is localised growth that depends on polarised secretion. The actin cytoskeleton functions in bud site selection, polarised movement of secretion vesicles to the bud region and possibly in secretion itself (Dunn and Shortle, 1990; Novick and Botstein, 1985; Shortle *et al.*, 1984). Furthermore, actin is involved in organelle movement and positioning (Drubin *et al.*, 1993), nuclear migration, nuclear division and cytokinesis (Palmer *et al.*, 1992). More recent work shows a role for actin in early spindle positioning in budding yeast (Beach *et al.*, 2000; Theesfeld *et al.*, 1999; Yin *et al.*, 2000). In addition to these functions, actin is also involved in endocytosis (Benedetti *et al.*, 1994; Holtzman *et al.*, 1993; Kubler and Riezman, 1993). Transformation and response of the actin cytoskeletion can be triggered by intracellular signals (cyclin/Cdc28p complexes) or by extracellular signals, such as changes in osmolarity or nutrient availability. Another extracellular signal, mating pheromone, results in polarised organisation of the actin cytoskeleton for the formation of the mating projectile, the shmoo (Chowdhury *et al.*, 1992; Kron and Gow, 1995; Read *et al.*, 1992).

The organisation of the actin cytoskeleton in budding yeast undergoes changes which are cell cycle dependent (Adams and Pringle, 1984; Kilmartin and Adams, 1984) (Figure 2D). In early G_1 of the cell cycle cortical actin patches and cables are evenly distributed and 'randomly' orientated at the inner the cell surface (Mulholland *et al.*, 1994). As shown in microscopy studies most actin fibres run along the inner surface of cells and do hardly extend into the cytoplasm (Botstein *et al.*, 1997). After Start of the cell cycle, a concentration of actin patches at the bud site can be observed with actin cables oriented towards the bud site (Kilmartin and Adams, 1984; Li *et al.*, 1995). In early bud phase (G_1/S transition), actin patches localise at the bud tip were bud growth predominantly takes place. When the bud reaches a certain size, actin patches distribute over the whole bud surface and isotropic bud growth occurs (Farkas *et al.*, 1974; Tkacz

and Lampen, 1972). During cytokineses actin patches form a contractile ring in the bud neck from which cables emanate. Here, cell division will take place.

Myosins are motor proteins which interact with actin filaments to provide translocation of actin cables and movement along actin cables. Myosins are divided in different subclasses according to similarities in motor and tail domains. Budding yeast has five myosins. The *S. cerevisiae* conventional myosin Myo1p (class II) is mainly involved in cell separation (Rodriguez and Paterson, 1990; Sweeney *et al.*, 1991; Watts *et al.*, 1987). The four unconventional myosins of budding yeast all belong to the class I and V myosins. The class V myosins are actin based motor proteins which are involved in polarised growth throughout different organisms (Mercer *et al.*, 1991; Prekeris and Terrian, 1997; Provance *et al.*, 1996). The yeast class V Myo2p motor protein, is an essential protein required for polarised growth, transport of secretory vesicles (Govindan *et al.*, 1995) and spindle orientation (Beach *et al.*, 2000; Yin *et al.*, 2000). In mutants, the normal actin localisation in the bud is disturbed and secretory vesicles accumulate in the mother cell (Johnston *et al.*, 1991). Loss of Myo2p function finally results in ceasation of budding (Govindan *et al.*, 1995; Reck-Peterson *et al.*, 2000). Some mutant cells also show defects in spindle orientation (Beach *et al.*, 2000; Yin *et al.*, 2000). In these cells myo2p fails to provide the polarisation of Kar9p at the bud cortex. In wild type cells Kar9p moves via binding to Myo2p to the bud cortex and captures microtubules through interaction with the microtubule-binding protein Bim1p thereby orientating the spindle. Mutants in *MYO2* can be rescued by high gene dosage of *SMY1* and *SMY2* (Lillie and Brown, 1994). *SMY1* is one of the six kinesin-related proteins in yeast and the only one that does not assist with spindle functions. Instead, Smy1p is involved in polarised cell growth (Lillie and Brown, 1994; Lillie and Brown, 1998). Smy1p and Myo2p co-localise and the two proteins interact in their putative cargo-carrying domains (Beningo *et al.*, 2000). Deletion of *SMY1* does not result in spindle orientation defects (Yin *et al.*, 2000) and the relevance of this interaction of an actin motor with a putative microtubule motor is unknown. The other multi-copy suppresser, *SMY2*, is a novel non-essential gene. High gene dosage of *SMY2* can also suppress mutations in other genes. These are for example, mutations in genes coding for proteins involved in vesicular transport (*SEC22*, *BET1*, *SEC16*) and in transcription

(*SPT15*) (Lillie and Brown, 1994). The fission yeast homologue of *SMY2* is *MPD2* which was isolated in a high gene dosage suppresser screen of fission yeast *cdc7* mutants (Cullen *et al.*, 2000). The budding yeast homologue of *CDC7*, *CDC15*, is part of the mitotic exit network (see 1.2) and localises to the budding yeast SPB (Xu *et al.*, 2000). Furthermore, Myo2p binds to calmodulin and the two proteins co-localise throughout the cell cycle (Brockerhoff *et al.*, 1994) and are found in regions with high concentrations of cortical actin patches. However, they do not co-localise with the cortical actin patches (Brockerhoff *et al.*, 1994).

The performance of the actin cytoskeleton is tightly regulated to ensure rearrangements during the cell cycle at the right time. The timing of bud emergence is triggered by the cyclin dependent kinase *CDC28* (Lew and Reed, 1993, 1995) and requires complex formation with the *CLN* G_1 cyclins (Figure 2A). The organisation of the actin cytoskeleton is mediated by the Rho-like GTPases in signalling pathways in response to these intracellular stimuli and also to extracellular growth signals (Tapon and Hall, 1997; Van Aelst and D'Souza-Schorey, 1997).

1.4 Microtubule organising centres

Microtubule organising centres (MTOCs) are a group of morphologically different organelles that are analogous in function. As mentioned above, they serve as focus points for microtubules and provide functions in mitosis necessary for successful cell duplication (see 1.4.4). Historically, the different types of MTOCs were named according to their morphology. The MTOC of animal cells was discovered by the cell biologists Boveri and van Beneden in the 19th century (Boveri, 1900). They observed a structure in the centre of the cells they studied from which fibres emanated. This organelle was named the 'centrosome'. The centrosome duplicated prior to mitosis and associated with the spindle poles. Theodor Boveri at first believed he found the 'material of inheritance' but later realised that he discovered one of the key players in partitioning this material now known as chromosomes. The functional equivalent of the centrosome in yeast is called the spindle pole body (SPB) and was discovered as a 'fibre apparatus' by Robinow and Marak in 1966. The SPB is structurally different from the centrosome. While the centrosome consists of a pair of centrioles and

pericentriolar material (see 1.4.1), the SPB is a multi-layered disk-like structure (see 1.4.2.1). The SPB does not contain a structure related to the centriole (see 1.4.1). However, it seems that microtubule organisation at both MTOCs is mediated by homologous proteins which are part of a complex called the gammasome or γ-tubulin ring complex in animal cells and the γ-tubulin complex in yeast (see 1.4.3 and 1.4.4). Although SPBs and centrosomes are very different in structure, more homologous proteins have been discovered and these are discussed in 1.4.3. The centrosome and the SPB of budding yeast are so far the best-characterised MTOCs. The third type of MTOC is the basal body which is structurally very similar to the centriole. Basal bodies are found at the plasma membrane and they nucleate the assembly of flagella and cilia. In most land plants, microtubule nucleation proteins are not associated with a defined structure such as the centrosome (Vaughn and Harper, 1998). Therefore, no conventional centralised MTOC can be defined.

Although lately, there has been some controversy about the role of the MTOCs (see 1.4.4) the main function remains the nucleation and organisation of microtubules (see 1.4.4). MTOCs are being studied in a variety of organisms. This study specialises on the SPB of the yeast *Saccharomyces cerevisiae*, but for comparison, the animal centrosome is discussed in more detail. In addition, significant homologies to or differences in MTOCs of organisms are described.

1.4.1 The centrosome

The animal centrosome is about 1 μm^3 in size and is made up by around 100 proteins. Some of those proteins require microtubules to be localised at the centrosome others localise independently. Some proteins stay at the centrosome throughout the cell cycle and others appear at a particular time and then dissociate or are degraded. The centrosome can be divided into two structurally different parts, a pair of centrioles and the centrioles surrounding pericentriolar material (Figure 4A). Presumably, the pair of centrioles serves as scaffold on which the pericentriolar material assembles.

Each centriole consists of a cylindrical array of nine triplets of microtubules which are connected with each other. These specialised microtubules are very stable which might

be due to post-translational modification such as poly-glutamylation (Bobinnec *et al.*, 1998). It has been shown in the algae *Chlamydomonas* that delta-tubulin is required for the triplet structure because without delta-tubulin cells are only able to produce microtubule doublets (Dutcher and Trabuco, 1998). The two centrioles differ in appearance with the older centriole displaying spoke like appendages at the end distal to its partner (Lange and Gull, 1996; Paintrand *et al.*, 1992). Both centrioles are linked together at the proximal end by specialised fibres. These fibres allow mobility, since one centriole moves around in a certain radius in a cell cycle dependent manner while its partner seems to be mainly stationary (Piel *et al.*, 2000). An additional protein of centrioles is centrin, a homologue of the budding yeast Cdc31p and it is found in the lumen of centrioles (Paoletti *et al.*, 1996).

The basic element of the pericentriolar material is a network of 12-15 nm filaments which other components associate with. Localisation of proteins can be cell cycle dependent and therefore, the pericentriolar material changes during the cell cycle reaching a peak at metaphase to anaphase transition with the low point at telophase in most cells. Microtubule nucleation functions are carried out by components of the pericentriolar material while centrioles do not seem to be directly involved in this process (Moudjou *et al.*, 1996; Tassin *et al.*, 1998). However, this traditional model is being debated lately. The main protein-complex necessary for the nucleation process is the γ-tubulin ring complex (see 1.4.4) which contains γ-tubulin and a variety of associated proteins. Another protein, which localises to the pericentriolar material is pericentrin, a large 220 kd protein (Doxsey *et al.*, 1994). Pericentrin forms a complex with γ-tubulin which assembles into a organised lattice (Dictenberg *et al.*, 1998). Recently, a pool of Hsp83, a member of the highly conserved Hsp90 family, was found to localise to *Drosophila* centrosomes throughout the cell cycle (Lange *et al.*, 2000). Hsp90 function was shown to be necessary for centrosome separation and maturation as well as spindle formation and chromosome segregation (Lange *et al.*, 2000).

Figure 4: Microtubule organising centres. (**A**) Cartoon of the centrosome. The centrosome consists of two centrioles (violet and green) which are linked by fibres (red) and of the pericentriolar material (grey). The mature 'mother' centriole (blue) has spoke-like appendages (pink) near its distal end. Microtubules (blue) are nucleated by the pericentriolar material. 'Reprinted from *Current biology*, Vol. 9, Urbani and Stearns, The centrosome, page No. R315, copyright (1999), with permission from Elsevier Sciences.' (**B**) Electron micrograph of isolated *S. cerevisiae* SPBs connected via a mitotic spindle. The outer (OP), central (CP) and inner (IP) plaque are indicated. (**C**) 2.3 nm tomographic slice of a budding yeast cell. The SPB (C1) is a multi-layered structure which is embedded in the nuclear envelope (NE). Microtubules (MT) can be seen attached to the inner plaque (IP). A hook-like structure (H) is visible at the side of the central plaque The half-bridge (HB) forms a one-sided extension of the SPB. The half-bridge (C2) is a specialisation of the nuclear envelope and consists of five distinct layers (see arrowheads). 'Reprinted from *Molecular Biology of the Cell*, (1999, volume 10, 2017-2031), with permission by the American Society for Cell Biology.' CP: central plaque, H: hook, HB: half-bridge, IL: intermediate layer, IP: inner plaque, MT: microtubules, NE: nuclear envelope, OP: outer plaque.

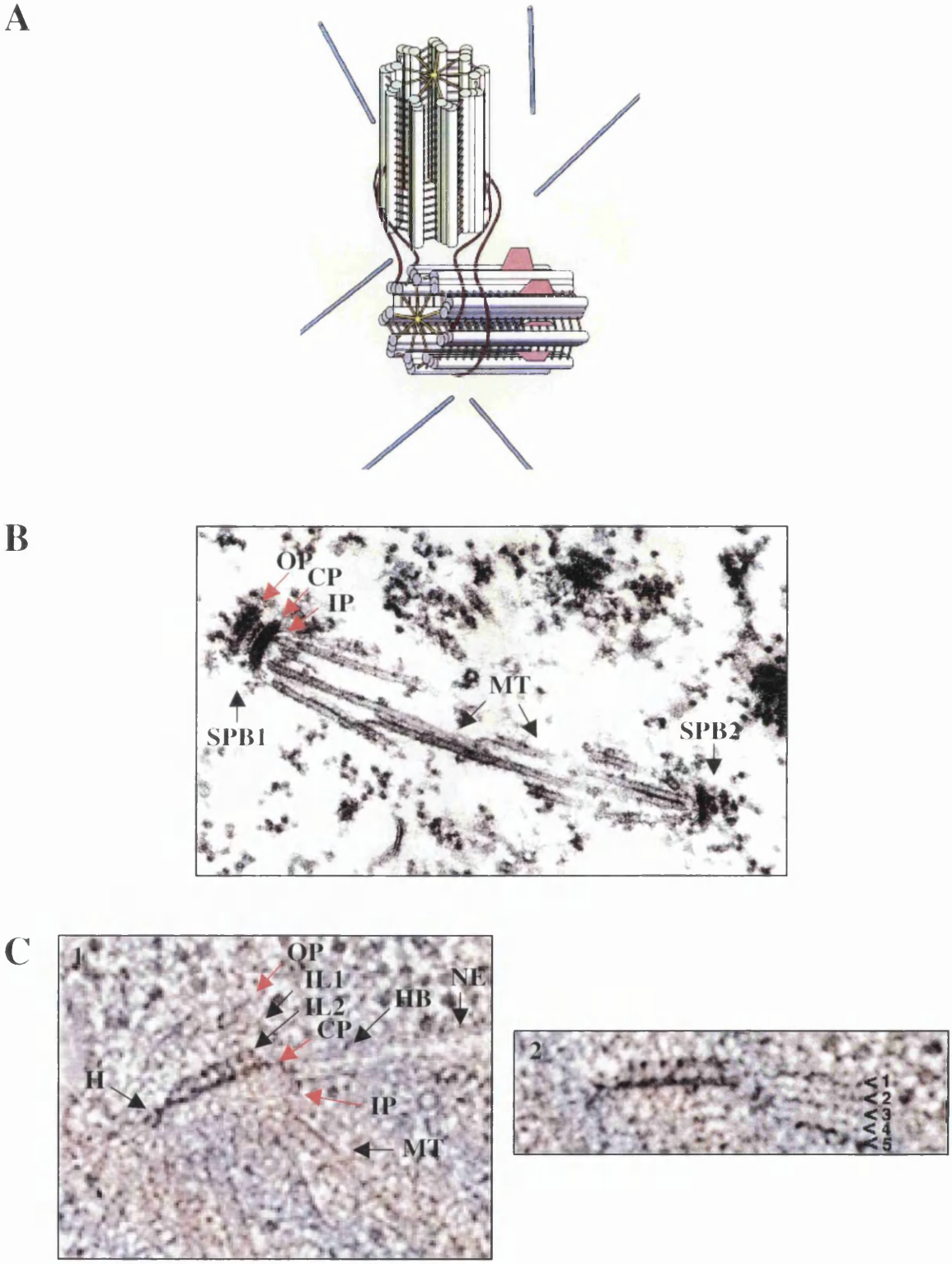

Figure 4: See facing page for figure legend.

1.4.2 The spindle pole body (SPB)

1.4.2.1 Morphology of the SPB

The SPB of *S. cerevisiae* is organised in distinct layers (Byers and Goetsch, 1974) which are connected to each other. The vertical extension, through the layers, remains constant but the horizontal size of the SPB can differ. In haploid cells the SPB is about half the size (horizontally) compared to the SPB of diploid cells. This change in size might be explained by the necessity of the diploid SPB to nucleate twice as many microtubules to connect the doubled number of chromosomes. The nomenclature of the different layers was introduced by Bullitt *et al.* (1997) who proposed that the SPB consists of five distinct layers (Figures 4B and 5). Recent studies using high-voltage electron tomography by O'Toole *et al.* (1999) support this model. The layers are defined as follows. The first distinct layer on the cytoplasmic site is termed outer plaque (OP) and is the site of cytoplasmic microtubule attachment. The following structures are the first intermediate layer (IL1) and the electron dense second intermediate layer (IL2). The central very electron dense layer which is at level with the nuclear envelope is called the central plaque (CP). The central plaque might be connected to the nuclear envelope with a hook-like structure, discovered by O'Toole *et al.* (1999). So far no components of the hook-like extension of the central plaque have been identified. On the nuclear side of the SPB the inner plaque (IP) is formed by the capped microtubule ends and here, the nuclear microtubules are anchored to the SPB. Horizontal sections through the layers show that IL2 contains a crystalline hexagonal lattice which is most likely a densely packed crystal of Spc42p (Bullitt *et al.*, 1997). Molecules in the central plaque section seem less spaced than in IL2. The other layers do not show ordered packing by high-voltage electron tomography (O'Toole *et al.*, 1999).

The SPB has a one-sided extension which is distinct from the nuclear envelope. This structure is called the half-bridge or if it connects the duplicated SPBs, the bridge. O'Toole *et al.* (1999) propose that the half-bridge consists of at least five distinct layers (Figure 4C) of which layer 2 is continuous with layer 5 and layer 3 is continuous with layer 4. Layer 1 lies at the cytoplasmic face of the bridge and does not

appear to be continuous with any of the other layers (Figure 4C). Layer 1 connects the bridge structure to the SPB via its interaction with a region between the central plaque and IL2 at the edge of the SPB. Cytoplasmic microtubules can be seen attached to the half-bridge in special stages of the cell cycle (see 1.4.2.2.5). At the end of the bridge, distal to the SPB a small structure forms in G_1/S which is called the satellite, the precursor of the new SPB (see 1.4.2.2.6).

1.4.2.2 Components of the SPB

1.4.2.2.1 Proteins forming inner and central regions of the SPB

Rout and Kilmartin (1990) identified three SPB components by raising a bank of monoclonal antibodies against an enriched SPB fraction. One of the proteins was 110 kD in size and it could be localised to the inner plaque of the SPB by immunolabelling EM using the original antibody from the screen (Rout and Kilmartin, 1990). The gene coding for the 110 kD protein, now named *SPC110* (spindle pole body component of 110 kD) is essential, but deletion of only the predicted coiled-coil domain of the protein is viable. Interestingly, deletion of the coiled-coil region results in a change in size of the inner plaque. The coiled-coil domain is non-essential but it is proposed that it provides flexibility of the inner plaque necessary for microtubule attachment (Kilmartin *et al.*, 1993) (Figure 5).

Spc110p was re-discovered later in two screens designed to identify calmodulin interacting proteins. Calmodulin is a ubiquitous eukaryotic Ca^{2+}-binding protein which is involved in cell signalling. One of these screens was aimed to search for proteins which compensate mutants in calmodulin (Geier *et al.*, 1996). The other screened an expression bank for calmodulin-binding proteins (Mirzayan *et al.*, 1992). Spc110p indeed contains a calmodulin binding site in its C-terminus (Stirling *et al.*, 1994) and mutations in the binding site, prevent calmodulin binding *in vitro* and Spc110p function *in vivo* (Geier *et al.*, 1996; Kilmartin *et al.*, 1993; Kilmartin and Goh, 1996; Stirling *et al.*, 1994, 1996).

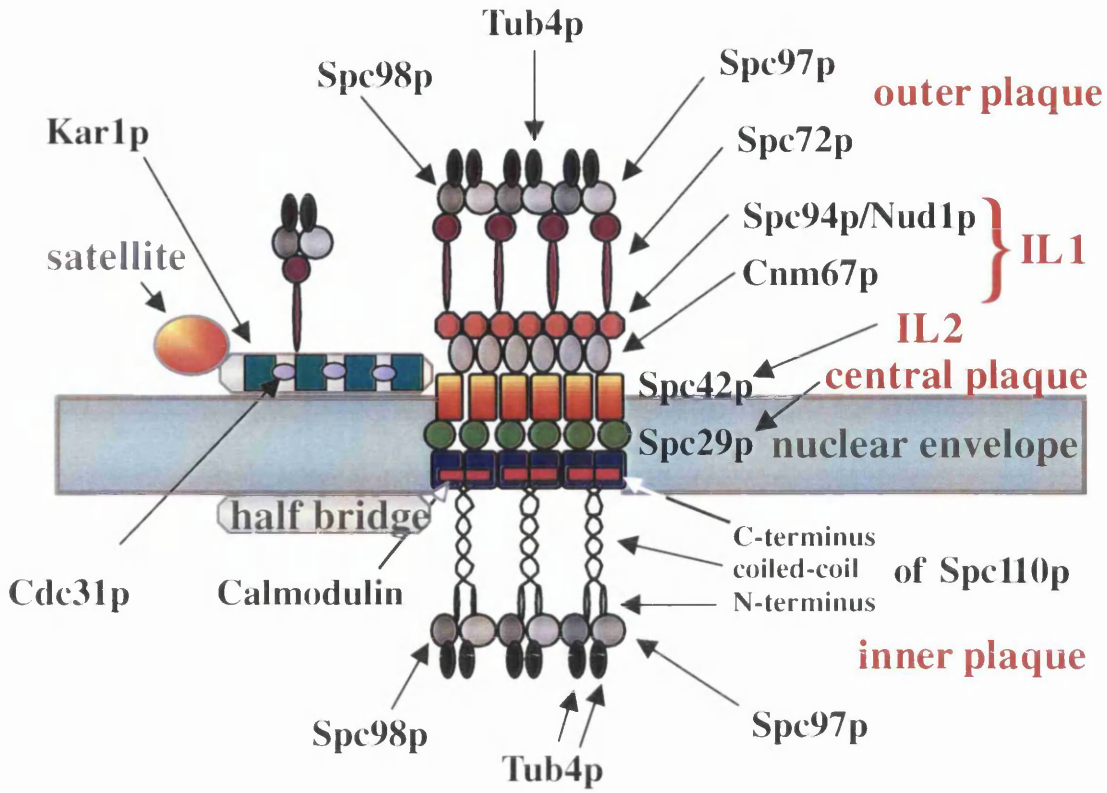

Figure 5: Molecular model of the *S. cerevisiae* SPB. The SPB is a mulit-layered structure consisting of outer plaque, intermediate layer 1 (IL1), intermediate layer 2 (IL2), central plaque and inner plaque. The SPB is embedded in the nuclear envelope throughout the cell cycle via the central plaque. Microtubules attach to the outer and inner plaque and in G_1 to the half-bridge. The half-bridge is a one-sided extension of the SPB and is a specialisation of the nuclear envelope. The precursor of the new SPB occurs in late G_1 at the distal end of the half-bridge (Byers and Goetsch, 1974; Byers *et al.*, 1978; Byers, 1981a, 1981b). The γ-tubulin complex consisting of Tub4p, Spc97p and Spc98p functions in the nucleation of microtubules (Sobel and Snyder, 1995; Geissler *et al.*, 1996; Marschall *et al.*, 1996; Knop and Schiebel, 1997; Knop *et al.*, 1997) and is localised at the outer and inner plaque (Rout and Kilmartin, 1990; Spang *et al.*, 1996a; Knop *et al.*, 1997). The γ-tubulin complex is connected to the central plaque via Spc110p and Spc72p (Kilmartin and Goh, 1996; Knop and Schiebel, 1997; Knop *et al.*, 1997; Chen *et al.*, 1998). The amino-terminus of Spc72p interacts with Spc97p and Spc98p (Knop and Schiebel, 1998). The carboxy-terminus of Spc110p including the calmodulin binding site is located near the central plaque (Geiser *et al.*, 1993; Stirling *et al.*, 1994; Spang *et al.*, 1996a) while the amino-terminus interacts with the γ-tubulin complex in the nucleoplasm (Spang *et al.*, 1996a; Knop and Schiebel, 1997). Spc94p/Nud1p and Cnm67p form the intermidiate layer 1 (Adams and Kilmartin, 1999; Elliott *et al.*, 1999). Spc42p is the main portein of the intermediate layer 2 (Bullitt *et al.*, 1997) and Spc29p binds to Spc42p and to the C-terminus of Spc110p (Adams and Kilmartin, 1999; Elliott *et al.*, 1999). Kar1p and Cdc31p are components of the half-bridge (Rose and Fink, 1987; Spang *et al.*, 1993, 1995).

The *SPC110* mutants fail to form a functional mitotic spindle (Kilmartin and Goh, 1996). Mutants in calmodulin are also unable to organise spindle microtubules and the majority of mutant cells arrests at the restrictive temperature containing only one SPB (Sun *et al.*, 1992). Calmodulin is localised at the central region of the SPB as shown by electron microscopy (Spang *et al.*, 1996a; Sundberg *et al.*, 1996) (Figure 5). This localisation is consistent with the interaction of calmodulin with the C-terminus of Spc110p which is localised in the central plaque region while the N-terminal domain of Spc110p extends into the inner plaque (Kilmartin and Goh, 1996; Spang *et al.*, 1996a; Sundberg *et al.*, 1996).

Two-hybrid experiments showed that the C-terminus of Spc110p additionally interacts with Spc42p, a component of the intermediate layer 2, while the N-terminus of Spc110p does not (Adams and Kilmartin, 1999). These findings were confirmed by the affinity precipitation of a complex containing mainly ProA-Spc110p, Spc42p, calmodulin and Spc29p (Elliott *et al.*, 1999; Knop and Schiebel, 1997). Analysing this complex, Elliott *et al.* (1999) showed that Spc29p interacts with the N-terminus of Spc42p and with the C-terminus of Spc110p in the yeast two-hybrid system. Furthermore, mutants in *SPC29* are lethal when combined with *cmd1-1*, *spc110-2* or *spc42-9* demonstrating that the proteins are functionally related. Thus, the C-terminal domain of Spc110p interacts with calmodulin and Spc29p. Presumably those proteins mediate the interaction of Spc110p with the N-terminus of Spc42p in the central region of the SPB (Figure 5). Inner and central regions of the SPB are therefore 'polar' in their organisation and the lateral extension is determined by interacting proteins.

Spc42p is like Spc110p predicted to be a coiled-coil protein. The putative coiled-coil domain of Spc42p is located in the central region of the protein and is essential for protein function (Donaldson and Kilmartin, 1996). Electron micrographs of cells overexpressing the protein show a large polymeric disc structure which extends from the side of the central region of the SPB along the cytoplasmic face of the nuclear envelope (Bullitt *et al.*, 1997; Donaldson and Kilmartin, 1996). This layer is composed entirely of phosphorylated Spc42p (Bullitt *et al.*, 1997). The lateral extension proposes that it is a bilayer (Bullitt *et al.*, 1997; Donaldson and Kilmartin, 1996) but it is assumed that this is an effect of overexpression and only a single layer of Spc42p

forms the intermediate layer 2 (Bullitt *et al.*, 1997). Electron microscopy of frozen preparations of the Spc42p structure revealed that it contains a crystalline array with hexagonal symmetry proposing a highly organised pattern for Spc42p (Bullitt *et al.*, 1997). Bullitt *et al.* (1997) concluded from their findings that Spc42p has the ability of self-assembly. Furthermore, that the Spc42p layer is the base structure of the SPB on which other layers of the SPB are added on in the fashion of crystal like self-assembly. However, this model does not offer an explanation for the size control of the SPB. If the size of the Spc42p lattice determines the size of the SPB how is the lattice itself controlled?

All interactions described above for Spc110p involve the C-terminus of the protein. A synthetical lethal screen to identify mutations that enhance the phenotype of temperature sensitive *spc110* mutants identified mutations in the *SPC97* and *SPC98* genes. Mutations in *SPC97* affect both N-and C-terminal *spc110* alleles, while mutations in *SPC98* are only synthetical lethal with mutations in the N-terminal *SPC110*. Spc110p interacts weakly with Spc97p and strongly with Spc98p in the two-hybrid system (Nguyen *et al.*, 1998). Spc97p and Spc98p and are part of the γ-tubulin complex (Geissler *et al.*, 1996; Knop and Schiebel, 1997) which is proposed to play a role in microtubule nucleation (see 1.4.4). A direct interaction of Spc110p with the yeast γ-tubulin Tub4p has not been shown. Therefore, Spc110p via its interactions with Spc97p and Spc98p tethers γ-tubulin to the inner plaque. A functional inner plaque provides the basis for nuclear microtubule attachment and proper spindle formation.

1.4.2.2.2 Components of the outer plaque

Elliot *et al.* (1999) observed a small fraction of Cnm67p in an affinity precipitate of Spc110p-ProA. Two-hybrid analysis showed two interactions for Cnm67p. The C-terminus of Cnm67p binds to the C-terminus of Spc42p (Adams and Kilmartin, 1999; Elliott *et al.*, 1999) and the N-terminus of Cnm67p interacts with Spc94/Nud1p in the two-hybrid system (Elliott *et al.*, 1999). Cnm67p was first identified to be a component of the SPB by Brachat *et al.* (1998) who determined the localisation of the GFP-tagged protein at the outer plaque (Figure 5). Further analysis of the gene revealed that mutants are defective in spindle orientation and nuclear migration resulting in the

formation of multi-nucleate and anucleate cells (Brachat *et al.*, 1998). Spc94p/Nud1p is a component of the outer plaque (Wigge *et al.*, 1998) (Figure 5) and it is essential. Mutants in *SPC94/NUD1* are unable to exit from mitosis and cells arrest with a large bud (Adams and Kilmartin, 1999).

Another component of the outer plaque is Spc72p (Figure 5). In contrast to *CNM67*, *SPC72* is essential in some but not all strain backgrounds (Knop and Schiebel, 1998; Soues and Adams, 1998). Deletion of *SPC72* in a W303 strain in which the gene is non-essential results in abnormal spindle positioning and aberrant nuclear migration. This phenotype was the result of a lack of cytoplasmic microtubules nucleated by the outer plaque. The *spc72* mutant cells do not arrest in the cell cycle, they break through the chromosome segregation block and undergo cytokinesis. This results in aploid and polyploid cells containing multiple SPBs (Soues and Adams, 1998).

The microtubule nucleation defect of the outer plaque in these mutants can be explained by the following interactions of Spc72p with other SPB components. Firstly, Spc72p interacts with Spc97p and Spc98p in the yeast two-hybrid system. Both proteins as mentioned above, are part of the yeast γ-tubulin complex, a protein complex involved in the nucleation of microtubules at the MTOCs throughout different species (see 1.4.3 and 1.4.4). Spc72p also shows a positive result in the two-hybrid system with the yeast γ-tubulin as bait, if Spc97p and Spc98p are co-overexpressed. All four proteins can be immunoprecipitated using anti-HA antibodies against the HA-epitope tag of Spc72p (Knop and Schiebel, 1998). This shows that Spc72p interacts with the γ-tubulin complex at the outer plaque and it is therefore analogous in function to Spc110p at the inner plaque (see 1.2.2.1).

Furthermore, Spc72p interacts with Stu2p. These two proteins associate in the yeast two-hybrid system and can be co-immunoprecipitated (Chen *et al.*, 1998). Stu2p is a component of the SPB but it also localises to microtubules. It is able to bind microtubules in vitro and might therefore be involved in attachment, organisation and dynamics of microtubule ends at the SPB (Wang and Huffaker, 1997).

1.4.2.2.3 Components which associate with SPBs and centromeres

Wigge *et al.* (1998) identified a protein named Ndc80p/Tid3p by MALDI-MS analysis of enriched SPBs fractions. This protein was identical to the 80 kD component discovered by Rout and Kilmartin (1990) in an early experiment using a monoclonal antibody approach. Ndc80p is localised close to SPBs as seen by immunoelectron microscopy (Rout and Kilmartin, 1990) and its localisation at the SPB does not change throughout the cell cycle (Wigge *et al.*, 1998). In addition, Ndc80p was detected at early short spindles by fluorescence microscopy (Wigge *et al.*, 1998). In anaphase cells, speckles of Ndc80p appear which might be at the positions of centromere DNA (Zheng *et al.*, 1999). It is also in anaphase that mutants in *NDC80* display defects. The SPB in these mutants is duplicated properly and the two SPBs are connected via a mitotic spindle but the chromatin can be seen mainly associated with only one SPB which remains in the mother cell. Therefore anaphase cells have large buds which contain one SPB but no or little DNA (Wigge *et al.*, 1998). Ndc80p was shown to be related to the human HEC protein with 26 % identity at the N-terminus and 36 % identity at the C-terminus (Wigge *et al.*, 1998). The human HEC protein localises to the kinetochore (Chen *et al.*, 1997a) a specialised region of the chromosome involved in microtubule attachment. Furthermore, the protein is probably involved in the regulation of proteasome-mediated degradation of mitotic cyclins (Chen *et al.*, 1997b). Due to the homology of Ndc80p with the centromere protein HEC and its mutant phenotype, Ndc80p might also have functions at the yeast kinetochore. This assumption is also supported by the speckled localisation of Ndc80p in anaphase which might represent kinetochore staining. Kinetochores are known to cluster in vicinity of the SPB probably through microtubule-kinetochore interactions (Goh and Kilmartin, 1993; Goshima and Yanagida, 2000; Hyland *et al.*, 1999). Taken together, Ndc80p could qualify as a shared component of SPBs and centromeres (Wigge *et al.*, 1998; Zheng *et al.*, 1999).

As another genetic interaction, *ndc80* is conditional lethal with *ctf19* (Hyland *et al.*, 1999). Ctf19p is possibly another shared component of SPBs and centromeres because Ctf19p localises to nuclear face of the SPB and it interacts with *CEN* DNA of the

centromeres (Hyland *et al.*, 1999). *Ctf19* mutants also display a severe chromosome missegregation phenotype (Hyland *et al.*, 1999).

1.4.2.2.4 Components which are shared by SPBs and nuclear pores

There are various hints that connections between SPBs and nuclear pore complexes (NPCs) exist. Nuclear pores are multi-protein complexes in the nuclear envelope which mediate nucleocytoplasmic transport. The best example for a shared component is Ndc1p, a transmembrane protein of the nuclear envelope which localises to both NPCs and SPBs. Co-localisation of Ndc1p with the nuclear pore component Nup49p and the SPB component Spc42p showed the localisation of Ndc1p at both organelles by immunofluorescence (Chial *et al.*, 1998). In detail studies of Ndc1p by immunoelectron microscopy revealed that Ndc1p localises to regions of NPCs and SPBs which are in contact with the nuclear envelope (Chial *et al.*, 1998). The *NDC1* gene was first discovered in a screen for cell cycle mutants (Moir *et al.*, 1982). *Ndc1-1* mutant cells fail to separate the chromosomes in mitosis but this does not result in a block of the cell cycle (Thomas and Botstein, 1986). It was shown, that the chromosome segregation defect is due to the failure of *ndc1* mutant cells to properly duplicate their SPBs. SPB duplication occurs but the new SPB is not inserted in nuclear envelope and the parental SPB organises a monopolar spindle (Winey *et al.*, 1993). Although SPB duplication is impaired in *ndc1* mutants, NPCs are functionally normal in these cells (Chial *et al.*, 1998). Yeast cells are very sensitive to altered gene dosage of *NDC1* which results in aneuploid and polyploid cells (Chial *et al.*, 1999). The *NDC1* gene has a homologue in fission yeast (*Schizosaccharomyces pombe*) which is called *Cut11+*. In fission yeast, the SPB is not constantly anchored in the nuclear envelope like the budding yeast SPB but it must be embedded in the nuclear envelope to organise the spindle in mitosis. Cut11p localises to mitotic SPBs in fission yeast and it is required for the cell cycle-dependent SPB anchoring in the nuclear envelope and therefore, for the formation of the bipolar spindle. Cut11p was also shown to associate with NPCs (West *et al.*, 1998). Analogue to the function of Cut11p it was proposed that Ndc1p functions in the insertion of organelles into the nuclear envelope (Chial *et al.*, 1998).

Interestingly, the deletion of the gene coding for the non-essential nucleoporin, Pom152p, suppresses the SPB duplication defect of *ndc1* mutants (Chial *et al.*, 1998). The mechanism by which this takes place is as yet unknown. Pom152p, a transmembrane protein, forms part of the peripheral membrane ring of the nuclear pore (Strambio-de-Castillia *et al.*, 1995; Wozniak *et al.*, 1994) and it was proposed that its localisation at the nuclear pore coincides with that of Ndc1p (Rout *et al.*, 2000). Pom152p, was also identified by MALDI analysis of isolated SPBs (Wigge *et al.*, 1998) but like two more nuclear pore components (Nic96p, Nup85p) identified in this experiment, Pom152p was classified as contaminant.

A SPB component recently discovered to be present at nuclear pores is the budding yeast centrin, Cdc31p (see 14.2.2.5). Centrin is a ubiquitous component of MTOCs (see 1.4.3). In budding yeast, Cdc31p is localised at the half-bridge and it is involved in SPB duplication (see 1.4.2.2.5). Rout *et al.* (2000) identified Cdc31p by MALDI analysis of highly enriched nuclear pore complexes but they were unable to localise Cdc31p at nuclear pores because Cdc31p-ProA fusion proteins were non-functional. Therefore, the assumption that Cdc31p is a true component of nuclear pores is based on co-enrichment of Cdc31p with Pom152p in nuclear envelope preparations and on co-fractionation of Cdc31p with the known nuclear pore components Nic96p and Nup159p (Rout *et al.*, 2000).

1.4.2.2.5 Proteins of the bridge structure

So far, only two permanent components of the bridge structure, Kar1p and Cdc31p are known. Both proteins were localised to the half-bridge by electron microscopy (Spang *et al.*, 1993, 1995). The genes coding for the two half-bridge components were firstly identified in genetic screens which determined the role of the proteins based upon the consequences of loss of their function. Mutants in *KAR1* were isolated due to the loss of nuclear fusion (karyogamy) during mating (Conde and Fink, 1976) and Kar1p indeed contains a domain that is essential for karyogamy. Another part of the protein is required for SPB localisation and association with the other half-bridge component Cdc31p (Biggins and Rose, 1994; Spang *et al.*, 1995; Vallen *et al.*, 1992a, b). *CDC31* was identified in a screen for cell division mutants (Pringle and Hartwell, 1981). Cells

lacking Karlp or Cdc31p block cell cycle progression and arrest with an enlarged single SPB with an indistinct half-bridge and no satellite (Byers, 1981b). The function of Karlp and Cdc31p is therefore required for early steps in SPB duplication (see 1.4.5.2.2).

In addition to its function in SPB duplication, Cdc31p is involved in morphogenesis and cell integrity. This function is fulfilled via an interaction with Kic1p (Sullivan *et al.*, 1998), an essential protein kinase that phosphorylates substrates in a Cdc31p-dependent manner. Most likely, this interaction does not take place at the half-bridge since Cdc31p can also be found in the cytoplasm (Biggins and Rose, 1994). *KIC1* mutants have no SPB duplication defect but mutations in the kinase domain of Kic1p result in abnormal bud morphology, unusual actin distribution and cell lysis (Sullivan *et al.*, 1998). Certain *cdc31* alleles also show defects other than in SPB duplication. These mutants have an elongated bud morphology and they display cell wall defects leading to cell lysis (Sullivan *et al.*, 1998).

Other components of the half-bridge are the outer plaque component Spc72p and the γ-tubulin complex. However, their localisation at the half-bridge is temporary and cell cycle dependent. In G_1 of the cell cycle cytoplasmic microtubules emanate from the half-bridge (Byers and Goetsch, 1975) in addition to outer plaque organised cytoplasmic microtubules. For the nucleation of microtubules at the half-bridge Spc72p and the γ-tubulin complex associate with the half-bridge in G_1. The N-terminal domain of Spc72p interacts with the C-terminal domain of Karlp in vitro and vivo thereby, targeting the γ-tubulin complex to the half-bridge (Pereira *et al.*, 1999).

1.4.2.2.6 Components of the satellite

The satellite it a small globular structure which appears at the end of the half bridge in G_1 of the cell cycle. The satellite reassembles the precursor of the new SPB. In initial steps of duplication it enlarges into a duplication plaque which is then inserted into the nuclear envelope. Adams and Kilmartin (1999) tested which known SPB components associate with the satellite and the duplication plaque by immunolabelling electron microscopy of cells expressing GFP- fusions of *SPC42*, *NUD1*, *CNM67*, *SPC29* and

SPC110. Spc42p, Nud1p, Cnm67p were found at both satellite and duplication plaque, while Spc29p could only be clearly detected at the satellite. Spc110p instead, is not associated with any of both structures. Therefore, proteins (Spc42p, Nud1p, Cnm67p) which also localise to the cytoplasmic side of the SPB seem to dominate the early structures of SPB duplication. The Spc110p protein which mainly composes the inner plaque of the SPB, might therefore localise to the 'new' SPB from the nuclear side at a later stage, possibly after insertion of the duplication plaque into the nuclear envelope (Adams and Kilmartin, 1999).

1.4.2.2.7 Further proteins associated with SPBs

In an experiment using MALDI analysis of enriched SPBs fractions Wigge *et al.* (1998) confirmed existing SPB components and identified several novel SPB associated proteins. Of those proteins identified, many have not yet been characterised in more detail but they will be mentioned here for completeness. One of the components isolated is Spc34p. It localises to the SPB and all along the mitotic spindle by immunofluorescence and immunolabelling electron microscopy (Wigge *et al.*, 1998). Spc34p interacts in the yeast two-hybrid system with Spc19p (Uetz *et al.*, 2000), another component identified in the MALDI-MS experiment (Wigge *et al.*, 1998). Spc19p displays the same localisation as Spc34p (Wigge *et al.*, 1998). In addition to its interaction with Spc34p, Spc19p interacts with the ribosomal protein Rpn5p and Ndc80p/Tid3p (a shared component of SPBs and kinetochores, see 1.4.2.2.3), in the yeast two-hybrid system (Uetz *et al.*, 2000). Two more SPB components, Spc24p and Spc25p, firstly isolated by Wigge *et al.* (1998) show an interaction in the yeast two-hybrid system with each other (Winzeler *et al.*, 1999). Spc24p also interacts genetically with Prp11p, a pre-mRNA splicing factor, Ssk22p, a MAP kinase kinase, Ste50p a protein involved in spore wall formation and Fir1p, a protein involved in mRNA processing (Cho *et al.*, 1998). The relevance of these genetic interactions is not yet proven. Finally Spc105p, a potential trans-membrane protein, also localises to the SPB region. It is mainly concentrated at one side of the SPB with the gold staining on the cytoplasmic as well as on the nuclear face of the nuclear envelope (Wigge *et al.*, 1998).

1.4.3 Homologous proteins of MTOCs

Various components of the budding yeast SPB have homologues in other organisms. Several examples have been mentioned throughout the text and will be summarised here.

Centrin/caltractin is a ubiquitous component of MTOCs and it was originally identified in basal body of *Chlamydomonas reinhardtii* (Huang *et al.*, 1988; Salisbury *et al.*, 1988). The yeast centrin, Cdc31p (Baum *et al.*, 1986a; Errabolu *et al.*, 1994; Spang *et al.*, 1993) is most closely related to the human HsCEN3 more than to the other two human centrins HsCEN1 and HsCEN2 (Middendorp *et al.*, 1997; Salisbury, 1995). All human centrin isoforms are located in the distal lumen of centrioles (Middendorp *et al.*, 1997) while Cdc31p localises to the half-bridge. Centrin 3, as Cdc31p, has a role in centrosome reproduction since injection of recombinant HsCen3p or of RNA encoding HsCen3p in one blastomere of two-cell stage *Xenopus laevis* embryos results in under-cleavage and inhibition of centrosome duplications (Middendorp *et al.*, 2000). HsCEN3 does not complement mutations or deletion of *CDC31* in *S. cerevisiae*, but specifically blocks SPB duplication which indicates that the human protein acts as a dominant negative form of *CDC31*.

Another MTOC component conserved from yeast to humans is γ-tubulin (see 1.4.4). The *S. cerevisiae* γ-tubulin gene *TUB4* has 35 – 40 % homology to other γ-tubulins. Two other components of the γ-tubulin complex are highly conserved proteins. The yeast *SPC97* (Knop *et al.*, 1997) and *SPC98* (Geissler *et al.*, 1996 ;Rout and Kilmartin, 1990) genes have homologues in higher eukaryotes (Martin *et al.*, 1998; Murphy *et al.*, 1998; Tassin *et al.*, 1998). Spc97p is homologous to the human hGCP2 and the *Drosophila* Dgrip84 while Spc98p is homologous to HSSc98/hGCP3 in humans and Xgrip109 in *Xenopus* and Dgrip109 in *Drosophila*. This is an example for a protein complex conserved during MTOC evolution.

The budding yeast Ndc80p (see 1.4.2.2.3) has 45 % similarity with human HEC protein (Wigge *et al.*, 1998). HEC is localised at centromeres but not at MTOCs. Functionally expressed in yeast, human HEC protein localises to the nucleus (Zheng *et*

al., 1999) and Ndc80p can be functionally replaced with human HEC protein when expressed under the *NDC80* promotor (Zheng *et al.*, 1999).

Furthermore, *NDC1* (see 1.4.2.2.4) is homologous to the *S. pombe CUT11*. Both proteins are proposed to function in insertion of the SPB into the nuclear envelope.

1.4.4 The function of MTOCs

The main function of MTOCs is proposed, as the name already suggests, to be the nucleation and the organisation of microtubules. There has been some controversy about the role of MTOCs in cell division in higher eukaryotes because it was shown that bipolar spindles form in the absence of centrosomes. The microtubules forming those spindles originate from chromosomes and self-organise into mitotic spindles (Waters and Salmon, 1997). Consequently, centrosomes do not seem to be required for spindle formation. This was also shown in the fly *Sciara coprophila*. Unfertilised fly oocytes which do not harbour centrosomes can develop parthenogenetically. Nuclear division of these oocytes takes place via chromosome organised bipolar spindles (de Saint Phalle and Sullivan, 1998). These findings argue against the role of the MTOC as the unique microtubule organiser of the cell. However, the spindles of the fly oocytes are not properly orientated in the cell and cytoplasmic microtubules are not observed to connect to the spindle poles. Cytoplasmic microtubules are normally required for the spindle orientation and they are usually nucleated by MTOCs. *Chlamydomonas rheinhardtii* spindles which have developed without MTOCs, also show random spindle positioning in relation to the cleavage furrow (Ehler *et al.*, 1995). This shows that MTOCs are required at spindle poles to nucleate astral microtubules thereby ensuring proper spindle positioning and therefore functional cell division.

The best candidate for the universal microtubule nucleator of MTOCs is γ-tubulin. γ-tubulin is a conserved component of all MTOCs (Stearns *et al.*, 1991; Zheng *et al.*, 1991) (see 1.4.3). γ-tubulin was first identified in a screen for suppression of the *A. nidulans benA33* β-tubulin mutation. The β-tubulin mutant displays hyper stable microtubules which are overcome by mutation of γ-tubulin (Oakley and Oakley, 1989). The requirement of γ-tubulin for microtubule nucleation was proven by Joshi *et al.*

(1993) who showed that injection of anti-γ-tubulin antibodies blocks microtubule nucleation in mammalian cells. Mutations in γ-tubulin result in disruption of MTOC function of *A. nidulans, S. pombe, S. cerevisiae* and *D. melanogaster* (Horio *et al.*, 1991; Martin *et al.*, 1997; Spang *et al.*, 1996b; Sunkel *et al.*, 1995). In budding yeast, conditional lethal mutants in the γ-tubulin gene *TUB4* have disorganised non-functional spindles with less than the normal amount of MTs (Sobel and Snyder, 1995; Spang *et al.*, 1996b).

The γ-tubulin complex was first identified in *Xenopus* egg extract and here it includes α-and β-tubulin and proteins of 195, 133, 109, 75 kD (Zheng *et al.*, 1995). In the *Xenopus* centrosomes, part of the complex is organised in an open ring structure with a 25-28 nm diameter (Zheng *et al.*, 1995). These characteristic ring structures were also isolated from *Drosophila* pericentriolar material (Moritz *et al.*, 1995a, b). In yeast, the γ-tubulin complex does not display a ring like structure. This might be due to its small size (6S compared to 25 S in embryonic and somatic cells). While the γ-tubulin ring complex consists of at least five different proteins, the yeast complex most likely contains two molecules of the yeast γ-tubulin Tub4p and one molecule of Spc97p and Spc98p each (Knop and Schiebel, 1997). Spc97p and Spc98p were identified in yeast and have now been cloned in *Drosophila, Xenopus* and humans (see 1.4.3).

The yeast Tub4p localises to the inner and outer plaque structures of the SPB by immunoelectron microscopy (Spang *et al.*, 1996b) and so do Spc97p and Spc98p (Knop and Schiebel, 1997; Rout and Kilmartin, 1990). At the outer plaque, the γ-tubulin complex binds to Spc72p which connects to the central plaque via spc94p/Nud1p and Cnm67p (see 1.4.2.2.2). At the inner plaque, Spc110p connects the γ-tubulin complex to the central plaque (see 1.4.2.2.1). At the outer plaque the γ-tubulin complex nucleates cytoplasmic microtubules and at the inner plaque nuclear microtubules. In yeast microtubule minus ends appear rounded in the electron micrograph (Pereira and Schiebel, 1997). Such capped microtubule ends have now also been described in vertebrates (Rodionov *et al.*, 1999; Wiese and Zheng, 2000).

Since no direct interaction between γ-tubulin and α-or β-tubulin has been shown, nucleation models are still theoretical. In yeast the γ-tubulin complex is supposed to interact with microtubule minus ends possibly with the help of the microtubule binding protein Stu2p (Saunders, 1999). For microtubule nucleation by the γ-tubulin ring complex of higher eukaryotes two models exist. The ring/helix nucleation model by Oakley (1992) and Zheng *et al.* (1995) suggests, that γ-tubulin forms a helical ring on which microtubules assembles by direct interaction of α-tubulin with γ-tubulin. The protofilament model by Erickson and Stoffler (1996) proposes that α- and β-tubulin subunits would interact with a γ-tubulin filament. α- and β-tubulin will assemble into the form of a sheet which than curves up into a cylindrical microtubule. The second model takes into account that α- and β-tubulin form sheets in vivo and that minus ends of microtubules are free for dynamic instability.

Recently, functions of the budding yeast MTOC in cell cycle regulation have been proposed (Bardin *et al.*, 2000; Pereira *et al.*, 2000). As described in 1.2, proteins of the spindle positioning checkpoint (Bub2p, Bfa1p, Tem1p) localise to the SPB in a cell cycle dependent manner and positioning of one SPB in the bud is necessary to allow exit from mitosis. If defects in the spindle positioning occur and the SPB does not reach the bud, cell cycle progression is inhibited. Further data suggest that other cell cycle proteins like Cdc15p, Cdc5p etc. also localise to the SPB. Taken together, the SPB might play a central role in cell cycle regulation.

1.4.5 Duplication of MTOCs

In mitosis, every cell needs two functional MTOCs to form the poles of the mitotic spindle, to help with the positioning of the spindle in the cell and to assist with the separation of the chromosomes. Since each cell inherits only one MTOC, the MTOC has to be duplicated before mitosis. The duplication must be tightly regulated that only one duplication event occurs per cell cycle and that finally two functional MTOCs exist at the right time and in the right place.

1.4.5.1 Duplication of centrosomes

In G_1 of the animal cell cycle each cell harbours one centrosome consisting of a pair of centrioles with the surrounding pericentriolar material. At approximately the same time as DNA duplication, this is at the G_1 to S transition, centrosome duplication starts. Firstly, centrioles move apart and once separated new centrioles grow orthogonal to the original ones. In early G_2 the duplicated centrosomes can be observed side by side and each contains a complete pair of centrioles (Chretien *et al.*, 1997). This process of centrosome duplication is called semiconservative since each resulting centrosome posses one new and one old centriole (Kochanski and Borisy, 1990). The theory exists that the pre-existing centriole is the nucleator. This is the case for typical somatic cells which must have an existing centriole to create a new centriole. But it is also known, that some animal and plant cells form basal bodies and centrioles *de novo* therefore new centrioles are not strictly templated by existing ones. In late G_2 and mitosis, the duplicated centrioles move to opposite sides of the nuclear envelope. The migration of the centrosomes is dependent on kinesin microtubule motor proteins. When the nuclear envelope brakes down microtubles attach to chromosomes and after mitosis is completed, cytokinesis takes place.

1.4.5.2 Duplication of the budding yeast SPB

1.4.5.2.1 Duplication process

The duplication of the *S. cerevisiae* SPB begins in G_1 of the cell cycle with the formation of the satellite. The satellite is detectable by electron microscopy as a small electron dense structure on the cytoplasmic face of the half-bridge. It is always located at the side of the half-bridge distal to the existing SPB (Byers, 1981a; Byers and Goetsch, 1974). The structure of the satellite is either spherical in haploid cells or plaque-like in tetraploid cells (Adams and Kilmartin, 1999). It is mainly a small copy of the cytoplasmic/central core of the existing SPB (Adams and Kilmartin, 1999) (see 1.4.2.2.6). The satellite sits on top of the half-bridge but both structures are closely associated (O'Toole *et al.*, 1999). At this stage the precursor of the new SPB is not inserted in the nuclear envelope which is consistent with the finding that the satellite

does not contain Spc110p (see 1.4.2.2.6) and does not nucleate nuclear microtubules (Adams and Kilmartin, 1999).

The appearance of the satellite is the first morphological marker for the beginning of SPB duplication. When the small bud emerges, SPBs have already been duplicated but they are usually still connected by the bridge. In G_1-phase, the satellite enlarges and forms the duplication plaque which still contains the cytoplasmic SPB components described in 1.4.2.2.6 (Adams and Kilmartin, 1999) but not the nuclear Spc110p protein. Although, there might be other components present which have not yet been identified. At this stage, an elongation of the half-bridge under the duplication plaque occurs but the cytoplasmic phase of the half-bridge seems to stay constant (Adams and Kilmartin, 1999). The half-bridge layers are supposed to fuse at the distal end and here, a nuclear pore like structure is often present (Adams and Kilmartin, 1999). How the duplication plaque inserts into the nuclear envelope is not clarified. Two hypotheses exist. One model is that the half-bridge which is supposed to be extended under the duplication plaque retracts and reduces itself to its normal size thereby allowing nuclear components to assemble onto the duplication plaque from the nuclear side. The other theory suggests that the retraction of the half-bridge is passive and that Spc110p assembles onto the duplication plaque from the fusion point of the half-bridge (Adams and Kilmartin, 1999).

After insertion of the duplication plaque into the nuclear envelope two side-by-side SPBs connected via the bridge can be observed (Byers, 1981a). Now nuclear microtubules are nucleated from both SPBs and these interdigitate at sharp angles (O'Toole *et al.*, 1999). When the SPBs move apart the bipolar spindle forms and it consists of numerous short and some long microtubules (O'Toole *et al.*, 1999). A question that still has to be answered is whether the bridge is cleaved in the middle and equally distributed or whether the bridge is cleaved at the side, leaving one SPB without a bridge structure.

1.4.5.2.2 Proteins involved in SPB duplication

Several proteins are known to be involved in the SPB duplication process. Their identification is mainly the result of mutant analysis. The different proteins can be categorised for requirement in early, intermediate or late stages of duplication according to the mutant phenotype.

A protein that functions at early and late stages of SPB duplication is the dual specific kinase Mps1p. However, most conditional lethal mutants in *MPS1* display defects in early SPB duplication. Cells arrest with a single SPB that connects to an enlarged half-bridge. These mutant cells do not show any satellite formation (Winey *et al.*, 1991). The *mps1-737* mutant shows defects in a later stage of duplication. Mutant cells are able to initially form satellites but most cells arrest containing only one single SPB with a reduced half-bridge. In some of these cells an additional small SPB-like structure is observed (Schutz and Winey, 1998). This SPB is unable to nucleate microtubules and can not function in spindle formation. Taken together, Mps1p is involved in multiple steps of duplication.

The same duplication defect as in 'early' *MPS1* mutants was observed in mutants of the heat shock transcription factor *HSF1*. In *hsf1* mutants, the SPB is unduplicated and the half-bridge is enlarged (Zarzov *et al.*, 1997). It is unknown whether this is due to a direct function of Hsf1p at the SPB or if it is an effect of the lack of *HSP/HSC82* expression observed in the *hsf1* mutants (Zarzov *et al.*, 1997).

The yeast centrin Cdc31p and its half-bridge localiser Kar1p (see 1.4.2.2.5) are both required at the same time point early in SPB duplication (Rose and Fink, 1987a). Mutants in *CDC31* and *KAR1*, do not form a satellite but cause enlargement of the existing SPB (Baum *et al.*, 1986a). Mutants in *KAR1* can be rescued by overexpression of *CDC31* (Salisbury, 1995) and its mutated form *cdc31-16* which makes cells *KAR1* independent (Vallen *et al.*, 1994). Mutants in *KAR1* can also be rescued by high gene dosage of *DSK2*. This suppression is specific for SPB duplication and the additional karyogamy defect is not suppressed. Dsk2p is a nonessential ubiquitin-like protein

which has not been detected at the SPB (Biggins *et al.*, 1996). High gene dosage of *DSK2* is also sufficient to rescue the complete deletion of *KAR1* (Biggins *et al.*, 1996).

Another gene product that functions early in SPB duplication is Rpt4p/Pcs1p. It is a protein of the 19 S regulatory particle of the proteasome (Glickman *et al.*, 1998) also called the proteasome cap subunit (McDonald and Byers, 1997). The proteasome is required for degradation of ubiquitinated proteins throughout the cell cycle, including degradation of cyclins (see 1.2). Conditional lethal mutants of *RPT4/PCS1* arrest as large budded cells in G_2 of the cell cycle with only one SPB which nucleates a monopolar spindle (McDonald and Byers, 1997). DNA duplication and bud formation is not effected in these mutants. Fully functional Rpt4p-GFP localises to the nuclear envelope and ER (endoplasmic reticulum) throughout the cell cycle where the main proteasomal activity takes place. Taken together, Rpt4p a component of the proteasome might be involved in degradation of proteins required for SPB duplication (McDonald and Byers, 1997).

The central plaque component Spc42p is also required for proper SPB duplication. It seems to function at an intermediate stage of the duplication process because mutants in *SPC42* have a single SPB with disordered material associated with the cytoplasmic site of the half-bridge. This might indicate that the enlargement of the satellite into the duplication plaque is compromised in these mutants (Donaldson and Kilmartin, 1996).

The following proteins are involved in late events in SPB duplication and mutants show similar phenotypes to the 'late' *MPS1* mutant allele *mps1-737*. Mutants in *MPS2* were isolated in the same screen as *MPS1* mutants, a screen for cells containing monopolar spindles (Winey *et al.*, 1991). The defect in these *MPS2* monopolar spindle mutants can be explained by incomplete SPB duplication. Mutant cells which temporarily arrest in G_2 contain the original SPB organising a monopolar spindle and in some cases a small SPB-like structure. The small SPB resides on the cytoplasmic face of the nuclear envelope and only nucleates cytoplasmic microtubules (Winey *et al.*, 1991). The lack of nuclear microtubules might be the consequence of the incomplete insertion of the new SPB into the nuclear envelope and its lack of the inner plaque structure (Winey *et al.*, 1991). Similar phenotypic features are observed in

mutants in *NDC1* (see 1.4.2.2.4). These mutants start to duplicate the SPB but the duplicated SPB is not inserted into the nuclear envelope (Winey *et al.*, 1993). The original SPB organises a monopolar spindle which connects to all chromosomes (Winey *et al.*, 1993). The mutant cells undergo asymmetric segregation with all chromosomes located at one pole (Thomas and Botstein, 1986). It was proposed that Mps2 and Ndc1p function in insertion of the duplication plaque into the nuclear envelope.

CDC37 was originally identified in a screen for mutants that arrest at Start in G_1 (Reed, 1980). The *cdc37-1* mutants arrest as unbudded cells in G_1 and remain mating pheromone responsive (Reed, 1980). Interestingly, SPB duplication proceeds past Start and cells have side-by-side SPBs at the arrested stage (Schutz *et al.*, 1997). The new SPB is incomplete since it lacks outer plaque material. Further hints that Cdc37p is involved in SPB duplication come from genetic experiments. *CDC37* is a high gene dosage suppresser of *mps1-1* mutants which show an early SPB duplication defect and *mps1* and *cdc37* are co-lethal (Schutz *et al.*, 1997). Mutants in *CDC37* cause the loss of Mps1p kinase activity but the level of Mps1p in the cells remains constant (Schutz *et al.*, 1997). The mammalian homologue of Cdc37p is a subunit of the Hsp90 chaperone complex which associates with several protein kinases (Stepanova *et al.*, 1996).

The SPB component Spc29p is required in late SPB duplication (Adams and Kilmartin, 1999; Elliott *et al.*, 1999). Mutant cells in late G_1 of the cell cycle contain two SPBs but one of those SPBs is smaller in size. The SPBs nucleate spindle microtubules but the spindle is asymmetric with the smaller SPB nucleating less microtubules (Adams and Kilmartin, 1999). However, later in the cell cycle mainly one SPB per cell is observed by immunofluorescence and only about 20 % of mutant cells still show a second SPB signal. It is therefore assumed that the smaller SPB disintegrates in the majority of mutant cells (Adams and Kilmartin, 1999; Elliott *et al.*, 1999).

1.4.5.2.3 Involvement of the *PKC1* MAP kinase pathway in SPB duplication

Khalfan *et al.* (2000) searched for high copy suppressers of the double deletion mutant Δ*dsk2* Δ*rad23* which is defective in early steps of SPB duplication. As expected they found that high gene dosage of *CDC31* overcomes the defect as shown before by Biggins *et al.* (1996). In addition, they identified two genes of the *PKC1*-pathway, *SLG1/WSC1* and *PKC1* itself, that can suppress the deletion mutant. The *PKC1*-pathway is a MAP kinase signalling pathway involved in numerous cell processes including cell wall integrity and bud emergence at the G_1/S transition (Gray *et al.*, 1997; Marini *et al.*, 1996; Mazzoni *et al.*, 1993; Zarzov *et al.*, 1996). One of the proteins identified in the suppresser screen, Slg1p, functions as a plasma membrane protein that signals Pkc1p via the small GTPase Rho1p (Jacoby *et al.*, 1998; Verna *et al.*, 1997). Pkc1p the other protein identified by Khalfan *et al.* (2000) activates the subsequent MAP kinase module consisting of Bck1p, Mkk1p/ Mkk2p and Mpk1p (Irie *et al.*, 1993; Lee *et al.*, 1993; Lee and Levin, 1992). In addition, high gene dosage of *SLG1* and *PKC1* partially suppresses the *kar1-Δ17* and *cdc31-2* mutants which are also known to show SPB duplication defects (see 1.4.5.2.2). The downstream components *BCK1* and *MPK1* were also able to suppress the defects of the *kar1-Δ17* strain. Further genetic studies revealed that mutants in *SPC110* coding for a inner plaque component can be suppressed by high-copy number of *PKC1* and *SLG1* (Khalfan *et al.*, 2000). The *Spc110-220* mutation leads to defective SPB assembly because of reduced interaction between Spc110p and calmodulin (Sundberg *et al.*, 1996). Therefore, *PKC1*, *SLG1*, *MPK1* and *BCK1*, all of which are genes coding for components of the MAP kinase cascade, show genetic interactions with genes coding for proteins involved in SPB duplication.

1.4.5.3 Similarities of MTOC duplication in different organisms

The duplication process of the budding yeast SPB has often been described as template mechanism. The template would be the satellite on which the other SPB components assemble. Although, there is no structural evidence, the template mechanism has also been proposed for centriole duplication. This is based on the finding that the procentriole always assembles at a set distance of about 70 nm from the proximal end

of the existing centriole. The occurrence of the procentriole in a set location led to the suggestion that a template structure might be attached to the existing centriole in this place (Rattner and Phillips, 1973; Robbins *et al.*, 1968).

The duplication process of the fission yeast SPB shows some similarities to the duplication of the budding yeast SPB. In fission yeast, the new SPB assembles on the end of a bridge structure attached to the existing SPB (Ding *et al.*, 1997). This is analogous to the assembly of the satellite and the duplication plaque at the end of the half-bridge in budding yeast. However, it appears that the new fission yeast SPB uses the existing SPB as a source for building material since the 'old' SPBs decreases in size while the new one grows. This has not been observed in budding yeast cells where the established SPB stays mainly constant in size throughout the cell cycle. The budding yeast SPB is embedded in the nuclear envelope throughout the cell cycle (Byers, 1981a) and the new SPB is inserted into the nuclear envelope during duplication. The fission yeast SPB resides just outside the nuclear envelope apart from mitosis. In mitosis the fission yeast SPBs have to insert into the nuclear envelope to form the spindle poles since there is no nuclear envelope breakdown. Therefore, fission yeast inserts completely duplicated SPBs into a fenestration of the nuclear envelope while budding yeast inserts the duplication plaque into the nuclear envelope. So far only one of the components involved in the insertion process has been identified but this component is homologue in both organisms. This is the fission yeast Cut11p and its budding yeast homologue Ndc1p (see 1.4.2.2.4).

An indication that certain steps of MTOC duplication might be conserved in all organisms comes from the finding that centrin is a common component of all MTOCs. Mutants in the budding yeast centrin, *CDC31*, block formation of the satellite and lead to enlargement of the remaining unduplicated SPB (see 1.5.2.2) (Baum *et al.*, 1986b; Byers, 1981b; Schild *et al.*, 1981). The *Chlamydomonas reinhardtii* centrin/caltractin which is found in basal bodies, is essential for accurate basal body duplication and separation (Taillon *et al.*, 1992) and for microtubule severing (Sanders and Salisbury, 1989, 1994). Another example is the centrin of the green alga *Spermatozopsis similis* which localises to fibres connecting the new probasal body to the existing basal body (Lechtreck *et al.*, 1999). Centrin 3 which is the closest relative to the budding yeast

Cdc31p out of the three human centrins has a role in centrosome reproduction. This was shown in an experiment by Middendorp *et al.* (2000) who showed that injection of recombinant HsCen3p or of RNA encoding HsCen3p into one blastomere of two-cell stage *Xenopus laevis* embryos resulted in inhibition of centrosome duplication.

1.5 Aim of thesis: characterisation of Bbp1p

In our laboratory, a screen for high gene dosage suppressers of conditional lethal mutants in *SPC98* resulted in the identification of *BBP1* (S. Geissler, *unpublished data*). *BBP1* was also isolated in our laboratory in a two-hybrid screen for interacting proteins of the SPB component Spc29p (Schramm *et al.*, 2000).

BBP1 had been identified before in a two-hybrid screen for proteins interacting with *BFR1* (Xue *et al.*, 1996). *BFR1* itself was isolated as a high-gene dosage suppresser of Brefeldin A induced lethality (Jackson and Kepes, 1994). The drug Brefeldin A causes the disassembly of the Golgi complex due to inhibition of the small G protein Arf1p (Peyroche *et al.*, 1999). High gene dosage of *BFR1* was also shown to rescue mutants in *SEC17* (Jackson and Kepes, 1994). The gene product of *SEC17* is involved in vesicle targeting and/or fusion (Clary *et al.*, 1990; Griff *et al.*, 1992). More recently, Bfr1p was shown to be part of the polyribosome-mRNP complex (Lang and Fridovich-Keil, 2000) where it associates with the mRNP complex protein Scp160 and the poly (A)-binding protein Pab1p.

Xue *et al.* (1996) investigated the effect of depletion of *BBP1*. They constructed a *bbp1* deletion strain which contained wild type *BBP1* under the *GAL* promoter. The strain was incubated on glucose medium to deplete Bbp1p, and the cells continued to grow for 16 h to 18 h. FACS analysis showed that some cells increased in ploidy after 16 h. Immunofluorescence revealed that spindle formation was defective in these cells since duplicated SPBs were not connected via a spindle.

The genetic interactions of *BBP1* with genes coding for the known SPB components Spc98p and Spc29p indicated a potential function of Bbp1p at the SPB. Furthermore, the spindle defect of cells depleted of *BBP1* suggested an implication of Bbp1p in the

formation of a functional spindle, one of the main tasks of SPBs. Taken together, Bbp1p was a promising candidate for a novel SPB component with functions in mitosis. In this study, this theory was followed up in different experiments. The localisation of Bbp1p potentially at the SPB was to be determined by fluorescence microscopy and immunoelectron microscopy. In addition, interactions of Bbp1p with known SPB components were to be tested by two-hybrid and suppression analysis. To identify novel interactors of Bbp1p, affinity precipitates of Bbp1p were analysed by MALDI-MS. If these experiments were to show that Bbp1p is a SPB component, the cellular function of Bbp1p was to be determined by overexpression experiments and by analysis of conditional lethal mutants. Finally, a molecular model of the SPB including Bbp1p was to be proposed.

2. Materials and Methods

2.1 Materials

2.1.1 Chemicals

All chemicals were purchased from Sigma (Dorset, UK), Merck (Darmstadt, Germany), Gibco (Paisley, UK) or Fisher Scientific (Loughborough, UK), unless specified otherwise.

2.1.2 Buffers

Frequently used buffers are listed here. All buffers were prepared with double distilled water. Some buffers were autoclaved (121 °C, 2.0 bar) as indicated.

Blotting-buffer:
48 mM Tris
39 mM glycine
0.037 % (w/v) SDS
20 % (v/v) methanol

HU-buffer:
200 mM Tris-HCl (pH 6.8)
8.0 M urea
5 % (w/v) SDS
0.1 mM EDTA
15.0 mg/ml DTT
0.1 % (w/v) bromophenol blue (Roth, Karlsruhe, Germany)

Laemmli-buffer:
25 mM Tris
192 mM glycine
0.1 % (w/v) SDS

PBS:
50 mM $NaPO_4$
150 mM NaCl
pH 7.5
autoclaved

Qiagen buffer 1:	20 mM Tris-HCl (pH 8.0) 10 mM EDTA (pH 8.0) 100 µg/ml RNAse
Qiagen buffer 2:	200 mM NaOH 1 % (w/v) SDS
Qiagen buffer 3:	3.0 M potassium acetate
6 x loading buffer DNA:	0.25 % (w/v) bromophenol blue (Roth, Karlsruhe, Germany) 0.25 % (w/v) xylene cyanole FF 15 % (w/v) Ficoll 400 (Pharmacia, Uppsala, Sweden)
Stripping buffer:	62.5 mM Tris (pH 6.7) 2 % (w/v) SDS 100 mM β-mercaptoethanol
50 x TAE buffer:	2.0 M Tris-acetic acid (pH 7.7) 50 mM EDTA autoclaved
10 x TBS:	25 mM Tris-HCl (pH 7.5) 150 mM NaCl autoclaved
TBS-T:	1 x TBS 0.1 % (v/v) Tween 20 pH 7.5

2.1.3 Enzymes

Restriction enzymes were purchased from New England Biolabs (Beverly, USA), Roche (Lewes, UK), Pharmacia (Uppsala, Sweden) and Gibco (Paisley, UK).

Taq DNA polymerase was purchased from Perkin Elmer, Wellesley, USA (Amplitaq) or Eurogentec, Southampton, UK (Goldstar). Vent polymerase was obtained from New England Biolabs (Beverly, USA).

Klenow enzyme and alkaline phosphatase were purchased from Roche (Lewes, UK).

RNAse A and DNAse I, were purchased from Sigma (Dorset, UK).

Gluculase was obtained from NEN (Boston, USA), zymolyase from Seikagaku Corporation (Tokyo, Japan) and mutanase (Novozym 234) was a gift from Novo Nordisk (Copenhagen, Denmark).

2.1.4 Kits

Big Dye™ squencing kit	Applied Biosystems (Warrington, UK)
ECL™	Amersham Pharmacia (Uppsala, Sweden)
Qiaex™	Qiagen, (Hilden, Germany)
Qiagen™ Plasmid Midi Kit	Qiagen (Hilden, Germany)

2.1.5 Standards

2.1.5.1 DNA standards

The size of DNA-fragments on agarose gels was determined with the 1 kb DNA extension ladder from Gibco (Paisley, UK). This standard consists of fragments with a size of 40 kb, 20 kb, 15 kb, 10 kb, 8,144 bp, 5,090 bp, 4,072 bp, 3,054 bp, 2,036 bp, 1,636 bp, 1,018 bp and 506 bp.

2.1.5.2 Protein standards

For the determination of molecular weights of proteins on SDS polyacrylamide gels (PAGE), the SDS-PAGE broad range standard from BioRad (Hemel Hempstead, UK) was used. This standard consists of myosin (200,000 D), β-galactosidase (116,250 D), phosphorylase B (97,400 D), serum albumin (66,200 D), ovalbumin (45,000 D), carbonic anhydrase (31,000 D), trypsin inhibitor (21,500 D), lysozyme (14,400 D) and aprotinin (6,500 D).

2.1.6 Primer

A and B primers for the amplification of yeast genes were designed to anneal about 300 bp upstream of start and 300 bp downstream of stop. Two-hybrid primers were constructed to be 'in frame' and to include a start or a stop codon. Sequencing primers were constructed according to the specific application. For the cloning of inserts, restriction sites were constructed in the oligonucleotides.

S1- and S2-primers were used for the deletion of yeast genes. S2- and S3-primer pairs were suitable for C-terminal epitope tagging of yeast genes. S1-, S2- and S3-primers for the amplification of pYM modules (Knop *et al.*, 1999) were constructed as follows:

All S-primers contain firstly, chromosomal sequences for homologous recombination and secondly, nucleotide sequences for the amplification of the pYM modules. S1 (forward) primers contain 50 bases of the gene-specific sequence upstream from the start codon including the start codon plus 5'CGTACGCTGCAGGTCGAC3' for the amplification of the pYM modules. S2 (reverse) primers contain 50 bases of the gene-specific sequence downstream from stop including the stop codon plus 5'ATCGATGAATTCGAGCTCG3' sequence for the amplification of the pYM modules. S3 (forward) primers are identical to the 50 bases of the gene-specific sequence upstream of the stop codon not including the stop codon and contain the 5'CGTACGCTGCAGGTCGAC3' sequence for amplification of the module.

Table I: Primers

Name	Sequence	Description
BBP1-A	cgggatccGTCCTCAGTATCATTATTAACAATG	(*Bam*H I)
BBP1-A2	cgggatccGGAGCCGGGTAAAGCGCGCATG	(*Bam*H I)
BBP1-B	tccgctcgagACAGCTCGTGTTGAGTGATG	(*Xho* I)
BBP1-2H1	cgggatccgtATGAATCAGGAAGACAACACG	(*Bam*H I)
BBP1-2H2	cgggatccgtatgGATAGACAATTACTATGTCCGGG	(*Bam*H I/artificial start)
BBP1-2H3	tccgctcgagctaCAGGTCTCTACTGTTCAAGTC	(*Xho* I/artificial stop)
BBP1-M1	GACCCGTTTTTGTGTCGCTCG	
BBP1-M2	AGAGACAATTTCGCGTTGCACC	
BBP1-PCR5'	CTCTTGGAACAATAGCGGTC	
BBP1-PCR3'	CTTCGATCATGGCACCC	
BBP1-PCR3'2	GTCCGGTATGATTACTGACGGCAGGACTAC	

***Table I** continued*

BBP1-SEQ5`-3545	CTGGTCTGGATTCAACGCTCCATAGGAAG	
BBP1-SEQ3`-4316	CGGATAGTCTTTGCTTCAATGTTTG	
BBP1-S1	GTCAATCTTCGAAGGAGCATAGAGGCGAATGACTACTGAACAATGcgtacgctgcaggtcgac	
BBP1-S2	AGAGTCGTAACTGTTATTTCCATTGTGGAATGGAGTCCTGTCCTAatcgatgaattcgagctcg	
BBP1-S3	AGAAAAGATACTTCTGCTGGTTCGAATATTTTTTCAACAGGACAAcgtacgctgcaggtcgac	
BFR1-A	cgggatccCGTAAGCGTGGCTACTGCATTG	(*Bam*H I)
BFR1-B	tccgctcgagCAGGTGCAATGTCCCACGCCTTC	(*Xho* I)
BFR1-2H1	cgggatccgtATGTCCTCCCAACAACACAAG	(*Bam*H I)
BFR1-S1	TATCAACGTAATAGCATATTTTCTAACAACACAGCCATTGCCATGcgtacgctgcaggtcgac	
BFR1-S2	AATGAAGAAAGATCAGGAGAAAAATTTTTTTCTACTTCAGGTTTAatcgatgaattcgagctcg	
BFR1-S3	AAAAGATTGAAAGAACAGGAAGAGTCTGAAAAAGATAAAGAAAATcgtacgctgcaggtcgac	
MPS2-A	cgggatccCTTGTGTAAATGCCTTCACGGG	(*Bam*H I)
MPS2-B	tccgctcgagCAACGCTGCCACGCACATTATTTTG	(*Xho* I)
MPS2-2H1	cgggatccgtATGAGTAACGGTGCGTTTGATGC	(*Bam*H I)
MPS2-2H2	tccgctcgagTTAAATGCCGAATACTCTACTATATGCG	(*Xho* I)
MPS2-2H3	cgggatccgtatgGTATATGCTCATGACACACCATCC	(*Bam*H I/artificial start)
MPS2-2H4	tccgctcgagttaCCATATGTTGGAGGGAACCGCGGA	(*Xho* I/artificial stop)
MPS2-GFP	cgggatccATGAGTAACGGTGCGTTTGATGC	(*Bam*H I)
MPS2-M1	GTTCCTATGAGCTTCGATTGCC	
MPS2-M2	GGACACCTGCCAGTAAAGCGAAACAG	
MPS2-S1	GAAAGAAAGCTTTACAAACAATTCTGTCTTTGACAACGTAAGTATGcgtacgctgcaggtcgac	
MPS2-S2	TATTTTCACTGTGTATGAAGTGGCACGGTGCAAAGGCCAAGGTTTAatcgatgaattcgagctcg	
MPS2-S3	CAAATGCCAATGTGGATGACGCATATAGTAGAGTATTCGGCATTcgtacgctgcaggtcgac	
POM152-A	gcgggatccCTGGTATTATAGAAATAGAGTTTC	(*Bam*H I)
POM152-B	tccccgggCGGATAGGTCATTGAGCCAATTTC	(*Sma* I)
POM152-2H1	gcgggatccgtATGGAGCACAGATATAACGTG	(*Bam*H I)
POM152-S1	TAGATTTATCATACCAGATACGTTTATCAGGAGGCTTGTATAATGcgtacgctgcaggtcgac	
POM152-S2	TATTGCGGGAAAGAAAAATTTCATCAGACTTTCTTGTAATATTTAatcgatgaattcgagctcg	
POM152-S3	ACAGATGCTTATTGTTTTGCCAAAAATGATCTTTTTTTCAATAACcgtacgctgcaggtcgac	
SEC66-A	cgggatccCGATATCAGTAGTATAGG	(*Bam*H I)
SEC66-B	tccgctcgagGTGAGCAAGAAGAAGGGTAGAAAACAC	(*Xho* I)
SMY2-A	aaaactgcagGGTAGGTGATGACGTCCACAGCAA	(*Pst* I)
SMY2-B	tccccgggGAATTTGTCATTATCTGCGTT	(*Sma* I)
UMP1-A	cgggatccTTCAATCCATTCTGTGTTCCC	(*Bam*H I)
UMP2-B	tccgctcgagTGCGGACTATATAGGACACTA	(*Xho* I)

Capital letters indicate nucleotide sequences homologue to the chromosomal DNA sequence. Artificially created restriction sites are underlined.

2.1.7 Plasmids

Table II: Plasmids

Name	Description	Source or reference
p415-*ADH*	p415 containing *ADH* promotor	(Mumberg *et al.*, 1995)
p425-*GAL1*	p425 containing *GAL1* promotor	(Mumberg *et al.*, 1994)
pACT II	two-hybrid vector: pRS425 containing *GAL4-HA*	(Durfee *et al.*, 1993)
pAL1	pET28c containing $MPS2^{1-307}$	A. Camasses
pBG2A	pRS425 containing *DSK2*	B. Geier
pCS1	pGEX-5X-1 containing *BBP1*	this study
pCS7	pGEX-5X-1 containing $BBP1^{1-237}$	this study
pCS8	pGEX-5X-1 containing $BBP1^{202-385}$	this study
pCS9	p425-*GAL1* containing *BBP1*	this study
pCS14	pRS425 containing *BBP1*	this study
pCS15	pRS315 containing *BBP1*	this study
pCS16	pRS316 containing *BBP1*	this study
pCS17	pRS414 containing *BBP1*	this study
pCS51	pRS304 containing *bbp1-1*	this study
pCS52	pRS304 containing *bbp1-3*	this study
pCS53	pRS304 containing *bbp1-2*	this study
pCS55	pEG202 containing *BFR1*	this study
pCS58	pACTII containing *BFR1*	this study
pCS61	pACTII containing $MPS2^{1-307}$	this study
pCS71	pRS315 containing *MPS2*	this study
pCS72	pRS425 containing *MPS2*	this study
pCS78	pRS316 containing *MPS2*	this study
pCS84	p415-*ADH* containing *BFR1*	this study
pCS85	Yep13 clone 61 containing *UMP1*, *SEC66* and *SMY2*	this study
pCS86	pRS425 containing *SEC66*	this study
pCS88	pRS425 containing *UMP1*	this study
pCS91	pRS425 containing *SMY2*	this study
pEG202	two-hybrid vector: 2 μm, *HIS3*-vector with *LexA DNA-binding domain*	(Gyuris *et al.*, 1993)
pET28c	*E. coli* expression vector containing His_6 under control of the T7 promotor	Novagen, Madison, USA
pFL44	2 μm, *URA3*-based yeast-*E. coli* shuttle vector	C. Mann
pFL44-HSC1	pFL44 containing *HSC82*	C. Mann
pFL44-HSF1S	pFL44 containing *MPS2*	C. Mann
pGEX-5X-1	*E. coli* expression vector containing GST under control of the lacZ promotor	Pharmacia, Uppsala, Sweden
pGP1	p414-*GAL1* containing *SPC98*	G. Pereira
pLysS	*E. coli* expression vector containing gene coding for T7 lysozyme	(Studier, 1991)
pMM5	two-hybrid vector: pRS423 containing *GAL1-LexA-Myc*	M. Knop
pMM6	two-hybrid vector: pRS425 containing *GAL1-GAL4-HA*	M. Knop
pMK11	pRS425 containing *SPC97*	(Knop *et al.*, 1997)
pMK15	pACT II containing *SPC97*	(Knop *et al.*, 1997)
pMK16	pEG202 containing *SPC97*	(Knop *et al.*, 1997)
pMK26	pRS414containing *SPC97*	M. Knop

Table II *continued*

Name	Description	Source or reference
pMK51	p414-*GAL1* containing *SPC97*	M. Knop
pRS304	*TRP1*-based yeast integration vector	(Sikorski and Hieter, 1989)
pRS305	*LEU2*-based yeast integration vector	(Sikorski and Hieter, 1989)
pRS315	*CEN6, LEU2*-based yeast-*E. coli* shuttle vector	(Sikorski and Hieter, 1989)
pRS316	*CEN6, URA3*-based yeast-*E. coli* shuttle vector	(Sikorski and Hieter, 1989)
pRS414	*CEN6, TRP1*-based yeast-*E. coli* shuttle vector	(Sikorski and Hieter, 1989)
pRS423	2 μm, *HIS3*-based yeast-*E. coli* shuttle vector	(Christianson *et al.*, 1992)
pRS425	2 μm, *LEU2*-based yeast-*E. coli* shuttle vector	(Christianson *et al.*, 1992)
pRS426	2 μm, *URA3*-based yeast-*E. coli* shuttle vector	(Christianson *et al.*, 1992)
pSE3	pRS425 containing *SPC29*	(Elliott *et al.*, 1999)
pSE10	pRS425 containing *SPC34*	S. Elliott
pSE17	pRS425 containing *SPC42*	S. Elliott
pSE63	pMM5 containing *SPC29*	S. Elliott
pSE64	pMM6 containing *SPC29*	S. Elliott
pSE65	pMM5 containing *BBP1*	S. Elliott
pSE66	pMM6 containing *BBP1*	S. Elliott
pSE67	pMM5 containing $MPS2^{1\text{-}307}$	S. Elliott
pSE68	pMM6 containing $MPS2^{1\text{-}307}$	S. Elliott
pSE69	pMM5 containing *CDC31*	S. Elliott
pSE70	pMM6 containing *CDC31*	S. Elliott
pSE71	pMM5 containing *KAR1-ΔTM*	S. Elliott
pSE72	pMM6 containing *KAR1-ΔTM*	S. Elliott
pSE83	pMM5 containing *cdc31-16*	S. Elliott
pSE84	pMM6 containing *cdc31-16*	S. Elliott
pSG21	pEG202 containing *TUB4*	S. Geissler
pSG26	pACT II containing *SPC98*	S. Geissler
pSG46	pACT II containing *TUB4*	S. Geissler
pSG56	pEG202 containing *SPC98*	S. Geissler
pSM39	pRS315 containing *KAR1*	E. Schiebel
pSM234	pRS425 containing *CDC31*	E. Schiebel
pSM271	pRS425 containing *SPC98*	E. Schiebel
pSM292	pRS426 containing *CMD1*	E. Schiebel
pSM347	pRS426 containing *TUB4*	E. Schiebel
pSM375	pRS414 containing *SPC98*	E. Schiebel
pSM458	pRS426 containing *SPC72*	E. Schiebel
pSM535	pRS425 containing *SPC19*	E. Schiebel
pSM538	pRS425 containing *SPC25*	E. Schiebel
pSM541	pRS425 containing *SPC24*	E. Schiebel
pSM544	pRS425 containing *SPC105*	E. Schiebel
pSM553	pRS425 containing *TUB1*	E. Schiebel
pSM554	pRS425 containing *RBL2*	E. Schiebel
pSM568	pRS425 containing *CNM67*	E. Schiebel
pSM603	pRS425 containing *STU2*	E. Schiebel

Table II *continued*

Name	Description	Source or reference
pSM733	pRS305 containing *mps2-2*	E. Schiebel
pSM734	pRS305 containing *mps2-42*	E. Schiebel
pSM740	pRS315 containing *SPC42-GFP-kanMX6*	E. Schiebel
pSM743	pRS426 containing *MPS2*	E. Schiebel
pSM751	pRS426 containing *BBP1*	E. Schiebel
pSM782	pRS315 containing *SPC110-GFP-kanMX6*	E. Schiebel
pYM1	pFA6a-kanMX6 containing 3HA	(Knop *et al.*, 1999)
pYM4	pFA6a-kanMX6 containing 3Myc	(Knop *et al.*, 1999)
pYM5	pFA6a-His3MX6 containing 3Myc	(Knop *et al.*, 1999)
pYM6	pFA6a-*klTRP1*containing 9Myc	(Knop *et al.*, 1999)
pYM8	pFA6a-kanMX6 containing TEV-ProA-7HIS	(Knop *et al.*, 1999)
pYM12	pFA6a-kanMX6 containing yEGFP	(Knop *et al.*, 1999)
YEp13	2 μm, *LEU2*-based yeast-*E. coli* shuttle vector	(Broach *et al.*, 1979)

2.1.8 *E. coli* strains

Plasmids listed above were transformed (see 2.2.8.5.1) and amplified in either of the following strains:

DH5α — *deoR endA1 gyrA96 hsdR17*($r_k^- m_k^-$) *recA1 relA1 supE44 thi-1* Δ(*lacZYA-argFV169*) ϕ*80*δ*lacZ*Δ*M15* F^- λ^-; Clontech, Palo Alto, USA

SURE — $e14^-$($McrA^-$) Δ(*mcrCB-hsdSMR-mrr*)171 *endA1 supE44 thi*-1 *gyrA96 relA1 lac recB recJ sbcC umuC*::Tn5 (Kan^r) *uvrC* [F' *proAB lacI*^{q}ZΔ(*M15* Tn*10* (Tet^r)]; Stratagene, La Jolla, USA

BL21 (DE3) pLysS — *E. coli* B F^- *dcm ompT hsdS*($r_\beta^- m_\beta^-$) *gal* (DE3) [pLysS Cam^r)^a; Stratagene, La Jolla, USA

2.1.9 Yeast strains

Table III: Yeast strains

Name	Genotype-construction	Source or reference
ALY1	*MAT***a** *ura3-52 lys2-801 ade2-101 trp1*Δ63 *his3*Δ*200 leu2*Δ*1* Δ*mps2::HIS3MX4* pCS78	A. Camasses
CJY16	*MAT***a** *ura3-52 lys2-801 ade2-101 trp1*Δ63 *his3*Δ*200 leu2*Δ*1 SPC24-3HA*-kanMX6	C. Janke
CMY677	*ura3-52 lys2-801 ade2-101 trp1*Δ63 *leu2*Δ*1 cdc28-109*	C. Mann
CMY936	*ura3-52 lys2-801 ade2-101 trp1*Δ63 *leu2*Δ*1 hsf1-82*	C. Mann
ESM357	*MAT*α *ura3-52 his3*Δ*200 leu2*Δ*1*	E. Schiebel
ESM400	*MAT*α *ura3-52 trp1*Δ63 *leu2*Δ*1 mps1-1*	E. Schiebel
ESM401	*MAT*α *ura3-52 his3*Δ*200 mps2-1*	(Elliott *et al.*, 1999)
ESM527	*MAT***a** *ura3-52 lys2-801 ade2-101 trp1*Δ63 *his3*Δ*200 leu2*Δ*1 spc29-2*	(Elliott *et al.*, 1999)
ESM480	*MAT***a** *ura3-52 lys2-801 ade2-101 trp1*Δ63 *his3*Δ*200 leu2*Δ*1 SPC25-3HA*-kanMX6	E. Schiebel
ESM578	*MAT***a** *ura3-52 lys2-801 ade2-101 trp1*Δ63 *his3*Δ*200 leu2*Δ*1 spc29-3*	(Elliott *et al.*, 1999)
ESM780	*MAT***a** *ura3-52 lys2-801 ade2-101 trp1*Δ63 *his3*Δ*200 leu2*Δ*1* Δ*mps2::HIS3MX4* pCS78	E. Schiebel
ESM786	*MAT***a** *ura3-52 lys2-801 ade2-101 trp1*Δ63 *his3*Δ*200 leu2*Δ*1*::pSM733 *mps2::HIS3MX4*	E. Schiebel
ESM787	*MAT***a** *ura3-52 lys2-801 ade2-101 trp1*Δ63 *his3*Δ*200 leu2*Δ*1*::pSM734 *mps2::HIS3MX4*	E. Schiebel
ESM834	*MAT***a** *ura3-52 lys2-801 ade2-101 trp1*Δ63 *his3*Δ*200 leu2*Δ*1* Δ*sst1::URA3 NDC80-6HA-klTRP1*	E. Schiebel
SGY37	*MAT***a** *ura3-52::URA3-lexA-op-LacZ trp1 his3 leu2*	(Geissler *et al.*, 1996)
YAS8	*MAT***a** *ura3-52 lys2-801 ade2-101 trp1*Δ63 *his3*Δ*200 leu2*Δ*1* Δ*sst1::URA3*	(Spang *et al.*, 1995)
YCS1	*MAT***a**/α *ura3-52 lys2-801 ade2-101 trp1*Δ63 *his3*Δ*200 leu2*Δ*1 BBP1*/Δ*bbp1::HIS3MX4*	this study
YCS3	*MAT***a** *ura3-52 lys2-801 ade2-101 trp1*Δ63 *his3*Δ*200 leu2*Δ*1 BBP1-3HA-kanMX6*	this study
YCS4	*MAT***a** *ura3-52 lys2-801 ade2-101 trp1*Δ63 *his3*Δ*200 leu2*Δ*1 BBP1-ProA-kanMX6*	this study
YCS5	*MAT***a** *ura3-52 lys2-801 ade2-101 trp1*Δ63 *his3*Δ*200 leu2*Δ*1 BBP1-3Myc-kanMX6*	this study
YCS6	MATα *ura3-52 his3*Δ*200 leu2*Δ*1 BBP1-GFP-* kanMX6	this study
YCS17	*MAT***a** *ura3-52 lys2-801 ade2-101 trp1*Δ63 *his3*Δ*200 leu2*Δ*1* Δ*bbp1::HIS3MX4* pCS16	this study
YCS18	*MAT*α *ura3-52 his3*Δ*200 leu2*Δ*1* pCS9	this study
YCS47	*MAT***a** *ura3-52 lys2-801 ade2-101 trp1*Δ63 *his3*Δ*200 leu2*Δ*1 BBP1-9MYC-klTRP1*	this study
YCS50	*MAT***a** *ura3-52 lys2-801 ade2-101 trp1*Δ63 *his3*Δ*200 leu2*Δ*1 BFR1-9MYC-klTRP1*	this study
YCS53	*MAT***a** *ura3-52 lys2-801 ade2-101 trp1*Δ63 *his3*Δ*200 leu2*Δ*1 BFR1-3HA*-kanMX6	this study
YCS56	*MAT***a**/α *ura3-52 lys2-801 ade2-101 trp1*Δ63 *his3*Δ*200 leu2*Δ*1 BFR1*/Δbfr1*::HIS3MX4*	this study
YCS64	*MAT***a** *ura3-52 lys2-801 ade2-101 trp1*Δ63::pCS51 *his3*Δ*200 leu2*Δ*1* Δ*bbp1::HIS3MX4*	this study
YCS65	*MAT***a** *ura3-52 lys2-801 ade2-101 trp1*Δ63::pCS51 *his3*Δ*200 leu2*Δ*1* Δ*bbp1::HIS3MX4*	this study
YCS66	*MAT***a** *ura3-52 lys2-801 ade2-101 trp1*Δ63::pCS53 *his3*Δ*200 leu2*Δ*1* Δ*bbp1::HIS3MX4*	this study
YCS67	*MAT***a** *ura3-52 lys2-801 ade2-101 trp1*Δ63 *his3*Δ*200 leu2*Δ*1* Δ*bfr1::HIS3MX4*	this study
YCS70	*MAT***a** *ura3-52 lys2-801 ade2-101 trp1*Δ63::pCS51 *his3*Δ*200 leu2*Δ*1* Δ*bbp1::HIS3MX4* Δ*sst1::URA3*	this study
YCS72	*MAT***a** *ura3-52 lys2-801 ade2-101 trp1*Δ63::pCS53 *his3*Δ*200 leu2*Δ*1* Δ*bbp1::HIS3MX4* Δ*sst1::URA3*	this study
YCS75	*MAT***a**/α *ura3-52 lys2-801 ade2-101 trp1*Δ63 *his3*Δ*200 leu2*Δ*1 MPS2*/Δ*mps2::HIS3MX4*	this study
YCS78	MATα *ura3-52 his3*Δ*200 leu2*Δ*1 MPS2-GFP-kanMX6*	this study

***Table III** continued*

Name	Genotype-construction	Source or reference
YCS84	*MATa ura3-52 lys2-801 ade2-101 trp1*Δ63 *his3Δ200 leu2Δ1 BBP1-3Myc-kanMX6 MPS2-3HA-HIS3MX6*	this study
YCS88	*MATa ura3-52 lys2-801 ade2-101 trp1*Δ63 *his3Δ200 leu2Δ1 MPS2-3HA-kanMX6*	this study
YCS94	*MATa ura3-52 lys2-801 ade2-101 trp1*Δ63 *his3Δ200 leu2Δ1 Δmps2::HIS3MX4*	this study
YCS108	*MATa ura3-52 lys2-801 ade2-101 trp1*Δ63 *his3Δ200 leu2Δ1 POM152-6HA-klTRP1*	this study
YCS109	*MATa ura3-52 lys2-801 ade2-101 trp1*Δ63::pCS51 *his3Δ200 leu2Δ1 Δbbp1::HIS3MX4* pSM740	this study
YCS110	*MATa ura3-52 lys2-801 ade2-101 trp1*Δ63::pCS51 *his3Δ200 leu2Δ1 Δbbp1::HIS3MX4* pSM782	this study
YCS111	*MATa ura3-52 lys2-801 ade2-101 trp1*Δ63 *his3Δ200 leu2Δ1*::pSM734 *mps2::HIS3MX4 POM152::kanMX6*	this study
YCS112-1	*MATa ura3-52 lys2-801 ade2-101 trp1*Δ63::pCS51 *his3Δ200 leu2Δ1 Δbbp1::HIS3MX4 POM152::kanMX6*	this study
YCS112-2	*MATa ura3-52 lys2-801 ade2-101 trp1*Δ63::pCS53 *his3Δ200 leu2Δ1 Δbbp1::HIS3MX4 POM152::kanMX6*	this study
YCS113	*MATa ura3-52 lys2-801 ade2-101 trp1*Δ63 *his3Δ200 leu2Δ1 spc29-2 POM152::kanMX6*	this study
YPH499	*MATa ura3-52 lys2-801 ade2-101 trp1*Δ63 *his3Δ200 leu2Δ1*	Sikorski and Hieter (1989)
YPH501	*MATa*/α *ura3-52 lys2-801 ade2-101 trp1*Δ63 *his3Δ200 leu2Δ1*	Sikorski and Hieter (1989)
YPH500	*MATα ura3-52 lys2-801 ade2-101 trp1*Δ63 *his3Δ200 leu2Δ1*	Sikorski and Hieter (1989)
31CG37	*MATa lys2-801 ade2-101 trp1*Δ63 *his4 cdc37-1*	B. Wickner

2.1.10 Antibodies

Table IV: Antibodies

Antibody	dilution	source
goat anti-mouse CY2	1:200	Dianova, Hamburg, Germany
goat anti-mouse CY3	1:500	Dianova, Hamburg, Germany
goat anti-rabbit CY2	1:200	Dianova, Hamburg, Germany
goat anti-rabbit CY3	1:1000	Dianova, Hamburg, Germany
goat anti-mouse nanogold	1:100	Nanoprobe, New York, USA
goat anti-rabbit nanogold	1:100	Nanoprobe, New York, USA
goat anti-mouse peroxidase	1:4,000	Dianova, Hamburg, Germany
goat anti-rabbit 12 nm gold	1:40	Jackson Immuno Research, West Grove, USA
goat anti-rabbit peroxidase	1:5,000	Dianova, Hamburg, Germany

Table IV continued

Antibody	dilution	source
mouse anti-HA (12CA5)	1:20	E. Schiebel
mouse anti-his	1:200	Dianova, Hamburg, Germany
mouse anti-Myc (9E10)	1:20	E. Schiebel
mouse anti-Myc	1:500	Roche, Lewes, UK
mouse anti-tubulin (WA3)	1:20	E. Schiebel
rabbit anti-Bbp1p	1:200	this study
rabbit anti Cnm67p	1:800	E. Schiebel
rabbit anti-Kar1p	1:100	E. Schiebel
rabbit anti-Mps2p	1:200	this study
rabbit anti-Spc24p	1:200	E. Schiebel
rabbit anti-Spc42p	1:1000	E. Schiebel
rabbit anti-Spc72p	1:200	E. Schiebel
rabbit anti-Spc97p	1:200	E. Schiebel
rabbit anti-Spc98p	1:500	E. Schiebel
rabbit anti-Spc110p	1:500	E. Schiebel
rabbit anti-Tub4p	1:1000	E. Schiebel

2.1.11 Media

All media were autoclaved unless specified otherwise.

2.1.11.1 Media for yeast

YPD:
10 g yeast extract
20 g bacto peptone
20 g glucose
to final volume 1 l of H_2O

YPAD:
1 l YPD
100 mg adenine

YPD-plates:
1 l YPD
20 g agar

G418-plates:
200 ml autoclaved YPD/agar-medium at less than 50 °C
0.2 g G418 in 20 ml H_2O, sterile filtered

SC-medium:

6.7 g bacto-yeast nitrogen base without amino acids
20 g glucose
2 g drop out mix
to final volume 1 l of H_2O

drop out mix:
ammino acid mix:

adenine	5 g
alanine	20 g
arginine	20 g
asparagine	20 g
aspartate	20 g
cysteine	20 g
glutamine	20 g
glutamate	20 g
glycine	20 g
inositol	20 g
isoleucine	20 g
lysine	20 g
methionine	20 g
para-aminobenzoic acid	2 g
phenylalanine	20 g
proline	20 g
serine	20 g
threonine	20 g
tyrosine	20 g
valine	20 g

36.7 g of the ammino acid mix were mixed with the following ammino acids/bases for the specific drop out mix:

histidine	2 g
leucine	4 g
uracil	2 g
tryptophan	2 g

SC-plates:

6.7 g bacto-yeast nitrogen base without amino acids
20 g glucose
2 g drop out mix (see above)
to final volume 0.5 l of H_2O

20 g agar
to final volume 0.5 l of H_2O

Both solutions were autoclaved separately and after cooling down to 50 °C, they were mixed slowly.

SC-Raf-medium:
1.34 g bacto yeast nitrogen base without amino acids
0.4 g drop-out mix
4 g raffinose
to final volume 0.2 l of H_2O
sterile filtered

SC-Raf/Gal-medium:
1.34 g bacto yeast nitrogen base without amino acids
0.4 g drop-out mix
4 g raffinose
4 g galactose
to final volume 0.2 l of H_2O
sterile filtered

SC-Raf/Gal-plates:
1.34 g bacto yeast nitrogen base without amino acids
0.4 g drop-out mix
4 g raffinose
4 g galactose
to final volume 0.1 l of H_2O
sterile filtered

4 g bacto-agar in 100 ml H_2O, autoclaved

Both solutions were mixed after they had cooled down to 50 °C

5-FOA-plates:
1.34 g bacto yeast nitrogen base without amino acids
0.4 g drop out mix SC-Ura
4 g glucose
10 mg uracil
0.2 g 5-FOA
to final volume 0.1 l of H_2O
sterile filtered

4 g bacto-agar in 100 ml H_2O, autoclaved

Both solutions were mixed after they had cooled down to 50 °C.

Spo-plates:
2.5 g yeast extract
15 g KAc
0.4 g glucose
20 mg: His, Leu, Lys, Trp, Met, Arg
40 mg : Ade, Ura, Tyr
100 mg Phe
350 mg Thr

20 g agar
to final volume 1 l of H_2O

2.1.11.2 Media for bacteria

SOC-medium:
20 g bacto tryptone
5 g yeast extract
20 g glucose
2.5 mM KCl
10 mM NaCl
10 mM $MgCl_2$
10 mM $MgSO_4$
to final volume 1 l of H_2O

TY-medium:
10 g bacto-tryptone
5 g yeast extract
5 g NaCl
pH 7.5
to final volume 1 l of H_2O

TY-plates:
1 l TY-medium
20 g bacto-agar

TY with ampicillin:
Ampicillin (stock solution: 100 mg/ml in H_2O) diluted 1:1000 in TY-medium
For plates: TY-plate solution was autoclaved and cooled down, then ampicillin was added.

TY with chloramphenicol:
chloramphenicol (stock solution: 34 mg/ml in ethanol) diluted 1:1000 in TY-medium
For plates: TY-plate solution was autoclaved and cooled down, then chloramphenicol was added.

TY with kanamycin:
kanamycin (stock solution: 30 mg/ml in H_2O) diluted 1:1000 in TY-medium
For plates: TY-plate solution was autoclaved and cooled down, then kanamycin was added.

2.1.12 Filters and membranes

Chromatography paper 3 mm	Whatman, Maidstone, UK
Mobicol filter columns (1 ml, 90 µm pore size)	Bioscience, Cramlington, UK
Nalgene® bottle top filter (250 ml, 500 ml)	Nalge Nunc International, Rochester, USA
Protran® nitrocellulose transfer membrane	Schleicher & Schuell, Dassel, Germany
Supor® Acrodisc® 32 (0.45 µm)	Pall Corporation, Ann Arbor, USA

2.1.13 Photographic material

Super RX Fuji medical X-ray film	Fuji Photo Film Co., LTD, Tokyo, Japan

2.1.14 Equipment

ABI Prism™ 377 DNA sequencer	Perkin Elmer (Wellesley, USA)
AC211S balance	Sartorius (Goettingen, Germany)
Axiophot microscope	Zeiss (Jena, Germany)
Beat beater	Biospec Products (Bartlesville, USA)
Capacitance Extender	Biorad (Hemel Hempstead, UK)
Centrifuge 4K15	Sigma (Dorset, UK)
Centrifuge 5417C and 5417R	Eppendorf (Hamburg, Germany)
Chilled CCD camera C5985	Hamamatsu (Bridgewater, USA)
Chilled CCD camera controller	Hamamatsu (Bridgewater, USA)
Clean bench Lamin Air® HB 2448	Heraeus Instruments (Hanau, Germany)
Delta 350, Mettler pH-electrode	Mettler (Giessen, Germany)
Diamond knife	TAAB (Aldermasten, UK)
DU650 spectrophotometer	Beckman (Fullerton, USA)

Electron microscope Zeiss 902	Zeiss (Jena, Germany)
FACScan	Becton & Dickinson (Franklin Lakes, USA)
Gel blotter	Max Planck Institute technial support (Munich, Germany)
Gel electrophoresis chamber	Biometra (Goettingen, Germany)
Gene Pulser™	Biorad (Hemel Hempstead, UK)
Genie 2 plus computer	Viglen (Alperton, UK)
HT shaker	Infors AG (Bottingen, Switzerland)
Incubators B12, BK600, B6420 and Cytoperm	Heraeus Instruments (Hanau, Germany)
Laserjet 2100 M	Hewlett Packard (Boise, USA)
Mettler isoCall balance	Mettler (Giessen, Germany)
Mettler PE360 balance	Mettler (Giessen, Germany)
Microferm® fermentor	New Brunswick Scientific Co. Inc. (Edison, USA)
Microfuge™ II and J-6B centrifuge	Beckman (Fullerton, USA)
Microwave	Panasonic (Tokyo, Japan)
Milli Q® and Milli RO Watersystems	Millipore (Watford, UK)
Mini-Protean II™ gel electrophoresis chamber	BioRad (Hemel Hempstead, UK)
Mini-sub® cell GT gel electrophoresis chamber	BioRad (Hemel Hempstead, UK)
Multi Drive XL	Pharmacia (Uppsala, Sweden)
OCE 3107C printer	OCE (Venlo, Netherlands)
OCE 3165 printer	OCE (Venlo, Netherlands)
Omega™ autoclave	Prestige™ (Medical Blackburn, UK)
Orbital shaker	Forma Scientific (Marjetta, USA)
Personal cycler	Biometra (Goettingen, Germany)
Polytron PT 3100	Kinematica (Lucerne, Switzerland)
Power Mac G4	Apple Macintosh (USA)

Power Pack P25	Biometra (Goettingen, Germany)
Power supply EPS 3500	Pharmacia (Uppsala, Sweden)
Power supply modell 200/2.0	BioRad (Hemel Hempstead, UK)
Pulse Controller	Biorad (Hemel Hempstead, UK)
RCT basic stirrer	IKA Labortechnik (Staufen, Germany)
Reichert Ultracut S	Leica (Wetzlar, Germany)
Rollermixer SRT2	Stuart Scientific (Stone, UK)
Scanner Arcus II	Agfa (USA)
Sonopuls GM 200	Bandelin electronics (Berlin, Germany)
Sorvall® RC5B centrifuge	Kendro (Bishop's Stortford, UK)
The imager™	Appligene (Heidelberg, Germany)
Thermal printer 8670 PS	Kodak (USA)
Thermomixer 5436	Eppendorf (Hamburg, Germany)
Tip sonicator UW 200	Bandelin electronics (Berlin, Germany)
Ultra Cut S Microtone	Zeiss (Jena, Germany)
Ultrasound incubator Transsonic 420	Elma® (Singen, Germany)
UV transiluminator UVI-tec	UVP Inc. (San Gabriel, USA)
Vacuum concentrator	Bachhofer (Reutlingen, Germany)
Varifuge 2.3RS	Heraeus Instruments (Hanau, Germany)
Vortexer VF2	IKA-labortechnik (Staufen, Germany)
Vortex-Genie 2™	Scientific Laboratories (Bohemia, USA)
Wide mini-sub® cell gel electrophoresis chamber	BioRad (Hemel Hempstead, UK)
X-omat 480 RA processor	Kodak (USA)

2.1.15 Software

Amplify 1.2	Bill Engels (Madison, USA)
CellQuest	Becton & Dickinson (Franklin Lake, USA)
DNA strider™ 1.2	Christian Marck (Gif-Sur-Yvette Cedex, France)
Endnote 3.0	Niles Software Inc. (Berkley, USA)
Fotolook	Agfa (USA)
Freehand 7.0	Macromedia (USA)
Nestcape Communicator 4.7	Netscape Communicator Corporation (USA)
NIH Image1.62	National Institutes of Health (USA)
Photoshop 5.0	Adobe (USA)
Powerpoint® 97 SR-1	Microsoft® Corporation (Santa Rosa, USA)
Word 97 SR-1	Microsoft® Corporation (Santa Rosa, USA)

2.1.16 Internet services

The following internet services were used:

Entrez-PubMed:	http://www.ncbi.nlm.nih.gov:80/entrez/query.fcgi
ExPASy	http://www.expasy.ch/
MIPS	http://www.mips.biochem.mpg.de
SIT	http://www.genome.ad.jp/SIT/SIT.html
SGD	http://genome-www.stanford.edu/cgi-bin/SGD/
SOSUI	http://sosui.proteome.bio.tuat.ac.jp/sosuiframe0.html

2.2 Methods

2.2.1 Polymerase chain reaction (PCR)

DNA fragments were amplified by PCR. Plasmid and chromosomal DNA were used as template. The DNA polymerase activity was dependent on the $MgCl_2$ concentration. The annealing temperature was adjusted for each primer pair ([n(A,T) x 2 °C + n(C,G) x 3 °C] – 4 °C). The elongation time was calculated as 1 min per 1 kb. Samples were usually cycled 25 times (n=25).

2.2.1.1 Amplification of genes

The following PCR conditions were used as standard for the amplification of genes. In general, three different $MgCl_2$ concentrations were tested.

Table V: PCR pipette schemata for the amplification of genes

	in µl	1	2	3
Template (200 ng)	1	✓	✓	✓
Primer 3' (10 µM)	1	✓	✓	✓
Primer 5' (10 µM)	1	✓	✓	✓
10 x PCR buffer	10	✓	✓	✓
dNTPs (2 µM)	10	✓	✓	✓
$MgCl_2$ (25 mM)	variable	8	16	24
Vent polymerase	0.2	✓	✓	✓
Taq DNA polymerase	0.3	✓	✓	✓
H_2O	ad 100	68.5	60.5	52.5

The thermocycler was programmed as follows:

Denaturing	4 min	94 °C
Cycle:		
Denaturing	1 min	94 °C
Annealing	1 min	50 to 65 °C dependent on oligonucleotides
Elongation	1 min/kb	72 °C
n=25		
Elongation (fill in)	5 min	72 °C

2.2.1.2 Colony PCR

Colony PCR is a method to amplify DNA fragments from yeast directly without isolation of DNA prior to the PCR reaction. This technique was mainly used to check the integration of genes into the yeast chromosome by amplification of the marker gene. Therefore, 1 ml yeast culture (OD_{600}=0.8) was incubated with 50 µl zymolyase (1 mg/ml H_2O) at RT for 10 min. The spheroblasted cells were harvested by centrifugation (2,700 rcf, 1 min, RT) and the supernatant was discarded. The pellet was incubated at 92 °C for 5 min before it was used as a template for the PCR reaction. The oligo-nucleuotides for the amplification of chromosomal markers were designed to prime in the marker gene and upstream and downstream of the marker gene in the original chromosomal regions. The following substances were added to each template:

Table VI: PCR pipette schemata for colony PCR

	in µl
Primer 3' (10 µM)	0.25
Primer 5' (10 µM)	0.25
10 x PCR buffer	2.5
dNTPs (2 µM)	2.5
$MgCl_2$ (25 mM)	1.25
Taq DNA polymerase	0.5
H_2O	17.75

Standard conditions for the thermo cycler:

Denaturing	2 min	94 °C
Cycle:		
Denaturing	30 sec	94 °C
Annealing	30 sec	50 °C
Elongation	1 min 30 sec	72 °C
n=25		
Elongation (fill in)	5 min	72 °C

2.2.1.3 Mutagenic PCR

Mutagenic PCR, PCR under in-optimal conditions, was employed to produce faulty copies of wild type genes, which could be used to construct conditional lethal mutants in yeast. Firstly, the optimal conditions ($MgCl_2$ concentration, annealing temperature, elongation time) for the amplification of the DNA fragment were established as in 2.2.1. For the mutagenic PCR, the concentration of dATP was varied and/or $MnCl_2$ was added to compete for Mg^{2+}- binding of the DNA polymerase. These conditions lead to mistakes by the amplification of the DNA fragment causing mutations in the sequence. In addition, Goldstar (see 2.1.3), a DNA polymerase was used which is known to frequently make mistakes during the amplification. Several conditions were tested:

Table VII: PCR pipette schemata for mutagenic PCR

	in µl	+	1	2	3	4	5
Template (200 ng)	1	✓	✓	✓	✓	✓	✓
Primer 3' (10 µM)	1	✓	✓	✓	✓	✓	✓
Primer 5' (10 µM)	1	✓	✓	✓	✓	✓	✓
10 x PCR buffer	10	✓	✓	✓	✓	✓	✓
dCTPs (2 µM)	2	✓	✓	✓	✓	✓	✓
dGTPs (2 µM)	2	✓	✓	✓	✓	✓	✓
dTTPs (2 µM)	2	✓	✓	✓	✓	✓	✓
dATPs (2 µM)	variable	2	0.4	2	2	0.8	0.8
$MgCl_2$ (25 mM)	optimal	✓	✓	✓	✓	✓	✓
$MnCl_2$ (25 mM)	variable	-	-	4	6	4	6
goldstar	0.5	✓	✓	✓	✓	✓	✓
H_2O	ad 100	68.5	60.5	52.5	52.5	52.5	52.5

The PCR mix was cycled under optimal conditions established before (see 2.2.1).

2.2.1.4 Amplification of cassettes

Conditions for the amplification of cassettes for epitope tagging and deletion of genes were established as described in 2.2.1. Templates were chosen according to the application (see 2.2.16 and 2.2.17). The different plasmids (pYM1, pYM4, pYM5, pYM6, pYM8 and pYM12) are listed in Table II. S1/S2-primer pairs (see 2.1.6) were

used for the amplification of deletion cassettes and S2/S3-primer pairs (see 2.1.6) for epitope tagging. PCR reactions were cycled under the following standard conditions:

Denaturing	5 min	94 °C
Cycle:		
Denaturing	1 sec	94 °C
Annealing	1 sec	54 °C
Elongation	2 min 30 sec	72 °C
n=25		
Elongation (fill in)	5 min	72 °C

2.2.2 Precipitation of DNA

Plasmid DNA was precipitated with ethanol or isopropanol. For the ethanol precipitation, two volumes of ethanol (ice cold) and 1/10 volume of 3 M sodium acetate were added to one volume of DNA. The sample was incubated on ice for 10 min, before centrifugation in an Eppendorf centrifuge at 4 °C for 20 min.

For the isopropanol precipitation, 2 volumes of isopropanol and 1/10 volume of 3 M sodium acetate were added to one volume of DNA. The DNA was precipitated by centrifugation in an Eppendorf centrifuge at RT for 20 min.

The precipitate was washed in 70 % (v/v) ethanol, dried in the vacuum concentrator for 5 min and taken up in an appropriate volume of H_2O.

2.2.3 Restriction digest

The conditions (buffer, temperature) for restriction digests were chosen according to the manufacturer. Restriction of DNA with two restriction endonucleases (double digest) was done simultaneously if both enzymes had sufficient activity (more than 75 %) under the same conditions. Otherwise the digests were done in succession. After completion of the first digest the enzyme was inactivated (heat inactivation or phenol chloroform extraction) before the second enzyme was added. In addition, if the enzymes had different optimal buffers, the partially restricted DNA was precipitated

(ethanol or isopropanol precipitation) and taken up in the optimal buffer for the second restriction enzyme.

2.2.4 Gel electrophoresis

2.2.4.1 Separation of DNA

Nucleic acids were separated via the standard method of agarose gel electorphoresis which employs the migration of the negatively charged DNA in the electric field (Sambrook *et al.*, 1989). The concentration of the agarose gels and the time of the electrophoresis were adjusted according to the expected fragment size. TAE-buffer and a current of 90 V were used as standard conditions. The DNA probes were loaded onto the gels after addition of 1/6 volume of DNA loading buffer (see 2.1.2). The Gibco 1 kb ladder was used as size marker (see 2.1.5.1).

2.2.4.2 Separation of proteins (SDS-PAGE)

Proteins were separated under denaturing conditions by SDS-PAGE (Laemmli, 1970). BioRad Miniprotean gel systems were used for small acrylamide gels with concentrations of 8, 10, 12 and 18 % according to the expected size of the proteins. The Biometra gel system was useful for the separation of proteins on gradient gels due to the larger gel size. 4 % stacking gels were used for both systems.

Table VIII: Acrylamide gels for SDS-PAGE

type of gel	**8 %**	**10 %**	**12 %**	**18 %**	**4 % stacking gel** (for 2 Miniprotean gels)
acrylamide (30 %) in ml	2.7	3.35	4.0	6.0	0.65
1.5 M Tris-HCl (pH 8.8) in ml	2.5	2.5	2.5	2.5	-
0.5 M Tris-HCl (pH 6.8) in ml	-	-	-	-	1.25
H_2O in ml	4.7	4.0	3.4	1.35	3.1
10 % (w/v) SDS in µl	100	100	100	100	50
10 % (w/v) APS in µl	50	50	50	50	25
TEMED in µl	5	5	5	5	5

For the gradient gels, 8 % and 18 % solutions were prepared, whereby for the 18 % mixture 1 ml of H_2O was replaced with 1 ml 50 % (v/v) glycerol. Both solutions were mixed with help of a gradient mixer while the gel was poured.

Protein samples were taken up or mixed with HU-buffer and were incubated at 65 °C for 5 min. After 5 min centrifugation at 15,300 rcf, up to 20 µl (Miniprotean) or 30 µl (gradient gel) were loaded onto the gel.

The gradient gels were run at 25 mA and 200 V per gel for up to 6 h. The conditions for the Miniprotean gels were 25 mA and 180 V per gel, with the running time dependent on the percentage of the gel. Laemmli running buffer (see 2.1.2) was used for both applications.

2.2.5 Staining techniques

2.2.5.1 Staining of DNA

Agarose gels containing DNA which had been separated by electrophoresis were stained for 20 min in an ethidium bromide solution (20 ng in 20 ml H_2O). Afterwards, the gels were washed in H_2O for 20 min before the DNA was analysed with the UV transiluminator.

2.2.5.2 Staining of proteins

The choice of the staining method was dependent on the expected protein amount. Coomassie Blue staining was used as standard method. The more sensitive Fairbanks method (Fairbanks *et al.*, 1971) was suitable to stain protein bands containing as less as 100 ng of protein. If Fairbanks staining was unsuccessful, protein gels were destained and re-probed by silver staining.

2.2.5.2.1 Coomassie Blue staining

The acrylamide gel was incubated in staining solution consisting of 0.25 % (w/v) Serva blue G (Serva, Heidelberg, Germany), 7 % (v/v) acetic acid and 50 % (v/v) methanol for a minimum of 30 min. Afterwards, the gel was washed in destain solution

(7 % (v/v) acetic acid, 50 % (v/v) methanol) until the background was again transparent. The gel was finally washed in H_2O and was stored in H_2O at 4 °C, or was dried in the gel dryer.

2.2.5.2.2 Fairbanks staining

The Fairbanks method was mainly used to stain gradient gels. Firstly, the gel was incubated in destain solution (7 % (v/v) acetic acid, 50 % (v/v) methanol) before it was transferred to the staining solution (25 % (v/v) isopropanol, 10 % (v/v) acetic acid, 0.05 % (w/v) Serva blue G (Serva, Heidelberg, Germany)). After 45 min of staining the gel was slowly destained in 10 % (v/v) isopropanol, 10 % (v/v) acetic acid, 0.005 % (w/v) Serva blue G for 30 min and then in 10 % (v/v) acetic acid, 0.002 % (w/v) Serva blue G for 30 min. Finally, the gel was incubated in 10 % (v/v) acetic acid until the background was reduced completely. The gel was washed several times in H_2O before it was dried in the gel dryer or it was stored in H_2O at 4 °C.

2.2.5.2.3 Silver staining

This silver staining method was suggested by A. Shevchenko (EMBL, Heidelberg, Germany; *personal communication*) as suitable for staining of proteins which should be analysed by MALDI-MS (see 2.2.26). The chemicals used in this protocol do not covalently modify proteins and therefore, do not interfere with the identification of peptide weights by MALDI-MS.

The SDS-gel was rinsed two times for 2 min in H_2O. The gel was incubated for 1 h in H_2O on a shaker. The longer the washing time the more of the yellowish background could be removed. The gel was incubated in 0.02 % (w/v) sodium thiosulfate for 2 min. After two washes with H_2O the gel was submerged in chilled 0.1 % (w/v) silver nitrate for 30 min on a shaker in the cold room. The silver nitrate solution was discarded and the gel was rinsed twice for 30 sec in H_2O. The gel was developed in a solution consisting of 0.04 % (v/v) formaldehyde in 2 % (w/v) sodium carbonate. The developer solution was replaced if it turned yellow. The staining was stopped by discarding the developing solution and addition of 1 % (v/v) acetic acid. The gel was

washed several times in 1 % (v/v) acetic acid. The gels were stored in 1 % (v/v) acetic acid at 4 °C.

2.2.6 Extraction of DNA from agarose gels

Nucleic acids were isolated from agrose gel slices using the Qiaex™ gel extraction kit (Qiagen).

2.2.7 Culture of strains

2.2.7.1 Culture of E. coli strains

Liquid cultures of *E.coli* were inoculated by transferring cells from freezer stocks, plates or pre-cultures with sterile glass pipettes into the appropriate growth medium. TY-medium (see 2.1.11.2), a non-selective growth medium was used for growing DH5α and Sure cells. TY-Ampicillin-medium (see 2.1.11.2) was used for the selection of plasmids carrying the *bla* gene for ampicillin resistance (pRS-vectors, pGEX-5X-1, pEG202, pACTII). TY-chlorampenicole-medium (see 2.1.11.2) selected for plasmids with the chloramphenicol marker (pLysS) and TY-kanamcyin for the pET28c plasmid harbouring the *kan* gene. The culture volume was dependent on the application. In general, cultures were incubated overnight at 37 °C. In special cases, cultures were incubated shorter and at lower temperatures, for example to avoid degradation of proteins expressed in the pGEX or the pET vector systems.

If *E. coli* cells were grown on plates, the medium was selected accordingly (see above) and plates were incubated overnight at 37 °C. Strains from liquid culture were plated out using a sterile spatula. Cells from freezer stocks or plates were transferred using sterile glass pipettes or sterile tooth picks.

2.2.7.2 Culture of yeast strains

In contrast to *E. coli*, yeast can not be grown successfully in liquid culture if inoculated directly from freezer stocks. Therefore, yeast cells from freezer stocks were firstly incubated on plates. Newly made yeast strains that are yeast strains which have been

genetically manipulated were usually grown on plates first. For growth of yeast cells in liquid culture, a pre-culture was inoculated with cells from plates and incubated overnight. The main culture was inoculated with the pre-culture considering the growth rate of the strain and the culture volume. For example, a YPH499 culture which had been incubated at OD_{600}=0.003 would have a OD_{600}=0.8 after about 12 h. The optimum growth temperature of wild type strains is 30 °C. Temperature sensitive mutants were incubated at the permissive temperature before shift to the restrictive temperature. The growth medium was dependent on the application. Wild type strains were grown in YPD, YPAD or SC-complete medium (see 2.1.11.1). Plasmids were selected for by growth in SC-medium lacking the amino acid or base whose synthesis was encoded by the selective marker of the plasmid. If strains were manipulated by chromosomal integration of genes, the transformation was established by growth on selective medium before these strains were grown on non-selective medium.

If large culture volumes were needed, yeast strains were grown in fermenters. Up to 36 l of culture could be obtained.

2.2.8 Cloning

In this study, transgenic *E. coli* strains containing plasmid-DNA coding for yeast genes were produced. Yeast strains were altered to carry plasmids coding for additional copies of genes or mutated yeast genes. Chromosomal copies of yeast genes were manipulated by deletion, mutation and epitope tagging.

Genes were amplified by PCR and the primers were often designed to harbour restriction sites for endonucleases to simplify the cloning. Plasmids were first amplified in *E. coli* before transformation into yeast. The integration of DNA into the yeast chromosome is possible due to homologues recombination.

2.2.8.1 Preparation of vectors

Plasmid DNA was prepared by restriction digest. After the restriction digest, the enzymes were inactivated by heat (65 °C, 10 min) or phenol/chloroform extraction. The plasmid backbone was separated from the cut out fragment by agarose gel

electrophoresis (see 2.2.4.1). The plasmid was subsequently extracted from the gel (see 2.2.6). If only one enzyme was used for the linearisation of the vector or if the enzyme was a blunt-end cutter, the DNA ends had to be dephosphorylated to avoid re-ligation. Therefore, 3 µg of cut plasmid were taken up in 89 µl H_2O, 10 µl alkaline phophatase buffer and 1 µl alkaline phosphatase and incubated at 37 °C for 1 h. The alkaline phosphatase was inactivated by incubation at 65 °C for 1 h. The plasmid DNA was precipitated and taken up in 30 µl H_2O.

2.2.8.2 Preparation of inserts

Genes were amplified by PCR (see 2.2.1). They were either ligated into vectors using restriction sites in the PCR primers or in the gene itself. After the restriction digest (see 2.2.3), DNA fragments were separated by agarose gel electrophoresis (see 2.2.4.1) and the gene was isolated by gel extraction (see 2.2.6).

In addition, some fragment were ligated blunt end, if no suitable restricition sites were available. Therefore, sticky ends were filled in with Klenow polymerase. For this, the following reaction mix was prepared and the mixture was incubated for 3 h at 37 °C:

200 ng of DNA
5 mM NTPs each
1 u Klenow enzyme
2 µl Klenow buffer
made up to 20 µl H_2O

After the fill in reaction, the Klenow enzyme was heat inactivated (65 °C, 10 min) and the DNA was precipitated (see 2.2.2), washed and dried and then taken up in H_2O. The fragments could then be ligated into plasmids (see 2.2.8.3).

2.2.8.3 Ligation

For the ligation of DNA fragments into plasmids, 50 ng plasmid DNA, 1 µl ligation buffer 0.4 µl ATP (25 mM), 1 µl ligase and 200 ng fragment-DNA in an final volume of 10 µl were incubated overnight in the cryostate at 13 °C.

2.2.8.4 Competent cells

In this study, competent yeast and *E. coli* cells were used for transformation. *E. coli* cells were usually sensitised by the $CaCl_2$-method. For the transformation of *E.coli* (see 2.2.8.5.1) with yeast-mini DNA which is low in DNA concentration, electro-competent cells were prepared. Lithium chloride competent yeast cells were used for the transformation with plasmids and PCR fragments.

2.2.8.4.1 Competent *E.coli* cells

2.2.8.4.1.1 $CaCl_2$-competent cells

Firstly, a 10 ml TY pre-culture was inoculated with DH5α (see 2.2.7.1) cells. It was incubated overnight at 37 °C. Secondly, 0.5 ml of pre-culture were transferred into a flask with 100 ml TY- medium. This culture was incubated at 37 °C until OD_{600}=0.3 to 0.4 was reached (about 3 to 4 h). Afterwards the culture was incubated on ice for 10 min. The cells were harvested by centrifugation at 4 °C at 2,700 rcf for 5 min. The pellet was resuspended in 5 ml cold 50 mM $CaCl_2$ and the cells were again harvested by centrifugation. After the $CaCl_2$ washing step had been repeated once more, the cells were taken up in 0.5 ml $CaCl_2$. The cells were used immediately or glycerin was added to a final concentration of 20 % and the cells were frozen in liquid nitrogen and stored at – 80 °C.

2.2.8.4.1.2 Electro-competent cells

An *E.coli* culture was prepared as described in 2.2.8.4.1.1 and the culture was chilled on ice for 30 min. The cells were harvested by centrifugation at 4 °C at 1,090 rcf for 10 min. The pellet was taken up in ice cold water and the cells were harvested again by centrifugation. This washing step was repeated twice more. The pellet was taken up in

an equal volume of ice-cold 10 % (v/v) glycerol. Cells were used immediately for transformation (see 2.2.8.5.1) or were frozen in liquid nitrogen and stored at – 80 °C.

2.2.8.4.2 Competent yeast cells

Yeast medium (10 ml) was inoculated and this pre-culture was incubated overnight at the optimal temperature for the specific yeast strain. The following day, 200 ml of medium were inoculated with the pre-culture (OD_{600}=0.003) and the culture was harvested by centrifugation (4 °C, 1,090 rcf, 5 min) at OD_{600}=0.6 to 0.8. The cells were resuspended in one culture volume of H_2O and the cells were again harvested by centrifugation. The pellet was then taken up in ¼ culture volume of LiSorb and the cells were spun down by centrifugation. The supernatant was removed completely and the cells were resuspended in 300 µl LiSorb per 50 ml culture volume. Salmon sperm DNA that had been denatured at 95 °C for 5 min was cooled on ice and 5 µl DNA were added to 50 µl yeast cells. The cells were used immediately or were frozen for storage at – 80 °C.

LiSorb: 100 mM LiOAc
10 mM Tris-HCl (pH 8.0)
1 mM EDTA (pH 8.0)
1 M Sorbitol
sterilfiltered

2.2.8.5 Transformation

Competent *E. coli* and yeast cells prepared as described in 2.2.8.4. were used for transformation.

2.2.8.5.1 Transformation of bacteria cells

2.2.8.5.1.1 Transformation of $CaCl_2$-competent cells

50 µl of $CaCl_2$-competent *E. coli* cells were incubated with up to 5 µg of plasmid DNA on ice for up to 1.5 h. Cells were heat shocked at 42 °C for 60 sec, before they were taken up in 1 ml SOC-medium (see 2.1.11.2). They were incubated in a shaker at 37 °C

for one hour. Cells were harvested in an Eppendorf centrifuge (4 °C, 2,700 rcf, 5 min), taken up in 100 µl TY-medium (see 2.2.11.2) and plated out on selective plates.

2.2.8.5.1.2 Transformation of electro-competent cell

100 µl of electro-competent *E. coli* cells were incubated with up to 2 µg of plasmid DNA in a 100 µl electroporation cuvette on ice for up to 1 h. The cells were transformed using a BioRad electroporator at the following settings: 1.8 kV, 100 Ohms and 125 µFD. The cells were taken up in 1 ml SOC medium and treated as described in 2.2.8.5.1.1.

2.2.8.5.2 Transformation of yeast cells

Lithium competent yeast cells (50 µl, see 2.2.8.4.2) were mixed with 0.5 to 5 µl plasmid DNA (up to 5 µg) and 300 µl LiPEG (see below) by vortexing. The mixture was incubated at RT for 20 min. DMSO (35 µl) was added to the cells under vortexing. The cells were incubated at 42 °C (wild type: 15 min; conditional lethal mutants: 5 min) and afterwards were harvested by centrifugation (4 °C, 1,090 rcf, 5 min). Cells were taken up in 200 µl PBS and were transferred onto selective plates. Transformations using the marker gene for kanamycin resistance were taken up in 3 ml YPD-medium and were incubated at 30 °C for 3 h before transfer on selective plates.

LiPEG: 100 mM LiOAc
10 mM Tris-HCl (pH 8.0)
1 mM EDTA (pH 8.0)
40 % (w/v) Polyethylene glycol
sterilfiltered

2.2.9 Freezer stocks

2.2.9.1 Freezer stocks of E. coli strains

A liquid culture of *E. coli* cells (1 ml) was mixed with 0.5 ml 50 % (v/v) glycerol in a sterile cryo-tube by vortexing. The sample was stored immediately at – 80 °C.

2.2.9.2 Freezer stocks of yeast strains

About 10 mm^3 of fresh yeast cells from liquid cultures or plates were transferred into a sterile cryo-tube containing 1 ml 15 % (v/v) glycerol. The cells were dispersed by vortexing. To avoid the sedimentation of cells, the mixture was quickly frozen by placing the tubes on dry ice before storage in the – 80 °C freezer.

2.2.10 Isolation of DNA

2.2.10.1 Isolation of plasmid DNA from E. coli

Plasmid DNA was isolated from *E. coli* cells by alkaline lysis. For the isolation of Mini-DNA (up to 20 ng) cells of 1 ml culture were harvested by centrifugation (4 °C, 2,700 rcf, 5 min) in an Eppendorf centrifuge. The pellet was taken up in 300 µl Qiagen buffer 1 (see 2.1.2). After addition of 300 µl Qiagen buffer 2 (see 2.1.2), the solution was mixed gently and before Qiagen buffer 3 (see 2.1.2) was added and the solution was again mixed with care. The sample was spun in an Eppendorf centrifuge (4 °C, 20,800 rcf, 20 min) and the supernatant was transferred into a new Eppendorf tube. The plasmid DNA was precipitated by addition of 0.5 ml isopropanol and centrifugation (RT, 20,800 rcf, 20 min). After washing and drying, the DNA was taken up in 50 µl H_2O.

Larger amounts of plasmid DNA (up to 200 µg) were isolated from a 50 ml *E. coli* culture using the Qiagen MIDI kit (see 2.1.4).

2.2.10.2 Isolation of plasmid DNA from yeast (plasmid rescue)

DNA containing plasmid DNA was isolated from yeast. Since the yield is usually very low, the plasmids were then transformed into *E. coli* cells for amplification.

Cells of 1 ml yeast overnight culture or about 2 mm^3 of yeast cells from a fresh plate were washed in 1 ml of H_2O. The cells were pelleted by centrifugation (4 °C, 1,090 rcf, 5 min), taken up in 0.5 ml of S-buffer (see below) and incubated for spheroblasting at 37 °C for 30 min. After the cells were spheroblasted (cells were dark and round under

the light microscope), they were lysed in 0.1 ml lysis solution (see below) by incubation at 65 °C for 30 min. 3 M potassium acetate (166 µl) was added and the cells were chilled on ice for 10 min. The sample was spun in an Eppendorf centrifuge (4 °C, 20,800 rcf, 10 min) and the supernatant was transferred into a new tube before the DNA was precipitated by adding 0.8 ml of cold ethanol. After the pellet was washed with 70 % (v/v) ethanol, the DNA was dried and taken up in 40 µl of H_2O. About 2 µl of DNA were used for the transformation of 100 µl of *E. coli* cells (see 2.2.8.5.1.2).

S-buffer:
10 mM K_2HPO_4 pH 7.2
10 mM EDTA
50 mM β-mercaptoethanol
50 µg/ml zymolyase (25 T)

Lysis solution:
25 mM Tris-HCl pH 7.5
25 mM EDTA
2.5 % (v/v) SDS

2.2.10.3 Isolation of chromosomal DNA from yeast

Chromosomal DNA was isolated from yeast as template for the amplification of wild type genes. Furthermore, for the testing of chromosomal integration of epitope tags or deletion of genes by amplification of marker genes by PCR.

Cells of a 1.5 ml yeast culture (OD_{600}=1.0) were harvested by centrifugation (4 °C, 1,090 rcf, 5 min) and the cells were washed with 1 ml of H_2O. The cells were taken up in 200 µl Qiagen buffer 1 (see 2.1.2) containing 2 ml β-mercaptoethanol and 0.04 mg zymolyase (20,000 U/mg). The mixture was incubated at 37 °C for 1 to 2 h. The tubes were occasionally inverted to stop the sedimentation of cells. After this spheroblasting step, 200 µl Qiagen buffer 2 (see 2.1.2) were added and the solutions were mixed carefully. The cells were incubated at 65 °C for 20 min to complete the formation of spheroblasts. Qiagen buffer 3 (200 µl, see 2.1.2) was added and the cells were set on ice for 15 min to precipitate proteins. The solution was centrifuged (RT, 15,300 rcf, 3 min) and the supernatant was transferred into a new tube. The chromosomal DNA was precipitated by addition of 600 µl isopropanol and incubation at RT for 5 min. The sample was centrifuged at RT and 15,300 rcf for 30 sec and the supernatant was

removed. The DNA pellet was incubated in 1 ml of 70 % (v/v) ethanol for at least 10 min to allow the diffusion of salt ions into the washing solution. After centrifugation (RT, 15,300 rcf, 30 sec) the pellet was dried very shortly, the DNA was taken up in 35 µl of H_2O and was incubated at RT on a shaker for at least 15 min. The chromosomal DNA was stored at – 20 °C.

2.2.11 Measurement of DNA concentration

The concentration of plasmids and oligonucleotides was measured according to Sambrook (1989). The DNA was diluted 1:1000 with H_2O and the absorption was measured at 260 nm (A_{260}) using a Beckman spectrometer. The concentration of the DNA was calculated with the following formulas whereby S represents the size of the DNA in kilobases:

Single stranded DNA: C (pmol/µl) = A_{260}:(10 x S)

Double stranded DNA: C (pmol/µl) = A_{260}:(13.2 x S)

2.2.12 Measurement of protein concentrations

The concentration of proteins was measured by the TCA-method (Trichloroacetic acid). For example, protein concentrations were measured to load equal amounts of proteins on SDS-PAGE gels and to ensure that samples contained similar amounts of total yeast extract for immunoprecipitations. Proteins were concentrated in solution by the following protocol. 300 µl of protein solution were mixed with 300 µl 30 % (w/v) TCA. The suspension was measured in the photometer at 340 nm (A_{340}). If necessary the measurement was calibrated using BSA solutions of known concentrations.

2.2.13 Western blotting

Proteins that had been separated by SDS-PAGE (see 2.2.4.2) were transferred onto nitrocellulose membranes (see 2.1.12) by electro blotting. Therefore, the acrylamide gel was soaked in blotting buffer (see 2.1.2) for at least 5 min. One sheet of nitrocellulose, slightly larger in size than the protein gel and 6 sheets of 3 mm

Whatman paper (see 2.1.12) which were larger than the nitrocellulose sheet were soaked in blotting buffer for 3 min. A sandwich consisting of 3 Whatman sheets, one nitrocellulose sheet, the protein gel topped with 3 Whatman papers was formed in a blotting apparatus. The standard blotting conditions were a maximum of 0.2 mA per gel for 1.5 h. Proteins on nitrocellulose sheets were stained with Ponceou S solution (1 % (v/v) acetic acid, 0.5 % (w/v) Ponceau S) for 2 min before the background was reduced by washing with H_2O.

In general, blots were blocked in TBS (see 2.1.2) containing 1 % (w/v) milk powder (Premier Brand, Moreton, UK) overnight at 4 °C. The blots were washed twice with TBS before they were incubated at RT for up to 1.5 h with the primary antibody (see 2.1.10) in TBS or TBS containing 0.1 % (w/v) milk. The antibody solution was discarded and the blots were washed up to 5 times with TBS or TBS containing 0.1 % (v/v) Tween 20. After incubation at RT with the secondary antibody (see 2.1.10) coupled to horse radish peroxidase (HRP) for up to 1 h in TBS or TBS containing 0.1 % (w/v) milk, the blots were washed 3 times with TBS containing 0.1 % (v/v) Tween 20 and twice with TBS or 5 times with TBS. The blots were probed with the ECL kit (see 2.1.4) and fluorescence emission was recorded on X-ray films (see 2.1.13).

2.2.14 Automated sequencing

Plasmid DNA was sequenced by automated cycle sequencing using an ABI sequencer. This method is based on the principle method developed by Sanger et al. (1977). For this study, fluorescent labelled bases were used (Big dye labelling mix, ABI) to terminate the elongation reaction. The primer was chosen according to the application. Double strand DNA (200 to 500 ng) and about 25 ng of primer DNA were mixed with 6 µl ABI Big-dye and the reaction mix was cycled in a thermal cycler with the following programme:

Denaturing	5 min	95 °C
Cycle:		
Denaturing	30 sec	95 °C
Annealing	10 sec	55 °C
Elongation	4 min	60 °C

n=25

The DNA was then precipitated by ethanol precipitation (see 2.2.2), washed and dried. Preparation of sequencing gels, loading of gels and the analysis of the data were provided by the in-house sequencing service.

2.2.15 FACS analysis

The flow analysis cytometry system (or originally called the method of 'Fluorescence Activated Cell Sorting', FACS (Bonner *et al.*, 1972)) was used to measure the DNA content of yeast cells. The DNA content is a good indicator for the cell cycle stage of yeast cells.

Cells of a 5 ml yeast culture (OD_{600}=0.4 to 1.0) were sonicated for 1 min in the ultra sound bath before they were harvested by centrifugation (4 °C, 510 rcf, 10 min) in an Eppendorf centrifuge. The pellet was resuspended in 2 ml 70 % (v/v) ethanol and the cells were incubated for at least 2 h on a roller. The cells were again spun, the supernatant was discarded and the cells were taken up in 0.5 ml 50 mM Tris-HCl (pH 7.8). The cells were pelleted by centrifugation and were resuspended in 0.5 ml 50 mM Tris-HCl (pH 7.8). This washing step was repeated once more and the pellet was taken up in 0.8 ml 50 mM Tris-HCl (pH 7.8). 200 µl of RNAse A (5 mg/ml 50 mM Tris-HCl (pH 7.8)) were added and the cells were incubated on a roller at RT overnight. The next day 100 µl RNAse A (5 mg/ml 50 mM Tris-HCl (pH 7.8)) were added and the cells were incubated at 37 °C for 1 h. The cells were spun, taken up in 0.5 ml of pepsin (5 mg/ml 55 mM HCl) and were incubated at 37 °C for 30 min. After centrifugation, the cells were washed with 1 ml buffer w (200 mM Tris-HCl (pH 7.5) containing 211 mM NaCl and 78 mM $MgCl_2$) and were pelleted again. The cells were

then resuspended in 0.5 ml of buffer w and 55 µl of 500 µg/ml propidium iodide in water were added. The cells were incubated for at least 15 min. Afterwards 50 µl cell suspension were transferred into a FACS tube (Falcon 2052) containing 2 ml 50 mM Tris-HCl (pH 7.8). The cells were again sonicated in the ultra sound bath for 2 min before reading on the FACS. A minimum of 50,000 events was measured at 'Low Flow' rate. Forward and side scatters were analysed with the CellQuest software (see 2.1.16).

2.2.16 Epitope tagging of yeast strains

Epitope tagging of yeast genes was done using PCR based techniques (Knop *et al.*, 1999; Longtine *et al.*, 1998; Schneider *et al.*, 1995; Wach *et al.*, 1997) and homologues recombination in yeast. Modules, containing the genes coding for epitope tags and selection markers were used as PCR templates. In this study, cassettes for 3'-tagging with GFP-, Myc-, HA- and Protein A were used (Knop *et al.*, 1999) (see 2.1.7). Selection markers were KanMX6, His3MX6 (Wach *et al.*, 1994, 1997) and the *TRP1* gene from *Kluyveromyces lactis* (*klTRP1*). The primers (S2 and S3 primers, see 2.1.6) were designed to amplify cassettes and to contain homologues regions for the integration into the chromosome. Amplification of cassettes by PCR was done as described in 2.2.1.4. PCR products were precipitated by ethanol precipitation (see 2.2.2), were washed and taken up in water. Haploid wild type strains like YPH499 and ESM357 (see 2.1.9) were transformed (see 2.2.8.5.2) with the PCR product and the integration of cassettes into the chromosome was controlled on selection plates. Integration was additionally tested by colony-PCR (see 2.2.1.2) and Western blotting with antibodies directed against the tags (see 2.2.13).

2.2.17 Construction of yeast deletion strains and shuffle strains by microscopic dissection (spore analysis)

One copy of a specific gene was deleted in the diploid YPH501 strain by replacing the ORF with a marker gene. The primers (S1 and S2 primer, see 2.1.6) were designed to amplify the marker gene. In addition, they contained flanking regions homologous to sequences upstream and downstream of the coding region. The markers were amplified

by PCR (see 2.2.1.4) using the pFA6-kanMX4 or pFA6-HIS3MX6 modules (Wach *et al.*, 1994) (see 2.1.7). The PCR products were precipitated by ethanol precipitation (see 2.2.2), were washed and taken up in water. They were transformed (see 2.2.8.5.2) into diploid YPH501 (see 2.1.9) cells and the integration of cassettes into the chromosome was controlled on selective plates (SC-His or kanamycin plates). Integration was additionally tested by colony-PCR (see 2.2.1.2).

The constructed strain was then further investigated by spore analysis. Firstly, the strain was forced to sporulate due to sub-optimal growth conditions. Therefore, cells were plated out on SPO-plates (see 2.1.11.1) which only provided ¼ of the optimal amino acid content required for normal growth. Cells were incubated for up to 4 d at 23 °C. Formation of tetrads containing four spores was controlled under the phase contrast microscope. Tetrads (2 mm^3) were scraped of the SPO-plate and were taken up in 200 µl of H_2O. 3 µl of zymolyase 20T (stock solution: 27 mg/ml H_2O) were added and the cells were incubated at RT for up to 10 min. The terades were separated into 4 single spores with the dissecting microscope. Firstly, the spores were incubated on YPD-plates. If all four spores were able to grow and two out of four spores were able to grow after replica plating (see 2.2.19) on selective plates, the deleted gene was non-essential. If only two out of four spores grew on non-selective plates and these two spores did not grow on selective plates, the deleted gene was essential for growth.

Shuffle strains are strains which lack the chromosomal copy of a gene, but carry a wild type copy of this gene on a *CEN*-based *URA3*-plasmid. These strains were constructed as follows. A diploid strain with one copy of a specific gene replaced with a marker (*HIS3*, *KAN*) was transformed (see 2.2.8.5.2) with a pRS316 plasmid carrying a wild type copy of the specific gene with its own promoter. The strain then underwent spore analysis. Colonies which evolved from a single spore and carried the deletion marker (*HIS3* or *KAN*) as well as the *URA3* marker were selected.

2.2.18 Construction of conditional lethal yeast strains

Conditional lethal mutants are yeast strains which carry mutations in a specific gene or a specific region of a gene. The strains were selected that the mutation only leads to a

growth defect if the strain is incubated above the permissive temperature. In this study, temperature sensitive mutants in *BBP1* and *MPS2* were constructed using PCR techniques and homologous recombination. Defects leading to the growth inhibition were analysed and potential functions of the gene product were proposed.

For the construction of a conditional lethal yeast strain, the selected gene was mutagenised by PCR (see 2.2.1.3). A CEN plasmid containing the wild type copy of the gene was constructed (see 2.2.8) and two restriction sites were selected to cut out a region of the gene which should be mutated. The mixture of mutated PCR fragments obtained in the different mutagenic PCR reactions and the plasmid containing flanking regions of the wild type gene were transformed (see 2.2.8.5.2) into the shuffle strain (see 2.2.17). If homologues recombination took place, the PCR fragment had been ligated into the cut vector and the yeast strain obtained the ability to grow on plates selective for the plasmid marker gene. Transformants were incubated at 23 °C (permissive temperature) on plates selective for the markers of the shuffle strain and the multi-copy plasmid. At least 50,000 colonies were investigated. The cells were replica plated (see 2.2.19) on 5-FOA plates to select against the *URA3*-plasmid of the shuffle strain carrying the wild type gene (see 2.2.20). The remaining colonies were replica plated on plates selecting for the marker gene of the multi-copy plasmid and were tested for growth at 30 °C, 33 °C, 35 °C and 37 °C. Colonies which were unable to grow at these temperatures were selected and the plasmids were isolated by yeast DNA isolation (see 2.2.10.2). The plasmids were then transformed into *E. coli* cells (see 2.2.8.5.1.2), were amplified and then isolated using the Qiagen Midi kit (see 2.2.6). The plasmids were re-transformed into the yeast shuffle strain. Transformants were replica plated on 5-FOA-plates and were tested for growth above 23 °C. Inserts of plasmids which were still able to cause a synthetic lethal phenotype were cloned into yeast integration vectors and the genes were integrated into the chromosome. Conditional lethal mutants were analysed throughout the cell cycle using FACS analysis (see 2.2.15), immunofluorescence (see 2.2.33.2) and morphological electron microscopy (see 2.2.34.1).

2.2.19 Replica plating

Replica plating is a technique to transfer yeast colonies from one plate to another thereby the original pattern of colonies is maintained. Yeast cells were grown on plates and the yeast colonies were transferred onto a sterile velvet cloth, which was held in place on a solid plastic cylinder. The pattern was then transferred onto other plates by carefully pressing the new plate onto the velvet. The plates were incubated for 1 day at the appropriate temperature.

2.2.20 5-FOA selection

Plasmids containing the *URA3* marker gene could be counter selected for by incubation of strains on 5-FOA (5-fluoro-orotic acid) plates. Strains which contain a *URA3* gene can convert 5-FOA to 5-fluoro-uridine monophosphate (5-FUMP) which will be converted into fluorodeoxyuridine which is a potent inhibitor of thymidylate synthetase and therefore toxic to cells. Taken together, cells which keep the *URA3* plasmid, die due to accumulation of the toxic metabolite and cells which loose the *URA3* plasmid are able to grow unaffectedly on 5-FOA plates (see 2.1.11.1). Cells were incubated on 5-FOA plates for up to 3 d. Cells which grew on 5-FOA-plates but not on plates lacking uracil were selected.

2.2.21 α-factor arrest

Yeast cells can be arrested in the cell cycle with the help of the mating pheromone α-factor. α-factor is produced by haploid α-type cells to signal haploid **a**-type cells their wish to mate. Once in contact with α-factor, haploid **a**-type cells will form a mating projectile (shmoo) and arrest in G_1.

Yeast strains (mat **a**) were grown in liquid culture until OD_{600}=0.3 to 0.4. α-factor (stock solution: 1 mg α-factor/ml DMSO) was added in a dilution of 1:100 (wild type cells) or 1:1000 (bar $^-$ yeast strains) and the cultures were incubated for up to 2.5 h in a shaker (wild type: 37 °C, conditional lethal strains: 23 °C). A culture was regarded as arrested in G_1 if more than 90 % of cells had developed a shmoo. The shmoo was

visible under the light microscope. Cells were released from α-factor by washing the cells three times with YPD-medium.

2.2.22 Preparation of total cell extract

2.2.22.1 Lysis of E. coli cells by sonication

E. coli cells were lysed by sonication. For example, cells from a 400 ml culture (OD_{600}=0.4) were harvested by centrifugation (4 °C, 2,700 rcf, 5 min) and the pellet was taken up in 20 ml PBS and transferred into a 50 ml Falcon tube. 5 mM benzamidin, 1 mM EDTA and 1 mM PMSF were added and the Falcon tube was placed on ice for sonication. The cells were lysed up to 8 times for 2 min with an output of the tip sonicator of 40 %. When over 90 % of cells appeared dark and broken under the light microscope, 1 % (v/v) Triton-X-100 was added and the cells were incubated on ice for 30 min to complete the lysis. The lysed cells were centrifuged (4 °C, 10,600 rcf, 5 min) and the supernatant contained the soluble fraction of proteins while proteins insoluble under these conditions, remained in the pellet. The supernatant obtained with this method was for example used for the purification of GST-fusion proteins from *E. coli* (see 2.2.25.1).

2.2.22.2 Lysis of yeast cells using TCA

This rather quick way of producing total cell extract from yeast was mainly used to check the expression of yeast gene fusions (see 2.2.16) by Western analysis (see 2.2.13).

A yeast culture of 1.5 ml (OD_{600}=0.8) was harvested by centrifugation (4 °C, 1,090 rcf, 5 min) in an Eppendorf centrifuge. The pellet was taken up in 1 ml of H_2O. The cells were again centrifuged and taken up in 1 ml of H_2O containing 150 µl 1.85 M NaOH and 7.5 % (v/v) of β-mercaptoethanol. The solution was mixed by vortexing and 150 µl of 55 % (w/v) TCA were added and the cells were incubated on ice for 10 min. The lysed cells were centrifuged (4 °C, 20,800 rcf, 10 min) and the supernatant was removed. The precipitated proteins were taken up in HU-buffer and the sample was incubated at 65 °C for 15 min to dissolve the denatured proteins. The sample was

centrifuged (RT, 20,800 rcf, 5 min) to pellet insoluble fragments. It was loaded on an acrylamide gel and proteins were separated by SDS-PAGE (see 2.2.4.2).

2.2.22.3 Lysis of yeast cells with glass beads

Lysis of yeast cells using glass beads was used for producing cell extract suitable for affinity purification of protein complexes (see 2.2.25). Firstly, the extraction conditions had to be established for each protein:

A yeast culture (200 ml) was grown to OD_{600}=0.8 and the cells were harvested by centrifugation (4 °C, 1,090 rcf, 5 min). The pellet about 1 g of cells was taken up in 3 ml of basis-buffer (50 mM Tris-HCl pH 7.5, 10 mM EDTA, 1 mM EGTA, 5 % (v/v) glycerol) containing 100 mM NaCl and proteinase inhibitors (complete MINI, Roche, Lewes, UK). Ice cold acid washed glass beads (∅ 425-600 µm, Sigma, Dorset, UK) were added up to 3 mm below the surface of the solution. The cells were lysed by vortexing up to 24 times for 30 sec. The samples were cooled on ice in between vortexing. The supernatant was taken of with a pipette and was divided into six Eppendorf tubes and the samples were centrifuged (4 °C, 20,000 g, 10 min). A sample of the supernatant was kept at – 20 °C and the rest was discarded. One pellet each was resuspended in the following buffers:

1. basis-buffer (see text above), 100 mM NaCl

2. basis-buffer (see text above), 100 mM NaCl, 1 % (v/v) Triton-X-100

3. basis-buffer (see text above), 1 M NaCl, 1 % (v/v) Triton-X-100

4. basis-buffer (see text above), 1 M NaCl, 1 % (w/v) SDS

5. RIPA (20 mM Tris-HCl pH 7.4, 150 mM NaCl, 1 % (v/v) Triton-X-100, 0,5 % (w/v) desoxycholate, 1 % (w/v) SDS)

6. RIPA (see above), 1 M NaCl

A small stirring bar was added and the samples were stirred on ice for 30 min. The samples were centrifuged (4 °C, 20,000 g, 10 min) and each supernatant was mixed with an equal volume of HU-buffer (see 2.1.2). Each pellet was resuspended in 400 µl HU-buffer and all samples were incubated at 65 °C for 10 min. The samples were centrifuged (4 °C, 20,000 g, 10 min) and analysed by SDS-PAGE (see 2.2.4.2) and Western blotting (see 2.2.13). The best extraction conditions for Bbp1p and Mps2p were established as basis-buffer, 100 mM NaCl, 1 % (v/v) Triton-X-100. The total yeast extract was then prepared as follows:

Yeast cultures with a volume of 200 ml to 12 l were grown to OD_{600}=0.6 to 1.2 and were harvested by centrifugation (4 °C, 1,090 rcf, 10 min). The pellet was resuspended in the optimal extraction buffer (2 ml buffer/g cells; see above) excluding the detergent and proteinase inhibitors (complete MINI, Roche, Lewes, UK). The cells were lysed by vortexing with glass beads as described above. Pellets up to 4 g were lysed in Falcon tubes while larger amounts were lysed in the bead beater (see 2.1.14). The detergent was added to the cell/buffer/glass bead solution and the sample was stirred on ice for up to 40 min. The liquid was transferred into a new centrifuge tube and the samples was centrifuged (4 °C, 20,000 g, 10 min). The supernatant was used for the affinity purification of proteins (see 2.2.25).

2.2.23 Preparation of polyclonal antibodies

In this study, antibodies against Bbp1p and Mps2p were raised in rabbits. In both cases GST-fusion proteins were expressed in *E. coli* and the proteins were purified using glutathion sepharose (see 2.2.25.1) before they were used for the immunisation. Antibodies were raised against the N-terminus of the proteins only.

2.2.23.1 Immunisation

Before the first immunisation 2 ml of blood were taken as pre-immunserum sample. The blood was incubated at 37 °C for 1 h and was then kept over night at 4 °C. The blood sample was centrifuged at RT and 2,000 rcf in a 15 ml Falcon tube in a Beckman centrifuge. The supernatant was kept at – 20 °C.

For the first injection, 500 µl of purified protein (1 mg protein/ml, see 2.2.25.1) were mixed with 1 ml complete Freund's Adjuvant (Sigma, Dorset, UK) with the ultrasonicator. The second immunisation was timed about 4 weeks after the first injection. For this injection and the two following injections, always four weeks apart, 500 µl of purified protein were mixed with 1 ml incomplete Freund's Adjuvant (Sigma, Dorset, UK) with the ultrasound mixer shortly before the application.

2.2.23.2 Test bleed

After the second immunisation, 2 ml of blood sample were taken. The blood was incubated at 37 °C for 1 h and was then kept over night at 4 °C. The sample was centrifuged at RT and 2,000 rcf in a 15 ml Falcon tube in a Beckman centrifuge. The supernatant contained the antibodies and the pellet was discarded. A protein blot was prepared, which contained six lanes with the epitope tagged version of the protein and six lanes loaded with cell extract from yeast cells over-expressing the specific protein. The blot was arranged in a special apparatus (Max Planck Institute technical support, Munich, Germany), in which the serum could be applied in narrow chambers in different dilutions. The blots were treated as for normal Western blotting (see 2.2.13). The serum was applied in 5 different dilutions (1:10, 1:50, 1:100, 1:500, 1:1000). Two lanes were tested with pre-immunserum which served as negative control. According to the quality of the signal, the number of further immunisations was decided.

2.2.23.3 Affinity purification of antibodies

Firstly, one pre-column containing CNBr-sepharose (Pharmacia, Uppsala, Sweden) coupled to GST and a main column containing CNBr-sepharose coupled to the antigen (GST-Bbp1p, GST-Mps2p) were prepared. Therefore, the antigen-GST fusion proteins were purified as described under 2.2.25. The purified proteins were filled into a dialyse tube. For the pre-column, BL21 pLysS cells containing pGEX-5X were induced with IPTG (compare 2.2.25) and the cells were harvested by centrifugation. The pellet was resuspended in 10 to 20 ml CB-buffer (100 mM $NaHCO_3$, 0.5 M NaCl, pH 8.3) and were lysed with the tip sonicator as described in 2.2.22.1. The lysed cells were centrifuged (4 °C, 20,000 g, 10 min) and the supernatant was filled in a dialyse tube.

The two protein solutions were dialysed against CB-buffer (see above) at 4 °C overnight. Meanwhile, the CNBr-resin was prepared. CNBr-spharose (2 g) was swelled in 400 ml 1 mM HCl for 15 min. The resin was washed on a glass filter with 400 ml of 1 mM HCl with a spatula. The resin was transferred into a Falcon tube and the HCl was aspirated off. The sepharose was washed in 10 volumes CB-buffer (4 °C, 510 rcf, 2 min). The dialysed protein samples were mixed with two volumes of CNBr-sepharose each. They were incubated at RT for 2 h to allow the binding of the proteins to the sepharose. The matrix was pelleted by centrifugation (4 °C, 510 rcf, 2 min) and the supernatant was removed. The beads were either resuspended in 0.2 M glycine pH 8.0 or in 1.0 M ethanolamine pH 9.0 followed by an incubation at RT for 2 h. The beads were washed once in 100 mM NaOAc pH 4.0, 0.5 M NaCl (4 °C, 510 rcf, 2 min) before they were packed into disposable polystyrene columns (Pierce, Rockford, USA). Each column was washed three more times with 100 mM NaOAc pH 4.0, 0.5 M NaCl, subsequently with 2 volumes PBS. PBS 1 % (w/v) SDS was added to the columns and when the buffer had penetrated the matrix, the columns were sealed and incubated at 65 °C for 40 min. The columns were again washed with 2 volumes PBS 1 % (w/v) SDS at RT. Afterwards, the columns were washed with 4 volumes of PBS 1 % (v/v) Triton-X-100. The pre-column was placed above the main column and the serum was applied (flow rate: 5 ml/1 h). When all the serum had penetrated, 2 volumes PBS were added to the pre-column. The pre-column was removed and the main column was washed with 3 volumes PBS 1 % (v/v) Triton-X-100 and 4 volumes PBS. Before the elution of the antibody, the main column was cooled down to 4 °C. For the elution, 1 ml cold glycine-buffer (0.2 M glycine, 1 mM EGTA, pH 2.5) was added to the column. The flow through was collected in an Eppendorf tube containing 300 µl 1 M Tris-HCl pH 8.0 which neutralised the solution. The eluate and the Tris-buffer were mixed immediately and the mixture was kept on ice. The elution was repeated seven times. Then, 1 ml 4 M guanidium-HCl pH 7.0 was added to the main column and the flow through was collected. This step was repeated four times. All fractions were tested for protein with Bradford reagent (Sigma, Dorset, UK). The glycine solutions which contained protein were pooled and so were the guanidium solutions and 0.2 % (w/v) BSA was added. Both solutions were dialysed against PBS at 4 °C

overnight. The dialysed antibody solutions were aliquoted and stored at – 80 °C. Affinity purified antibodies were tested by Western blotting (see 2.2.13).

2.2.24 Coupling of antibodies to beads

Antibodies were immobilised to sepharose beads (protein A sepharose 4 Fast Flow, Amersham Pharmacia, Uppsala, Sweden; protein G sepharose 4B Fast Flow, Sigma, Dorset, UK) for the immunoprecipitation of proteins from yeast (see 2.2.25.3).

Sepharose beads (1 ml) were washed (4 °C, 200 rcf, 5 min) twice in 5 ml PBS to remove the storage buffer. The binding capacity of spharose beads is about 25 mg to 35 mg of IgG per 1 ml drained beads depending on the product. Sepharose beads (1 ml) were incubated overnight at 4 °C with 1 to 5 ml of antibody solution in PBS to allow the binding of the antibody to protein A/G. Polyclonal antibodies directed against a specific protein or mouse monoclonal anti-HA (12CA5) or anti-Myc (9E10) (see 2.1.10) antibodies were used. The beads were sedimented by centrifugation (4 °C, 200 rcf, 5 min), the supernatant was removed and the beads were washed twice with 10 ml of 0.2 M sodium-borate buffer (pH 9.0). The beads were resuspended in 10 ml of 0.2 M sodium-borate buffer (pH 9.0). Dimethylpimelimidate (50 mg) was added to a final concentration of 20 mM. The beads were incubated with the cross linking agent for 1 h at RT. The beads were spun down by centrifugation (4 °C, 200 rcf, 5 min) and they were washed once with 10 ml 0.2 M ethanoldiamine (pH 8.0). They were incubated in 10 ml of 0.2 M ethanoldiamine (pH 8.0) at RT for 2 h to quench any remaining cross linker activity. The beads were pelleted (4 °C, 200 rcf, 5 min), the supernatant was discarded and the beads were washed in 10 ml PBS. The beads were stored in 5 ml PBS containing 0.1 % (w/v) sodium azide at 4 °C. To check the coupling efficiency, an equal volume of beads was sampled before and after the cross linking reaction. The beads were taken up in HU-buffer (see 2.1.2) and they were incubated at 65 °C for 10 min. The two samples were analysed by SDS-PAGE (see 2.2.4.2). The crosslinked antibodies were not eluted from the matrix. In contrast, the uncoupled IgGs were released and were detectable in the Coomassie Blue stained gel (see 2.2.5.2.1).

2.2.25 Affinity chromatography

Proteins were enriched from bacteria and yeast cell extract by affinity chromatography.

2.2.25.1 Purification of GST-protein-fusions from E.coli

The pGEX-5X vector system was used for the expression of yeast genes in *E. coli.* Yeast genes were ligated into the pGEX-5X-1 vector (see 2.1.7) and were cloned into the BL21 pLysS strain (see 2.2.8). The pLysS vector encodes lysosyme which is expressed continuously and simplifies cells lysis. The gene is under control of the *tac* promotor which is activated by the inactivation of the lac I^q suppresser by addition of IPTG. The vector was constructed that the expressed protein will contain a GST-tag. This GST-tag will allow the purification of the protein via binding to glutathione sepharose. Strains were selected for chloramphenicol (pLysS) and ampicillin (pGEX-5X-1) resistance.

Firstly, the optimal induction conditions were established. 1.5 ml of TY-Amp-chloramphenicol-medium were inoculated with the specific Bl21 strain and cells were incubated at 37 °C overnight. The next day, 10 ml of selective medium were inoculated with 200 µl overnight culture and were incubated at 30 °C for 2 h. IPTG was added to a final concentration of 0.2 mM and the culture was incubated on a shaker at 30 °C for another 3 to 4 h. The cells were harvested by centrifugation (4 °C, 2,700 rcf, 5 min). The pellet was taken up in 50 µl of HU-buffer (see 2.1.2) and the sample was incubated at 65 °C for 10 min. The samples were analysed by SDS-PAGE (see 2.2.4.2) and Coomassie Blue staining (see 2.2.5.2.1). If the protein was degraded, different concentrations of IPTG and varied incubation times were tested. The optimal conditions for the isolation of Bbp1p and Mps2p were 0.5 mM IPTG for 2 h at 30 °C.

For the purification, the volume of the culture was scaled up to 400 ml and the induction was done under the established conditions. The cells were lysed as described in 2.2.22.1. Glutathione sepharose 4 B (1 ml; Amarsham Pharmacia, Uppsala, Sweden) was washed twice with PBS (4 °C, 200 rcf, 5 min) before it was added to the cell lysate. To allow the binding of GST to the beads, the solution was incubated on an

overhead mixer at 4 °C for 2 h. The beads were washed once in PBS containing 0.1 % (v/v) Triton-X-100 and twice in PBS (4 °C, 200 rcf, 5 min). The beads were finally taken up in 10 ml PBS and were loaded on disposable polystyrene columns (Pierce, Rockford, USA). The beads were washed with PBS until the flow through was free of proteins. The protein content of the flow through was checked with Bradford reagent (Sigma, Dorset, UK). For the elution of the protein 1 ml 10 mM glutathion in 50 mM Tris-HCl pH 8.0 was added to the sealed column. After 10 min, the flow through was collected. This procedure was repeated twice more. Of each flow through 10 µl were mixed with 10 µl HU-buffer (see 2.1.1). The samples were analysed by SDS-PAGE (see 2.2.4.2) and Coomassie Blue staining (see 2.2.5.2.1).

2.2.25.2 Enrichment of ProA-fusion proteins from yeast extract

Protein A (ProA) binds IgGs with high affinity and therefore it is possible, to enrich ProA tagged proteins using IgG sepharose beads (Amarsham Pharmacia, Upsala, Sweden). The following protocol was used to isolate Bbp1p-ProA fusion proteins and the interacting protein Mps2p. Yeast cells (15 g), either of cells expressing Bbp1p-ProA or of YPH499 cells (wild type control) were lysed in the beat beater under optimal extraction conditions for Bbp1p-ProA (see 2.2.22.3; basis-buffer: 50 mM Tris-HCl pH 7.5, 10 mM EDTA, 1 mM EGTA, 5 % (v/v) glycerol containing 100 mM NaCl and 1 % (v/v) Triton-X-100). A sample of total yeast extract was mixed with an equal volume of HU-buffer (see 2.1.2) and was kept at – 20 °C. This sample was used as control for the total concentration of the target protein.

IgG sepharose beads (4 ml bed volume) were washed in 10 ml 0.5 M acetic acid pH 3.4. The beads were sedimented by centrifugation (4 °C, 200 rcf, 5 min). The supernatant was discarded and the beads were washed with TST (50 mM Tris-HCl pH 7.6, 150 mM NaCl, 0.05 % (v/v) Tween 20) until the pH was neutral. This procedure was repeated once more. The beads were packed into two disposable 2 ml polystyrene columns (Pierce, Rockford, USA). The columns were cooled to 4 °C and one was loaded with wild type yeast extracts and the other with the Bbp1-ProA yeast extract. The columns were washed with following buffers at a flow rate of 0.3 ml/min:

20 ml basis buffer (see text above), 0,35 M NaCl, 1 % (v/v) Triton-X-100

5 ml basis buffer (see text above), 0,5 M KCl, 1 % (v/v) Triton-X-100

10 ml basis buffer (see text above), 0,5 M NaCl, 1 % (v/v) Triton-X-100

20 ml TST (see text above)

5 ml 5 mM ammonium acetate (NH_4OAc) pH 6.5

5 ml 5 mM NH_4OAc pH 5.5

5 ml 5 mM NH_4OAc pH 5.0

The proteins were eluted by addition of 4.5 ml 0.5 M NH_4OAc pH 3.5. The eluate was collected and divided into 0.8 ml portions which were dried in the vacuum concentrator over night. The dried pellet was taken up in H_2O and was dried again in the speed vac. This step was repeated until all salt was removed. Each pellet was taken up in 30 µl of HU-buffer (see 2.1.2) and was incubated at 65 °C for 10 min.

The sepharose beads were taken up in HU-buffer and were incubated at 65 °C for 10 min. The samples were centrifuged (RT, 15,300 rcf, 5 min) and the supernatant was stored at –20 °C. This sample was used as a control for the elution efficiency.

All samples were analysed by SDS-PAGE (see 2.2.4.2) and Fairbanks staining (see 2.2.5.2.2). Unique protein bands were analysed by MALDI-MS (see 2.2.26).

2.2.25.3 Immunoprecipitation of yeast proteins

Proteins and their interacting protein partners were enriched by immunoprecipitation. Therefore, HA- and Myc-fusion proteins or wild type proteins were precipitated using antibodies against the HA- and Myc-epitopes or against proteins directly. The optimal extraction conditions for each protein were established as described in 2.2.22.3 and cell extracts were prepared accordingly. In this study, the optimal extraction buffer for proteins was established as basis-buffer (50 mM Tris-HCl pH 7.5, 10 mM EDTA, 1 mM EGTA, 5 % (v/v) glycerol) containing 100 mM NaCl and 0.5 % (v/v) Triton-X-100. A sample of the total yeast extract was mixed with an equal volume of HU-buffer (see 2.1.2) and was kept at –20 °C. This sample was used as control for the total concentration of the target protein. Sepharose beads which had been coupled to

antibodies were prepared as in 2.2.24. The sepharose beads were washed twice in basis-buffer (4 °C, 200 rcf, 5 min). About 50 µl of drained beads were added to the yeast extract of 0.5 g yeast pellet. Proteinase inhibitors were added (complete MINI, Roche, Lewes, UK) and the yeast lysate sepharose mixture was incubated in a roller mixer at 4 °C for 4 h. The beads were harvested by centrifugation (4 °C, 200 rcf, 5 min) and the supernatant was taken off. A sample of the supernatant was mixed with an equal volume of HU-buffer (see 2.1.2) and was kept at –20 °C. This sample was used, in combination with the sample of total yeast extract (see above) as control for the binding efficiency of the antibody beads. The beads were washed once in 1.5 ml extraction buffer (see above), before they were transferred into spin columns (Mobicol, MoBiTec, Bioscience, Cramlington, UK). The beads were washed in the spin columns twice with extraction buffer and 3 times with basis-buffer (see above; 4 °C, 200 rcf, 5 min). The bottom of the columns was sealed and an equal volume of HU-buffer was added to the sepharose beads. After the top had been sealed, the columns were incubated at 65 °C for 20 min to brake the protein-antibody binding. The columns were placed in an Eppendorf tube and the HU-buffer containing the dissolved proteins was harvested as flow through by centrifugation (4 °C, 15,300 rcf, 5 min). The proteins were analysed by SDS-PAGE and/or Western blotting. In some cases, protein bands were identified by MALDI-MS (see 2.2.26).

The following control experiments were undertaken to test the specificity of the precipitation. As control for the immunoprecipitation of fusion-proteins, a wild type strain was treated identically to the strain with the tagged gene. To detect non-specific binding in a precipitation using antibodies recognising the yeast protein directly, two controls were done. Firstly, sepharose A/G beads which had been treated with the same coupling reagent were used for a mock precipitation. This control would have shown unspecific binding of yeast proteins to beads. Secondly, beads coupled to an unrelated polyclonal antibody or to pre-immunserum were used for the precipitation. Here, non-specific binding of antibodies to yeast proteins would have been detected.

2.2.26 MALDI-MS

Analysis of proteins by MALDI-MS (Karas and Hillenkamp, 1988) was performed in collaboration with Anna and Andrej Shevchenko (EMBL, Heidelberg, Germany). The samples were digested with trypsin and the mass of the resulting peptides was determined after ionisation by time of flight. The mass of the trypsin peptides is characteristic for each protein. Since the whole yeast genome is sequenced, all ORFs and hypothetical ORFs are known and the proteins can be identified according to the peptide masses.

2.2.27 *In vitro* binding assay

In this study, the binding of 6His-N-Mps2p to GST-Bbp1p, GST-N-Bbp1p and GST-C-Bbp1p was investigated by *in vitro* binding. Therefore, 6His-N-Mps2p, GST-Bbp1p, GST-N-Bbp1p, GST-C-Bbp1p and GST were expressed in *E.coli* as described in 2.2.25.1. Cells were lysed according to 2.2.22.1. Triton-X-100 was added to final content of 0.1 % (v/v) to the lysate of cells expressing 6His-N-Mps2p. The lysate was incubated for up to 1 h on ice. Meanwhile, GST-Bbp1p, GST-N-Bbp1p, GST-C-Bbp1p and GST were bound to glutathion sepharose as described in see 2.2.25.1 Methods for the purification of proteins from *E. coli*. After the binding the sepharose resins were washed once in PBS containing 0.1 % (v/v) Triton-X-100 and twice in PBS (4 °C, 510 rcf, 2 min). Of each resin 50 µl were taken off and were kept at 4 °C (control sample for binding to resin). The 6His-N-Mps2p lysate was centrifuged (4 °C, 20,800 rcf, 10 min). A 50 µl sample of the 6His-N-Mps2p supernatant was frozen (control samples for expression of 6His-N-*MPS2*. The rest of the supernatant was divided in four equal portions which were incubated with the four different resins at 4 °C for 1 h. After the incubation, the resins were washed once in PBS, 0.1 % (v/v) Triton-X-100 and twice in PBS (4 °C, 510 rcf, 2 min) before they were transferred into a spin column (Mobicols). The resins were washed three times more with PBS. Finally, the resins and all other control samples were resuspended in HU-buffer and the mixtures were incubated at 65 °C for 10 min. Glutathion sepharose beads and larger particles were sedimented by centrifugation (RT, 20,800 rcf, 5 min) and the samples were analysed by SDS-PAGE (see 2.2.4.2) and Western blotting (2.2.13).

2.2.28 Yeast two-hybrid analysis

In this study, the yeast two-hybrid system (Fields and Song, 1989) was used to study the interaction of SPB components. The transcriptional activator Gal4p is composed of a DNA binding domain ($Gal4p^{DNA}$) and an acidic transactivation domain ($Gal4p^{TA}$). These two distinct regions can be fused to other proteins. Re-union of the two domains via interaction of the fusion-proteins lead to restoration of the transcriptional activity. As consequence, the functional transcripition of the *LacZ* reporter, coding for β-galactosidase is initiated. β-galactosidase metabolises X-Gal, whereby a blue indigo dye accumulates after oxidation. Here, the bacterial DNA-binding protein LexA was use instead of the $Gal4p^{DNA}$ domain.

Genes were amplified by PCR (see 2.2.1.1) and were cloned (see 2.2.8) in frame into the two-hybrid vectors. Different combinations of two-hybrid vectors containing the $LexA^{DNA}$ (pEG202, pMM5) or the $Gal4p^{TA}$ (pACTII, pMM6) domains were used. Plasmids were transformed into Mata and Matα yeast strains and transformants were selected on SC-Leu (pACTII, pMM6) or SC-His (pEG202, pMM5) plates. Strains were combined by replica plating (see 2.2.19) and mating on YPD-plates. Diploids were selected on double selective plates (SC-His-Leu). Diploid cells were overlaid with top agar containing the X-Gal substrate. The top agar was prepared as follows: 0.5 M sodium phosphate (pH 7.0), 1 % (w/v) SDS, 20 mM KCl, 2 mM $MgCl_2$ solution was prepared and heated to 40 °C. Low melting agarose (400 mg) was dissolved in 30 ml H_2O and cooled to 50 °C. The two solutions were mixed slowly and 1 ml of X-Gal (stock solution: 40 mg/ml dimethyl formamide) was added. The plates were overlaid and cells with very strong two-hybrid interactors already turned blue after 5 min.

In this study, the *GAL1* promotor of the pMM5 and pMM6 plasmids (see 2.1.7) was expressed sufficiently without galactose induction.

2.2.29 Suppression analysis

The principle of suppression analysis is that slight overexpression of one or more genes might be able to complement for the function of a defective gene. Conditional lethal

mutants which show a growth defect due to mutations in a single gene, can therefore be investigated for rescue of growth by overexpression of other yeast genes. The protein encoded by the overexpressed gene might take over or help with the functions of the protein encoded by the defective gene or work downstream of the non-functional gene. In some cases, negative suppression occurs. Thereby, overexpression of a gene leads to an increase in the growth defect of the mutant by possibly, further inhibiting the defective protein encoded by the mutated gene directly or indirectly. Taken together, suppression events are a good indication for the possible interaction of proteins or for the similarity in the cellular function of genes.

Conditional lethal mutants were transformed (see 2.2.8.5.2) with mulit-copy or single copy plasmids containing ORFs of yeast genes expressed from their own promoter. The strains were selected for the marker gene of the plasmid and cells were tested for growth at the restrictive temperature (positive suppression) or for growth inhibition at the permissive temperature (negative suppression).

In case of the Δ*mps2* suppression screen, a library (YEp13) was transformed (see 2.2.8.5.2) into the *MPS2* shuffle (see 2.2.17) strain. The transformants were selected for the wild type plasmid (shuffle strain with pRS316-*MPS2*) and for the library plasmid (*LEU*-based plasmid pFL44), as well as for the deletion of *MPS2* (*HIS3* marker gene). After counter-selection for the wild type plasmid on 5-FOA-plates (see 2.2.20), the transformants were tested for growth at the restrictive temperature. The inserts of the YEp13-library coded for 5 kb to 10 kb of yeast chromosomal DNA. In order to ensure the entire yeast genome was covered 50,000 transformants were screened for suppression. The plasmids leading to suppression were isolated by plasmid rescue (see 2.2.10.1). The plasmids were again transformed into the *MPS2* shuffle strain and were tested for suppression as described above. Plasmids, which still mediated suppression, were sequenced (see 2.2.14) and identified genes were subcloned and again tested for suppression as described above.

2.2.30 Geldanamycin assay

Geldanamycin is a benzoquinoid ansamycin and was initially thought to inhibit protein tyrosine kinases (DeBoer *et al.*, 1970). It is now known that geldanamycin blocks the interaction of substrates with Hsp90 (Whitesell *et al.*, 1992).

For the geldanamycin assay (Morano *et al.*, 1999), overnight cultures of yeast strains were grown until OD_{600}=0.6 and about 2 x 10^6 cells were harvested by centrifugation (4 °C, 1,090 rcf, 5 min). The cells were taken up in 200 µl of YPAD-medium and were mixed with 3 ml of autoclaved and cooled (to 50 °C) YPAD-medium containing 0.8 % (w/v) agar. The agar/cell solution was evenly spread over a YPD-plate and the top agar was left to solidify. Aliquots of 2 mM geldanamycin in DMSO and of DMSO alone (10 µl) were spotted onto the top agar. The plates were dried before incubation at 23 °C for 3 d.

2.2.31 Isolation of nuclei

A yeast culture (12 l) was grown in a fermenter until OD_{600}=0.8. The cells were harvested by centrifugation in a Sorvall centrifuge (4 °C, 2,000 rcf, 15 min). The pellets were taken up in water and they were pooled together. Cells (10 µl) were counted under the microscope and the whole cell content was calculated. The cells were harvested by centrifugation (4 °C, 2,000 rcf, 15 min). The cells were resuspended in cold spheroblasting buffer (1.2 M sorbitol, 25 mM KPi-buffer pH 6.5, 10 mM β-mercaptoehtanol) so that the cell concentration was about 1.5 x 10^9 cells/ml spheroblasting buffer. Per 1 ml spheroblasting buffer, 75 µl glusulase, 20 µl zymolyase (stock solution: 10 mg/ml spheroblasting buffer) and 10 µl mutanase (stock solution: 1 mg/ml spheroblasting buffer) were added. The cells were incubated at 30 °C on a shaker until the cells were spheroblasted (about 3 to 4 h). Digestion of the cell wall which is indicated by cells becoming dark and rounded was monitored under the phase contrast microscope. Meanwhile, Ficoll-400 was dissolved in 1.2 M sorbitol to produce a solution of 7.5 % (w/v) Ficoll. An equal volume of 1.2 M sorbitol was added to the spheroblasted cells and the spheroblasts were pelleted by centrifugation in the Sorvall GS3 rotor (4 °C, 2200 rpm, 15 min). The supernatant was taken off carefully and the

pellet was taken up in 45 ml of 1.1 M sorbitol. The Ficoll solution (30 ml per tube) was transferred into 50 ml Falcon tubes and 15 ml of spheroblast solution was added on top of each Ficoll cushion. The spheroblasts were filtered through the Ficoll cushion by centrifugation (4 °C, 2100 rcf, 30 min) in a Beckmann centrifuge. The spheroblasts were taken up with the help of a glass pipette in the following solution per 10^{10} cells: 10 ml PVP-solution (8 % (w/v) PVP40, 1.57 g KH_2PO_4, 1.46 g K_2HPO_4, 152 mg $MgCl_2$ per 1 l H_2O, pH 6.5), 60 µl solution P (2 mg pepstatin A and 90 mg PMSF in 5 ml ethanol), 24 µl Triton-X-100 ultra pure. The spheroblasts were placed on ice and they were lysed for at least three times with the polytron (see 2.1.14) at 12,000 rpm for 3 min. Lysis was checked by removing a small aliquot, staining the DNA with DAPI (1 µg/ml) and analysing the sample under the fluorescent microscope. If the small DAPI dots, which resembled the nuclei, could be seen free from cell material, the lysis was completed. An equal volume of 0.6 M sucrose-PVP was added to the lysed spheroplasts and the solution was mixed before centrifugation in the GSA-rotor (4 °C, 12,000 rpm, 10 min). The pellet was taken up in 180 ml of 1.7 M sucrose-PVP. The solution was mixed with the polytron for 2 min at 2,000 rpm. Up to 12 sucrose gradients were prepared as follows: 8 ml of 2.3 M sucrose (n_D=1.4540) formed the bottom layer, 8 ml of 2.1 M sucrose (n_D=1.4420) the middle layer and 8 ml of 2.01 M sucrose (n_D=1.4370) the top layer. The concentration of the sucrose solutions had been adjusted exactly with help of a refractometer (see 2.1.14). Each gradient was overlaid with 15 ml of lysed spheroblasts in 1.7 M sucrose-PVP. The tubes were balanced using 1.0 M sucrose-PVP. The gradients were centrifuged in the SW28-rotor in a vacuum centrifuge (4 °C, 14,000 rpm, 16 h). The gradient was sampled in 1 ml fractions. The fractions were analysed after addition of DAPI (1 µg/ml) under the fluorescence microscope. The nuclei were at the interface of gradient 2.1 M and 2.3 M sucrose. The refraction index of the fractions containing nuclei was adjusted to n_D=1.434 with 0.9 M sucrose-PVP if necessary. The yield of nuclei was determined by DNA measurement at 260 nm in the spectrometer. Therefore, 10 µl of nuclei containing gradient fraction were added to 1 ml of 1 % (w/v) SDS and were measured. As blank 1 ml of 1 % (w/v) SDS was measured (OD_{260}=140 equivals 10^{10} nuclei). The nuclei were spun in the 50.2 TI rotor (4 °C, 36,000 rpm, 1 h) and were stored at –80 °C.

2.2.32 Isolation of SPBs

SPBs were obtained by lysis of isolated nuclei (see 2.2.31). Therefore, 10^{10} nuclei were resuspended by vortexing in 1.0 ml lysis solution (1.5 % (v/v) Triton X-100, 2.0 % (w/v) digitonin, 20 % (v/v) DMSO, 0.1 mM $MgCl_2$), 10 µl solution P (2 mg pepstatin A and 90 mg PMSF in 5 ml ethanol) and 2 µl 2 % (w/v) DNAse I-solution (2 % (w/v) DNAse I in 0.25 M sucrose, 0.05 M tri-ethanolamine pH 7.4, 0.25 M KCl, 5 mM $MgCl_2$). The nuclei were incubated at RT for 10 min. Beforehand, several sucrose solutions were prepared in bt-buffer (0.01 M bisTris pH 6.5, 0.1 mM $MgCl_2$) for the gradient centrifugation. The sucrose concentrations were adjusted exactly (2.5 M: n_D=1.4533; 2.25 M: n_D=1.4414; 2.0 M: n_D=1.4295; 1.75 M: n_D=1.4174) with the refractometer. An equal volume of 2.5 M sucrose-bt-buffer was added to the lysed nuclei and they were centrifuged in a 50.2 TI rotor (4 °C, 5,500 rpm, 6 min). The supernatant was loaded onto a sucrose gradient prepared in a Beckman SW41 polycarbonate tube (Beckman, Fullerton, USA). The gradient consisted of a bottom layer of 0.75 ml 2.5 M sucrose-bt, the second layer of 2 ml of 2.25 M sucrose-bt, the third layer of 2 ml of 2.0 M sucrose-bt and the top layer of 2 ml 1.75 M sucrose-bt. If more than one gradient was loaded, the tubes were balanced with 1.0 M sucrose-bt-buffer. The tubes were spun at (4 °C, 29,000 rpm, 6 h) in a SW41 rotor in a vacuum ultra-centrifuge. The gradients were unloaded from the top in 1 ml fractions. The SPBs were usually at the interface of the 2.0 M and 2.25 M sucrose layers. A 10 µl sample of each fraction was taken up in 10 µl HU-buffer (see 2.1.2) and the samples were analysed by Western blotting (see 2.2.13) using antibodies against known spindle pole body components. The fractions with good signals in the Western blot were used for electron microscopy (see 2.2.34).

2.2.33 Fluorescence microscopy techniques

The localisation of proteins in the cell was determined by fluorescence microscopy. Either proteins were localised by fluorescence microscopy using GFP labelled proteins, or by indirect immunofluorescence microscopy with antibodies against proteins or epitope tags of proteins. A Chroma (Zeiss, Jena, Germany) filterset was used with the

following parameters: DAPI: G365, FT395, LP420; GFP/CY2: 450-490, FT510, LP 520; CY3: BP546, FT580, LP590.

2.2.33.1 Direct fluorescence microscopy using GFP

Strains, expressing proteins fused to GFP were constructed as described in 2.2.16. Cells were grown until OD_{600}=0.4 and 1 ml culture was harvested by centrifugation (4 °C, 1,090 rcf, 5 min). The pellet was taken up in 1 ml H_2O. The cells were spun down by centrifugation and were taken up in 200 µl H_2O containing 0.2 µg DAPI. Cells (5 µl) were immobilised on microscope slides which had been covered with a 0.4 % (w/v) low melting agarose coat beforehand. Fluorescent light emission from the GFP-tag and the DAPI stained DNA was detected with a Zeis Axiopot fluorescent microscope (see 2.1.14). Proteins could be localised in relation to the DAPI staining region (nucleus) and/or due to the pattern of GFP staining.

2.2.33.2 Indirect immunofluorescence

For the localisation of proteins which might be partially present in the cytoplasm, cells were prepared for immunofluorescence by formaldehyde fixation (Pringle *et al.*, 1989) followed by a second fixation with methanol/acetone. For SPB components methanol/acetone was used as sole fixative (J. Kilmartin, Cambridge, UK). With the second method, cytoplasmic localisation of proteins is missed, since the cytoplasm is mostly extracted.

Antibodies against SPB components (anti-Spc72p antibody) were used to label the SPB. Novel proteins like Bbp1p, Mps2p, Bfr1p and Pom152p were localised with antibodies against the epitope (HA, Myc) fused to the specific gene. Microtubules were stained with an anti-tubulin antibody. The DNA was visualised by DAPI staining.

2.2.33.2.1 Fixation and preparation of spheroblasts with the formaldehyde method

A yeast culture (10 ml) was grown to OD_{600}=0.8, 1 ml 1 M KPO_4 (pH 6.5). Formaldehyde (1.2 ml) was added and the cells were incubated at RT for up to 1 h. The

fixation time is crucial, since the length of the incubation with formaldehyde can affect the epitope and therefore, the recognition of the epitope by the antibody. The optimal fixation time for each protein was determined empirically and fixation times of 15 min, 30 min and 45 min were usually tested. The cells were harvested by centrifugation (4 °C, 510 rcf, 5 min), taken up in 1 ml SP-buffer (0.1 M KPO_4, 1.2 M sorbitol). This step was repeated twice more. After the third washing step, the cells were resupended in 0.9 ml SP-buffer containing 20 mM β-mercaptoethanol and 0.1 ml zymolyase (stock solution: 2.5 mg zymolyase 20T in 1 ml SP-buffer containing 20 mM β-mercaptoethanol). The cells were incubated at 30 °C for 15 to 45 min until cells were spheroblasted (about 90 % of cells appeared dark and round under the phase contrast microscope). The spheroblasts were put on ice for 5 min before sedimentation in an Eppendorf centrifuge (4 °C, 510 rcf, 2 min). The spheroblasts were washed 3 times with 1 ml of cold SP buffer (4 °C, 510 rcf, 2 min). Spheroblasts were used immediately or were kept at 4 °C for up to 24 h.

The cells were transferred onto microscopy well slides as follows. Firstly, 20 µl poly-lysine were added to each well. After 2 min the poly-lysine was removed and each well was washed 5 times with H_2O. The microscopy slide was dried and 20 µl spheroblasts were added to each well. After 10 min, the solution was removed carefully and the slide was transferred into cold methanol for 5 min. After the slide was bathed in cold acetone for 30 sec, the slide was air dried for about 10 min. The application of antibodies is described in 2.2.33.2.3.

2.2.33.2.2 Fixation and preparation of spheroblasts for the methanol/acetone method

About 6 ml of yeast culture of a OD_{600}=0.8 were harvested by centrifugation (4 °C, 1,090 rcf, 5 min). The pellet was taken up in 1 ml 1.1 M sorbitol and 5 µl β-mercaptoethanol, 80 µl glusulase and 22 µl zymolyase 20T (stock solution: 27 mg/ml H_2O) were added. The cells were then incubated at RT for 30 to 60 min. The formation of spheroblasts was followed by light microscopy and when 90 % of the cells were dark and round, the cells were harvested by centrifugation (4 °C, 510 rcf, 2 min). The

spheroblasted cells were washed once in 1.1 M sorbitol (4 °C, 510 rcf, 2 min). The cells were then resuspended in 1 ml Wickerman solution (YPAD-medium containing 1.1 M sorbitol) and incubated at RT for 1 h. The cells were pelleted and washed for up to 3 times with 1.1 M sorbitol. After the final wash, the cells were taken up in 500 µl 1.1 M sorbitol. The cells were fixed on the microscope slide by bathing in methanol and acetone as described above.

2.2.33.2.3 Fluorescence labelling of proteins for light microscopy

The incubation of cells with antibodies was the same for both methods (described in 2.2.33.2.1 and 2.2.33.2.2). The cells on microscopy slides were blocked by addition of 20 µl PBS-1 % (w/v) BSA (PBS-B) to each well. After 20 to 60 min each well was washed twice with 20 µl PBS-B. The primary antibody in PBS-B (20 µl) was added to the cells and the incubation time was up to 1.5 h. The cells were washed five times with 20 µl PBS-B, before 20 µl of secondary antibody in PBS-B were applied. After 1 h the wells were washed up to six times with PBS. The slide was air dried before 4 µl DAPI/citiflour were added and the slide was sealed with a cover slip and nail varnish. The slide could be stored at – 20 °C for several months.

The following controls were done to distinguish between specific and non-specific binding of antibodies. If proteins were localised with antibodies against the epitope tag of the protein, a wild type strain was treated exactly the same as the strain expressing the protein fusion. If proteins were localised with antibodies specific for the protein itself, control cells were incubated only with the secondary antibody to test its specificity.

2.2.34 Electron microscopy techniques

In this study, the morphology of conditional lethal mutants in *BBP1* was analysed in the cell cycle. Therefore, samples to study the cell morphology were prepared for cells harvested at 45 min, 1 h, 1 h 15 min and 1 h 30 min after release from α-factor arrest (see 2.2.21) and were analysed by electron microscopy (EM).

Furthermore, proteins were localised by pre-embedding immunolabelling followed by electron microscopy. Bbp1p was localised using whole cells, isolated nuclei and isolated SPBs and Mps2p was localised using isolated SPBs only.

Samples for morphological and immunolabelling EM, were stained by pre-embedding staining with osmium and uranyl acetate. After embedding in Spurr-resin (see below) ultra thin samples were prepared with a microtone (see 2.2.34.3). For all samples serial sections were prepared apart from samples containing immunolabelled SPBs for whom preparation of serial sections was not possible (see 2.2.34.2.3). For post-embedding staining, the samples were contrasted with uranyl acetate in methanol (Stempak and Ward, 1964) before staining with lead citrate (Reynolds, 1963). All solutions used in these protocols were sterile filtered to avoid contamination of samples with particles.

2.2.34.1 Electron microscopy to study morphology

A culture of yeast (15 ml, OD_{600}=0.6 to 0.8) was harvested by centrifugation (4 °C, 1,090 rcf, 5 min). The pellet was washed in 5 ml phosphate-Mg-buffer (40 mM K_2HPO_4-KH_2PO_4 pH 6.5, 0.5 mM $MgCl_2$) and the cells were spun once more (4 °C, 1,090 rcf, 5 min). The pellet was taken up in 1 ml phosphate-Mg-buffer containing 2 % (v/v) glutaraldehyde and the cells were fixed at RT for 30 min under constant motion. The fixed cells were washed once in phosphate-Mg-buffer (4 °C, 1,090 rcf, 5 min) and were then resupended in 1 ml of pre-treatment solution (0.2 M Tris-HCl pH 9.0, 20 mM EDTA, 0.1 M β-mercaptoethanol). The cells were incubated at RT for 5 min before they were washed (4 °C, 510 rcf, 5 min) twice in phosphate citrate-buffer (0.17 M KH_2PO_4, 30 mM sodium citrate, pH 5.8). The cells were taken up in 0.9 ml phosphate citrate-buffer and after addition of 0.1 ml glusulase, the cells were spheroblasted at RT overnight. After centrifugation (4 °C, 510 rcf, 2 min), the supernatant was discarded and the cells were washed twice in 0.1 M sodium acetate pH 6.1. The pellet was taken up in 250 µl 2 % (v/v) osmium tetroxide in H_2O and the cells were contrasted at RT for 15 min in the dark. The cells were washed twice with H_2O before the cells were stained in 1 % (w/v) uranyl acetate in H_2O at RT for 1 h in the dark. After two more washing steps (with H_2O), the cells were dehydrated. Firstly, by incubation in 70 % (v/v) ethanol for 30 min. Secondly, in 95 % (v/v) ethanol for

30 min and subsequently, twice in ethanol which was free of H_2O. The cells were taken up in 0.5 ml Spurr resin (Agar Scientific, Stansted, UK) and were incubated for 1 h at RT. The cells were spun down by centrifugation (RT, 1,090 rcf, 5 min), the Spurr-resin was removed and cells were taken up in new 200 µl Spurr-resin and were transferred into an EM tube (Polysciences, Warrington, USA). The cells were pelleted by centrifugation (RT, 15,300 rcf, 15 min) in a horizontal Eppendorf centrifuge. The tubes were filled up to the top with Spurr-resin and the resin was polymerised at 65 °C for 8 h.

2.2.34.2 Immunolabelling electron microscopy

2.2.34.2.1 Immunolabelling electron microscopy using yeast cells

Yeast cells of a 10 ml culture (OD_{600}=0.8) of the strain YCS5-2 (*BBP1*-3Myc) were fixed for 45 min after addition of 1.2 ml formaldehyde (37 %) and 1 ml 1 M KPi-buffer (500 mM K_2HPO_4, 500 mM KH_2PO_4, pH 6.5). The cells were harvested by centrifugation (4 °C, 510 rcf, 5 min). The cells were washed three times with S-buffer (40 mM KPi, pH 6.5, 0.5 mM $MgCl_2$, 1.2 M sorbitol) before they were resuspended in 0.9 ml S-buffer containing β-mercaptoethanol and 0.1 ml zymolyase 20T (stock solution: 2 mg/ml S-buffer containing β-mercaptoethanol). The cells were spheroblasted at 30 °C for about 45 min until 90 % of cells appeared dark and rounded by phase contrast. The cells were chilled on ice for 5 min before they were washed three times in cold S-buffer (4 °C, 510 rcf, 5 min). The cells were finally washed once in blocking buffer (PBS, 1 % (w/v) BSA, 100 mM lysine, 0.1 % (v/v) Triton-X-100) containing proteinase inhibitors (Mini complete, Roche, Lewes, UK). The pellet was taken up in 0.5 ml blocking buffer containing the primary antibody (anti-Myc; Roche, Lewes, UK; dilution 1:500). The cells were incubated at RT for 1 h. The excess of primary antibody was washed off with blocking buffer (3 times), before the secondary antibody (goat anti-mouse nanogold, dilution 1:100, pre-absorbed, see below) in blocking buffer was applied. After 1 h incubation time the cells were washed three times in PBS. The antibodies were crosslinked in PBS containing 1 % (v/v) glutaraldehyde at RT for 15 min. After two washing steps with PBS the cells were washed twice more with H_2O.

The secondary antibody was coupled to ultra-small gold particles which had to be silver enhanced. The silver enhancement method by Danscher was optimised for the application (Danscher *et al.*, 1987).

Solution A: 100 g of gum arabic dissolved in H_2O ad final volume of 200 ml
Solution B: 200 mM Hepes-buffer pH 5.8
Solution C: 0.285 g hydrochinone in 5 ml H_2O (use immediately)
Solution D: 0.036 g silver lactate in 5 ml H_2O (use immediately, keep in the dark)

The Danscher solution was prepared with 5 ml solution A, 1 ml solution B, 1.5 ml solution C, 1 ml H_2O and 1.5 ml solution D. The cells were resuspended in 3 ml Danscher solution. Cells (1 ml) were transferred into 5 ml PBS to stop the silver enhancement reaction after 1 min, 5 min and 10 min. The cells were harvested by centrifugation and were washed twice in H_2O (4 °C, 510 rcf, 5 min). Pre-embedding staining with osmium tetroxide and uranyl acetate, dehydration of samples and polymerisation of the Spurr-resin was done as described in 2.2.34.1. Samples were serial sectioned (see 2.2.34.3) and stained (see 2.2.34.4).

The secondary antibody showed strong background staining during the optimisation of the protocol. Therefore, a batch of secondary antibody was incubated with fixed and spheroblasted cells for 1h, just like the incubation of cells with the primary antibody (see above). The cells were spun down by (4 °C, 20,800 rcf, 5 min), the supernatant containing the pre-absorbed antibody was kept at 4 °C and the dilution of the antibody was adjusted accordingly.

As control, wild type cells were treated exactly the same as the YCS5-2 cells.

2.2.34.2.2 Immunolabelling EM using isolated nuclei

The isolated nuclei (10^{10}, see 2.2.31) were taken up in 1 ml S-buffer (40 mM KPi, pH 6.5, 0.5 mM $MgCl_2$, 1.2 M sorbitol) containing 1/10 volume of fromaldehyde (37 %). The nuclei were fixed for 30 to 40 min and were washed twice in PBS (4 °C, 2,700 rcf, 5 min) before they were taken up in 0.5 ml blocking buffer (PBS, 1 % (w/v) BSA, 100 mM lysine, 0.1 % (v/v) Triton-X-100 and proteinase inhibitors (Mini

complete, Roche, Lewes, UK)). After incubation at RT for 30 min, the nuclei were washed three times in blocking buffer. The nuclei were taken up in blocking buffer containing the primary antibody (anti-Bbp1p antibody, dilution:1:5) and were incubated at RT for 1 h. This step was followed by 5 washing steps with blocking buffer. The nuclei were then incubated with the secondary antibody (goat anti-rabbit nanogold) in blocking buffer. The secondary antibody had been pre-absorbed with nuclei. Therefore, the antibody was incubated with fixed and blocked nuclei in the same way as described for the primary antibody (see before). The nuclei were spun down by centrifugation (4 °C, 20,800 rcf, 5 min) and the supernatant containing the pre-absorbed antibody was used for the incubation. The dilution of the antibody was adjusted accordingly. After the incubation with the pre-absorbed secondary antibody, the nuclei were washed twice in PBS 0.1 % (v/v) Triton-X-100 and twice in PBS.

The cross-linking of antibodies, the silver enhancement, de-hydration, embedding in Spurr-resin and the polymerisation were done as described for whole cells. Samples were serial sectioned (see 2.2.34.3) and were stained (see 2.2.34.4).

As a control for the specificity of the secondary antibody, nuclei were prepared as described above but the incubation step with the primary antibody was omitted.

2.2.34.2.3 Immunolabelling EM using isolated SPBs

One batch of SPBs (about 10^5) obtained as described in 2.2.32, was taken up in 0.5 ml Bt-Mg-buffer (10 mM BisTris, 0.1 M $MgCl_2$, pH 6.5) containing 5 % (v/v) sterile filtered formaldehyde and the SPBs were fixed at RT for 15 min. The fixation was stopped by dilution of the SPBs in 5 ml Bt-Mg-buffer. Meanwhile, glass tubes were prepared which contained adapters on which a cover slip could be placed. The glass tube was filled with some Bt-Mg-buffer, so that the cover slip was covered and 5 ml Bt-Mg-buffer containing the fixed SPBs were added. The tube was spun in a HB 6 Beckman rotor at 4 °C and 11,000 rpm for 12 min. The supernatant was aspirated off until 5 mm above the cover slip. The cover slip was taken out of the glass tube and was placed with the SPB-containing side on a drop of blocking buffer (PBS containing 1 % (w/v) BSA and 100 mM lysine) for 10 min. The cover slip was moved to a new

drop of blocking buffer and the incubation step was repeated. Afterwards, the cover slip was put head up on parafilm (American National Can, Chicago, USA). A drop of primary antibody diluted in blocking buffer (anti-Bbp1p and anti-Mps2p at dilution: 1:5) was placed on the cover slip. The SPBs were incubated for 1 h, before the antibody was aspirated off and the SPBs were washed 6 times with blocking buffer. This was done by placing a drop of blocking buffer on the cover slip and aspirating it off again. The secondary antibody (12 nm gold, goat anti-rabbit, dilution 1:40) was applied in a drop of blocking buffer for 1 h. Afterwards, the SPBs were washed 6 times with PBS. To cross-link the antibodies, the SPBs were incubated in a drop of PBS containing 1 % (v/v) glutaraldehyde at RT for 10 min. The SPBs were washed three times in H_2O before they were contrasted in 2 % (v/v) osmium tretroxide in H_2O in the fume hood for 15 min. The SPBs were washed again twice with a drop of H_2O, before they were de-hydrated with drops of 95 % (v/v) ethanol and 100 % ethanol. Finally, a drop of Spurr-resin was placed on the cover slip and SPBs were soaked for 1 h. The Spurr-resin was taken off and three gelatin EM capsules (Polysciences, Warrington, USA) filled with Spurr-resin were placed on the cover slip. After polymerisation of the Spurr-resin at 65 °C for 8 h, the glass cover slip was carefully removed with the help of tweezers. Since the layer of SPBs in the Spurr-resin is very thin, sections were cut (see 2.2.34.3), which contained a small line of SPBs. The SPBs were contrasted as described in 2.2.34.4.

2.2.34.3 Sectioning of samples

Sectioning of samples was provided by Margaret O'Prey (Technical Services, Beatson Institute, Glasgow). Ultra thin sections of samples were cut at 70 nm with the microtone using a diamond knife. The sections were floated of the knife into H_2O. Sections were transferred onto microscopy grids (300-mash grid, copper/rhodium; slot grid, cooper/palladium; both ∅ 3.05 mm; TAAB, Aldermasten, UK) which had been coated with 0.6 % (v/v) formvar (TAAB, Aldermasten, UK).

2.2.34.4 Post-embedding staining of samples

2.2.34.4.1 Staining with uranyl acetate

The samples were contrasted by post-embedding staining in a methanolic solution of uranyl acetate. Therefore, the microscopy grids were incubated in the dark for 5 min in a sterile filtered solution of 2 % (w/v) uranyl acetate in 70 % (v/v) methanol (Stempak and Ward, 1964). Each grid was taken up with a pair of tweezers and was secured with an elastic band. The grid remained on the pair of tweezers for the following steps. The grids were washed by moving them through about 10 drops of 70 % (v/v) methanol, which had been prepared in a multi-well porcelain dish. The grids were dried for at least 15 min, before they were stained with lead citrate (see below).

2.2.34.4.2 Staining with lead citrate

Reynolds' lead citrate stain (1963) was prepared as follows. CO_2-free water was made by autoclaving double-distilled water in a screw-capped bottle and sealing the flask while still very hot. 1.33 g of lead nitrate and 1.76 g of sodium citrate were mixed with 30 ml CO_2-free water by shaking. The milky solution turned clear after 5 to 7 ml of NaOH were added. The pH of the solution was between pH 12.0 and pH 12.1. A CO_2-free staining chamber was prepared by placing NaOH pellets on a wet piece of filter paper in a petri dish. A drop of lead citrate was placed in the middle of the petri dish and the grids were floated in lead citrate for 5 min. Each grid was taken up with a pair of tweezers and was placed in a drop of water. Afterwards, each grid was washed, still on the tweezers, under the constant flow of water from a squeeze bottle for about 1 min. The grids were dried for at least 15 min.

3. Results

3.1 Functional epitope tags of BBP1

The construction of functional epitope tags for Bbp1p was a prerequisite for the localisation and immunoprecipitation of the protein. Strains expressing *BBP1* fused to triple HA, triple Myc, protein A or single GFP were obtained as described in Material and Methods. The tags were generated by PCR (see 2.2.1.4) with primers *BBP1*-S2 and *BBP1*-S3 (see 2.1.6) using the modules pYM1, pYM4, pYM8 and pYM12 (Knop *et al.*, 1999) (see 2.2.16). The PCR products were analysed by gel-electrophoresis (see 2.2.4.1). As expected the DNA fragments were 1922 bp for 3HA, 1943 bp for 3Myc, 2225 bp for TEV-ProA-7HIS and 2562 bp for GFP (Figure 6A). After ethanol precipitation (see 2.2.2), the fragments were transformed into the yeast strains YPH499 (HA: YCS3; TEV-ProA-7HIS: YCS4; Myc: YCS5) or ESM357 (GFP: YCS6) and were selected for the kanMX6 marker (Wach *et al.*, 1994). The proper integration of constructs at the C-terminus of *BBP1* was tested by colony-PCR (see 2.2.1.2) using the *BBP1*-B primer and the *KAN*2 primer, which binds in the kanamycin gene. The PCR products confirmed the correct chromosomal integration of the modules (Figure 6B). The expression of the gene-fusions was tested by Western blotting (see 2.2.13) using anti-HA, anti-Myc and anti-ProA antibodies (Figure 6C). The sizes of the fusion-proteins were about 54 kD for Bbp1p-3HA, 57 kD for Bbp1p-3Myc and 64 kD for Bbp1p-TEV-ProA-7HIS. The expression of *BBP1-GFP* was analysed by fluorescence microscopy (see 2.2.33.1). Since *BBP1* is an essential gene (see 3.4.1) the protein-fusions were functional when they allowed the normal growth of the haploid yeast strains YPH499 and ESM357.

A Bbp1p-9Myc fusion protein was constructed as described above using the pYM6 module. It was only partially functional, since cells grew more slowly and contained elongated buds. This strain was not used for further experiments.

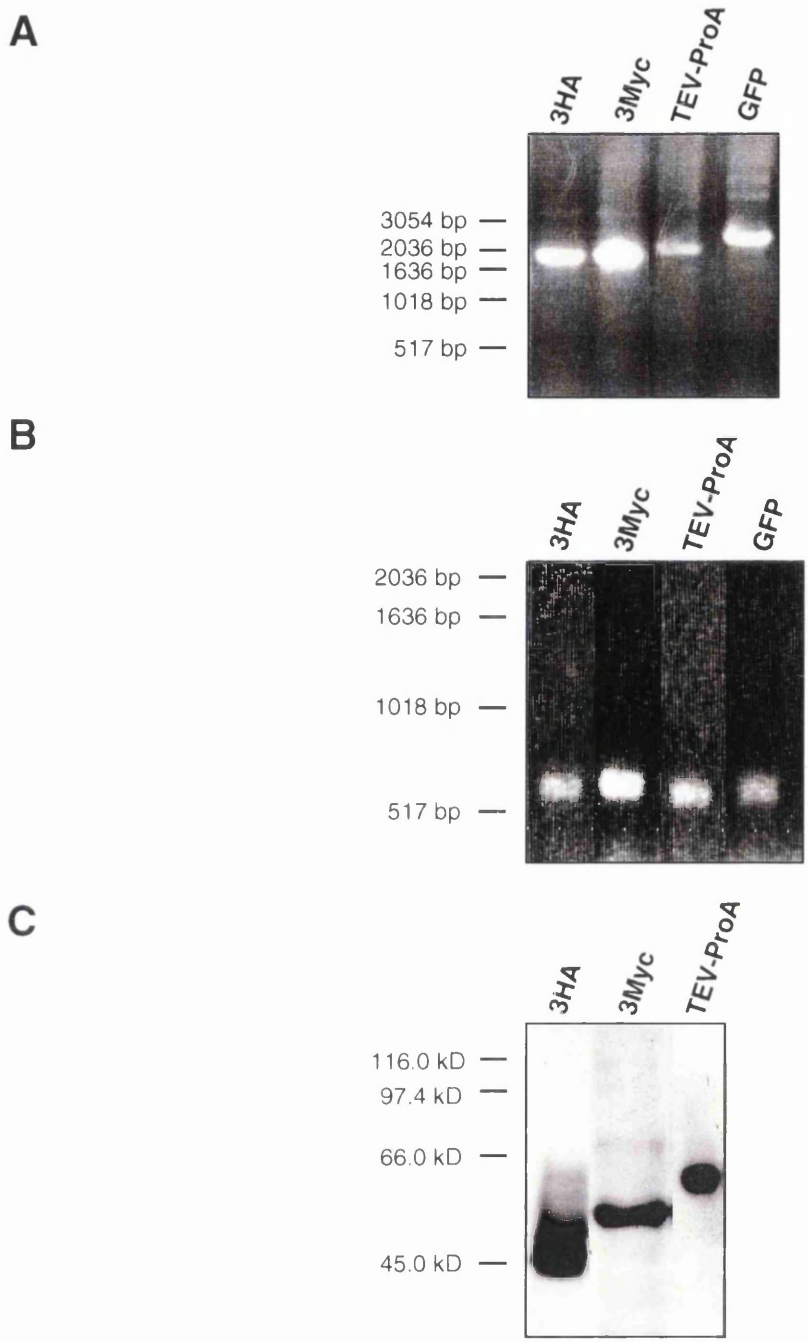

Figure 6: Epitope tagging of *BBP1*. (**A**) Cassettes for 3HA, 3Myc, TEV-ProA and GFP tagging of *BBP1* were amplified by PCR with primers *BBP1*-S2 and *BBP1*-S3 and the PCR products were checked by agarose gel-electrophoresis. (**B**) Insertion of tags into the chromosome was monitored by colony PCR using primers which prime in the selection marker (kanamycin) and downstream from the stop codon of *BBP1*. (**C**) Expression of *BBP1-3HA*, *BBP1-3Myc* and *BBP1-TEV-ProA* was controlled by Western blotting with antibodies recognising the specific epitope tags.

3.2 Antibodies specific for Bbp1p

Polyclonal Antibodies recognising Bbp1p were raised against Bbp1p-GST fusion proteins for identification of Bbp1p by Western blotting and for immunolabelling localisation of Bbp1p.

BBP1-GST and N-*BBP1*-GST fusions were obtained by cloning the ORF and the N-terminus of *BBP1* into the pGEX-5X-1 plasmid (pCS1 and pCS7-1, see 2.1.7). After transformation of the plasmids into the *E. coli* strain BL21 (DE3) pLysS, the best conditions for the expression of the gene-fusions were established as 0.5 mM IPTG for 2 h at 37 °C (see 2.2.25.1). Longer induction caused severe degradation of the fusion-protein and lower concentration of IPTG did not provide sufficient induction. Expression of full length *BBP1*-GST caused inclusion bodies and the protein was insoluble. The N-terminal Bbp1p-GST fusion protein was soluble and could be purified by binding to glutathione sepharose as described in 2.2.25.1. The purified protein was used for the immunisation of a rabbit (see 2.2.23). A course of four immunisations was sufficient to obtain serum that recognised protein bands at about 45 kD in a Western blot of total yeast extract of cells overexpressing Bbp1p (YCS18-1; *GAL1-BBP1*, Figure 7A). After affinity purification of the antibodies (see 2.2.23.3), the fraction of antibodies eluted with glycine/EGTA produced a strong signal at about 45 kD in a Western blot of total yeast extract of *GAL1-BBP1* cells (Figure 7B). The antibodies did not show a signal in Western blots using total yeast extract of wild type cells (data not shown). The antibodies recognised Bbp1p in Western blots of extracts from nuclei and SPBs and they were specific since only one single band was visible at about 45 kD (Figure 7C). Therefore, the antibodies specifically recognise Bbp1p and show a signal in Western blots containing sufficient amounts of protein. The antibodies were stored at – 20 °C and were used at a dilution of 1:200 for Western blotting.

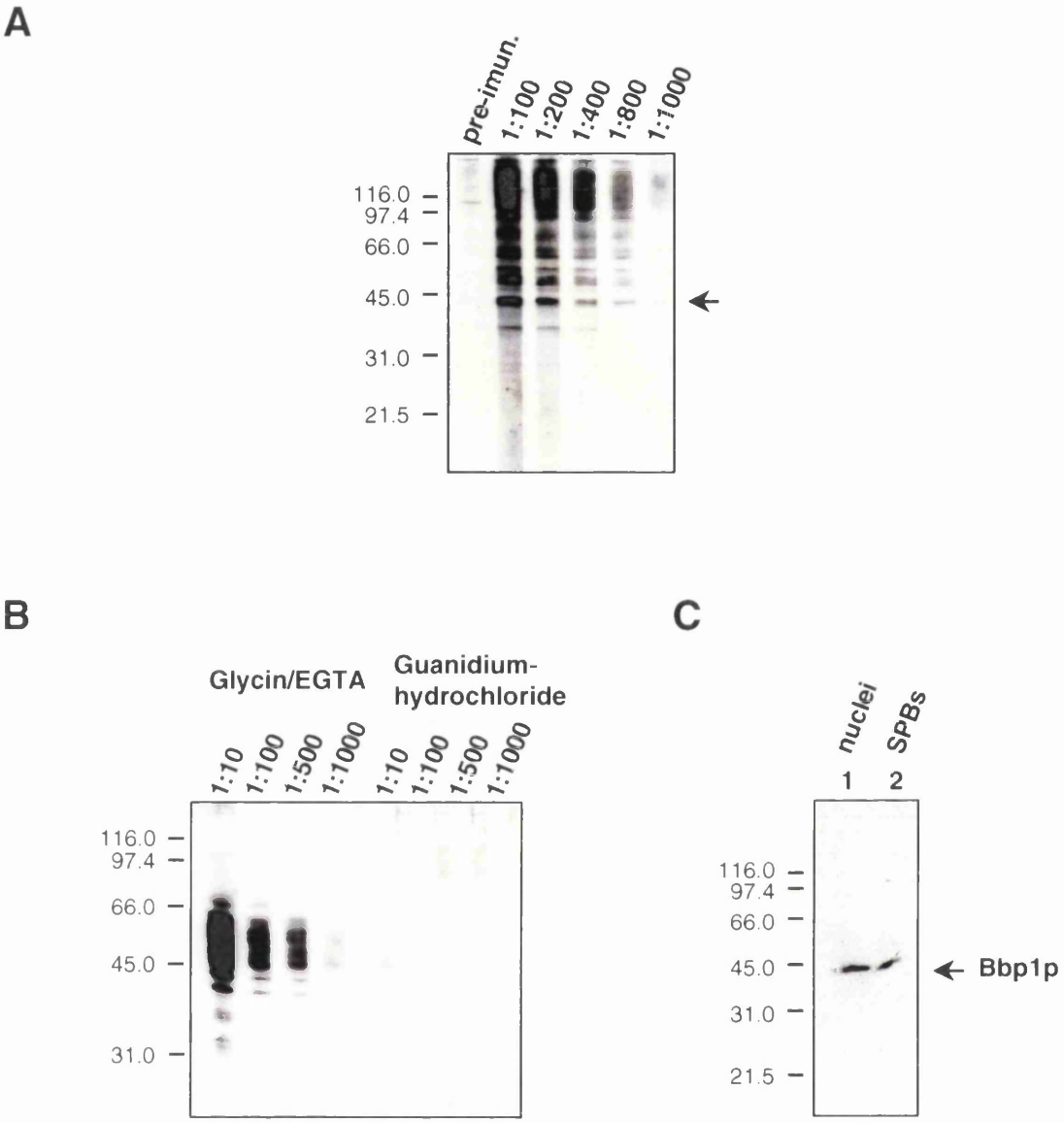

Figure 7: Antibodies which specifically recognise Bbp1p. (**A**) Western blots containing cell extract of cells overexpressing *BBP1* were probed with different dilutions of serum of the immunised rabbit. The rabbit serum contained antibodies recognising a protein band corresponding to the molecular weight of Bbp1p (about 45kD, indicated by arrow) which was not recognised by the pre-immunserum (first lane). (**B**) The immunopurified serum eluted with glycin/EGTA recognised protein bands at about 45kD in Western blots containing cell extract of cells overexpressing *BBP1*. (**C**) The immunopurified serum recognised a single protein band just below 45kD at a dilution of 1:200 in Western blots containing isolated nuclei (lane 1) or isolated SPBs (lane 2).

3.3 Cellular localisation of Bbp1p

Bbp1p was found as an interacting protein of Spc29p (S. Elliott, *published in* Schramm *et al.*, 2000), a component of the central plaque of the SPB (Adams and Kilmartin, 1999; Elliott *et al.*, 1999). This interaction with Spc29p could take place at the SPB and therefore Bbp1p or a pool of Bbp1p might be localised at the SPB as well. To prove this hypothesis the localisation of Bbp1p in the cell was determined by direct fluorescence, indirect immunofluorescence and immunolabelling electron microscopy.

3.3.1 Localisation of Bbp1p using GFP fusions

GFP has been used successfully to visualise various SPB components in yeast. Especially products of gene fusions of *SPC42* and *SPC72* with GFP show a very distinct dot-like staining by fluorescence microscopy which represents the SPB (Chen *et al.*, 1998; Schutz and Winey, 1998). Cells expressing *BBP1* fused to GFP (YCS6, see 3.1, see 2.2.16) were grown in liquid culture to early logarithmic phase, were harvested by centrifugation and investigated by fluorescence microscopy (see 2.2.33.1). To be able to observe a GFP-signal by fluorescent microscopy, the cells had to be washed in water to remove the YPD-medium which obstructed the documentation of the weak Bbp1p-GFP signal. The Bbp1p-GFP signal exhibited a single dot-like staining in unbudded cells and double dot-like staining in budded cells (Figure 8A). This is consistent with GFP signals observed for other SPB components. However, compared to the signals obtained for the SPB components Spc42p, Spc110p or Spc72p the Bbp1p-GFP signal was much weaker. In addition, dot-like staining could also represent staining of kinetochores which cluster near the SPB (Goh and Kilmartin, 1993; Goshima and Yanagida, 2000; Hyland *et al.*, 1999). Thus, Bbp1p is localised in distinct dot-like patterns which could indicate a localisation of Bbp1p at the SPB.

3.3.2 Localisation of Bbp1p at the SPB by indirect immunofluorescence

To investigate if the signal obtained by direct fluorescence microscopy represented a localisation of Bbp1p at the SPB, Bbp1p had to be co-localised with known SPB components by indirect immunofluorescence (see 2.2.33.2). For this experiment Bbp1p-3Myc was detected using mouse monoclonal 9E10 antibodies against the Myc-

tag of the protein. The SPB was marked with polyclonal antibodies (rabbit) against the outer plaque component Spc72p (Knop and Schiebel, 1998). The DNA was stained by DAPI and the blue staining roughly represented the area of the nucleus. Bbp1p-3Myc (YCS5) cells were grown to OD_{600}=0.8 and were fixed according to the methanol/acetone method (see 2.2.33.2.2). As secondary antibodies, goat-anti-mouse CY3 and goat-anti-rabbit CY2 antibodies were used (see 2.1.10). The wild type control (YPH499) sample showed some unspecific background staining for the anti-Myc/anti-mouse CY3 antibody combination (Figure 8, B1 and B2). However, the staining of Bbp1p-3Myc cells was distinctly different from the control strain (Figure 8, compare B1 and B2 with B3 and B4). The red coloured CY3 signal which represented Bbp1p was consistent with the dot-like pattern obtained in the GFP localisation experiment (compare Figure 8 A with Figure 8, B3 and B4) and co-localised with the green Spc72p signal (Figure 8, B3 and B4). Both, Spc72p and Bbp1p signals were in proximity to the blue staining for chromatin (Figure 8B). Due to co-localisation with the known SPB component Spc72p, Bbp1p is a component of the SPB.

3.3.3 Localisation of Bbp1p at the periphery of the central plaque by immunolabelling electron microscopy

To investigate which substructure of the SPB, Bbp1p associates with, isolated SPBs, nuclei and whole yeast cells were investigated by immunolabelling electron microscopy. YCS5 (Bbp1p-3Myc) cells were prepared for pre-embedding labelling (see 2.2.34.2.1). The optimal fixation for cells was determined as 3.5 % formaldehyde for 40 min. The primary antibody (Boehringer anti-Myc antibody) was used in a dilution of 1:500 and the secondary antibody which was coupled to ultra small gold particles (goat anti-mouse nanogold) was pre-absorbed with spheroblasts to reduce non-specific binding (see 2.2.34.2.1). The ultra-small gold particles were silver-enhanced by the Danscher method (see 2.2.34.2.1). After ultra-thin serial sectioning of Spurr embedded cells (see 2.2.34.3) the sections were placed onto microscopy grids and were stained with uranyl acetate and lead citrate (see 2.2.34.4). In 10 cases a gold signal representing Bbp1p was observed close to the central plaque (Figure 9A). As a control YPH499 cells were treated identically and the cells did not show any gold staining at the SPB (data not shown).

In the experiment described above, the morphology of yeast cells and of SPBs was not perfectly conserved. This was due to the harsh treatment of cells during spheroblasting and due to incubation of cells with detergent to allow the penetration of antibodies into the cell. Therefore, the localisation was repeated using isolated nuclei and isolated SPBs. Since the cell walls and most of the cytoplasmic material and in case of isolated SPBs, partially the nuclear envelope, had been removed by the isolation, antibodies had easier and better access to the SPB. Therefore, samples could be treated less harshly and the structure of SPBs was less affected by this procedure.

The isolated nuclei (see 2.2.31) were prepared for electron microscopy as described in Material and Methods (see 2.2.34.2.2). Anti-Bbp1p antibodies were used at a dilution of 1:5 and the secondary antibody coupled to ultra small gold particles was pre-absorbed with isolated nuclei and the dilution was adjusted accordingly. The ultra-small gold particles were silver-enhanced by the Danscher method (see 2.2.34.2.1). About 40 % of all 64 nuclei investigated showed labelling at the SPB (Figure 9B). The gold particles representing Bbp1p were found near the periphery of the central plaque (n=20). In cases in which the half-bridge was visible, the signal was close to the site where the half-bridge connects to the central plaque periphery (n=3). In three cases the gold particle stained the inner plaque. The control nuclei which had been incubated with the secondary antibody, did not show any SPB staining. Only, two out of 45 control nuclei investigated had staining at the nuclear envelope but not at the SPB.

The localisation of Bbp1p at the central plaque periphery was further confirmed using isolated SPBs (see 2.2.32). SPBs were fixed in 5 % formaldehyde (see 2.2.34.2.3). The anti-Bbp1p antibody was used at a dilution of 1:5 and the goat-anti-rabbit antibody coupled to 12 nm gold was used at a dilution of 1:1000. About 55 % of 60 SPBs investigated had staining at the side of the central plaque (Figure 9C). Side-by-side SPBs connected via the bridge structure were observed to have signals where the bridge connects to the central plaque or 180° opposite, on the other side of the central plaque (n=5) (Figure 9C).

Taken together, Bbp1p was shown to be a component of the SPB with a localisation at the central plaque periphery.

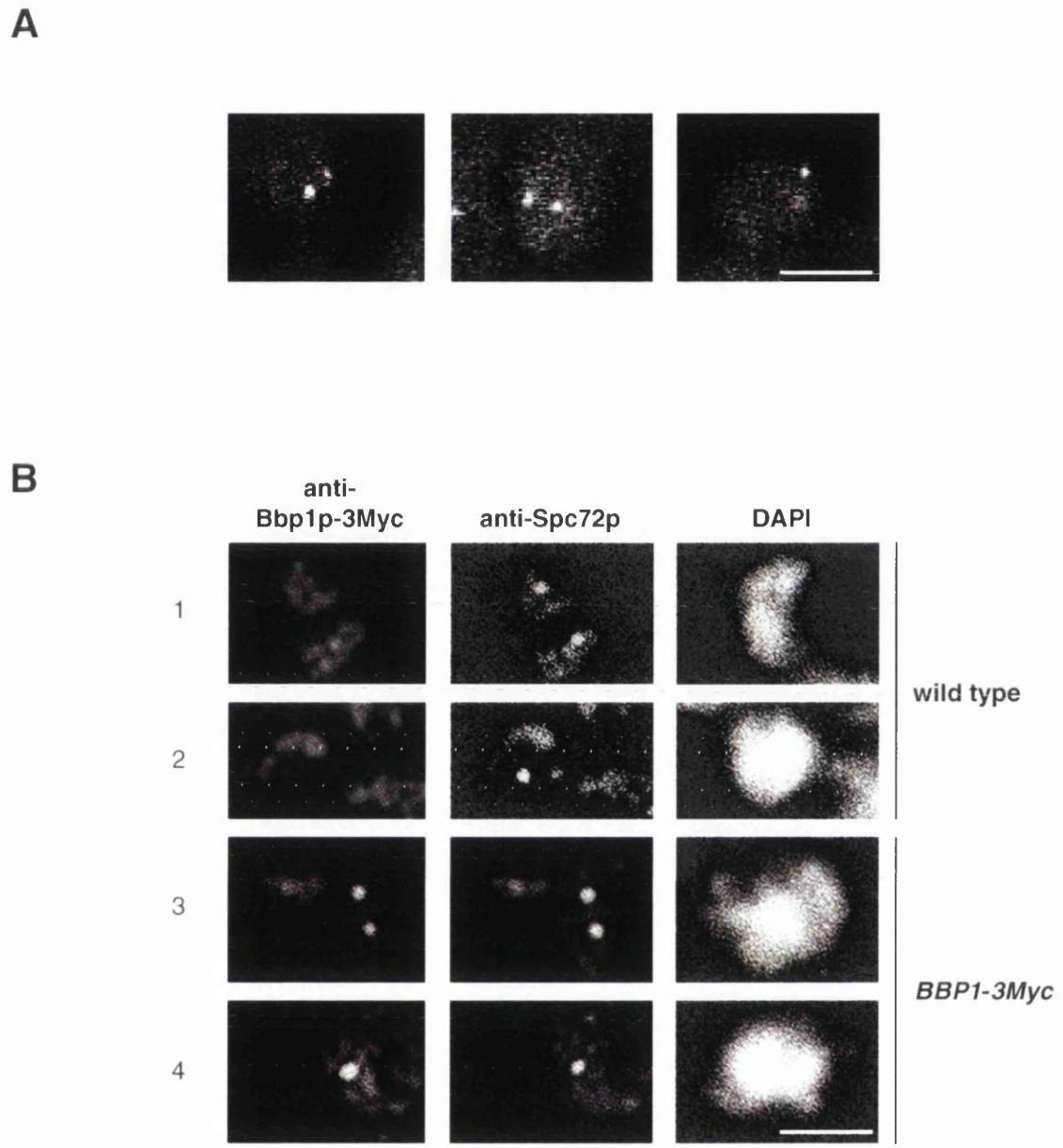

Figure 8: Bbp1p is localised at the SPB. (**A**) Cells expressing *BBP1*-GFP were investigated by fluorescence microscopy and dot-like signals typical for SPB staining were observed. (**B**) Indirect immunofluorescence of wild type cells (panel 1 and 2) and cells expressing Bbp1p-3Myc (panel 3 and 4). Bbp1p-3Myc was localised using mouse monoclonal anti-Myc antibodies (9E10). The SPB was labelled with antibodies against the outer plaque component Spc72p (rabbit anti-Spc72p) and the DNA was visualised by DAPI staining. The specific dot-like signal for Bbp1p which was not present in the wild type control co-localised with the Spc72p staining of SPBs. Bars (A and B), 5 µm.

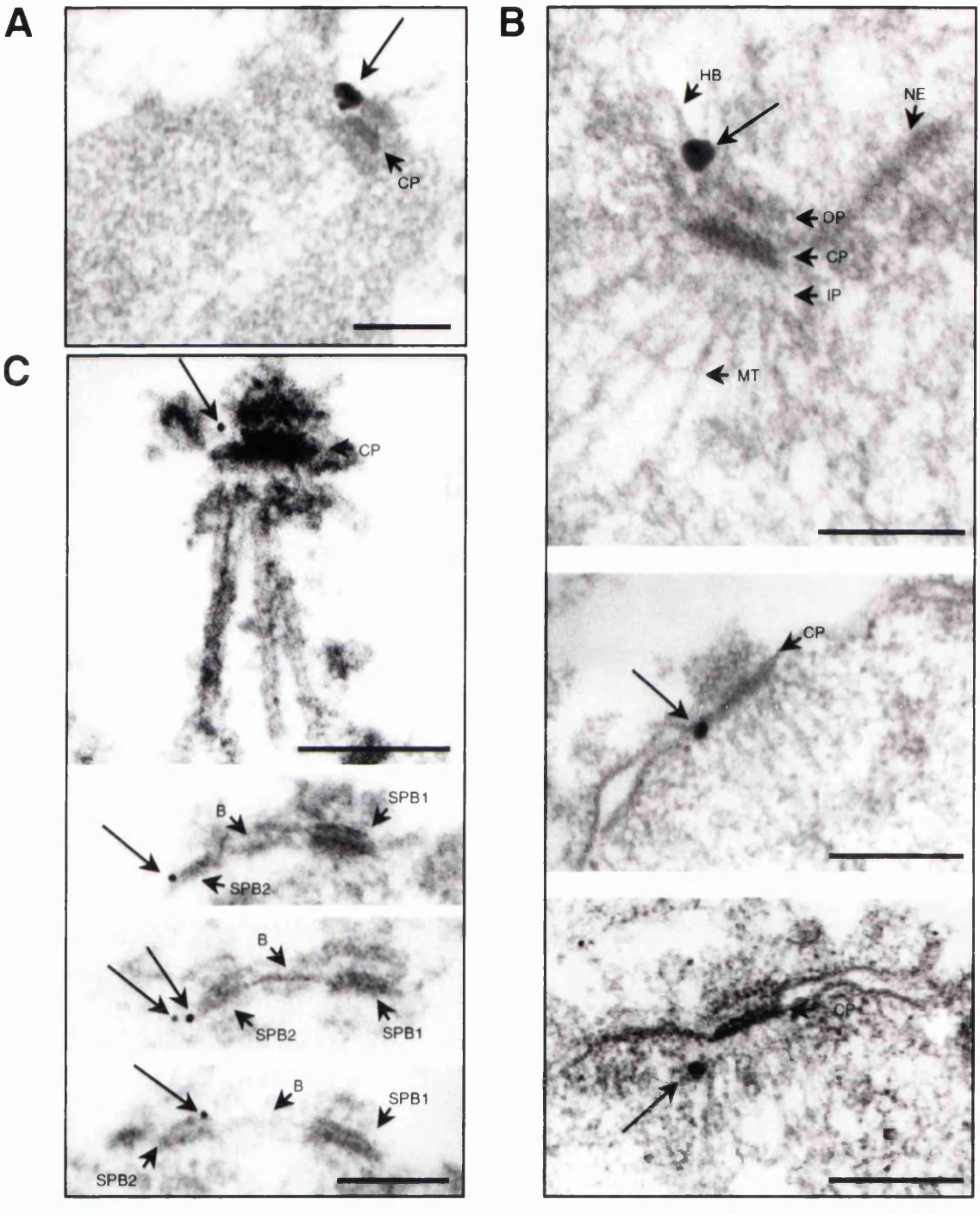

Figure 9: Bbp1p is associated with the central plaque periphery. Immunolabelling electron microscopy of *BBP1-3Myc* cells (**A**), isolated nuclei (**B**) or isolated SPBs (**C**) using mouse monoclonal anti-Myc antibodies (A) or immunopurified rabbit anti-Bbp1p antibodies (B and C). The secondary antibodies were conjugated to ultra small gold (A and B) or to 12 nm gold particles (C). Ultra small gold particles were silver enhanced. Gold staining represents Bbp1p (large arrows). Note: in a few cases (n=3) gold staining was found close to the inner plaque of the SPB (B, bottom right micrograph). B: bridge, CP: central plaque, HB: half bridge, IP: inner plaque, MT: microtubules, NE: nuclear envelope, OP: outer plaque; Bars (A-C), 0.25 µm.

3.4 The cellular role of Bbp1p

The following experiments were designed to reveal the functions of Bbp1p at the SPB and to elucidate its role in cellular processes.

3.4.1 *BBP1* is essential

To determine if *BBP1* is an essential gene YCS1, a diploid yeast strain in which one chromosomal copy of *BBP1* was replaced with the *HIS3* marker gene was constructed (see 2.2.17). YCS1 was forced by sub-optimal growth conditions to undergo meioses and transform cells into tetrads (see 2.2.17). The four spores of each tetrad were separated by microscopic dissection onto non-selective YPD-plates and were incubated for growth at 23 °C. Two spores should harbour wild type copies of *BBP1* while the other two spores should contain the *HIS3* marker gene instead. Two out of four spores managed to grow on non-selective plates (Figure 10A). These two spores did not contain the *HIS3* marker gene, since the colonies could not grow after replication on selective plates lacking histidine (data not shown). Therefore, spores which did not contain *BBP1* were unable to grow into colonies.

In addition, YCS1 was transformed with *BBP1* on a single copy *URA*3-based vector and the strain was analysed by microscopic dissection (data not shown). All four spores could grow on non-selective plates. If colonies grown up from four sister spores were replica plated on 5-FOA plates the *URA3*-based *BBP1* plasmid was lost (see 2.2.20) and only two colonies could grow. Cells of these colonies harboured the chromosomal wild type copy of *BBP1*. Thus, cells lacking Bbp1p were unable to grow and *BBP1* is an essential gene.

3.4.2 Overexpression of *BBP1* inhibits cell growth

A yeast strain overexpressing *BBP1* was constructed by placing *BBP1* under the control of the *GAL1*-promoter (pCS9) and transforming the p425-*GAL1*-*BBP1* plasmid into wild type (YPH499) yeast cells. The resulting strain, YCS18, was streaked out on 2 % raffinose/2 % galactose plates for induction of the *GAL1*-promoter. Induction of the *GAL1*-promoter can cause an overproduction of up to 1500-fold (Mumberg *et al.*,

1994). Some small colonies of the strain containing the p425-*GAL1-BBP1* plasmid were able to grow (Figure 10B, sector 1). Compared to the normally growing wild type strain (Figure 10B, sector 2), containing the p425-*GAL1* control plasmid, growth was strongly inhibited. The effect of *BBP1* overexpression was not as harmful for cells as overexpression of *SPC42* coding for a component of the IL2 which was used as a control (Figure 10B, sector 3). Overexpression of *SPC42* is known to be toxic and cells overexpressing Spc42p contain disc-shaped polymers associated with the SPB at the outer nuclear membrane (Bullitt *et al.*, 1997; Donaldson and Kilmartin, 1996). *BBP1* overexpression was toxic, however, slightly less than compared to *SPC42*.

In a second experiment, YCS18 cells were grown in liquid culture, for two days in SC-Leu medium containing 2 % raffinose to deplete glucose. Then, cells were harvested and transferred into SC-Leu medium containing 2 % raffinose and 2 % galactose for induction of the *GAL1*-promoter. The control strain containing the p425-*GAL1* plasmid was treated accordingly. Cells were harvested shortly before induction (0 h) and 3 h, 6 h, 8 h, 24 h and 48 h after induction for Western (see 2.2.13) and FACS analysis (see 2.2.15). Western blotting using anti-Bbp1p antibodies (Figure 10C) showed that Bbp1p was highly enriched in cells overexpressing Bbp1p (Figure 10C, S2) compared to non-induced cells (0 h) and cells containing the empty p425-*GAL1* plasmid (Figure 10C, S1). However, the anti-Bbp1p antibody did not show a signal for wild type levels of Bbp1p in Western blots as described in 3.2 before. Samples of the control strain (YPH499 p425-*GAL1*) and of YCS18 (*GAL1-BBP1*) cells of all time points were analysed by FACS (data not shown). There was no significant difference in the DNA content of cells highly overexpressing *BBP1* compared to wild type cells. Furthermore, cells overexpressing *BBP1* did not have any unusual phenotypes as investigated by light microscopy (data not shown). Immunofluorscence microcopy showed high levels of Bbp1p in the cytoplasm and the nucleus (data not shown). Cells overexpressing Bbp1p for 3 h were investigated by morphological electron microscopy and did not display any SPB defects (data not shown).

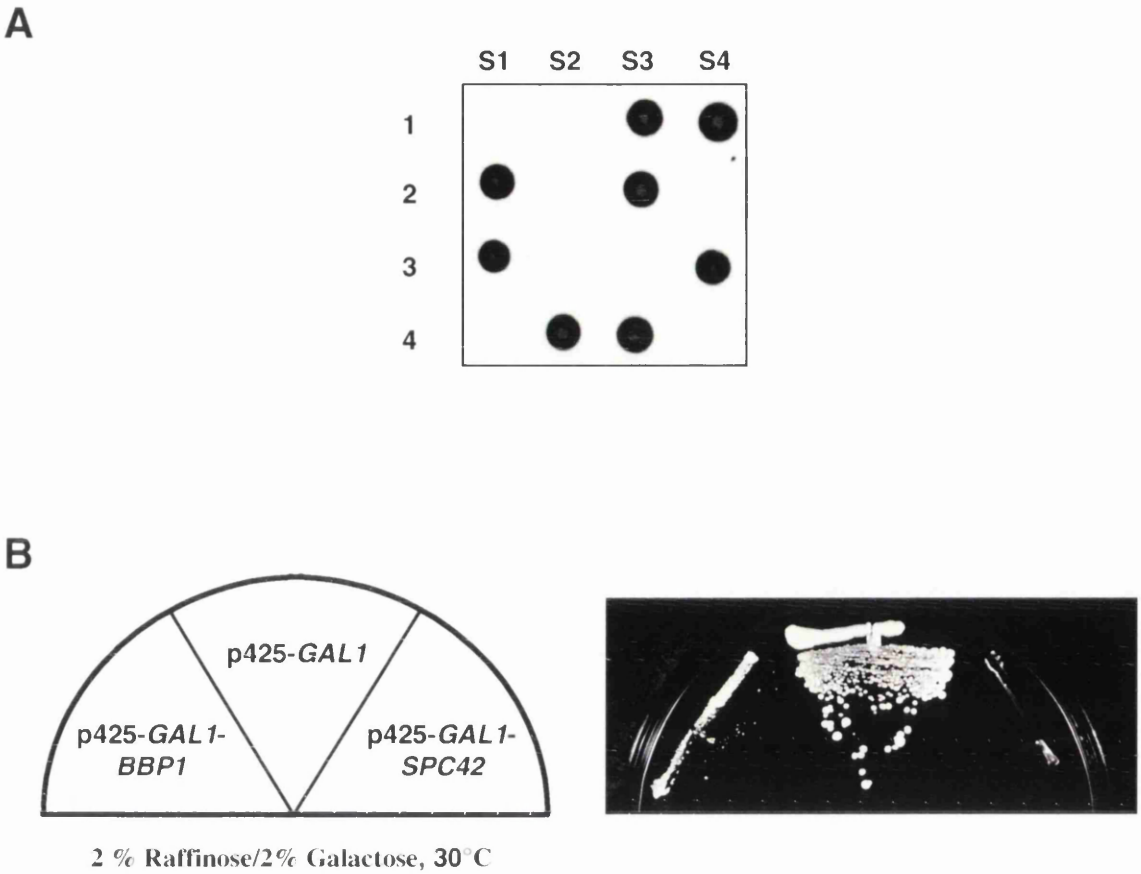

Figure 10: *BBP1* is an essential gene and its overexpression is toxic. (**A**) Sporeanalysis of YCS1 (*BBP1/Δbbp1::HIS3MX4*). Two out of four spores (S1, S2, S3, S4) lacked *BBP1* and were unable to grow into colonies. Four tetrades were dissected (lane 1-4) (**B**) Cells containing p425-*GAL1-BBP1* and p425-*GAL1-SPC42* were unable to grow on plates containing 2% Raffinose and 2% Galactose. The control cells containing p425-*GAL1* were able to grow. (**C**) Overexpression of *BBP1* under the *GAL1* promotor in liquid culture. Cells containing p425-*GAL1-BBP1 or* p425-*GAL1* were grown in 2 % Raffinose/2% Galactose medium and samples were taken at several time points after induction as indicated. Cell extracts were analysed by Western blotting with polyclonal rabbit anti-Bbp1p antibodies; strain S1: YPH499 containing p425-*GAL1*; strain S2: YPH499 containing p425-*GAL1-BBP1*.

3.4.3 Analysis of temperature sensitive mutants of *BBP1*

Since overexpression of *BBP1* neither caused a distinct arrest in the cell cycle nor an obvious alteration in the phenotype, conditional lethal mutants of *BBP1* were constructed as a tool to further investigate the function of Bbp1p.

3.4.3.1 Temperature sensitive mutants of BBP1

The function of Bbp1p was determined by the analysis of yeast strains carrying a mutated *BBP1* gene. Conditional lethal mutants of *BBP1* were constructed using PCR based techniques (see 2.2.18). Primers were designed to bind to the regions 167 bp upstream of start (*BBP1*-M1) and 138 bp downstream of stop (*BBP1*-M2) of *BBP1*, therefore, including the complete ORF of *BBP1*. Firstly, the optimal PCR conditions for the amplification of the *BBP1* containing fragment were determined as standard PCR conditions (see 2.2.1.1) with 2.5 mM $MgCl_2$ (template pCS14). For the mutagenic PCR these optimal conditions were changed as described in 2.2.1.3. PCR fragments obtained from reactions with 0.08 mM ATP and 1 mM $MnCl_2$ or 0.2 mM ATP and 1.5 mM $MnCl_2$ were selected. The ORF of *BBP1* contains two *Hpa*I restriction sites at 297 bp and 1327 bp downstream from start. This HpaI-fragment was cut out of *BBP1* which had been cloned into a single-copy *TRP1*-based vector (pCS17, pRS414-*BBP1*). The *Hpa*I-restricted vector and the PCR fragments obtained by mutagenic PCR were transformed into YCS17 (*BBP1* shuffle strain, see 2.2.17) and the transformants were selected for growth on plates lacking histidine and tryptophan. Due to homologues recombination the *Hpa*I-fragment was ligated into the cut pRS414-*BBP1* vector. About 25,000 transformants were obtained. The pRS316 plasmid carrying a wild type copy of *BBP1* was counter selected on 5-FOA plates (see 2.2.20) and afterwards colonies were replica plated on SC-His-Trp plates (see 2.2.19) and tested for failure to grow at different temperatures. As a result, 25 potentially temperature sensitive mutants were obtained. From these mutants, 17 of the pRS414-*bbp1* plasmids could be isolated by plasmid rescue (see 2.2.10.2) and were amplified in *E. coli*. After re-transformation into the *BBP1* shuffle strain 7 plasmids still caused a conditional lethal phenotype. Three strains with different restrictive temperatures were selected and the mutated

genes were integrated into the chromosomal *TRP1* locus. The mutations were confirmed by sequencing (see 2.2.14). Thus, the following strains were obtained:

YCS64 (*bbp1-1*)	restrictive temperature: 35 °C
	missense mutations: N97S, H135R, N234D, D243E
YCS65 (*bbp1-3*)	restrictive temperature: 37 °C
	missense mutations: M55T, N92D, E128D, N144M, I152K, I155R, L168I, V208D, E211G, K221R
YCS66 (*bbp1-2*)	restrictive temperature: 33 °C
	missense mutations: T66P, S106N, M230S

3.4.3.2 Suppression of conditional mutants of BBP1 by other SPB components

All three conditional lethal mutants of *BBP1* (*bbp1-1, bbp1-2, bbp1-3*) were tested for rescue of growth by overexpression of other SPB components and SPB associated proteins. Suppression of temperature sensitive mutants might be explained by the ability of the overexpressed protein to function downstream of the mutated protein or by its ability to take over or assist with the function of the mutated protein. Therefore, growth of the mutant strain at the restrictive temperature due to overexpression of another gene indicates a possible interaction or functional analogy of proteins. In this experiment various known SPB components were tested (Table VIIII). Firstly, all three mutants grew like wild type cells when additional copies of *BBP1* were reintroduced. Overexpression of *SPC42* coding for an IL2/central plaque component improved the growth of YCS64 and YCS66 strains very slightly. High gene dosage of *SPC34*, coding for a SPB component with unknown function (Wigge *et al.*, 1998), allowed *bbp1-2* to grow well at 33 °C and slightly at 35 °C. This effect was not observed in the case of *bbp1-1* and *bbp1-3*. An increase in the growth defect of *bbp1-1* and *bbp1-3* was recorded for the mild overexpression of the half-bridge component *KAR1* (see 3.6). Such an effect has been described before for conditional lethal mutants of *CDC31* (Vallen *et al.*, 1994) and *SPC29* (Elliott *et al.*, 1999). Additional copies of *SPC19*, *SPC24*, *SPC25*, *SPC29*, *SPC72*, *SPC97*, *SPC98*, *SPC105*, *STU2*, *CDC31*, *TUB1*, *TUB4*, *CMD1*, and *CNM67* did not affect the growth of the mutant strains.

Table VIIII: Effect of high gene dosage of indicated genes on mutants in *BBP*1 (*bbp1-1*, *bbp1-2* and *bbp1-3*)

YCS64 (*bbp1-1*)			**Temperature in °C**			
gene	**plasmid**	**plasmid name**	**30**	**33**	**35**	**37**
BBP1	pRS425	pCS14-2	+ + +	+ + +	+ + +	+ + +
SPC19	pRS425	pSM535-6	+ + +	+ +	-	-
SPC24	pRS425	pSM541-3	+ + +	+ +	-	-
SPC25	pRS425	pSM538-1	+ + +	+ +	-	-
SPC29	pRS425	pSE3-6	+ + +	+ +	-	-
SPC34	pRS425	pSE10	+ + +	+ +	-	-
SPC42	pRS425	pSE17-2	+ + +	+ + +	+	-
SPC72	pRS426	pSM458-1	+ + +	+ +	-	-
SPC97	pRS425	pMK11-15	+ + +	+ +	-	-
SPC98	pRS425	pSM271	+ + +	+ +	-	-
SPC105	pRS425	pSM544-1	+ + +	+ +	-	-
CNM67	pRS425	pSM568-1	+ + +	+ +	-	-
STU2	pRS425	pSM603-1	+ + +	+ +	-	-
KAR1	pRS315	pSM39-2	+ + +	-	-	-
CDC31	pRS425	pSM234-1	+ + +	+ +	-	-
TUB1	pRS425	pSM553-3	+ + +	+ +	-	-
TUB4	pRS426	pSM347-4	+ + +	+ +	-	-
CMD1	pRS426	pSM292-3	+ + +	+ +	-	-
	pRS315		+ + +	+ +	-	-
	pRS425		+ + +	+ +	-	-
	pRS426		+ + +	+ +	-	-
YCS65 (*bbp1-3*)			**Temperature in °C**			
gene	**plasmid**	**plasmid name**	**30**	**33**	**35**	**37**
BBP1	pRS425	pCS14-2	+ + +	+ + +	+ + +	+ + +
SPC19	pRS425	pSM535-6	+ + +	+ + +	+ +	-
SPC24	pRS425	pSM541-3	+ + +	+ + +	+ +	-
SPC25	pRS425	pSM538-1	+ + +	+ + +	+ +	-
SPC29	pRS425	pSE3-6	+ + +	+ + +	+ +	-
SPC34	pRS425	pSE10	+ + +	+ + +	+ +	-
SPC42	pRS425	pSE17-2	+ + +	+ + +	+ +	-
SPC72	pRS426	pSM458-1	+ + +	+ + +	+ +	-
SPC97	pRS425	pMK11-15	+ + +	+ + +	+ +	-
SPC98	pRS425	pSM271	+ + +	+ + +	+ +	-
SPC105	pRS425	pSM544-1	+ + +	+ + +	+ +	-
CNM67	pRS425	pSM568-1	+ + +	+ + +	+ +	-
STU2	pRS425	pSM603-1	+ + +	+ + +	+ +	-
KAR1	pRS315	pSM39-2	+ + +	+ + +	+	-
CDC31	pRS425	pSM234-1	+ + +	+ + +	+ +	-
TUB1	pRS425	pSM553-3	+ + +	+ + +	+ +	-
TUB4	pRS426	pSM347-4	+ + +	+ + +	+ +	-
CMD1	pRS426	pSM292-3	+ + +	+ + +	+ +	-
	pRS315		+ + +	+ + +	+ +	-
	pRS425		+ + +	+ + +	+ +	-
	pRS426		+ + +	+ + +	+ +	-

Table VIIII continued						
YCS66 (*bbp1-2*)			**Temperature in °C**			
gene	**plasmid**	**plasmid name**	**30**	**33**	**35**	**37**
BBP1	pRS425	pCS14-2	+ + +	+ + +	+ + +	+ + +
SPC19	pRS425	pSM535-6	+ + +	-	-	-
SPC24	pRS425	pSM541-3	+ + +	-	-	-
SPC25	pRS425	pSM538-1	+ + +	-	-	-
SPC29	pRS425	pSE3-6	+ + +	-	-	-
SPC34	pRS425	pSE10	+ + +	++	+	-
SPC42	pRS425	pSE17-2	+ + +	+	-	-
SPC72	pRS426	pSM458-1	+ + +	-	-	-
SPC97	pRS425	pMK11-15	+ + +	-	-	-
SPC98	pRS425	pSM271	+ + +	-	-	-
SPC105	pRS425	pSM544-1	+ + +	-	-	-
CNM67	pRS425	pSM568-1	+ + +	-	-	-
STU2	pRS425	pSM603-1	+ + +	-	-	-
KAR1	pRS315	pSM39-2	+ + +	-	-	-
CDC31	pRS425	pSM234-1	+ + +	-	-	-
TUB1	pRS425	pSM553-3	+ + +	-	-	-
TUB4	pRS426	pSM347-4	+ + +	-	-	-
CMD1	pRS426	pSM292-3	+ + +	-	-	-
	pRS315		+ + +	-	-	-
	pRS425		+ + +	-	-	-
	pRS426		+ + +	-	-	-

BBP1 complements the temperature dependent phenotype of mutants in *BBP1*. High gene dosage of *SPC42* rescues growth in *bbp1-1* and *bbp1-2* cells. *SPC34* is a high gene dosage suppresser of *bbp1-2* cells. *KAR1* on a centromer based plasmid has a negative effect on *bbp1-1* and *bbp1-3* cells. Strains were transformed with the indicated plasmids and cells were grown on plates for 3 d at the indicated temperatures. Wild type like growth is indicated by (+++) and slight growth by (+). (-) indicates no growth of strains at this temperature.

3.4.3.3 The temperature sensitive mutant bbp1-1 arrests in G_2 and is defective in chromosome segregation and proper spindle formation

The conditional lethal mutant *bbp1-1* (YCS64) was investigated throughout the cell cycle by FACS analysis and indirect immunofluorescence. *Bbp1-1* cells and wild type cells were grown in liquid culture at 23 °C, the permissive temperature of *bbp1-1* cells, to an OD_{600}=0.3. The cultures were arrested with α–factor in G_1-phase of the cell cycle (t=0) (see 2.2.21). After α–factor was removed by washing with YPD-medium the cells progressed synchronously through the cell cycle. Simultaneously, the cells were shifted to 37 °C, the restrictive temperature of *bbp1-1* cells. Samples of *bbp1-1* and control cells were taken at t=0 and every 30 min after release from G_1-arrest for 3 h.

Most wild type and *bbp1-1* cells were arrested in G_1-phase before release from α–factor arrest (t=0) as indicated by the 1n DNA content seen in the FACS analysis (Figure 11A). DNA replication was completed in both strains 1.0 h after release from α–factor arrest with cells now harbouring a 2n DNA content. Wild type cells underwent mitosis and separated their chromosomes between time points t=1 h and t=1.5 h returning to single cells with 1n DNA content (Figure 11A, Diagram 1). In contrast, *bbp1-1* cells arrested with a G_2 DNA content and did not complete mitosis (Figure 11A, Diagram 2).

SPB duplication (anti-Spc72p antibodies), spindle formation (anit-tubulin antibodies) and chromosome segregation (DNA stained with DAPI) were monitored throughout the cell cycle by immunofluorescence microscopy (see 2.2.33.2). The percentages of different morphological phenotypes of *bbp1-1* and wild type cells of the time-course samples were counted and are displayed in Table X. Wild type cells duplicated their SPBs, formed a mitotic spindle and separated their chromosomes (Figure 11, B1 and B2; Table X). *Bbp1-1* cells instead, showed various defects in mitosis (Figure 11, B3-B6; Table X). At 1.5 h after release, about 40 % of *bbp1-1* cells contained only one anti-Spc72p staining representing the SPB or two SPBs close together. This suggested that cells failed to duplicate their SPB or had disintegrated a non-functional SPB (Figure 11, B3). About 60 % of *bbp1-1* cells duplicated their SPB but displayed major mitotic spindle defects (Figure 11, B4-B6). If a mitotic spindle was visible it was an

asymmetrical spindle consisting of a large bundle of microtubules emerging from one SPB and only a few microtubules were nucleated by the other SPB (Figure 11, B4). The majority of cells with two spindle pole bodies (40 %) did not have a mitotic spindle. In these cells, one SPB was associated with a large array of microtubules and the other SPB only nucleated some, which seemed to be cytoplasmic microtubules (Figure 11, B5 and B6). Both SPBs always seemed to nucleate cytoplasmic microtubules which might explain why the positioning of the SPBs in the mitotic cells was normal. Most likely as an effect of the spindle defects, 99 % of *bbp1-1* cells failed to separate their chromosomes (Figure 11, B4-B6). The DAPI staining region always remained with the SPB that was able to nucleate the majority of microtubules. Interestingly, this functional SPB remained in the mother cell which could be identified as such because it still contained the mating projectile (shmoo) from the α-factor arrest. To summarise, immunofluorescence microscopy revealed that *bbp1-1* cells were defective in SPB duplication, spindle formation and DNA separation.

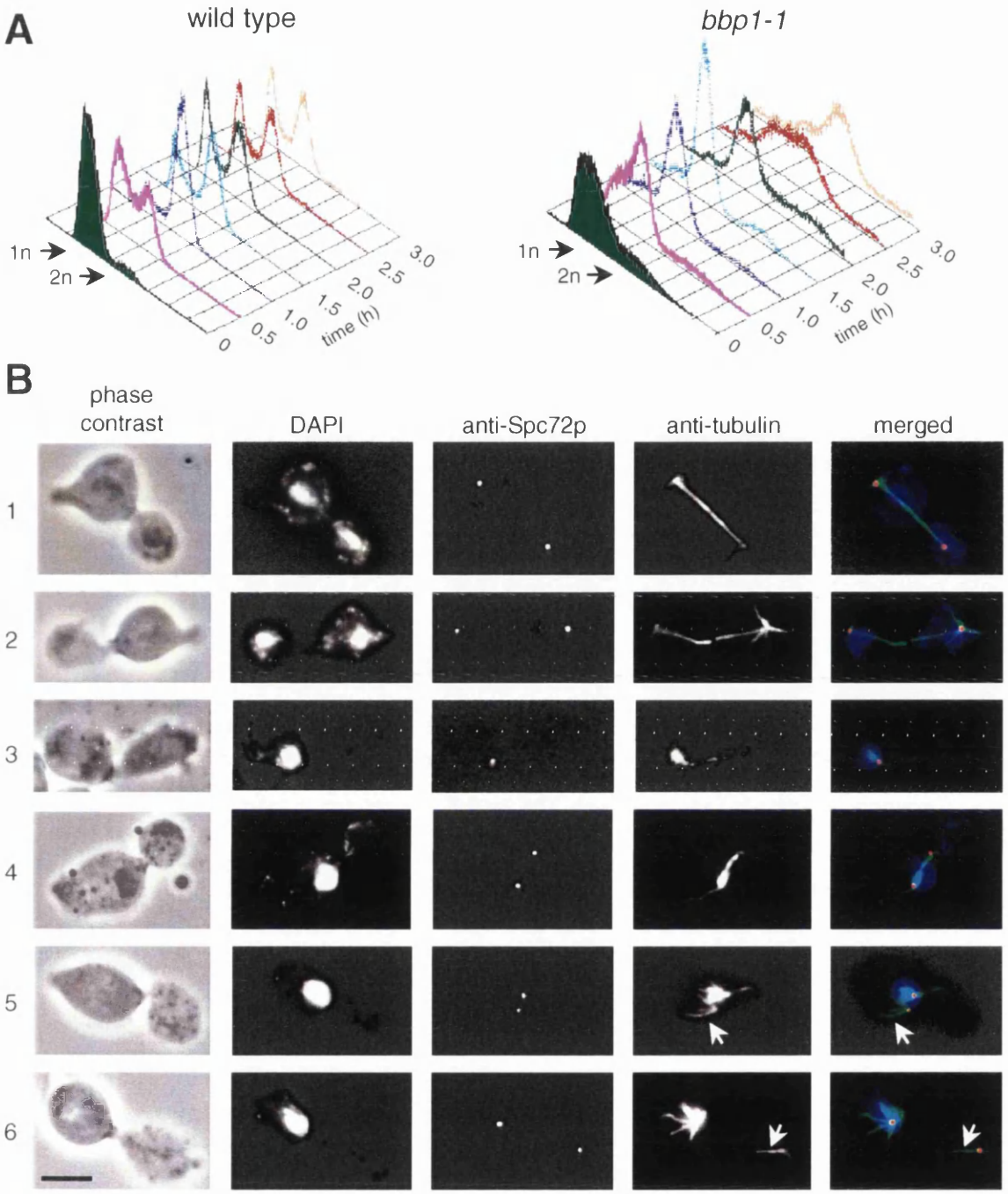

Figure 11: Mutants in *BBP1* are defective in spindle formation and chromosome segregation. Wild type and *bbp1-1* cells were arrested with α-factor in G_1 of the cell cylce. Cells were released from the arrest (t=0) and continued synchronously through the cell cycle. At the same time, cells were shifted to the the non-permissive temperature (37 °C). (**A**) The DNA content of wild type and *bbp1-1* cells was followed over time by flow cytometry. (**B**) Wild type (B1 and B2) and *bbp1-1* (B3-B6) cells were analysed 1.5 h after shift to 37 °C by indirect immunofluorescence with affinity-purified rabbit anti-Spc72p and monoclonal mouse anti-tubulin antibodies. The DNA was stained with DAPI. The anti-Spc72p (red), anti-tubulin (green) and DAPI (blue) signals were merged. Bar 5 µm.

Table X: Phenotypic Analysis of *bbp1-1*.

	time in h	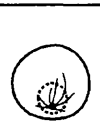	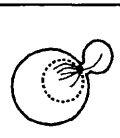	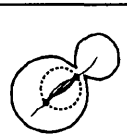	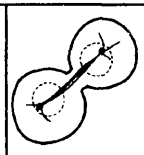	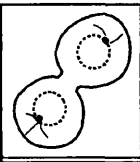	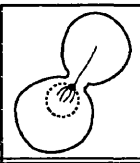	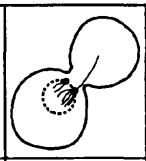	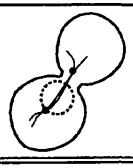	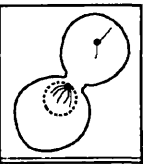
wild type	0	100	0	0	0	0	0	0	0	0
	0.5	25	70	5	0	0	0	0	0	0
	1.0	1	30	38	31	0	0	0	0	0
	1.5	30	3	2	60	5	0	0	0	0
bbp1-1	0	100	0	0	0	0	0	0	0	0
	0.5	18	82	0	0	0	0	0	0	0
	1.0	2	21	0	2	0	31	16	8	20
	1.5	0	0	0	1	0	40	2	14	43

Wild type and *bbp1-1* cells were synchronised with α-factor and shifted to 37 °C as described in Figure 11. Cells were prepared for immunofluorescence microscopy using rabbit anti-Spc72p and mouse anti-tubulin antibodies. DNA was stained with DAPI. About 200 cells were counted per time point. The SPB is indicated as dot. The DAPI staining region is drawn as a dotted circle. Values are given as percentages.

3.4.3.4 The bbp1-1 cells are defective in inner plaque formation

As shown in the immunofluorescence experiment 40 % of *bbp1-1* cells contained only one SPB at time points when wild type cells had already duplicated their SPBs and all *bbp1-1* cells with two SPBs, contained one SPB that was defective in microtubule nucleation. Therefore, it was assumed that *bbp1-1* cells fail to properly duplicate their SPB. To investigate the defects in duplication and especially, of the non-functional SPB, *bbp1-1* cells were examined by electron microscopy. Furthermore, components of the central and inner plaque of the SPB where tagged with GFP and the assembly of the new SPB was studied in *bbp1-1* cells by direct fluorescence microscopy.

3.4.3.4.1 Analysis of *bbp1-1* cells by morphological electron microscopy

Cultures of wild type and *bbp1-1* cells were synchronised in the cell cycle as described in 4.3.2 and samples were prepared for electron microscopy (see 2.2.34.1) at time-points t=1 h, t=1.25 h and t=1.5 h after shift to the non-permissive temperature. This time range was chosen according to the immunofluorescence experiment (see 3.4.3.3) which suggested that complications in SPB duplication occur in this time interval. *Bbp1-1* cells were able to perform initial steps of SPB duplication just like wild type cells. In G_1-cells (t=0.45 h) the enlarged satellite/duplication plaque was visible at the end of the half-bridge (n=20) (Figure 12A). The duplication plaque was still connected with the mother SPB via the half bridge (Figure 12A). Wild type cells then formed side-by-side SPBs (t=1.25 h) and the newly formed SPB was able to nucleate nuclear microtubules (Figure 12B, two serial sections). This step of SPB duplication was not observed in *bbp1-1* cells. Here, a second SPB could be seen still connected to the mother SPB via the bridge, as expected for side-by-side SPBs, but the new SPB did not have an inner plaque and did not nucleate nuclear microtubules (n=25) (Figure 12C, two serial sections). This suggested that the insertion of the duplication plaque is delayed or defective in *bbp1-1* cells. After 1.5 h only one normal looking SPB was observed in most serial sections through *bbp1-1* cells (n=50). Only in n=2 cases a small structure was seen which nucleated some nuclear and cytoplasmic microtubules and was located opposite a normally looking SPB (Figure 12, D and E; serial sections). These structures were very difficult to identify in serial sections of whole cells. Mainly,

because they only nucleated very few microtubules and they were only slightly larger than nuclear pores. Therefore, it was difficult not to mistake the small second SPB for a nuclear pore. This might explain why a second SPB was not identified in 60 % of cells as would have been expected from the immunofluorescence experiment (60 % of cells contained two SPB signals at t=1.5 h by immunofluorescence, compare 3.4.3.3). When a second SPB was detected in *bbp1-1* cells no proper spindle was seen connecting the two SPBs as normally the case for wild type cells (Figure 12, compare D and E with F). The few nuclear microtubules organised by the smaller SPB failed to connect to the microtubules of the other SPB. Although the small SPB nucleated fewer microtubules than normal, it must have developed some inner plaque structure, which nucleated microtubules via the γ-tubulin binding complex.

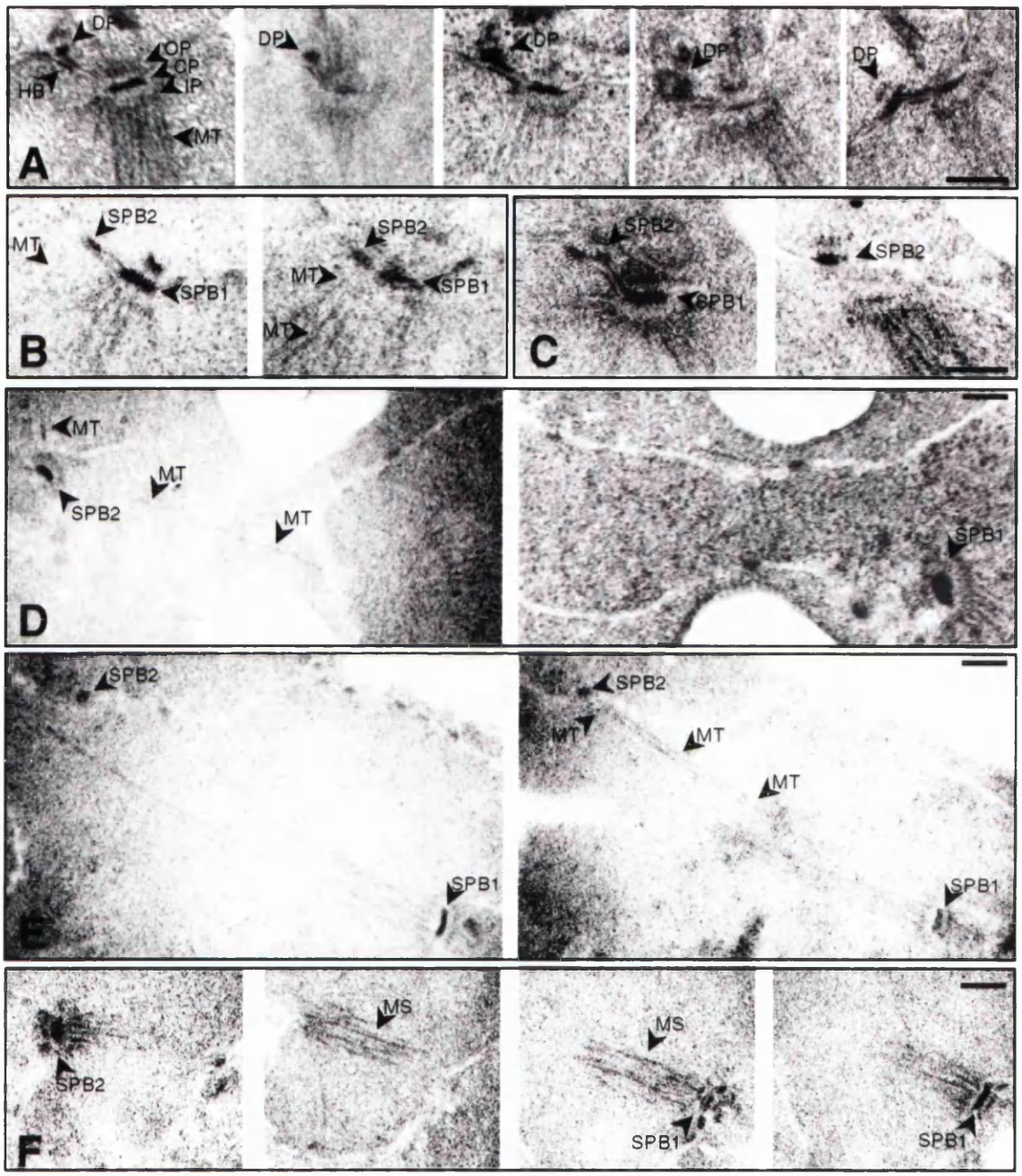

Figure 12: Mutants in *BBP1* are defective in SPB duplication. Synchronised wild type (**B** and **F**) and *bbp1-1* (**A**, **C**, **D**, **E**) cells were prepared for morphological EM 1 h (**A**), 1.25 h (**B**) and 1.5 h (**D** -**F**) after they had been shifted to 37°C (t=0). The mother SPB consists of an outer (OP), central (CP) and inner (IP) plaque. The duplication plaque (DP) is associated with the distal tip of the half-bridge (HB). Microtubules (MT) form functional mitotic spindles (MS) only in wild type cells. (**A**) Five micrographs of *bbp1-1* cells show the functional mother SPB with a normal duplication plaque. (**B**) Two serial sections through wild type side-by-side SPBs. (**C**) Two serial sections through *bbp1-1* cells. The duplication plaque (SPB2) is not properly inserted in the nuclear envelope (NE) and does not connect nuclear microtubules (MT). (**D** and **E**) Two serial sections through two nuclei of *bbp1-1* cells. SPB1 shows wild type morphology while SPB2 is smaller and associates with fewer nuclear microtubules. (**F**) Four serial sections through wild type cells. SPB1 and SPB2 form a mitotic spindle. Bars (A-F), 0.25 μm.

3.4.3.4.2 Analysis using GFP-tagged outer and central plaque components

To further investigate the defects of the smaller second SPB, *bbp1-1* strains were constructed which expressed *SPC42-GFP* or *SPC110-GFP* gene fusions. Spc42p is a SPB component which localises to the cytoplasmic side of the central plaque (Rout and Kilmartin, 1991). The inner plaque component Spc110p assembles into the SPB from the nuclear side (Kilmartin and Goh, 1996; Rout and Kilmartin, 1990) after the duplication plaque was inserted into the nuclear envelope (Adams and Kilmartin, 1999). The strains were arrested with α–factor and at t=1.5 h after release and shift to 37 °C, cells were analysed by fluorescence microscopy (Figure 13, A and B). GFP signals representing the inner (*SPC110*, Figure 13A) or central (*SPC42*, Figure 13B) plaque structures of SPBs were counted (Table XI). About 46 % of *bbp1-1 SPC42-GFP* cells had one and 54 % had two central plaque signals. For the strain containing a GFP marker for the inner-plaque it was observed that 84 % of cells had only one, while 16 % had two signals. In addition, the indirect immunofluorescence experiment (see 3.4.3.3) using antibodies against the outer plaque component Spc72p showed that 40 % of cells had one outer plaque staining and 60 % had two signals (Table X). Taken together, about 54 % to 60 % of cells contained two SPBs. But, only about one third of these duplicated SPBs had assembled an inner plaque structure. Interestingly, if two GFP signals were observed one was always fainter than the other one. This supported the finding by electron microscopy that one SPB was smaller than normal (Figure 12, C and D).

Taken together, *bbp1-1* cells displayed a defect in SPB duplication. The new SPB was smaller and could only with 30 % probability assemble an inner plaque. Small size and lack of an inner plaque structure lead to failure in microtubule nucleation, spindle formation and chromosome segregation.

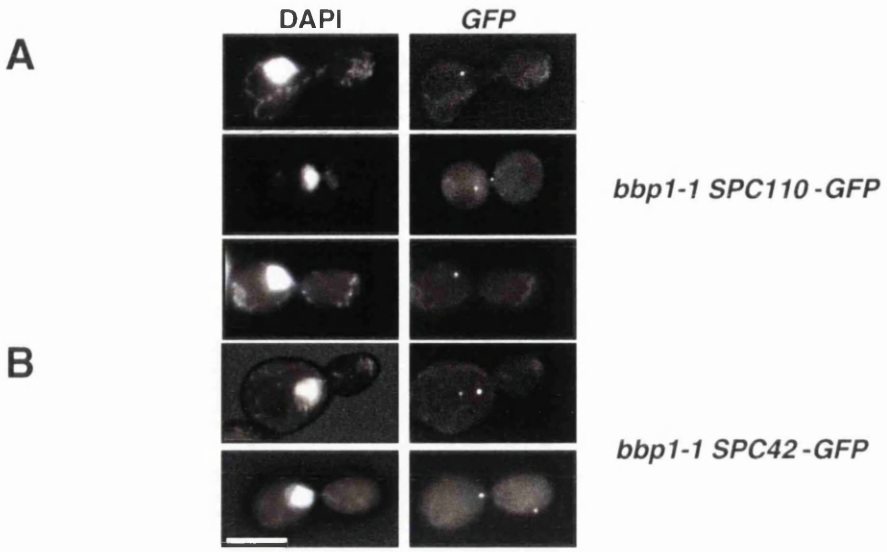

Figure 13: The majority of *bbp1-1* cells fails to assemble an inner plaque. *Bbp1-1* cells containing (**A**) *SPC110-GFP* or (**B**) *SPC42-GFP* were synchronised with α-factor. 1.5 h after release and shift to the non-permissive temperature (37 °C) cells were fixed with paraformaldehyde and DNA was stained with DAPI. The cells were analysed by fluorescence microscopy and 54 % of large budded *bbp1-1 SPC42-GFP* cells contained two SPB signals while only 16 % of *bbp1-1 SPC110-GFP* cells with two SPB signals were detected (see Table XI).

Table XI: The majority of *bbp1-1* cells fails to assemble an inner plaque

phenotype		*bbp1-1 SPC42*-GFP		*bbp1-1 SPC110*-GFP	
		counts	in %	counts	in %
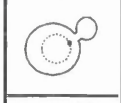	one SPB	1	46	0	84
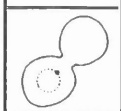	one SPB	25		48	
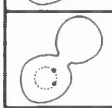	two SPBs	22	54	8	16
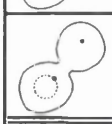	two SPBs	9		1	
total		57	100	57	100

Only about 54 % of ***bbp1-1*** cells contain two SPBs at the restricitve temperature. Only 1/3 of the duplicated SPBs contain an inner plaque structure. *Bbp1-1* cells containing *SPC42-GFP* (central plaque) or *SPC110-GFP* (inner plaque) were prepared as described in Figure 13 (see directly above). 57 cells were counted at 1.5 h after release from α-factor and shift to the non-permissive temperature (37 °C). The SPB is indicated as a dot. The DAPI staining region is drawn as a dotted circle.

3.4.4 Two-hybrid analysis of *BBP1* with components of the γ-tubulin complex

Since *BBP1* was originally identified as a high gene dosage suppresser of mutants in *SPC98*, the possible interaction of Bbp1p with Spc98p, a component of the γ-tubulin complex, was further investigated by two-hybrid analysis (see 2.2.28). *BBP1* fused to the LexA DNA-binding domain or to the *GAL4* activation domain did not show positive interactions in any combination with two-hybrid vectors containing *SPC98*, *SPC97* or *TUB4*, genes coding for the three components of the yeast γ-tubulin complex. Furthermore, *BBP1* did not interact with *TUB4* in the yeast two-hybrid system in a strain background slightly overexpressing *SPC97* or *SPC98*. Taken together, the two-hybrid system did not indicate any interaction of Bbp1p with components of the yeast γ-tubulin complex.

3.5 Bbp1p interacts with Bfr1p genetically

It had been reported by Xue et al. (1996) that Bbp1p interacts with Bfr1p in the yeast two-hybrid system. To investigate if Bfr1p could be interacting with Bbb1p the following experiments were designed.

3.5.1 Two-hybrid interactions of Bfr1p

BFR1 and *BBP1* were analysed in the yeast two-hybrid. Apart from *BBP1*, genes coding for SPB components like *SPC29*, *KAR1* and *CDC31* were tested for interaction with *BFR1*. In addition, *cdc31-16* that causes *CDC31* to be independent of *KAR1* was investigated (Vallen *et al.*, 1994). The genes were cloned into the yeast two-hybrid vectors pEG202 or pMM5 and pACTII or pMM6. The plasmids were transformed into YPH500 or SGY37 cells and two-hybrid vectors were combined by mating of yeast cells with opposite mating type. The resulting diploid cells were tested for interaction of proteins encoded by the two-hybrid vectors by X-Gal overlay assay (see 2.2.28). Blue colour indicated the interaction of proteins and could be seen for Bfr1p/Bbp1p, Bfr1p/Spc29p and Bfr1p/Cdc31p only in the combination with Bfr1p fused to the *GAL4* domain (Figure 14A). Bfr1p in the LexA vector pMM5, did not show these

interactions. Bfr1p did not show any interaction with Cdc31-16p, Kar1p or itself. As controls, interactions with the empty control plasmids were measured. All controls were negative, apart from Cdc31p with pMM6. However, the activation of the reporter gene was much weaker than seen for the Bfr1p/Cdc31p interaction. It was therefore concluded, that Bfr1p interacts with Bbp1p, Spc29p and Cdc31p in the yeast two-hybrid system.

3.5.2 *BFR1* is not a high gene dosage suppresser of conditional lethal mutants of *BBP1*

To further investigate if Bfr1p could interact with Bbp1p, conditional lethal mutants in *BBP1* were transformed with the pRS415 plasmid containing *BFR1* under the *ADH*-promotor (pCS84). Transformants were checked for growth at the restrictive temperature. High gene dosage of *BFR1* did not suppress the growth defect of the mutants (data not shown).

3.5.3 Bfr1p and Bbp1p do not co-precipitate

Proteins that interact with each other often form stable complexes which can be enriched by immunoprecipitation (Elliott *et al.*, 1999; Knop and Schiebel, 1997). If Bfr1p and Bbb1p interacted with each other it might be possible to precipitate the two proteins together. Wild type cells and cells expressing Bfr1p-3HA-tag were lysed under optimal extraction conditions for Bbp1p (100 mM NaCl, 1 % (v/v) Triton-X-100, see 2.2.22.3) and were incubated with anti-HA antibodies coupled to sepharose beads (see see 2.2.24 and 2.2.25.3). Immunoprecipitates were analysed by Western blotting using mouse monoclonal anti-HA and rabbit polyclonal anti-Bbp1p antibodies (see 2.2.13). Bfr1p-3HA had been precipitated and the control did not show any unspecific binding of Bfr1p-3HA to the sepharose beads. However, Bbp1p was not co-precipitated (data not shown).

3.5.4 Bfr1p is localised in the cytoplasm and at the nuclear envelope

It proved to be difficult to establish a direct interaction of Bbp1p and Bfr1p. However, a localisation of Bfr1p in proximity to Bbp1p at the SPB could confirm the possibility

of an interaction of the proteins, even if this interaction might not be direct but via other proteins. Bfr1p was localised by indirect immunofluorescence. Cells expressing *BFR1-9Myc* were prepared for immunofluorescence microscopy and were incubated with antibodies recognising the Myc epitope of the protein (see 2.2.33.2). The red CY3-signal of the secondary antibody representing Bfr1p showed cytoplasmic staining with a slight increase of the signal intensity around the DAPI stained DNA region (Figure 14B). As such, Bfr1p might be a cytoplasmic protein that is enriched at or around the nuclear envelope where it could potentially interact with Bbp1p.

3.6 Bbp1p interacts with the half-bridge component Kar1p

As described above (see 3.4.3.2), *KAR1*, on a centromere-based plasmid, increased the growth defect of *bbp1-1* and *bbp1-2* cells (Table VIIII, Figure 15A). This finding was especially interesting, since this was also the case for other conditional lethal mutants of SPB components like *spc29* and *cdc31* (Elliott *et al.*, 1999; Vallen *et al.*, 1994) which are also defective in SPB duplication. The *bbp1-1* mutant displayed a defect in proper SPB duplication (see 3.4.3.3 and 3.4.3.4) and Bbp1p was in some cases localised close to the half-bridge (see 3.3). An interaction with the half-bridge component Kar1p seemed likely and could be established using the yeast two-hybrid system (Figure 15B). *KAR1* in a yeast two-hybrid vector containing the *Gal4* activation domain interacted with *BBP1* fused to the *LexA* DNA-binding domain and activated the reporter gene. However, no positive signal was seen for the combination of *BBP1* fused to *Gal4* with *KAR1* fused to *LexA*. Taken together, Bbp1p interacts genetically with Kar1p by negative suppression and in the yeast two-hybrid system.

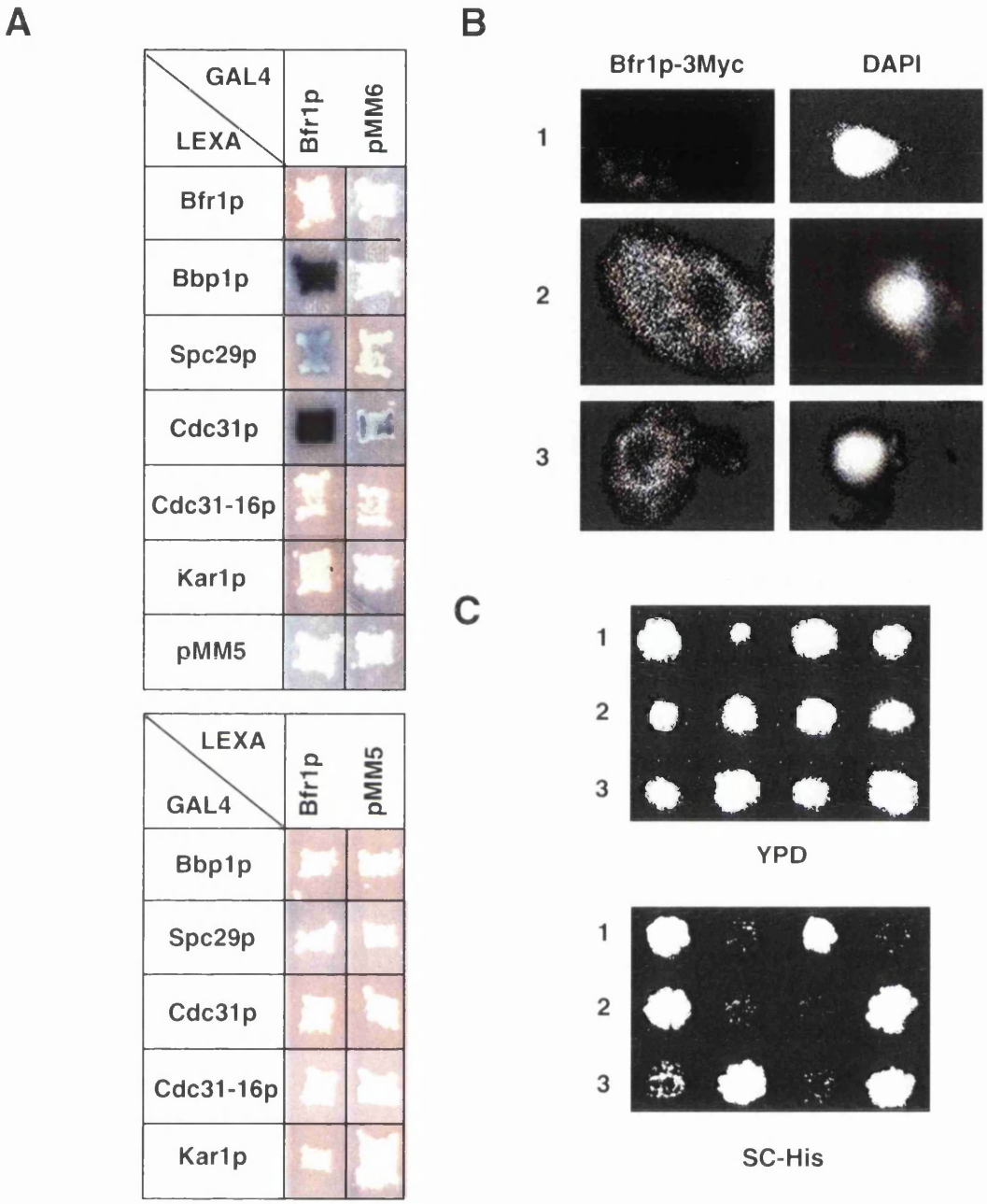

Figure 14: The non-essential *BFR1* codes for a cytoplasmic protein that is enriched at the nuclear envelope and interacts with SPB components. (**A**) Bfr1p interacts with the SPB components Bbp1p, Cdc31p and Spc29p in the yeast two-hybrid system, as indicated by the blue colour. Note: LexA-Cdc31p is slightly selfactivating. (**B**) Fluorescence microscopy of wild type cells (B1) and cells expressing Bfr1p-3Myc (B2 and B3). Cells were incubated with mouse monoclonal anti-Myc antibodies and DNA was stained with DAPI. (**C**) Sporeanalysis of YCS56 (*BFR1/Δbfr1::HIS3MX4*). All four spores can grow into colonies and two out of four spores harbour a copy of the *HIS3* gene.

A

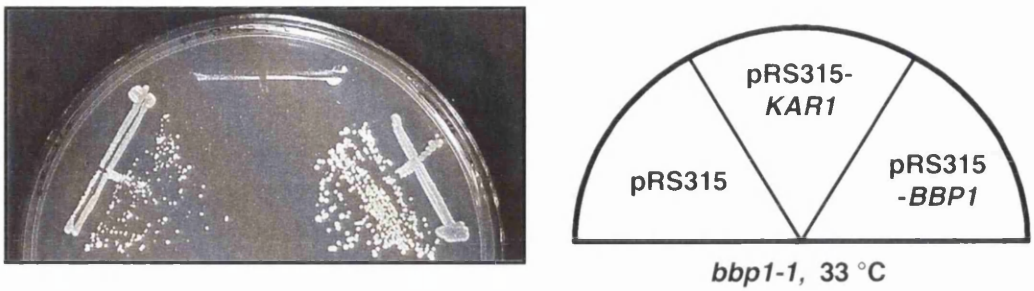

B

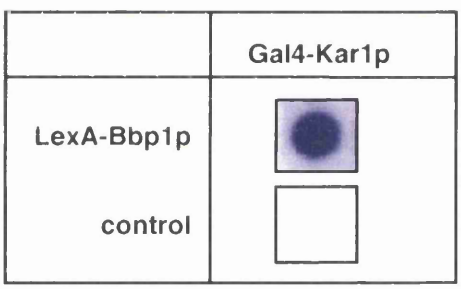

Figure 15: *BBP1* interacts with *KAR1*. (**A**) *KAR1* on a centromer-based plasmid increases the growth defect of *bbp1-1* cells. Strains were incubated for 3 d at 33 °C, a semi-permissive temperature for *bbp1-1*. (**B**) Bbp1p and Kar1p interact in the yeast two-hybrid system as indicated by the blue colour.

3.7 Bbp1p forms a complex with Mps2p

So far in this study, Spc34p and Kar1p were identified as proteins which interact with Bbp1p (see 3.4.3.2). Experiments that led to the finding of these interactions were designed to look specifically for interactions of Bbp1p with known SPB components. To identify novel proteins that directly interact with Bbp1p, Bbp1p-containing complexes were enriched by affinity chromatography.

3.7.1 Affinity precipitation of Bbp1p and identification of Mps2p

Bbp1p-ProA was enriched from cells carrying a functional gene fusion of *BBP1* and protein A. Wild type cells and cells expressing *BBP1-ProA* were lysed under optimal extraction conditions (see 2.2.23.3) and were incubated with IgG-sepharose beads to which protein A binds with high affinity (Knop and Schiebel, 1997). After several washing steps, proteins were eluted from the sepharose columns. The eluates were analysed on an 8 to 18 % SDS-PAGE gradient gel and proteins were stained according to Fairbanks (see 2.2.5.2.2). 15 g of cells were lysed to identify the bands of 45, 46 and 60 kD (Figure 16A). The binding of these proteins was dependent on the expression of *BBP1-ProA*, since they were not among the proteins of *BBP1* wild type cells that bound non-specifically to IgG-spharose (Figure 16A). The precipitates were analysed by Western blotting (see 2.2.13). The band at 60 kD was identified as Bbp1-ProA using anti-rabbit antibodies (data not shown) proving the immunoprecipitation of Bbp1p. However the known SPB components Kar1p, Spc110p, Cam1p, Tub4p, Spc97p and Spc98p were not present in the precipitate (data not shown).

Since two of the three protein bands remained unidentified, these protein bands were analysed by MALDI-MS in collaboration with Anna and Andrej Shevchenko at the EMBL, Heidelberg. The identification of proteins from yeast by MALDI-MS has been possible since the completion of the yeast genome sequence. Each protein band was digested with trypsin and the resulting peptide masses were determined by MALDI-MS (see 2.2.26). As expected, the protein band at 60 kD was identified as Bbp1p-ProA. The bands at 45 and 46 kD were identified as a duplet band of Mps2p (Figure 16B).

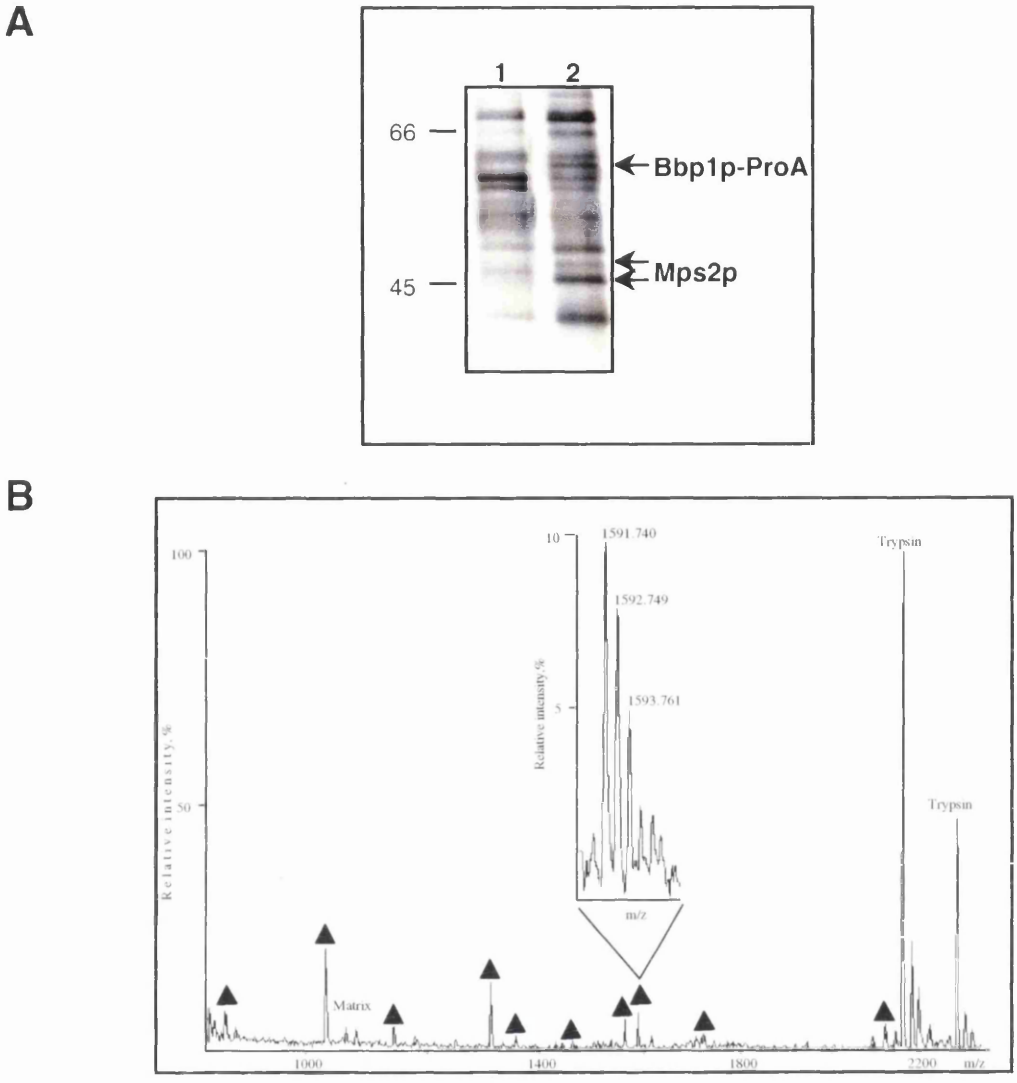

Figure 16: Mps2p affinity purifies with Bbp1p-ProA. (**A**) Bbp1p-ProA was enriched from lysates expressing Bbp1p-ProA by affinity purification using IgG sepharose beads (lane 2). The duplet band at about 45 kD was identified as Mps2p by MALDI (matrix-assisted laser desorption/ionisation) and was not present in the control lane (lane 1) which represents proteins that bound unspecifically to IgG sepharose. (**B**) Identification of Mps2p as Bbp1p interacting protein by MALDI. The mass spectrum acquired using 0.5 µl of the in gel digest of the 45 and 46 kD bands revealed 10 peptide ions, which matched the calculated masses of protonated tryptic peptides originating from Mps2p with mass accuracy better than 75 p.p.m (designated with filled triangles). These peptides covered about 30 % of the sequence of Mps2p. Ions that originated from the HCCA matrix ('Matrix') and intensive ions of autolysis products of trypsin ('Trypsin') are also designated in the spectrum. The inset presents an isotopically resolved cluster of the peptide ion with m/z 1591.740 [mass resolution of the instrument was better than 6500 (full width at half-maximum)].

At the time, *MPS2* was called *MMC1* (Mitotic mutability control 1) according to the MIPS (Munich, Germany) database. Data had been submitted suggesting a defect of *MMC1* mutants in mitosis. These data were published (Munoz-Centeno *et al.*, 1999) revealing that *MMC1* is *MPS2*. *MPS2* had been identified in 1991 in a screen for mutants with a defect in spindle formation (Winey *et al.*, 1991). Only at this later time point *MPS2* was allocated its DNA sequence in the database. *MPS2* functions in SPB duplication (Winey *et al.*, 1991) which is consistent with an interaction of Bbp1p and Mps2p since mutants in *bbp1* also show SPB duplication defects.

3.7.2 Verification of the MALDI-MS results by co-immunoprecipitation

The interaction of Bbp1p and Mps2p was verified by immunoprecipitation. The strains either expressed *MPS2-3HA BBP1-3Myc* or *MPS2 BBP1-3Myc* (control strain). Cells were lysed under the same conditions as in 3.7.1. Figure 17A (lane 1-4) shows Western blots of total yeast extract of these strains probed with anti-HA and anti-Myc antibodies. Cell lysates were incubated with anti-HA antibodies coupled to protein A sepharose and the precipitated proteins were analysed by SDS-PAGE (see 2.2.4.2) and Western blotting (see 2.2.13) using anti-HA and anti-Myc antibodies. Indeed, Bbp1p-3Myc was co-immunoprecipitated with Mps2p-3HA (Figure 17A, lane 6 and 8). This precipitation was specific, since it was not observed when the *MPS2 BBP1-3Myc* extract was used (Figure 17A, lane 5 and 7). Similarly, Mps2p-3Myc was co-immunoprecipitated with Bbp1p-3HA but not with Bbp1p using anti-HA antibodies (data not shown). This suggests that Bbp1p interacts with Mps2p and that both proteins are part of a common complex.

3.7.3 Bbp1p and Mps2p interact in the yeast two-hybrid system

The interaction of Bbp1p and Mps2p could also be verified using the yeast two-hybrid system (Figure 17B). *MPS2* and *BBP1* were fused to the *Gal4* or LexA domains. Both proteins interacted with each other in the two combinations. The plasmids combined with the empty vector controls were negative. Mps2p and Bbp1p were both able to interact with themselves and might therefore have the potential to form dimers.

A

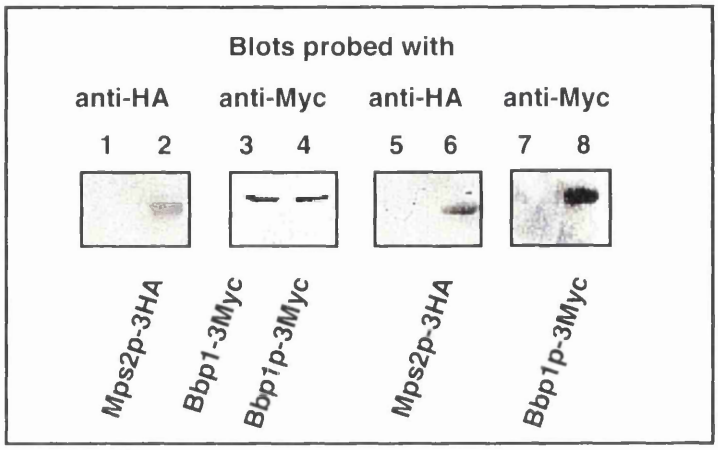

B

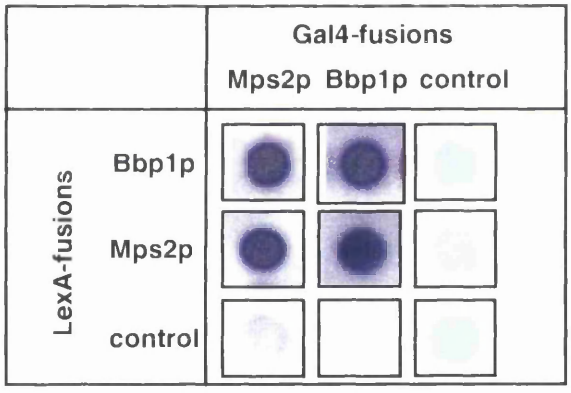

Figure 17: Bbp1p and Mps2p form a complex. (**A**) Bbp1p co-purifies with Mps2-3HA by immunoprecipitation. Lysates of cells expressing *BBP1-3Myc MPS2* (lane 1, 3, 5 and 7) or *BBP1-3Myc MPS2-3HA* (lane 2, 4, 6, 8) were analysed by Western blotting (lane 1-4) with the indicated antibodies or were incubated with anti-HA antibodies coupled to protein A sepharose beads for immunopurification (lane 5-8). Precipitated proteins were analysed by Western blotting with mouse monoclonal anti-HA (12CA5) antibodies (lane 5 and 6) or anti-Myc (9E10) antibodies (lane 7 and 8). (**B**) Bbp1p and Mps2p interact in the yeast two-hybrid system as indicated by the blue colour. Bbp1p and Mps2p also interact with themselves.

3.7.4 *MPS2* is a suppresser of temperature sensitive mutants of *BBP1*

Further genetic studies were undertaken to confirm the existence of the Bbp1p/Mps2p complex. Temperature sensitive mutants of *BBP1* (*bbp1-1, bbp1-2*) were transformed with *MPS2* on a multi-copy plasmid and transformants were incubated at the restrictive temperature. High gene dosage of *MPS2* rescued the growth of *bbp1-1* (Figure 18A, sector 2) and *bbp1-2* cells (data not shown). Cells containing the control plasmid could not grow at the restrictive temperature (Figure 18A, sector 1). This experiment indicated that *MPS2* was able to functionally support or substitute the defective *bbp1*.

3.7.5 *BBP1* is a suppresser of temperature sensitive mutants of *MPS2*

Temperature sensitive mutants for *MPS2* were constructed and investigated for high gene dosage suppression by *BBP1*.

3.7.5.1 Temperature sensitive mutants of *MPS2*

Temperature sensitive mutants of *MPS2* were constructed in a similar way to conditional lethal mutants of *BBP1* (see 3.4.3.1 and 2.2.18). The PCR conditions optimised for the mutagenic PCR of *BBP1* proved to be suitable for the amplification of *MPS2* from plasmid pCS71 with primers *MPS2*-M1 and *MPS2*-M2. The primers were designed to amplify a part of *MPS2* ranging from 146 bp downstream of start to 194 bp upstream of stop. The shuffle strain of *MPS2* (Δ*mps2*::*HIS3*, pRS316-*MPS2*; ESM780) was transformed with the isolated *MPS2* fragment obtained by mutagenic PCR and with pRS414-Δ*MPS2* lacking the B*su36*I/*Nde*I fragment (283 to 912 bp downstream of start). Homologous recombination occurred between the 5'- and 3'-terminal regions of pRS414-Δ*MPS2* and the mutated PCR fragment. Recombination resulted in circularisation of the pRS414 plasmid which was selected for by growth on medium lacking tryptophan. Temperature sensitive alleles were selected as described for *BBP1* (see 3.4.3.1). After integration into the *LEU* locus, two temperature sensitive mutants of *MPS2* were obtained:

ESM786 (*mps2-2*) restrictive temperature: 35 °C
missense mutations: I258V, S259Y

ESM787 (*mps2-42*) restrictive temperature: 37 °C
missense mutation: L191S

In addition, a conditional lethal mutant (*mps2-1*) from M. Winey's lab was used for the following experiment (see 3.7.1).

3.7.5.2 Suppression of temperature sensitive mutants of *MPS2*

All three conditional lethal mutants of *MPS2* were tested for high gene dosage suppression of *BBP1*. *Mps2-1, mps2-2* and *mps2-42* were transformed with pRS426-*BBP1* (pCS4) and were checked for growth at the restrictive temperature. *Mps2-2* (Figure 18B, sector 3) and *mps2-42* (data not shown) containing the pRS426-*BBP1* plasmid were able to grow at the restrictive temperature. In contrast, the conditional lethal phenotype of *mps2-1* was not rescued by high gene dosage of *BBP1* (Figure 18C, sector 3). This could indicate that the defect of *mps2-1* mutants is more severe than that of *mps2-2* and *mps2-42* and could not be rescued by high gene dosage of *BBP1*. It could also indicate dual or multiple functions of *MPS2*. Interestingly, m*ps2-1* cells flocculate when grown in liquid culture while *mps2-2* and *mps2-42* cells do not form cell clumps.

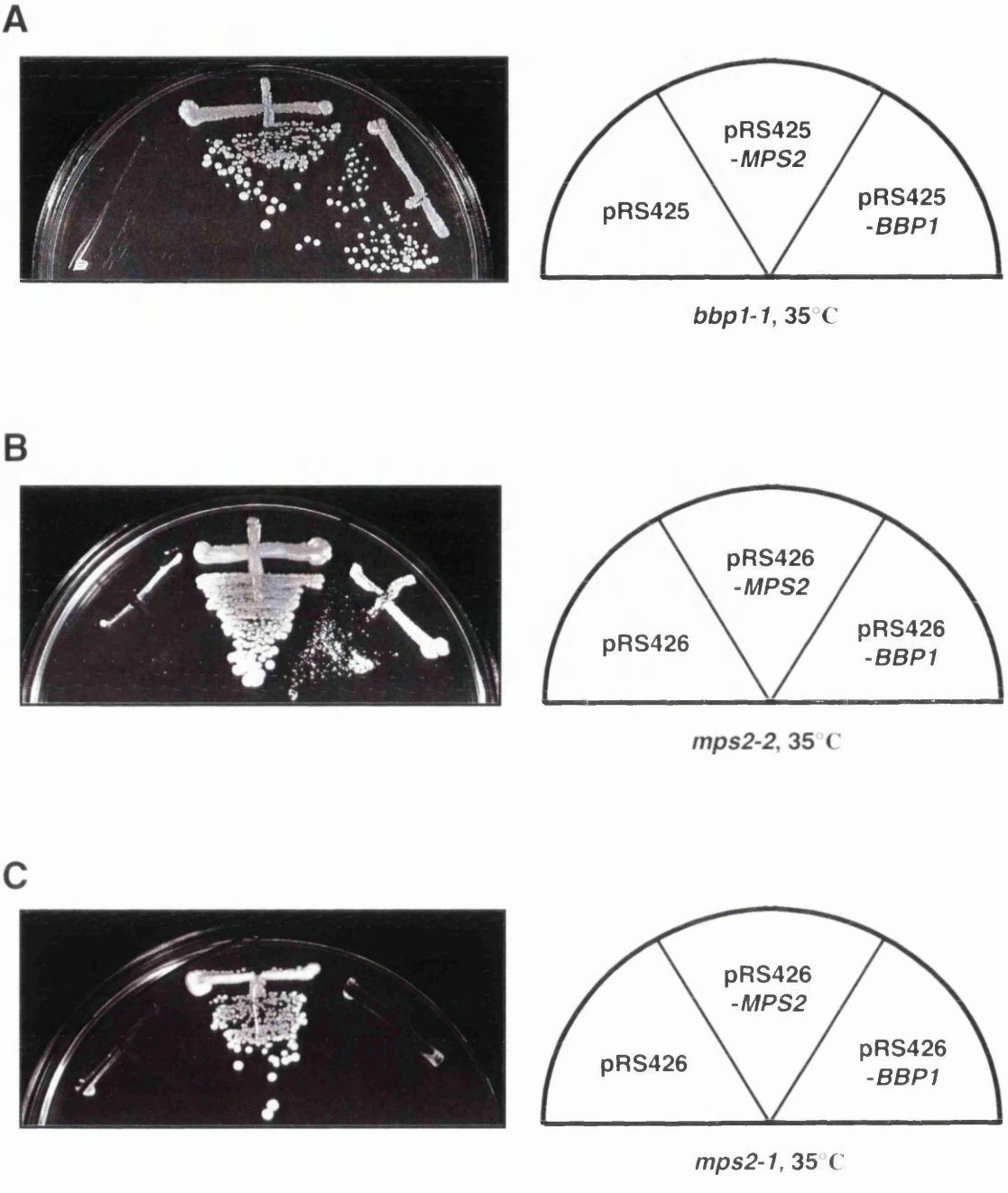

Figure 18: *MPS2* is a high gene dosage suppresser of *bbp1-1* cells and *BBP1* is a high gene dosage suppresser of *mps2-2* but not *mps2-1* cells. (**A**) *Bbp1-1* mutant cells were unable to grow at the restrictive temperature (35°C) containing pRS425. Complementation was observed by pRS425-*BBP1*. *MPS2* on pRS425 rescued the growth defect of *bbp1-1*. (**B**) Similarly, *mps2-2* cells were unable to grow at the restrictive temperature (35°C) containing pRS425. Complementation was observed by pRS425-*MPS2*. *BBP1* on pRS425 rescued the growth defect of *mps2-2* cells. (**C**) Instead, *mps2-1* cells were not rescued by high gene dosage of *BBP1*.

3.7.6 Bbp1p binds directly to Mps2p

Bbp1p and Mps2p interacted in the yeast two-hybrid system and showed a genetic interaction in the suppression experiment. Furthermore, both proteins were co-precipitated. All these experiment were performed in a yeast strain background and therefore, additional proteins were present which might have mediated the interaction of Bbp1p and Mps2p. To investigate if this had been the case, the interaction of bacterial expressed Bbp2p and Mps2p was tested in an in-vitro binding experiment (see 2.2.27). Full length GST-Bbp1p, N-terminal GST-Bbp1p$^{1-237}$ and C-terminal GST-Bbp1p$^{202-385}$ (pGEX-5X vector system) were purified from *E. coli* and immobilised to glutathione sepharose (see 2.2.25.1). The different beads were then incubated with cell extract from *E. coli* expressing His$_6$-Mps2p$^{1-307}$ (pET vector system) which lacked the membrane spanning region. After several washing steps, the proteins were eluted (see 2.2.27) and analysed by SDS-PAGE, Coomassie Blue staining (Figure 19, A1) and Western blotting with anti-GST (Figure 19, A2) and anti-His (Figure 19, A3) antibodies. His$_6$-Mps2p$^{1-307}$ bound to immobilised full length GST-Bbp1p (Figure 19A, lane 3), but not to the GST control beads (Figure 19A, lane 9). It interacted with similar efficiency with the C-terminal portion of Bbp1p (Figure 19A, lane 5), as with the full length Bbp1p (Figure 19A, lane 3). When His$_6$-Mps2p$^{1-307}$ was incubated with the N-terminal part of Bbp1p a faint protein band corresponding in size to His$_6$-Mps2p$^{1-307}$ was observed in some experiments (Figure 19A, lane 7). This band was not recognised by anti-His antibodies (Figure 19, A3, lane 7). It may represent a Bbp1p degradation product. Alternatively, His$_6$-Mps2p$^{1-307}$ might have bound weakly to the N-terminal part of Bbp1p, but the low amount of His$_6$-Mps2p$^{1-307}$ was not detected by the antibodies which recognised His$_6$ rather poorly. It should also be pointed out that the N- and C-terminal constructs of Bbp1p overlap by 36 aa which may be part of the binding region. Taken together, Mps2p interacts in vitro with the C-terminal half of Bbp1p. Since this experiment was carried out using bacterial expressed proteins this interaction was not assisted by additional yeast proteins and the interaction can be considered direct.

Figure 19: Binding of recombinant Bbp1p to Mps2p. (**A**) Bbp1p binds directly to Mps2p. GST-Bbp1p (lane 1 and 3), GST-C-Bbp1p$^{202-385}$ (lane 4 and 5), GST-N-Bbp1p$^{1-237}$ (lane 6 and 7) and GST (lane 8 and 9) bound to glutathione sepharose were incubated with (lane 3, 5, 7 and 9) or without (lane 1, 4, 6 and 8) His$_6$-N-Mps2p$^{1-307}$ (lane 2). The GST-Bbp1p derivates and associated proteins were eluted with sample buffer. The eluate was analysed by Coomassie Blue staining (A1) and by immunoblotting with anti-GST (A2) or anti-His (A3) antibodies. Protein bands (lane 2, 3, 5 and 7) corresponding in size to His$_6$-N-Mps2$^{1-307}$ are marked with an asterisk. (**B**) In *bbp1-1* cells Bbp1p and Mps2p form a complex at the permissive and the restrictive temperature. *Bbp1-1* cells were incubated for 3 h at 23 °C (lane 1 and 3) or 37 °C (lane 2 and 4). Lysates of cells were incubated with protein A sepharose beads coupled to rabbit anti-Mps2p antibodies and eluates were analysed by immunoblotting with rabbit anti-Bbp1p (lane 1 and 2) or rabbit anti-Mps2p (lane 3 and 4) antibodies.

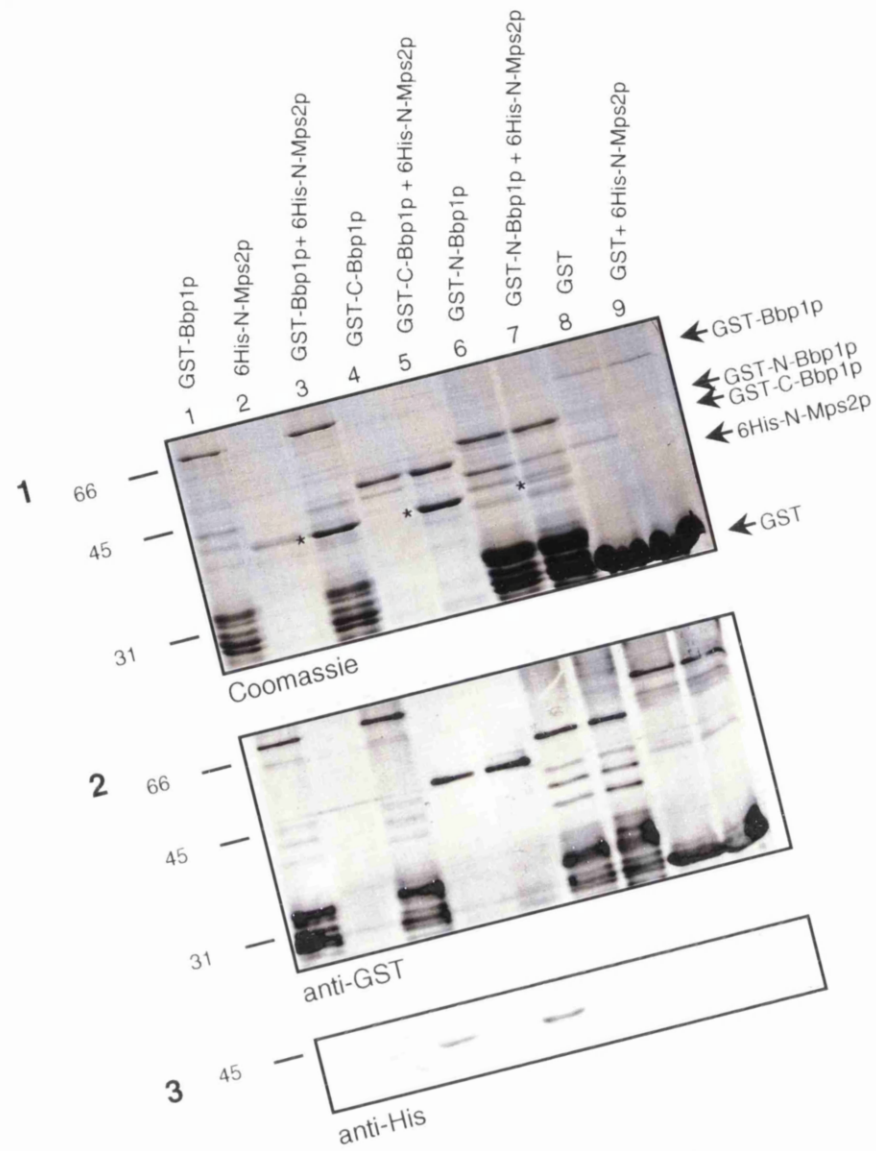

Figure 19: See facing page for figure legend.

3.7.7 Stability of the Bbp1p/Mps2p complex

Conditional lethal mutants in *BBP1* were unable to duplicate their SPB properly. This defect could be due to Bbp1p and Mps2p failing to interact. To address if the Bbp1p/Mps2p complex was affected in *BBP1* mutants, co-precipitation of Bbp1p and Mps2p was tested in *bbp1-1* cells incubated at the restrictive temperature. *Bbp1-1* cells were grown in liquid culture at 23 °C to OD_{600}=0.3. The culture was divided equally and incubated at the permissive (23 °C) and the restrictive temperature (37 °C) for up to 3 h. This incubation time was sufficient to arrest more than 95 % of *bbp1-1* cells in G_2. Cells of both cultures were lysed under optimal extraction conditions for Bbp1p (see 2.2.22.3) and the cell extract was incubated with sepharose beads coupled to anti-Mps2p antibodies (see 2.2.24). The precipitated proteins were analysed by SDS-PAGE (see 2.2.4.2) and Western blotting (see 2.2.13) with antibodies against Bbp1p and Mps2p. Mps2p was precipitated in slightly larger amounts in the culture incubated at the restrictive temperature (Figure 19B, lane 4) than at the permissive temperature (Figure 19B, lane 3). Bbp1p was co-precipitated under both conditions (Figure 19B, lane 1 and 2). Bbp1p showed slightly higher amounts in the precipitate of *bbp1-1* cells (Figure 19B, compare lane 1 with lane 2) which is most likely a consequence of the higher amount of Mps2p in the precipitate. To summarise, Bbp1p and Mps2p still formed a complex in *bbp1-1* cells.

3.8 Characterisation of Mps2p

As mentioned above *mps2-1* displayed a SPB duplication defect, such as the newly formed SPB was non-functional (Winey *et al.*, 1991). In addition, Mps2p directly interacted with Bbp1p (see 3.7.6) which was shown to be a SPB component (see 3.3). Taken together, it seemed likely that Mps2p itself is associated with the SPB. The following experiments were undertaken to support this hypothesis and to further study the function of *MPS2*.

3.8.1 Mps2p is localised at the SPB

Mps2p was localised by direct fluorescence microscopy, by indirect immunofluorescence microscopy and by immuno electron microscopy.

3.8.1.1 Localisation by direct fluorescence microscopy

As described for Bbp1p (see 3.3.1), GFP fused to *MPS2* was used as a reporter for the cellular localisation of Mps2p. Cells were prepared according to *Material and Methods* (see 2.2.33.1) and were investigated by fluorescence microscopy. The Mps2p-GFP signal was stronger than the Bbp1p-GFP signal, but still weaker than signals obtained for the central plaque component Spc42p or the outer plaque component Spc72p. Single cells usually contained one dot-like signal per cell (Figure 20, A1) whereas budded cells displayed two signals, which could represent the duplicated SPBs (Figure 20, A2). Thus, cells expressing *MPS2-GFP* exhibited typical SPB like staining.

3.8.1.2 Localisation by indirect immunofluorescence

Wild type cells and cells expressing fully functional epitope tagged Mps2p-3Myc were prepared for indirect immunofluorescence as described in 2.2.33.2 (compare to 3.3.2). Mouse monoclonal anti-Myc antibodies were used for the localisation of Mps2p-3Myc and antibodies against the outer plaque component Spc72p were employed to mark the SPB. The signals for Mps2p (red) and Spc72p (green) were merged (yellow) and co-localised (Figure 20, B3-B5). However, the signals did not overlap completely (red and green still visible in merge) which might indicate that Mps2p could be localised with a different substructure of the SPB than Spc72p. As a control, wild type cells were incubated with the same set of antibodies. Non-specific staining of cells by the anti-Myc antibody was not observed (Figure 20, B1 and B2). As speculated, Mps2p is a component of the SPB.

Figure 20: Mps2p is localised at the SPB. (**A**) Cells expressing *MPS2*-GFP were investigated by immunofluorescence microscopy and single (A1) or double (A2) dot-like signals, typical for SPB components, were observed. (**B**) Indirect immunofluorescence of wild type cells (lane 1 and 2) and cells expressing *MPS2-3MYC* (lane 3-5). Mps2p-3Myc was localised using mouse monclonal anti-Myc antibodies (9E10). The SPB was labelled with antibodies against the outer plaque component Spc72p (rabbit anti-Spc72p) and the DNA was visualised with DAPI. The dot-like signal for Mps2p-3Myc (red), which was not present in the wild type control, co-localised (green+red=yellow) with the Spc72p staining of the SPB (green). Note that Mps2p and Spc72p signals do not completely overlap (red and green still visible). (**C**) Mps2p is localised at the central plaque periphery (C1-C3) and near the outer plaque (C4-C6). Immunolabelling electron microscopy of isolated SPBs using immunopurified rabbit anti-Mps2p antibodies (C1-C6). The secondary antibodies were conjugated to 12nm gold particles. Gold staining represents Mps2p (large arrows). B: bridge, CP: central plaque, HB: half bridge, IP: inner plaque, MT: microtubules, NE: nuclear envelope, OP: outer plaque; Bars (A-B), 5 μm. Bar (C), 0.25 μm.

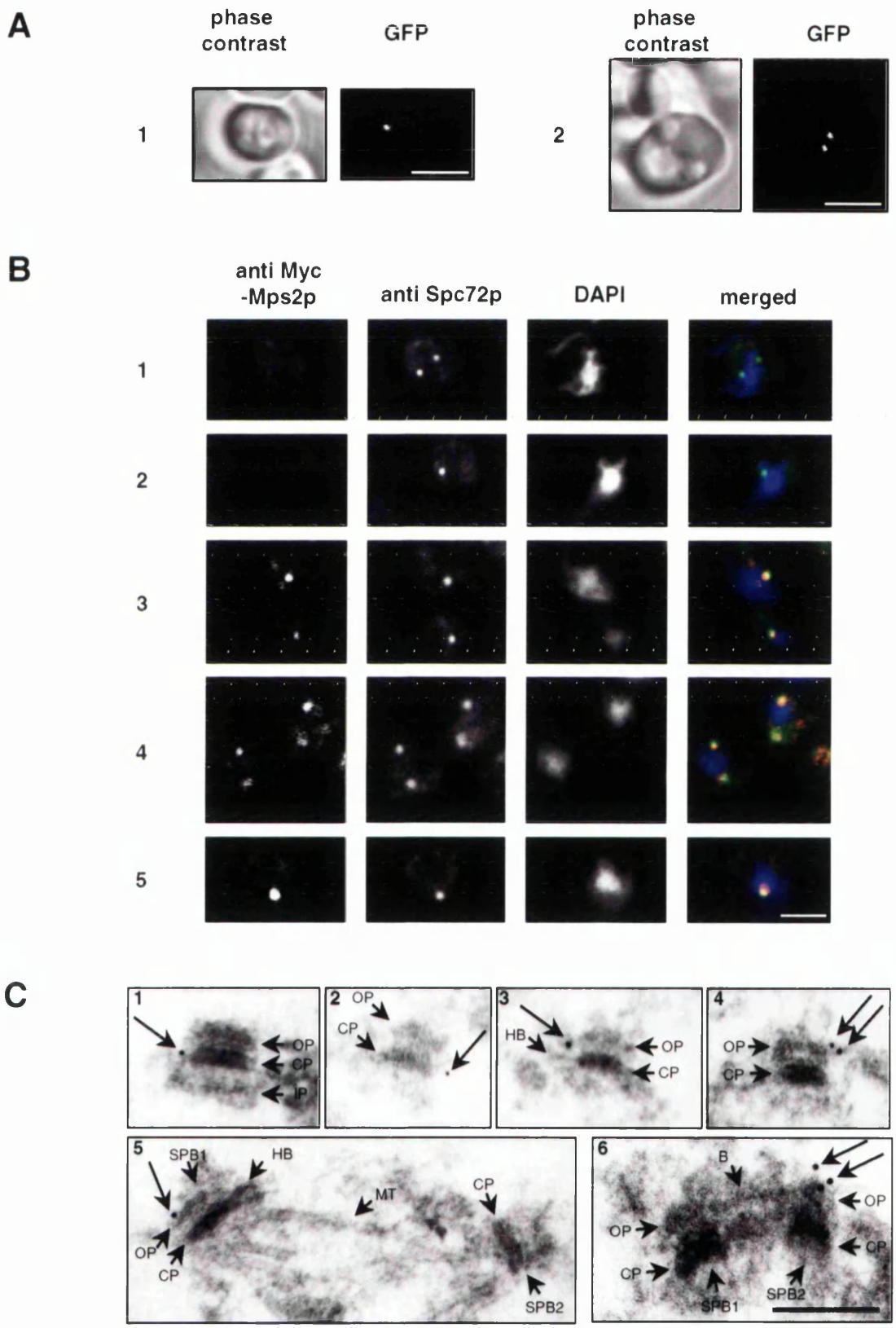

Figure 20: See facing page for figure legend.

3.8.1.3 Localisation by immunolabelling electron microscopy

To determine the localisation of Mps2p at the SPB in more detail, isolated SPBs (see 2.2.32) were prepared for electron microscopy (see 2.2.34.2.3). The SPBs were incubated with anti-Mps2p antibodies. The secondary antibody was a goat anti-rabbit antibody coupled to 12 nm gold particles. As control, SPBs were incubated only with the secondary antibody. The SPBs were embedded in Spurr resin, sectioned and contrasted with uranyl acetate and lead citrate (see 2.2.34.3 and 2.2.34.4). About 40 % of all SPBs investigated (n=40) had gold staining at the SPB (Figure 20C). In single SPBs, gold staining was observed at the side of the central plaque (n=9; Figure 20, C1-C3). This localisation was very similar to that of Bbp1p (Figure 9). In addition, gold particles close to the outer plaque were seen for single (n=2, Figure 20, C4), side-by-side (n=2, Figure 20, C6) and duplicated SPBs connected via mitotic spindle mircotubules (n=1, Figure 20, C5). Staining at the outer plaque had not been observed for Bbp1p. In some sections, the half-bridge was visible and the Mps2p staining was either opposite of (Figure 20, C5) or at the half-bridge (Figure 20, C3). The control SPBs did not show any staining (data not shown). Taken together, Mps2p is localised at the side of the central plaque and/or near the outer plaque.

3.8.2 Immunoprecipitation of Mps2p

When Mps2p was co-precipitated with Bbp1p no other protein had been identified as part of the complex. The immunoprecipitation of Mps2p could possibly reveal other components of the Bbp1p/Mps2p-complex. Wild type cells and cells expressing fully functional epitope tagged Mps2p-3HA were lysed under extraction conditions which were suitable for the isolation of the Bbp1p/Mps2p complex (see 2.2.22.3). Cell lysates were incubated with anti-HA antibodies immobilised to protein A sepharose beads (see 2.2.25.3). The purified proteins were firstly analysed by Western blotting (see 2.2.13). Mps2p-3HA and Bbp1p were present in the enriched protein fraction but not in the control, indicating that the immunoprecipitation was successful. The blots were also tested for the precipitation of other known SPB components. However, Spc42p, Spc72p, Cnm67p, Kar1p, calmodulin and Spc110p were not present in the precipitate. Consequently, the immunoprecipitate was analysed by SDS-PAGE (see 2.2.4.2) and

Fairbanks staining (see 2.2.5.2.2). Protein bands at 45 kD, 34 kD and 32 kD were excised from the gel and analysed by mass spectroscopy (see 2.2.26). The proteins at 45 and 32 kD were identified as Bbp1p. The band at 34 kD represented the 40S ribosomal protein Rps3p (data not shown). Therefore, Rps3p could potentially interact with Mps2p. However, it is known that ribosomal proteins are frequently found as contaminants of immunoprecipitates and this interaction was not further investigated.

3.8.3 Analysis of Δ*mps2* cells

3.8.3.1 Some Δmps2 cells are viable

A diploid strain was constructed which only carried one functional allele of *MPS2* while the other gene was disrupted by the *HIS3* marker (Δ*mps2*/*MPS2*::*HIS3*). Cells of this strain were sporulated and the spores were analysed by microscopic dissection (see 2.2.17). The separated spores were incubated at 23 °C on YPD plates. After 3 d, two out of four spores resulting from one single tetrad had grown into colonies. Cells of these colonies did not contain the *HIS3* marker, since the cells were not able to grow on selective medium (data not shown). Using a light microscope, micro-colonies could be seen in the areas where the other two spores were placed (data not shown). Therefore, Δ*mps2* spores were able to germinate. When the plates had been incubated for one week, small colonies became visible, but only 60 % of Δ*mps2* spores were able to grow into colonies (Figure 21). For these colonies the disruption of *MPS2* by the *HIS3* marker was confirmed by colony PCR. The Δ*mps2* cells were temperature sensitive since they were unable to grow at temperatures higher than 23 °C. Interestingly, Δ*mps2* cells were only partially complemented by *MPS2* since Δ*mps2* pRS316-*MPS2* cells were not able to grow at 37 °C. This might indicate that chromosome miss-segregation occurred during meiosis. In a further experiment, the shuffle strain of *MPS2* (Δ*mps2*::*HIS3*, pRS316-*MPS2*; ESM780) was incubated on 5-FOA plates to select against the *URA3*-based *MPS2* plasmid. No growth of the Δ*mps2* cells was observed. However, 5-FOA is slightly toxic even for wild type cells. To summarise, some Δ*mps2* cells were able to grow from spores into colonies on YPD plates but Δ*mps2* cells were unable to grow on 5-FOA. Cells that managed to grow

must have been suppressed by other proteins which can partially take over functions of Mps2p.

3.8.3.2 Phenotype of cells lacking MPS2

To gain more information about the cellular function of Mps2p, the deletion strain was analysed by immunofluorescence (see 2.2.33.2). Cells lacking *MPS2* were grown in liquid culture at 23 °C for 3 d to obtain efficient amount of cell material. Microtubules were visualised using anti-tubulin antibodies. The SPB was labelled using antibodies recognising the outer plaque component Spc72p and the chromatin positioning was monitored by DAPI staining.

Cells with wild type morphology including all stages of the cell cycle could be documented (Figure 22, 1 to 4). Early G_1 cells with one SPB (Figure 22, 1) and small budded cells with two SPBs connected by a short spindle (Figure 22, 2) were present in the culture. Large budded cells in late anaphase (Figure 22, 3) and telophase (Figure 22, 4) containing two SPBs and separated DNA were also observed.

On the other hand, various abnormal mutant phenotypes were documented (Figure 22, 5 to 10). Firstly, the shape of some mutant cells was different from wild type. Cells had elongated buds and/or were multi-budded. Cells displaying unusual morphology also showed abnormalities in chromosome segregation, microtubule distribution and SPB content (Figure 22, 7 to 10). Cells lacking *MPS2* could contain up to four SPBs (Figure 22, 7 to 10). Some of these SPBs did not connect to microtubules (Figure 22, 7 and 10) or nucleated very few microtubules (Figure 22, 9) Other SPBs nucleated an aster-like array of microtubules (Figure 22, 6 and 8) and some SPBs were connected by spindle-like structures (Figure 22, 5, 7 and 8). Most of these cells were unable to segregate their chromosomes (Figure 22, 6, 7, 9 and 10) and one main DAPI staining region was observed in these cells, even when they had a multi-budded phenotype. In some cases, the DNA was partially separated (Figure 22, 5 and 8). Taken together, the *MPS2* deletion strains displayed various phenotypes reaching from wild type appearance to highly defective cells.

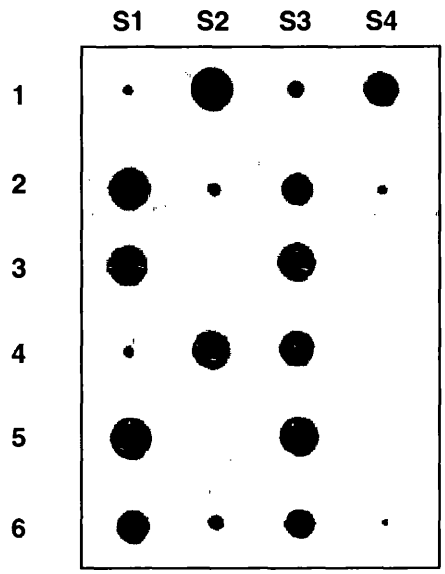

Figure 21: Cells lacking *MPS2* show a severe growth defect. Spore analysis of YCS75 (*MPS2/Δmps2::HIS3MX4*) reveals that some spores lacking *MPS2* are able to grow into colonies. Six tetrades (lane 1-6) were dissected into four spores (S1, S2, S3, S4) and were incubated at 23 °C for one week.

Figure 22: Cells lacking *MPS2* display wild type (1-4) and mutant phenotypes (5-10). Δ*mps2* cells were grown for 3 d at 23°C and were prepared for indirect immunofluorescence microscopy using rabbit anti-Spc72p to visualise the SPB and monoclonal mouse anti-tubulin antibodies. The DNA was stained with DAPI. The anti-Spc72p (red), anti-tubulin (green) and DAPI (blue) signals were merged. Bar, 5 μm.

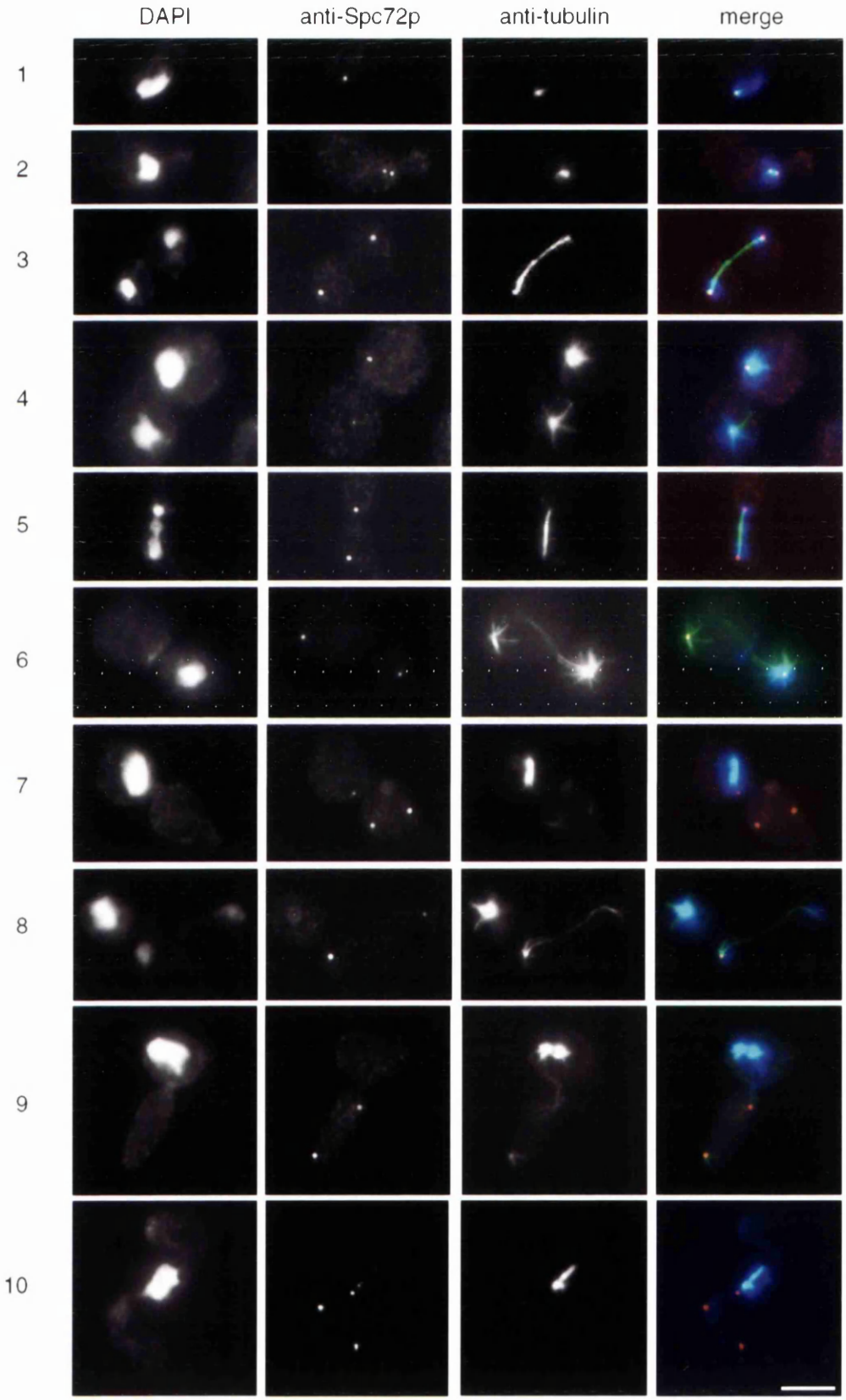

Figure 22: See facing page for figure legend.

3.8.3.3 BBP1 is unable to suppress the deletion of MPS2

If *BBP1* was the gene that suppressed Δ*mps2*, high gene dosage of *BBP1* should have a positive effect on the growth of the deletion strain. The *MPS2* shuffle strain (see 2.2.17), a strain lacking the chromosomal copy of *MPS2* but containing a wild type copy of *MSP2* on a centromere-based *URA3*-plasmid was transformed with *BBP1* on a multi-copy vector. As positive control pRS425-*MPS2* and as negative control pRS425 were transformed into the shuffle strain. Cells were counter selected for pRS316-*MPS2* on 5-FOA medium (see 2.2.20). Cells containing pRS425-*BBP1* or the empty vector control were unable to grow (data not shown). Cells containing the additional copies of *MPS2* grew like wild type cells. It cannot be excluded that Bbp1p takes over functions of Mps2p in the deletion strain but it does not have the potential to be the main protein supporting the growth of Δ*mps2* cells.

3.8.3.4 Multi-copy suppression screen

To identify the gene or genes responsible for the survival of the *MPS2* deletion, a screen for high gene dosage suppression of Δ*mps2* was carried out. The *MPS2* shuffle strain (see 2.2.17) was transformed with the yeast multi-copy library in plasmid YEp13 and transformants were selected on SC-His-Leu-Ura selective medium. About 50,000 transformants were replica plated (see 2.2.19) onto 5-FOA plates to counter select for the pRS316-*MPS2* plasmid (see 2.2.20). Altogether, 33 colonies were able to grow and thereof 18 YEp13 plasmids could be isolated and amplified in *E. coli* (see 2.2.10.2). These plasmids still allowed the growth of Δ*mps2* cells. The inserts of all plasmids were sequenced (see 2.2.14) and 15 contained a fragment from chromosome VII carrying *RPL7A*, *SNR39*, *SNR39B*, *MPS2*, *YGL074c* and *HSF1*. The complementation of Δ*mps2* by wild type *MPS2* was expected and indicated that the library was functional. All other three plasmids contained a fragment of chromosome II. The inserts varied slightly in size but all coded for *SEC66*, *SMY2* and *UMP1*. *SEC66*, codes for a glycoprotein which is part of an integral endoplasmic reticulum membrane protein complex that is required for translocation of presecretory proteins (Brodsky and Schekman, 1993; Feldheim *et al.*, 1993; Kurihara and Silver, 1993). Not much is known about *SMY2*, a gene that suppresses myosin 2 defects (Lillie

and Brown, 1994). *UMP1* is the gene for the 20S proteasome maturation factor (Ramos *et al.*, 1998). All three genes were amplified by PCR and were cloned into pRS425. The subcloned *SEC66*, *SMY2* and *UMP1* were transformed into the *MPS2* shuffle strain. As controls, the *MPS2* shuffle strain containing pRS425-*MPS2*, pRS425 or clone 61 (pCS85), one of the YEp plasmids isolated in the screen containing the chromosome II fragment, were used. All transformants grew at 23 °C on plates lacking leucine (Figure 23B). Cells containing pRS425-*UMP1*, pRS425-*SEC66* and pRS425 were unable to grow on 5-FOA medium (Figure 23, C and D). High gene dosage of *SMY2* rescued the growth of Δ*mps2* cells on 5-FOA medium in the same manner as clone 61. Cells containing the clone 61 or the pRS425-*SMY2* plasmids grew at 23 °C and 30 °C (Figure 23, C and D). However, these strains were unable to grow at higher temperatures. Therefore, high gene dosage of *SMY2* was able to suppress the growth defect of cells lacking Mps2p significantly.

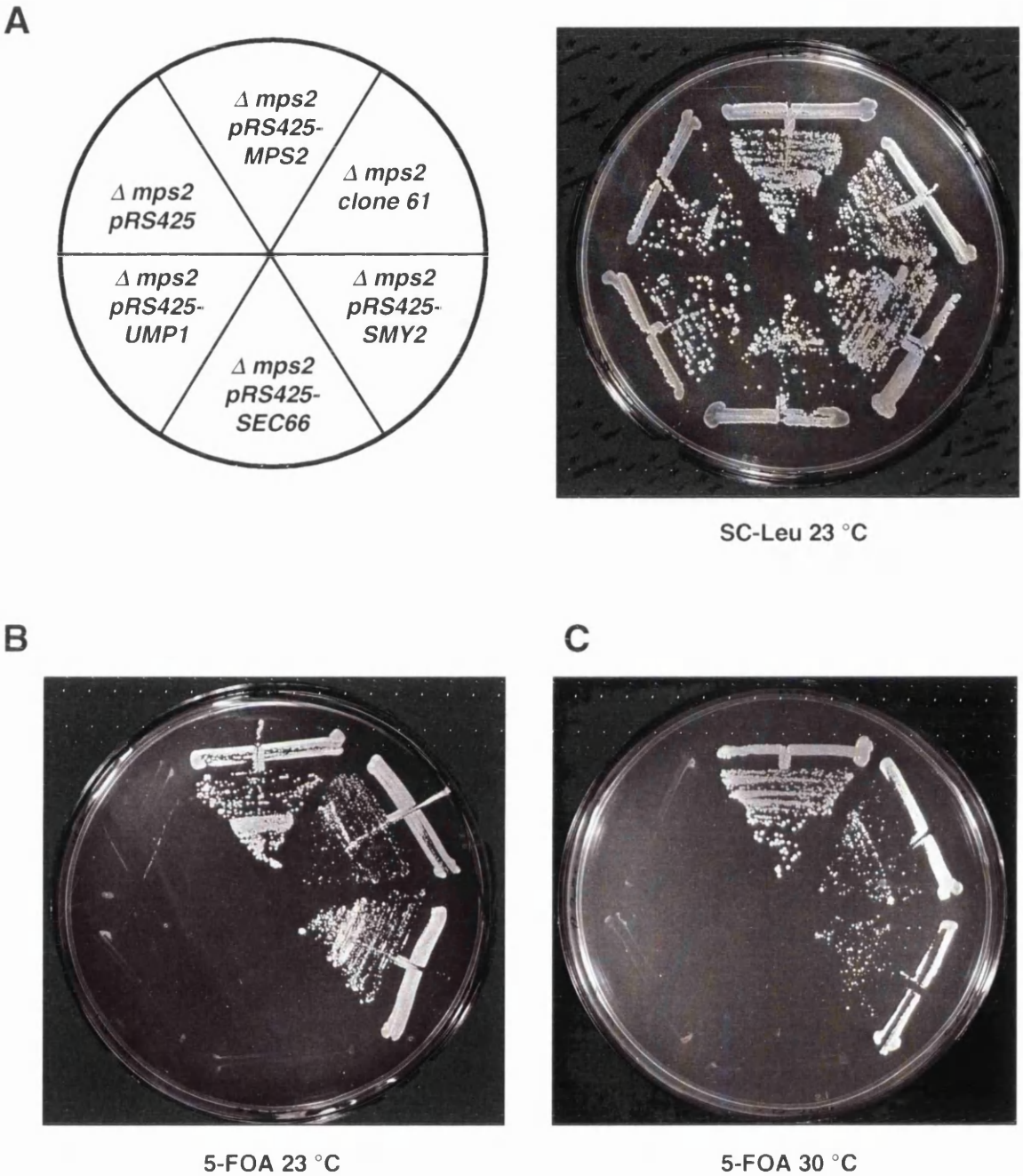

Figure 23: *SMY2* is a high gene dosage suppresser of Δ*mps2*. Clone 61, isolated in a multi copy suppresser screen of Δ*mps2* codes for the ORFs of *UMP1*, *SEC66* and *SMY2*. (**A**) The shuffle strain of *MPS2* containing the indicated plasmids is able to grow on SC-Leu plates at 23 °C. (**B** and **C**) *MPS2* complements the growth defect of Δ*mps2* cells. The *URA3*-based *MPS2*-plasmid was counter-selected on 5-FOA plates. High gene dosage of clone 61 and *SMY2* mediates growth of Δ*mps2* cells at 23 °C and 30 °C while *UMP1* and *SEC66* fail to do so.

3.9 Connections between the nuclear pore component Pom152p and the SPB

It had been shown by Chial et al. (1998) that the deletion of *POM152* coding for an abundant but nonessential nuclear pore component suppresses defects associated with mutations in *NDC1*. Ndc1p is a shared component of nuclear pores and SPBs and mutations in *NDC1* cause a SPB duplication defect (Winey *et al.*, 1993). Since mutants in *BBP1*, *MPS2* and *SPC29*, are defective in SPB duplication, the effect of the deletion of *POM125* in these mutant strains was tested.

3.9.1 Deletion of *POM152* in temperature sensitive mutants of *SPC29*, *BBP1* and *MPS2*

POM152 was deleted in *bbp1-1*, *bbp1-2*, *mps2-2* and *spc29-2* mutants using the KanMX disruption cassette (Knop *et al.*, 1999). The deletion of *POM152* was selected for on kanamycin plates. Transformants of *bbp1-1* and *bbp1-2* strains were then replica plated on SC-His-Trp plates to ensure that the deletion of *BBP1* and the integration of the *bbp1-1* and *bbp1-2* alleles were still present (Appendix 1). Accordingly, transformants of the *mps2-2* strain were selected on SC-His-Leu medium, to control the deletion of *MPS2* and the integration of *mps2-2* (Appendix 1). *Spc29-2* cells were only tested for the disruption of *POM152* by growth on kanamycin selective plates since the *spc29-2* mutant allele was directly integrated into the wild type gene (Appendix 1). The deletion of *POM152* was additionally proven by colony PCR (see 2.2.1.2). All four strains grew at the permissive temperature. *Bbp1-1* Δ*pom152*, *bbp1-2* Δ*pom152* and *mps2-2* Δ*pom152* were all able to grow at the restrictive temperature apart from *spc29-2* Δ*pom152* (Figure 24A). When a wild type copy of *POM152* was re-introduced into *bbp1-1* Δ*pom152* (Figure 24A), cells regained temperature sensitivity. This proved that deletion of *POM152* had the same 'positive' effect on *bbp1-1*, *bbp1-2* and *mps2-2* cells as on mutants in *NDC1*.

3.9.2 A fraction of the Pom152p pool is localised in proximity to the SPB

So far, Pom152p had only been described as a component of nuclear pores although the originial publication shows Pom152p staining at the SPB by immunoelectron microscopy (Wozniak *et al.*, 1994). In this study, the localisation of Pom152p in relation to the SPB was investigated by immunofluorescence (see 2.2.33.2). Pom152p-6HA was visualised using anti-HA antibodies and the SPB was marked with antibodies against the outer plaque component Spc72p. The staining pattern obtained from the anti-HA antibodies could be seen along the nuclear envelope and it was either dot-like or covered larger areas continuously (Figure 24B). In all cells investigated, a Pom152p signal was always located proximal to the SPB signal (Figure 24B, white arrows). This localisation was seen for SPBs containing single or duplicated SPBs.

3.9.3 Co-precipitation of Pom152p and Tdh3p

Genetic evidence suggested that Pom152p might be involved in SPB duplication (Chial *et al.*, 1998; this study). It had been shown by immunoprecipitation, that Pom152p interacts directly with the nuclear pore proteins Nic96p and Nup188p (Fabre and Hurt, 1997; Nehrbass *et al.*, 1996). However, SPB components were not identified in the precipitation. To exclude the possibility that further interactors of Pom152p had remained undiscovered, the immunoprecipitation of Pom152p was repeated. Wild type cells and cells expressing Pom152p-6HA were lysed under conditions optimal for the extraction of Bbp1p and Mps2p (see 2.2.22.3). Pom152p-6HA was enriched by immunoprecipitation using anti-HA antibodies immobilised to protein A sepharose beads (see 2.2.25.3). Western blot analysis (see 2.2.13) showed that Bbp1p and Mps2p were not present in the precipitate of Pom152p-6HA (data not shown).

The precipitates were also analysed by SDS-PAGE (see 2.2.4.2). In the Coomassie Blue stained gradient gel 5 unique protein bands were visible in the lane representing the Pom152p-6HA precipitation. The bands at 170 kD, 165 kD and 155 kD were identified by MALDI-MS (see 2.2.26) as Pom152p-6HA. This indicated that Pom152p-6HA had been slightly degraded during the experiment. The band at 66 kD did not contain enough material for identification by mass spectroscopy. The band at

37 kD was identified as Tdh3p, one of the three yeast glyceraldehyd 3-phosphate dehydrogenases (data not shown). Neither Nic96p nor Nup188p were precipitated under these conditions or they might not have been identified due to low amounts (data not shown). Taken together, no interaction with known SPB components could be detected.

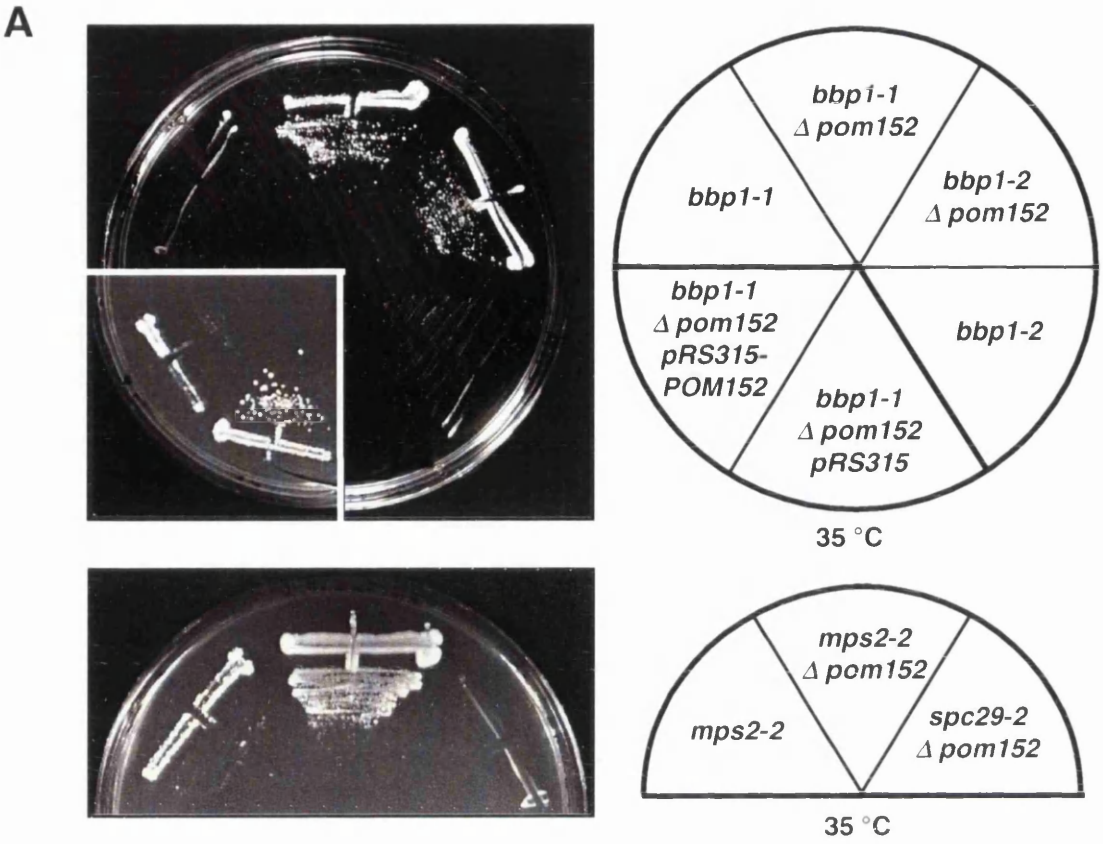

Figure 24: The nuclear pore component Pom152p might have functions at the SPB. (**A**) Deletion of *POM152* rescued the growth defect of mutants in *BBP1* and *MPS2* but not *SPC29* at the non-permissive temperature. If *POM152* was re-introduced into the *bbp1-1 Δpom152* strain, cells regained temperature sensitivity and were unable to grow at the non-permissive temperature. (**B**) Indirect immunofluorescence microscopy of cells expressing *POM152-6HA*. Pom152p-6HA (red) was localised at the nuclear envelope using mouse monclonal anti-HA antibodies (12CA5). The SPB was labelled with antibodies against the outer plaque component Spc72p (rabbit anti-Spc72p, green). The merge shows that a pool of Pom152p is always localised close to the dot-like signal for Spc72p representing the SPB. Bar, 2.5 µm.

3.10 The Spc24p/Spc25p/Ndc80p sub-complex

I. LeMasson (CEA/Saclay, France) identified *SPC24* in a two-hybrid screen with *MPS2* as bait. In collaboration with I. LeMasson, the possible interaction of Mps2p with Spc24p, a putative SPB component of unknown function was investigated. In our laboratory, this genetic interaction was followed up by immunoprecipitation (see 2.2.25.3). Mps2p was precipitated in cells expressing fully functional Spc24p-3HA using antibodies recognising Mps2p directly. Mps2p but not Spc24p-3HA was precipitated. In addition, Spc24p-3HA was precipitated using anti-HA antibodies coupled to sepharose beads. Spc24p-3HA, but not Mps2p were detected in the precipitate. Therefore, the two-hybrid interaction could not be supported by immunoprecipitation (data not shown).

Although Mps2p could not be detected in the precipitation of Spc24p-3HA, two unique bands, not present in the control precipitate were observed. Using MALDI-MS (see 2.2.26) the band of 70 kD was identified as Ndc80p which is a shared component of SPBs and centromeres (Wigge *et al.*, 1998). The band at 34 kD could not be identified due to low protein content. Shortly after, C. Janke in our laboratory, identified Ndc80p and Spc24p in a immunoprecipitation of Spc25p-3HA. This indicated that Spc24p might be part of a complex with Spc25p and Ndc80p. To verify this result, Spc25p-3HA and Ndc80p-6HA were precipitated using anti-HA antibodies (Figure 25). In both precipitates Spc24p could be detected using antibodies against Spc24p (Figure 25, lane 5 and 6). Spc24p was not present in the wild type control (Figure 25, lane 4). Therefore, Spc24p, Spc25p and Ndc80p are part of a common complex.

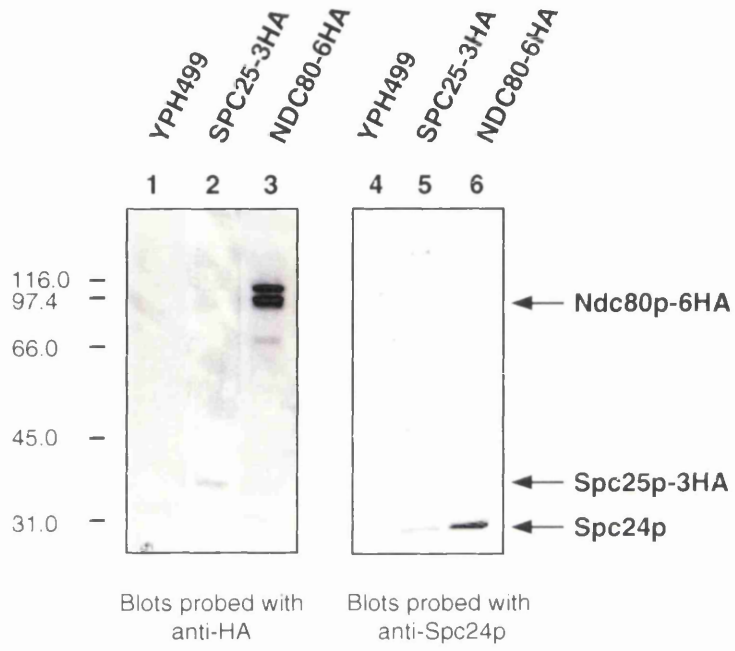

Figure 25: The SPB associated proteins Ndc80p, Spc24p and Spc25p form a novel complex. Spc24p (lane 5 and 6) co-precipitates with Spc25p-3HA (lane 2) and Ndc80p-6HA (lane 3). Lysates of wild type cells (lane 1 and 4) and cells expressing Spc25p-3HA (lane 2 and 5) or Ndc80p-6HA (lane 3 and 6) were incubated with anti-HA sepharose beads. The eluate was analysed by western blotting using mouse monoclonal anti-HA (lane 1-3) or rabbit polyclonal anti-Spc24p (lane 4-5) antibodies.

3.11 Hsc82p

3.11.1 Co-precipitation of Hsc82p and Mps2p in temperature sensitive mutants of *BBP1*

It was shown in earlier in this study (see 3.7.7) that Bbp1p and Mps2p form a complex in *bbp1-1* cells at the restrictive temperature. In this experiment Mps2p was precipitated from lysates of *bbp1-1* cells which had been incubated at 23 °C and 37 °C prior to precipitation. When the precipitates were analysed by SDS-PAGE (see 2.2.4.2) and Coomassie Blue staining (see 2.2.5.2.1), a very strong protein band at about 82 kD was observed in the precipitate of cells which had been incubated at 37 °C (Figure 26A). This protein band was identified by mass spectroscopy (see 2.2.26), as the constitutively expressed heat shock protein Hsc82p, a member of the HSP90 heat shock family. It is known that heat shock proteins are often precipitated by immunoprecipitation due to their ability to bind and fold proteins. However, it had been shown recently, that Hsp90 is a core component of the centrosome of *Drosophila* (Lange *et al.*, 2000). Furthermore, in budding yeast, mutants in the heat shock transcription factor *HSF1* are defective in *HSP90* expression and they have a defect in SPB duplication (Zarzov *et al.*, 1997). Therefore, the relation of *HSC82* with *MPS2* and *BBP1* was further investigated.

3.11.2 Geldanamycin Assay

Geldanamycin is a member of the benzoquinoid ansamycins, a class of naturally occuring antibiotics (DeBoer *et al.*, 1970). Geldanamycin is known to bind to Hsp90 thereby blocking the interaction of substrates with Hsp90 (Whitesell *et al.*, 1992). Morano *et al.* (1999) showed recently, that a mutant of *hsf1-583*, which is defective in cell cycle progression, is highly sensitive to geldanamycin. In an adaption of this experiment (see 2.2.30), the sensitivity of *hsf1-82* (mutant defective in SPB duplication) and of mutants of *MPS2* and *BBP1* to geldanamycin was tested. In addition, *cdc37*, *mps1* and *cdc28* cells were investigated for geldanamycin sensitivity. These are mutants in kinases, which act in the yeast cell cycles and all three mutants fail to duplicate their SPB (Schutz *et al.*, 1997; Winey *et al.*, 1991; Zarzov *et al.*,

1997). Geldanamycin and the control (DMSO) were applied to top agar layers containing the different strains and plates were incubated at 23 °C and 30 °C. *Hsf1-82*, *mps1-1* and *cdc28-109* were highly sensitive to geldanamycin even at the permissive temperature as seen by the inhibition of cell growth (Figure 26, C1-C3). Mutants of *BBP1*, *MPS2* and *CDC37* were not effected by geldanamycin (Figure 26, C4-C11) at the permissive or semi-permissive temperature (data not shown).

3.11.3 *HSC82* is a suppresser of a temperature sensitive mutant allele of *MPS2*

Mutants of *BBP1* (*bbp1-1* and *bbp1-2*) and *MPS2* (*mps2-1*, *mps2-2* and *mps2-42*) were tested for suppression by high gene dosage of *HSC82*. Only *mps2-42* cells were able to grow at the restrictive temperature due to overexpression of *HSC82* (Figure 26B, sector 3). *Bbp1-1*, *bbp1-2*, *mps2-1* and *mps2-2* did not benefit from high gene dosage of *HSC82*.

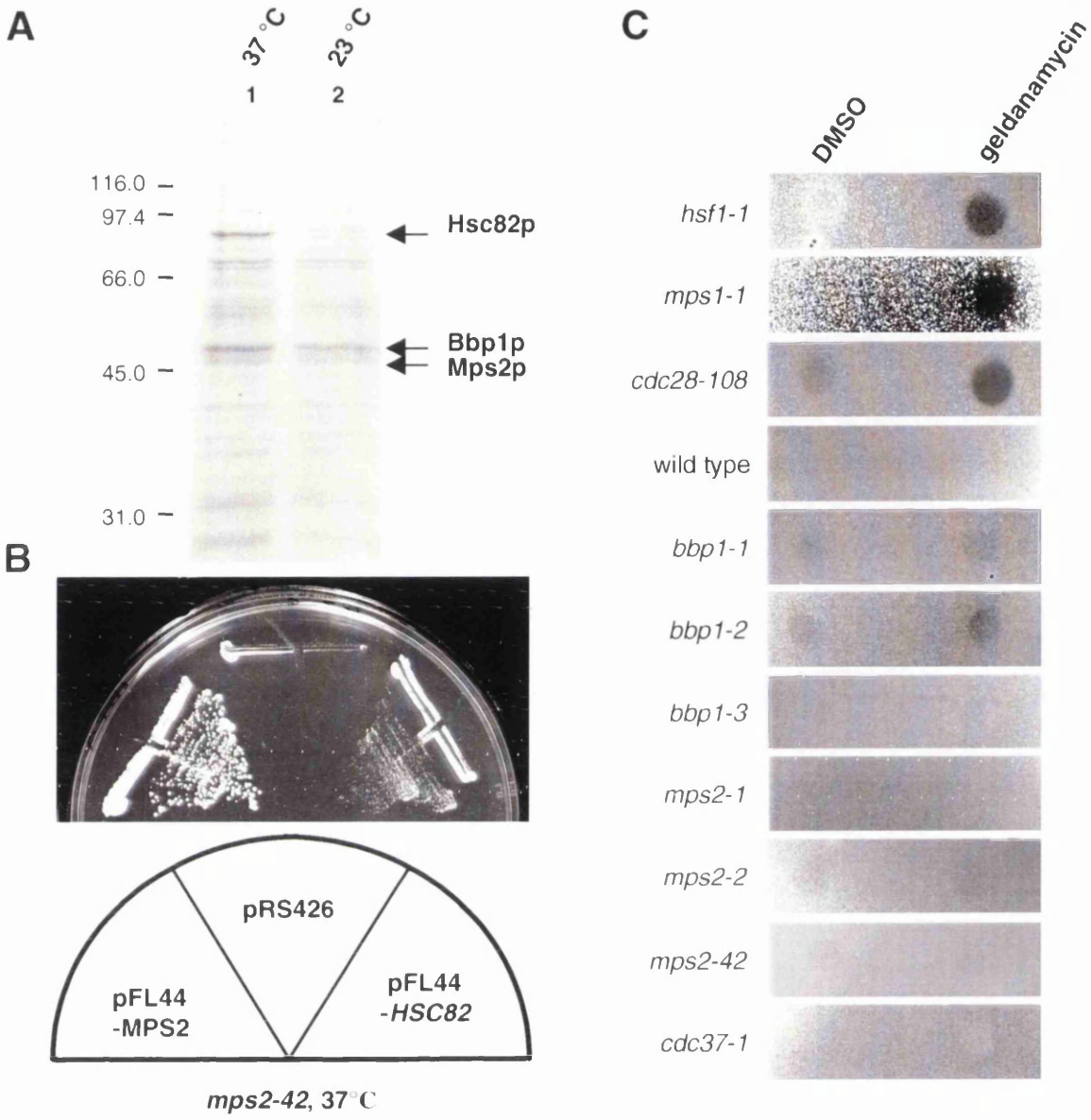

Figure 26: *HSC82* genetically interacts with *MPS2*. (**A**) Hsc82p and Bbp1p co-precipitate with Mps2p when *bbp1-1* cells were incubated at the restrictive temperature. *Bbp1-1* cells were incubated for 3 h at 23 °C (lane 2) or 37 °C (lane 1). Lysates of cells were incubated with protein A sepharose beads coupled to rabbit anti-Mps2p antibodies and eluates were analysed by SDS-PAGE and Fairbanks staining. The band at about 82kD (lane 1), which was not present in the control (lane 2), was identified as Hsc82p by MALDI-MS. (**B**) *HSC82* is a high gene dosage suppresser of *mps2-42* cells grown at the restrictive temperature. *MPS2* complements the growth defect of *mps2-42* cells while cells containing the empty control plasmid were unable to survive at 37 °C. (**C**) Mutants in *HSF1*, *MPS1* and *CDC28* are affected by the Hsp90 inhibitor geldanamycin. 10 µl of DMSO or 2 mM geldanamycin in DMSO were applied to the top agar layer containing cells of the indicated strains. Plates were incubated for 3 d at the permissive temperature.

4. Discussion

4.1 Bbp1p is a SPB component

The SPB is a multi-layered protein complex which functions in the nucleation and organisation of microtubules. In this study, Bbp1p was proven to be a novel component of the SPB. Firstly, Bbp1p was localised at the SPB using several microscopy techniques. Bbp1p was shown to localise to the SPB by fluorescence microscopy using Bbp1p fused to GFP. This result was also obtained by Wigge *et al.* (1998) who identified Bbp1p as a novel SPB component in the MALDI analysis of isolated SPBs. Furthermore, Bbp1p was co-localised with the known SPB component Spc72p by indirect immunofluorescence (this study). Bbp1p was present at the SPB throughout the cell cycle. These findings showed that Bbp1p is a component of SPBs. More detailed localisation studies using immunolabelling microscopy revealed the localisation of Bbp1p at the periphery of the central plaque (Figure 27A). This result was obtained in independent experiments using either anti-Myc antibodies to visualise Bbp1p-3Myc fusion proteins in whole cells or anti-Bbp1p antibodies to locate Bbp1p at SPBs of isolated nuclei or at isolated SPBs. Micrographs of SPBs containing a half-bridge showed gold staining representing Bbp1p either where the half-bridge connects to the central plaque or directly opposite. This particular localisation was also observed if a bridge linked two side-by-side SPBs. Here, Bbp1p might connect the SPB with the bridge-structure via its interaction with the central plaque component Spc29p and the half-bridge component Kar1p (see below). Since staining in proximity to the central plaque was observed when no bridge structure was visible, Bbp1p might be localised in a ring around the central plaque and not just at the site of bridge attachment or opposite (Figure 27B). In some cases staining was observed on the nuclear side of the SPB in proximity to the inner plaque. This however could be an artefact created by the distance of the gold particle from the protein itself caused by the length of the secondary and primary antibody. Otherwise, it could indicate that Bbp1p interacts with nuclear proteins on the nuclear face of the SPB. A localisation of Bbp1p throughout the central plaque itself could not be excluded by these experiments since such a pool of Bbp1p would hardly be accessible for the primary antibody.

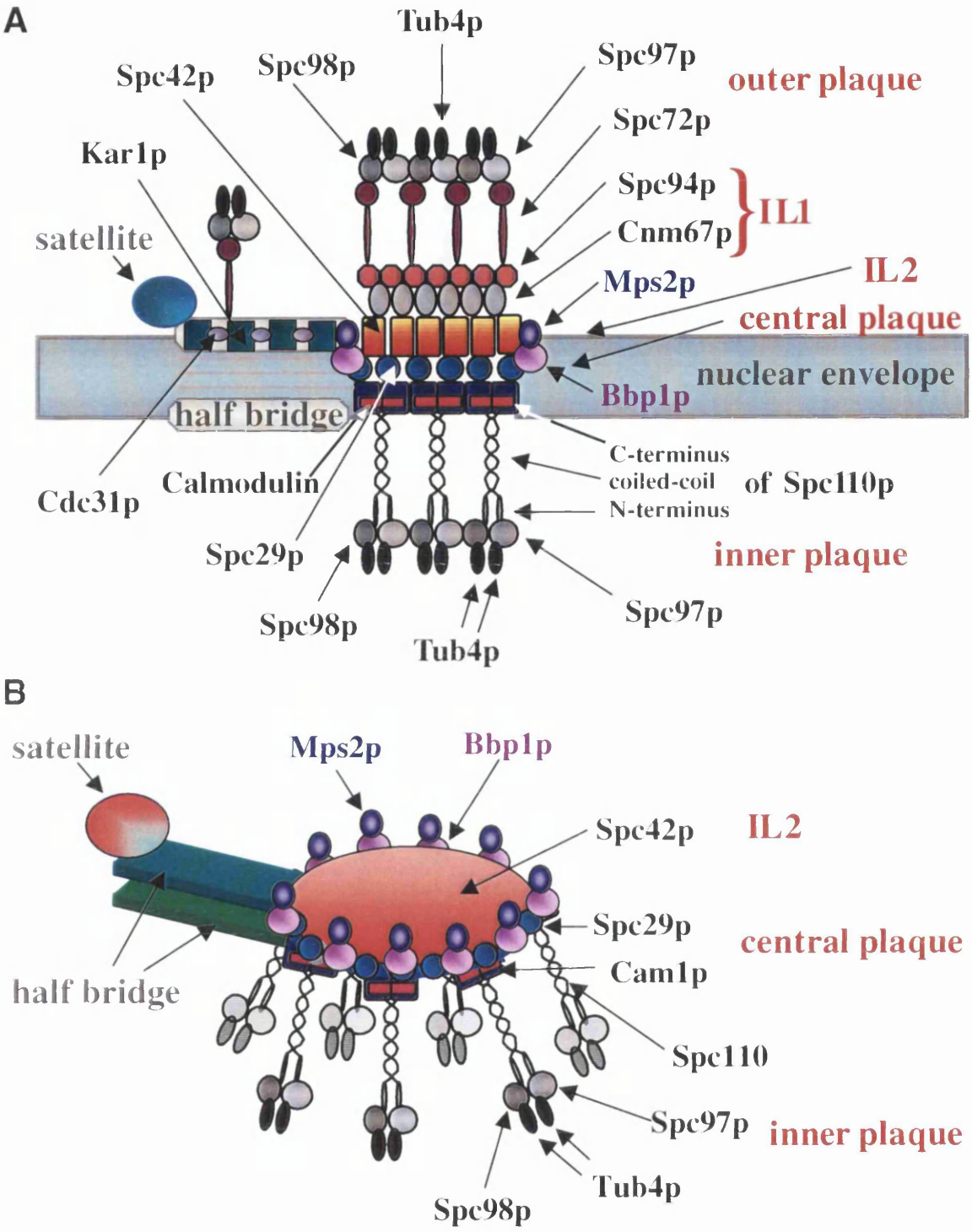

Figure 27: Model for the localisation of the Bbp1p/Mps2p complex at the central plaque periphery. Bbp1p interacts with the central plaque component Spc29p (Schramm *et al.*, 2000) which itself interacts with Spc42p and Spc110p (Adams and Kilmartin, 1999; Elliot *et al.*, 1999). Bbp1p further interacts with the half-bridge component Kar1p and might thereby connect the central plaque and the half-bridge. (**A**) Two dimensional layered organisation of the budding yeast SPB. (**B**) Three dimensional horizontal cut through the central core of the SPB.

The layers of the SPB are held together horizontally and vertically by the interaction of proteins within the layers. In this study, Bbp1p could be shown to interact with SPB proteins that are known to localise in vicinity of Bbp1p. In addition interactions with other SPB components and non-SPB components were observed (summarised in Figure 28).

Bbp1p was originally identified in two independent genetic screens. Firstly, as a high gene dosage suppresser of *spc98* conditional lethal mutants (S. Geissler, *unpublished data*) and secondly, as a suppresser of *spc29* conditional lethal mutants (S. Elliott, *published in* Schramm *et al.*, 2000). An interaction of Bbp1p with the central plaque component Spc29p is now well established. Bbp1p and Spc29p interact in the yeast two-hybrid system and by in vitro binding (S. Elliott, Schramm *et al.*, 2000). These findings suggest that Bbp1p and Spc29p interact directly. However, high gene dosage of *SPC29* could not rescue conditional lethal mutants in *BBP1*. Considering the fact that *BBP1* overexpression can rescue *spc29* conditional lethal mutants, this may indicate that Bbp1p functions later in the cell cycle than Spc29p.

No further evidence could be found for an interaction of Bbp1p with Spc98p, a protein of the γ-tubulin complex. High gene dosage of *SPC98* did not rescue mutants in *BBP1*. Spc98p was not present in immunoprecipitates of Bbp1p and both proteins did not show a positive signal in the yeast two-hybrid system. Therefore, it is unlikely that Bbp1p interacts with Spc98p. Furthermore, Bbp1p did not interact with the other two components of the budding yeast γ-tubulin complex, Spc97p and Tub4p, in the two-hybrid system. Spc97p and Tub4p as well as Cnm67p and Spc72p, which are outer plaque components, were not present in immunoprecipitates of Bbp1p.

In contrast, high gene dosage of *SPC42* a gene coding for an intermediate layer component suppressed *bbp1-1* and *bbp1-2* mutants. This genetic interaction could not be further established neither in the yeast two-hybrid system nor in affinity purification experiments. Nevertheless, the localisation of Bbp1p in proximity to the central plaque indicates the possibility of an interaction of the proteins. It may be that Bbp1p and Spc42p interact only temporarily during SPB duplication.

Furthermore, a genetic interaction between *BBP1* and *SPC34* was established. Spc34p was identified as a novel SPB component by Wigge *et al.* (1998). High gene dosage of *SPC34* suppresses the temperature dependent growth defect of *bbp1-2* cells. This findings are supported by the interaction of *BBP1* and *SPC34* in the yeast two-hybrid system (C. Janke, *unpublished data*). Since the cellular role of Spc34p is as yet unknown, further data are needed to allow conclusions about the function of this interaction.

Interestingly, Bbp1p interacted with the half-bridge component Kar1p in the yeast two-hybrid system. When additional copies of *KAR1* on a centromere-based plasmid were introduced into mutants in *BBP1* they caused an increase in the growth defect. Such an effect of *KAR1* deletion was recognised before for mutants in *CDC31* (Vallen *et al.*, 1994) and *SPC29* (Elliott *et al.*, 1999) which are both defective in SPB duplication (Adams and Kilmartin, 1999; Baum *et al.*, 1986a; Elliott *et al.*, 1999). How this effect occurs is not understood but it is an additional hint for functional similarities between Bbp1p and Spc29p and possibly Cdc31p, the yeast centrin.

4.2 Bbp1p forms a complex with Mps2p

Affinity enrichment of Bbp1p-ProA revealed the co-precipitation of a duplet protein band of about 45 kD which was identified as Mps2p by MALDI-MS analysis. This indicated a potential complex formation of Bbp1p with Mps2p. The interaction of Bbp1p and Mps2p was further proven in the yeast two-hybrid system and in immunoprecipitation experiments. Mps2p was co-precipitated with Bbp1p-3HA and vice versa, Bbp1p was co-precipitated with Mps2p-3HA.

The interaction between Bbp1p and Mps2p was direct and not mediated by other yeast proteins as shown in an in vitro binding experiment. Bacterial expressed N-terminal Mps2p which lacked the putative transmembrane segment (311-327 aa), bound to bacterial expressed full length or C-terminal Bbp1p. The N-terminal Mps2p construct contained the two potential coiled-coil domains (150-225 aa, 230-270 aa; Lupas *et al.*, 1991) of the protein. The C-terminal construct of Bbp1p also contained the putative

coiled-coil segment (320-360 aa; Lupas *et al.*, 1991). It could therefore be possible that Bbp1p and Mps2p interact via their coiled-coil domains.

MPS2 was first discovered in a screen for monopolar spindle mutants (Winey *et al.*, 1991). The mutants were shown to display a defect in late SPB duplication which caused the formation of monopolar spindles (Winey *et al.*, 1991). The *MPS2* gene was also isolated in a genetic screen with mutants in *CIN5* (Munoz-Centeno *et al.*, 1999). *CIN5* codes for a protein of the proteasome required for G_2/M transition (Ghislain *et al.*, 1993). Mutants in *CIN5* arrest with unsegregated chromosomes and it is assumed that proteolysis by the proteasome which is required for cells to enter anaphase is impaired. High gene dosage of *MPS2* inhibits growth of the *cin5* mutant at the semipermissive temperature of 30 °C. Mps2p contains 3 putative Cdc28p phosphorylation sites (Songyang *et al.*, 1994) and four potential destruction box sequences (Glotzer *et al.*, 1991) which could target the protein for destruction by the proteasome (Munoz-Centeno *et al.*, 1999). Therefore, Mps2p might be a substrate of the proteasome and its inefficient degradation might limit cell division (Munoz-Centeno *et al.*, 1999). Bbp1p and Mps2p co-immunoprecipitate in *bbp1-1* mutants which had been incubated for 3 h at the non-permissive temperature. The formation of the complex is therefore not impaired in these mutants. Mutants in *BBP1* arrest in G_2 and it could also be possible that the complex has to be disconnected or degraded for cell cycle progression. However possible degradation of Mps2p by the proteasome is still only hypothetical especially since Munoz-Centeno *et al.* (1999) showed that the concentration of Mps2p is nearly constant throughout the cell cycle except a slight decrease in G_1-S transition.

4.3 Mps2p is a component of SPBs

The finding that Bbp1p and Mps2p form a complex was followed up by the localisation of Mps2p. As expected Mps2p showed a localisation similar to Bbp1p. Mps2p-GFP displayed a typical SPB staining pattern and Mps2p localised close to Spc72p, a component of the outer plaque. As seen in the merged images, signals for Mps2p-3Myc and Spc72p overlapped (yellow) but not entirely (red and green). Therefore, Spc72p and Mps2p did not completely associate with the same SPB

substructures. This could be confirmed by immunolabelling microscopy using isolated SPBs. The gold signal representing Mps2p was mostly localised at the central plaque periphery, a localisation also seen for Bbp1p. Mps2p could be seen where the half-bridge connects to the central plaque or at the central plaque itself when no half-bridge was visible. This indicates that Mps2p like Bbp1p is localised in a ring like pattern at the level of the central plaque (Figure 27). In addition, gold staining was found at the outer plaque, where Spc72p is localised. Again, this could be an artefact created by the primary and secondary antibody but one micrograph showed staining of up to 3 gold particles which could indicate that this localisation is relevant. Munoz-Centeno *et al.* (1999) also localised Mps2p at SPBs by immunolabelling microscopy using whole cells expressing Mps2p-9Myc. In addition to the SPB staining, they observed staining for Mps2p at the nuclear envelope by immunofluorescence microscopy. Interestingly, Mps2p was also identified by Wigge *et al.* (1998) in the MALDI analysis of isolated SPBs but Mps2p was not further investigated in this publication. Taken together, Mps2p is a component of the SPB.

4.4 The Bbp1p/Mps2p complex functions in SPB duplication

Morphological electron microscopy studies of temperature sensitive mutants in *BBP1* showed that mutants are defective in late SPB duplication. Early steps like the enlargement of the satellite into a duplication plaque were normal in *bbp1-1* mutants but subsequent insertion of the duplication plaque into the nuclear envelope and formation of a functional inner plaque seemed to be defective. This was concluded because two fully functional SPBs were not observed in *bbp1-1* cells. If two side-by-side SPBs were investigated, one of the two SPBs connected via the bridge always lacked a complete inner plaque structure. If two separated SPBs were observed one SPB nucleated an apparently normal amount of microtubules while the other SPB nucleated non or only a few nuclear microtubules. Defects in inner plaque assembly possibly causing this microtubule nucleation defect were proven by direct fluorescence microscopy using SPB proteins fused to GFP as markers for the central and inner plaque structure. Only with 30 % probability contained both of the duplicated SPBs an inner plaque structure. GFP and immunofluorescence studies also showed that about 50 % of cells contained only one SPB. It was concluded that possibly the non-

functional SPB was disintegrated in most *bbp1-1* cells. Disintegration of the novel and defective SPB has been postulated for mutants in *spc29* and *spc110* (Adams and Kilmartin, 1999; Sundberg and Davis, 1997). The defects in SPB duplication observed in *bbp1-1* cells caused cells to fail in the formation of a functional spindle and in the separation of chromosomes. Therefore, mutant cells arrested in G_2 probably due to the spindle checkpoint which monitors unattached chromosomes.

The phenotype observed in *bbp1-1* mutants is nearly identical to that of *mps2-1* cells. Mutants in *MPS2* are defective in late SPB duplication (Winey *et al.*, 1991). After 4 h at the restrictive temperature about half of the mutant cells contain duplicated SPBs but the nascent SPB is not inserted into the nuclear envelope. The functional SPB nucleates nuclear and cytoplasmic microtubules while the second SPB only nucleates cytoplasmic microtubules. The smaller SPB-like structure was not found to connect to nuclear microtubules but was in some cases able to move away from the functional SPB probably via cytoplasmic microtubules. As consequence the two SPBs are not connected via a mitotic spindle and the cells arrest in G_2 with a monopolar spindle and unsegregated DNA (Winey *et al.*, 1991). The similarity between the two mutant phenotypes and the direct interaction of Bbp1p and Mps2p suggests that the Bbp1p and Mps2p function together in a complex in late SPB duplication.

A defect in SPB duplication was also observed for mutants in *SPC29* (Adams and Kilmartin, 1999; Elliott *et al.*, 1999). Most *spc29* mutant cells (66 %) contain only one SPB at the restrictive temperature. In about 30 % of cells a second SPB is visible which is smaller in size and only able to nucleate few microtubules. High gene dosage of *BBP1* is able to suppress this defect in *spc29-2* and *spc29-3* mutants (S. Elliott, *published in* Schramm *et al.*, 2000) indicating a functional similarity of both proteins. Overexpression of *MPS2* instead did not rescue *spc29* mutants (S. Elliott, *unpublished*). Spc29p did not show an interaction with Mps2p in the yeast two-hybrid system or by immunoprecipitation as shown for Spc29p and Bbp1p. Taken together, Spc29p has a role in SPB duplication and Spc29p might partially execute this function by interacting with the Bbp1p/Mps2p complex via Bbp1p.

That Bbp1p and Mps2p function together as a complex was further confirmed by the ability of each protein to suppress the mutant phenotype of the other protein. High gene dosage of *MPS2* was able to suppress the growth defect of *bbp1-1* and *bbp1-2* cells and overexpression of *BBP1* rescued the *mps2-2* and *mps2-42* mutants. The only exception was that *mps2-1* cells were not rescued by high gene dosage of *BBP1*. Importantly, only the mutation of the *mps2-1* allele (E39K) is not located in the predicted coiled-coil domain of Mps2p. If Bbp1p and Mps2p interacted via the coiled-coil region, Bbp1p might not be able to suppress mutations outside this region.

4.5 Functional similarities between the Bbp1p/Mps2p complex and Ndc1p

Ndc1p is a protein with functions in late steps of SPB duplication that is localised at nuclear pores and at SPBs. In more detail, a pool of Ndc1p co-localises with Spc42p by immunofluorescence microscopy and it was shown by immunolabelling microscopy that Ndc1p is located at the central plaque periphery (Chial *et al.*, 1998). The localisation of Ndc1p at the SPB is therefore identical to the localisation observed for Mps2p and Bbp1p. Furthermore, the phenotype of mutants in *NDC1* is similar to that observed in *mps2*, *bbp1* and *spc29* cells (Adams and Kilmartin, 1999; Elliott *et al.*, 1999; Thomas and Botstein, 1986; Winey *et al.*, 1991, 1993; this study). When mutants in *NDC1* contain two SPBs, one is normal in form and nucleates cytoplasmic and nuclear microtubules while the second SPB is smaller in size and only attaches to cytoplasmic microtubules. The defective SPB can move away from the mother SPB but it does not acquire its share of chromosomes which all remain connected to the functional spindle pole body. Ndc1p is not only a component of SPBs it also localises to nuclear pores but *ndc1* cells are actually not defective in nuclear pore function (Chial *et al.*, 1998). The fission yeast homologue of Ndc1p is Cut11p, a nuclear envelope protein and which is most likely to function as an anchor protein for the fission yeast SPB at the nuclear envelope in cell division (West *et al.*, 1998). Like Ndc1p, Cut11p also localises to nuclear pores (West *et al.*, 1998). It has been proposed that Ndc1p and Cut11p are not only homologous in their sequence but also in their function with a role in the anchorage and/or insertion of SPBs and nuclear pores into

the nuclear envelope. It was shown by Chial *et al.* (1998) that deletion of the nuclear pore component Pom152p rescues the cold sensitive growth defect of *ndc1* mutants. The mechanism of this phenomenon is not clear but wild type Pom152p seems to be antagonistic to the ndc1p mutant form. Furthermore, deletion of *POM152* in mutants of *BBP1* and *MPS2* also rescued the growth of mutant cells at the non-permissive temperature (this study, Figure 28). Deletion of *POM152* however had no positive effect on the growth of *spc29* mutant cells. This finding emphasises the functional similarity of Bbp1p and Mps2p with Ndc1p. Considering the localisation of Ndc1p at the central plaque and the similarity of the mutant phenotypes of *ndc1*, *bbp1* and *mps2*, Ndc1p might be functionally similar to Bbp1 and Mps2p. All three proteins might be involved in processes leading to the insertion of the duplication plaque into the nuclear envelope.

Interestingly, there is evidence that Pom152p might also be a shared component of nuclear pores and SPBs. Firstly, the original publication about the localisation of Pom152p (Wozniak *et al.*, 1994) contains micrographs which show localisation of Pom152p at the side of the central plaque of the SPB but the authors only commented on the localisation of Pom152p at nuclear pores. Secondly, Pom152p was identified by MALDI analysis of isolated SPBs (Wigge *et al.*, 1998) but was classified as contaminant. Finally, it was shown in this study by immunofluorescence microscopy that a pool of Pom152p was always present near SPBs. Taken together Pom152p might be a candidate for a protein which is shared by nuclear pores and SPBs, like Ndc1p.

In this study Pom152p was co-precipitated with Tdh3p, the budding yeast GAPDH (Figure 28). The relevance of this interaction was not further investigated. However, recently a MALDI analysis of highly enriched nuclear pores also identified Tdh3p as a potential nuclear pore component (Rout *et al.*, 2000) but the authors classified the protein as a contaminant. It might be interesting to consider a potential function of Tdh3p at nuclear pores or SPBs since the protein is known to have complex functions other than in glycolysis. Mammalian GAPDH is a membrane bound protein (Wooster and Wrigglesworth, 1976) with a Ca^{2+} dependent membrane fusion activity (Morero *et al.*, 1985). Furthermore, GAPDH can bind to the C-terminal region of α-tubulin (Kumagai and Sakai, 1983; Volker and Knull, 1997) and can cause tubulin

polymerisation and microtubule bundling (Huitorel and Pantaloni, 1985). GAPDH is known to be phosphorylated by a number of kinases including protein kinase C (Reiss *et al.*, 1996) and it has RNA binding activity (Ryazanov, 1985; Singh and Green, 1993). In yeast, *TDH3* was also isolated as a high gene dosage suppresser of mutations in *SEC61* (Esnault *et al.*, 1993) (Figure 28). Trimeric Sec61p forms the pore of the ER translocon but it is as yet unknown by which mechanism Tdh3p might be able to restore translocon activity. Speculating about the function of Tdh3p at the SPB, Tdh3p may interact with Pom152p to mediate steps in duplication plaque insertion or in inner plaque assembly.

4.6 Analysis of the Δmps2 deletion strain

BBP1 was regarded to be an essential gene since cells, which lacked a functional copy of *BBP1*, could not survive. In contrast, some cells lacking *MPS2* could grow very slowly at 23 °C but the majority of these cells displayed various severe mutant phenotypes. Cells were large and multi-budded and displayed defects in spindle formation and chromosome segregation. Interestingly, these cells could contain up to 4 SPBs. If the cellular defects in these cells were caused by malfunction of SPBs is not known since mutant cells have not yet been investigated by electron microscopy. FACS analysis of the Δ*mps2* strain showed that cells had 1n, 2n or 4n DNA contents (Munoz-Centeno *et al.*, 1999). High gene dosage of *BBP1* did not restore wild type growth in cells lacking *MPS2*. Therefore, it was unlikely that *BBP1* could be the main suppresser that mediated the slow growth of the deletion strain. A screen designed to identify high gene dosage suppressers of the *mps2* deletion strain identified one single candidate, *SMY2* (Figure 28). Overexpression of *SMY2* allowed cells lacking *MPS2* to grow at temperatures up to 30 °C. At 23 °C, cells with additional gene copies of *SMY2* grew with similar kinetics as wild type. The morphology of these cells was normal apart from the elongated form of the bud and the positioning of the bud at the side of the mother cell. This however could be a side effect of *SMY2* overexpression and should be followed up in future work.

The cellular role of Smy2p is as yet unknown but there are various hints for its putative function. *SMY2* had been identified in a screen for high gene dosage suppressers of

mutants in *MYO2*. *MYO2* encodes the yeast unconventional class V myosin, an actin associated motor protein which is involved in vesicle and organelle transport to the bud. Overexpression of *SMY2* can also suppress mutations in several other genes like *sec22*, *bet1* and *sec16* (Lillie and Brown, 1994) (Figure 28). The wild type products of these genes are involved in vesicular transport and vesicle fusion or vesicle formation (Espenshade *et al.*, 1995; Gimeno *et al.*, 1995; Newman *et al.*, 1990, 1992a, 1992b). Myo2p is also involved in directing the astral microtubules into the bud via an interaction with Kar9p (Yin *et al.*, 2000), thereby aligning the mitotic spindle. How could possible functions of Smy2p be related to functions of Mps2p? It might be that Mps2p has additional functions which are not closely related to its function at the SPB. The *mps2-1* mutant is not rescued by overexpression of *BBP1* and indeed, *mps2-1* cells show an additional defect not observed in *mps2-2* and *mps2-42* mutants. If *mps2-1* cells are grown in liquid culture cells floculate, which means that cells form clumps and sediment on the bottom of the flask. This phenotype is usually observed in mutants defective in cell wall formation. Cell wall formation is a process dependent on vesicular transport along the actin cytoskeleton and on vesicle fusion at the location of growth. Mps2p and Smy2p could possibly be involved in these processes but this is still to be proven. However to rescue the *MPS2* deletion mutant, Smy2p might have to compensate for functions of Mps2p directly at the SPB or at the nuclear envelope. This role of Smy2p remains to be determined in future work.

It was shown recently that the potential *S. pombe* homologue of *SMY2*, mpd2$^+$, suppresses the conditional lethal phenotype of mutants in *CDC7* (Cullen *et al.*, 2000). Cdc7p is a protein kinase which is essential for initiating septum formation a process required in fission yeast for cytokinesis (Fankhauser and Simanis, 1994). Cdc7p, like its budding yeast homologue Cdc15p, is localised at the SPB in mitosis (Sohrmann *et al.*, 1998; Xu *et al.*, 2000). In late anaphase Cdc7p localises to only one SPB (Sohrmann *et al.*, 1998) while it was shown for budding yeast that a portion of Cdc15p is found at the mother-bud neck at the end of telophase (Xu *et al.*, 2000). While Cdc7p is involved in the exit from mitosis by signalling the onset of septum formation (Sohrmann *et al.*, 1998), Cdc15p is part of the mitotic exit network required for degradation of B-type cyclins at the end of mitosis in budding yeast (Jaspersen *et al.*,

1998; Surana *et al.*, 1993). So far, it has not been investigated if high gene dosage of *SMY2* can rescue mutants in *CDC15* in budding yeast as indicated by the findings in fission yeast. However, if this was the case then Smy2p might have the potential to interact with Cdc15p and Mps2p at the SPB.

4.7 Bfr1p interacts with SPB components in the two-hybrid system

Bfr1p was shown to interact genetically with Bbp1p in the yeast two-hybrid system (Xue *et al.*, 1996; this study). The interaction of Bfr1p with other SPB components was also checked in the yeast two-hybrid system and Bfr1p was shown to interact with the half-bridge component Cdc31p and the central plaque protein Spc29p (this study). Localisation of Bfr1p by immunofluorescence microscopy revealed that the protein is cytoplasmic with a slight concentration at the nuclear envelope. An exclusive localisation or concentration at the SPB was not observed. About the function of Bfr1p can only be speculated despite several publications on the protein. Bfr1p was first identified in a screen for proteins that mediate resistance against the drug Brefeldin A (BFA) (Jackson and Kepes, 1994). Wild type yeast cells are resistant against the drug but if cells carry the *erg6* mutation they become sensitive ((Graham *et al.*, 1993; Shah and Klausner, 1993; Vogel *et al.*, 1993). In yeast, BFA binds to complexes of Sec7p and Arf1p-GDP thereby trapping the small G-protein of the Arf-family with its potential guanine nucleotide exchange factor Sec7p. As consequence Arf1p stays in the inactive GDP-bound form and COPI coat vesicle can not be assembled (Peyroche *et al.*, 1999). Transport to the Golgi and retrograde transport to the ER ceases and the Golgi disassembles and redistributes to the ER. Overexpression of *BFR1* causes complete resistance to BFA by an unknown mechanism (Jackson and Kepes, 1994). In addition, overexpression of *BFR1* partially suppresses the growth defect of mutants in *SEC17* a yeast gene coding for the homologue of the mammalian α-SNAP involved in vesicle targeting and/or fusion, respectively (Clary *et al.*, 1990; Griff *et al.*, 1992). This indicates that Bfr1p might have functions in vesicular transport. Interestingly, Smy2p the suppresser of the *mps2* deletion strain was also implicated in having functions in vesicular transport or fusion (see above).

More recently, Bfr1p was isolated in a complex with Scp160p, a potential member of the vigilin family that mainly associates with polyribosomes. Another component of the Scp160p complex isolated is Pab1p, a poly(A) binding protein (Lang and Fridovich-Keil, 2000). Scp160p can bind to ribohomopolymers and rRNA but not to tRNA (Weber *et al.*, 1997) and it localises to the cytoplasm with enrichment around the nuclear envelope and possibly the ER (Lang and Fridovich-Keil, 2000) a localisation similar to Bfr1p (this study). Deletion of *SCP160* in yeast is not lethal but results in various phenotypes including increased DNA content, missegregation of genetic markers during sporulation and abnormal cell morphology, including increased size and irregular shape (Wintersberger *et al.*, 1995). A deletion strain of *BFR1* is viable (Jackson and Kepes, 1994; this study) and shows similar phenotypes (Jackson and Kepes, 1994). Cells are enlarged in size and some cells are elongated and/or form multiple buds. About 20 % of cells show defects in nuclear segregation creating anucleate and polyploid cells (Jackson and Kepes, 1994). Therefore, Bfr1p and Scp160p show similar localisation and deletion phenotypes. Interestingly, Mps2p was co-purified with the ribosomal protein Rps3p (this study). Ribosomal proteins are often found to contaminate immunoprecipitates. On the other hand, this result could be an indication for the possibility of the interaction of Mps2p with ribosomes. However, more data are needed to confirm SPB ribosome interactions. In addition, interactions of Bfr1p with proteins involved in SPB duplication (Bbp1p, Cdc31p, Spc29p) still have to be connected to Bfr1p function in BFA-resistance, vesicular transport and as part of the Scp160p complex which binds to polyribosomes.

4.8 HSC82 might have functions at the SPB

In *Drosophila*, the chaperone Hsp90 is a core component of the centrosome (Lange *et al.*, 2000). Hsp90 localises to the centrosome throughout the cell cycle and its localisation is not microtubule dependent. Mutations in Hsp90 or treatment with Hsp90 inhibitors result in abnormal centrosome separation and maturation. As consequence aberrant spindles are formed and chromosomal separation is impaired. Therefore, Hsp90 seems to be essential to ensure proper centrosome functions (Lange *et al.*, 2000). Other functions of Hsp90 include the promotion of protein folding (Wiech *et al.*, 1992), keeping proteins in a folding compatible state for other chaperones

(Freeman and Morimoto, 1996) and the prevention of protein unfolding and aggregation (Miyata and Yahara, 1992).

In budding yeast two isoforms of Hsp90, the constitutively expressed Hsc82p and the highly inducible Hsp82p are present and expression of one of the two isoforms is essential (Borkovich *et al.*, 1989). So far, it is unknown whether Hsp90 is also a component of the yeast SPB. In this study, the constitutively expressed isoform *HSC82* was found to co-precipitate with the Bbp1p/Mps2p complex in mutant cells incubated at the restrictive temperature but not at the permissive temperature. The relevance of this interaction for the function of the complex in SPB duplication is not known. Interestingly, mutants in *HSF1*, a gene coding for a transcription factor of Hsp90 are defective in spindle pole body duplication (Zarzov *et al.*, 1997). This duplication defect might be due to direct functions of Hsf1p at the SPB but could also be due to the defect of *hsf1* mutants in the synthesis of Hsp90. The latter might be more likely since high gene dosage of *HSC82* can restore the defects in *hsf1* mutants (Zarzov *et al.*, 1997). It was tested whether high gene dosage could also restore growth in *bbp1* and *mps2* mutants also defective in SPB duplication. Here, high gene dosage of *HSC82* suppressed cells carrying the *mps2-42* mutant allele only while growth of *mps2-1*, *mps2-2* and all *bbp1* mutants was not improved. It was shown by Morano *et al.* (1999) that cells containing only the truncated form of *HSF1*[1-583] are very sensitive to the drug geldanamycin, an inhibitor of Hsp90. Other mutants which show defects in SPB duplication were tested for sensitivity to geldanamycin at the permissive and semi-permissive temperature. Of those strains tested, wild type strains and mutants in *BBP1*, *MPS2* and *CDC37* did not show reduced growth by treatment with geldanamycin. The *cdc37-1* mutant was tested since mutant cells arrest with side-by-side SPBs. Of these SPBs, the novel SPB has a reduced outer plaque or lacks the outer plaque completely. In contrast, the *hsf1-82*, *mps1-1* and *cdc28-109* mutants were unable to grow on plates treated with geldanamycin. The *cdc28-109* is an allele of *CDC28* that shows mixed G_1- and G_2- arrest after transfer of an asynchronous culture to the restrictive temperature (Zarzov *et al.*, 1997). Interestingly, depletion of Hsp90 from yeast cells also results in cell cycle arrest at both G_1/S- and G_2/M-phase (Morano *et al.*, 1999) suggesting a complex requirement for Hsp90 function at important time points of Cdc28p/cyclin

activity. Mps1p has functions at early and late stages in SPB duplication (Schutz *et al.*, 1997; Schutz and Winey, 1998) and it is part of the spindle checkpoint with signalling activity via Mad1p (Hardwick *et al.*, 1996). Mutants in *MPS1* have been shown to be co-lethal with mutations in *HSC82* (Jones *et al.*, 1999). This genetic interaction and the effect of geldanamycin on *mps1-1* could indicate a function of Hsp90 either in SPB duplication or in checkpoint signalling, since Hsp90 was shown to be part of various signalling cascades. Taken together, these findings indicate effects of Hsp90 function on proteins implicated in SPB duplication.

4.9 A novel protein complex of SPB associated proteins

Ivan LeMasson (Saclay, Paris, France) found a genetic interaction of Mps2p with Spc24p in the yeast two-hybrid system (*personal communication*). This genetic interaction has lately been reported in a publication about interactions of coiled-coil proteins (Newman *et al.*, 2000). Spc24p was first identified as a novel SPB component by MALDI-MS analysis of isolated SPBs and Spc24p was localised at the nuclear side of SPBs by immunolabelling electron microscopy (Wigge *et al.*, 1998).

The potential interaction of Mps2p and Spc24p was investigated by co-immunoprecipitation, but purification of Mps2p or Spc24p with each other was unsuccessful. However, MALDI analysis of the precipitate of Spc24p-3HA revealed the co-precipitation of Ndc80p. *Vice versa*, Spc24p could be co-precipitated with Ndc80p-6HA, which indicated that Spc24p and Ndc80p might form a complex. This assumption is further supported by the known genetic interaction of Ndc80p and Spc24p in the yeast two-hybrid system (Cho *et al.*, 1998).

Ndc80p, is a protein which localises close to the nuclear side of the SPB, a localisation also shown for Spc24p and Spc25p (Rout and Kilmartin, 1990; Wigge *et al.*, 1998). The staining pattern of Ndc80p-GFP at the nuclear side of the SPB is punctuated which is characteristic for centromere staining. Centromeres are known to cluster near the nuclear side of the SPB (Goh and Kilmartin, 1993; Goshima and Yanagida, 2000; He *et al.*, 2000; Hyland *et al.*, 1999; Jin *et al.*, 2000). Ndc80p is a homologue of the human HEC protein (Wigge *et al.*, 1998) which is localised at human kinetochores.

Furthermore, *NDC80* is synthetical lethal with *CTF19* (Hyland *et al.*, 1999) a gene coding for a kinetochore component, which was shown to localise to the nuclear phase of SPBs (Hyland *et al.*, 1999). Taken together, this indicates that Ndc80p is a potential component of kinetochores (Rout and Kilmartin, 1990; Wigge *et al.*, 1998; Zheng *et al.*, 1999).

C. Janke in our laboratory investigated Spc25p a protein that potentially interacts with Spc24p (see above). Precipitation of Spc25p-3HA enriched a complex containing the Spc24p/Ndc80p-complex and Nuf2p, a protein that is localised at SPBs (Osborne *et al.*, 1994). The cellular localisation of the complex consisting of Spc24p, Spc25p, Ndc80p and Nuf2p was further investigated in a collaboration of our laboratory with the group of J. Lechner (Heidelberg). CHIP analysis proved the association of all proteins with centromere DNA. This association was dependent on Ndc10p a core kinetochore component (Janke *et al.*, *in press*).

Mutants in *NDC80* contain two morphological normal SPBs and cells are able to form an anaphase spindle of wild type morphology but fail to segregate duplicated chromosomes (Wigge *et al.*, 1998). This mutant phenotype taken together with the localisation of Ndc80p at the kinetochore led to the conclusion that mutants in *NDC80* are unable to attach microtubules to kinetochores, a task which might usually be fulfilled by the functional complex.

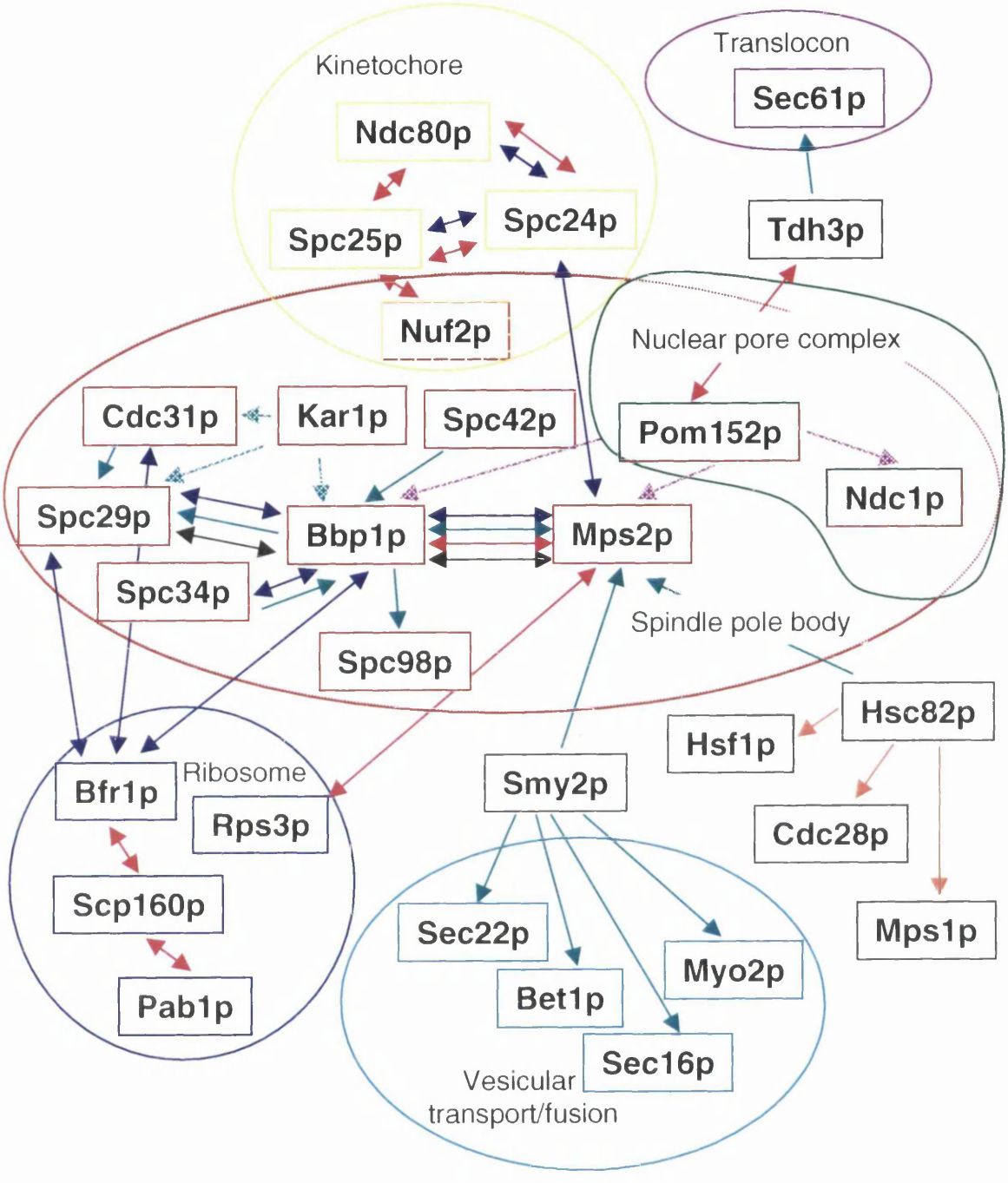

Figure 28: Complex interactions of Bbp1p and Mps2p with proteins of the spindle pole body, nuclear pore complex, ribosome, kinetochore, translocon and proteins involved in vesicular transport/fusion, cell signalling and other cellular processes.

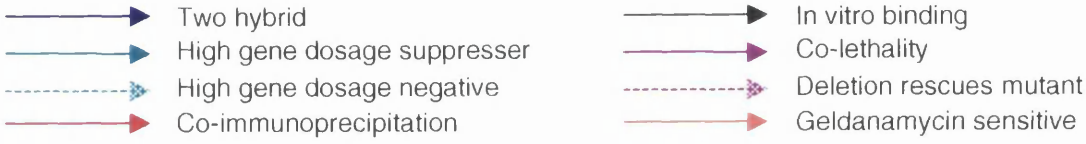

5. Conclusion

Bbp1p and Mps2p form a novel complex that functions in SPB duplication. The interaction of both proteins is direct and not mediated by other proteins. The complex is localised most likely in a ring-like structure around the central plaque periphery of the SPB thereby possibly anchoring the SPB in the nuclear envelope and connecting the central plaque to the half-bridge. This is supported by the interaction of Bbp1p with Spc29p a component of the central plaque of the SPB and by the interaction with Kar1p which is a component of the half-bridge. Bbp1p also shows genetic interaction with other SPB components like Spc34p and Spc42p. Furthermore, Bbp1p interacts with Bfr1p, a protein which is localised in the cytoplasm and at the nuclear envelope. Bfr1p is a protein of unknown function which mediates Brefeldin A resistance and associates with polyribosomes. Mutants in *BBP1* and *MPS2* display similar defects in SPB duplication which result in impaired mitosis and G_2 arrest. This phenotype can be rescued by deletion of *POM152*, a gene coding for a nuclear pore component, as observed before for mutations in *NDC1*. Mutants in *NDC1* show nearly identical defects as *bbp1* and *mps2* mutants and the proteins might have similar functions. A pool of Pom152p was shown to always be present in the proximity of SPBs and the protein might have direct function at the SPB. Cells lacking *MPS2*, which show various defects in spindle formation, SPB content and chromosomal segregation can not be rescued by high gene dosage of *BBP1* but by *SMY2*. Smy2p is a protein which might be involved in membrane fusion and/or vesicular transport. The mechanism of rescue has to be investigated further. This study also provides evidence that Hsp90 might have functions in SPB duplication. Hsc82p was found in the Bbp1/Mps2p complex in mutants of *BBP1*. Furthermore, high gene dosage of Hsc82p suppressed the *mps2-42* mutant. Inhibition of Hsp90 was lethal for mutants in *HSF1*, *MPS1* and *CDC28* which are all defective in SPB duplication. In addition to the Bbp1p/Mps2p-complex, a complex consisting of the SPB associated proteins Spc24p, Ndc80p and Spc25p was isolated. This complex might mediate the attachment of microtubules at kinetochores and is therefore essential for the formation of a functional mitotic spindle.

Bibliography

Adams, A.E. and Pringle, J.R. (1984) Relationship of actin and tubulin distribution to bud growth in wild- type and morphogenetic-mutant *Saccharomyces cerevisiae*. *J Cell Biol*, **98**, 934-45.

Adams, I.R. and Kilmartin, J.V. (1999) Localization of core spindle pole body (SPB) components during SPB duplication in *Saccharomyces cerevisiae*. *J. Cell Biol.*, **145**, 809-823.

Alberts, B., Bray, D., Lewis, M. and Raff, M. (1994) Molecular biology of the cell. *Garland New York*, **3rd edition**.

Bardin, A.J., Visintin, R. and Amon, A. (2000) A mechanism for coupling exit from mitosis to partitioning of the nucleus. *Cell*, **102**, 21-31.

Baum, P., Furlong, C. and Byers, B. (1986a) Yeast gene required for spindle pole body duplication: homology of its product with Ca2+-binding proteins. *Proc Natl Acad Sci U S A*, **83**, 5512-6.

Baum, P., Furlong, C. and Byers, B. (1986b) Yeast gene required for spindle pole body duplication: homology of its product with Ca^{2+}-binding proteins. *Proc. Natl. Acad. Sci. USA*, **83**, 5512-5516.

Beach, D.L., Thibodeaux, J., Maddox, P., Yeh, E. and Bloom, K. (2000) The role of the proteins Kar9p and Myo2p in orienting the mitotic spindle of budding yeast. *Curr Biol*, **10**, 1497-506.

Benedetti, H., Raths, S., Crausaz, F. and Riezman, H. (1994) The *END3* gene encodes a protein that is required for the internalization step of endocytosis and for actin cytoskeleton organization in yeast. *Mol Biol Cell*, **5**, 1023-37.

Beningo, K.A., Lillie, S.H. and Brown, S.S. (2000) The yeast kinesin-related protein Smy1p exerts its effects on the class V myosin Myo2p via a physical interaction. *Mol Biol Cell*, **11**, 691-702.

Biggins, S., Ivanovska, I. and Rose, M.D. (1996) Yeast ubiquitin-like genes are involved in duplication of the microtubule organizing center. *J Cell Biol*, **133**, 1331-46.

Biggins, S. and Rose, M.D. (1994) Direct interaction between yeast spindle pole body components: Kar1p is required for Cdc31p localization to the spindle pole body. *J. Cell Biol.*, **125**, 843-852.

Bloecher, A., Venturi, G.M. and Tatchell, K. (2000) Anaphase spindle position is monitored by the *BUB2* checkpoint. *Nat Cell Biol*, **2**, 556-8.

Bobinnec, Y., Moudjou, M., Fouquet, J.P., Desbruyeres, E., Edde, B. and Bornens, M. (1998) Glutamylation of centriole and cytoplasmic tubulin in proliferating non-neuronal cells. *Cell Motil Cytoskeleton*, **39**, 223-32.

Bonner, W.A., Hulett, H.R., Sweet, R.G. and Herzenberg, L.A. (1972) Fluorescence activated cell sorting. *Rev Sci Instrum*, **43**, 404-9.

Borkovich, K.A., Farrelly, F.W., Finkelstein, D.B., Taulien, J. and Lindquist, S. (1989) Hsp82p is an essential protein that is required in higher concentrations for growth of cells at higher temperatures. *Mol Cell Biol*, **9**, 3919-30.

Botstein, D., Chervitz, S.A. and Cherry, J.M. (1997) Yeast as a model organism [comment]. *Science*, **277**, 1259-60.

Boveri, T. (1900) Ueber die Natur der Centrosomen. *Zellen Studien*, **Heft 4**.

Brachat, A., Kilmartin, J.V., Wach, A. and Philippsen, P. (1998) *Saccharomyces cerevisiae* cells with defective spindle pole body outer plaques accomplish

nuclear migration via half-bridge-organized microtubules. *Mol Biol Cell*, **9**, 977-91.

Broach, J.R., Strathern, J.N. and Hicks, J.B. (1979) Transformation in yeast: development of a hybrid cloning vector and isolation of the *CAN1* gene. *Gene*, **8**, 121-33.

Brockerhoff, S.E., Stevens, R.C. and Davis, T.N. (1994) The unconventional myosin, Myo2p, is a calmodulin target at sites of cell growth in *Saccharomyces cerevisiae*. *J Cell Biol*, **124**, 315-23.

Brodsky, J.L. and Schekman, R. (1993) A Sec63p-BiP complex from yeast is required for protein translocation in a reconstituted proteoliposome. *J Cell Biol*, **123**, 1355-63.

Bullitt, E., Rout, M.P., Kilmartin, J.V. and Akey, C.W. (1997) The yeast spindle pole body is assembled around a central crystal of Spc42p. *Cell*, **89**, 1077-86.

Byers, B. (1981a) Cytology of the yeast life cycle. Cold Spring Harbor Laboratory Press, Cold Spring Harbor.

Byers, B. (1981b) Multiple roles of the spindle pole bodies in the life cycle of *Saccharomyces cerevisiae*. In Wettstein, D., Stenderup, A., Kielland-Brandt, M. and Friis, J. (eds.), *Molecular Genetics in Yeast*. Alfred Benzon Symp., Munksgaard, Copenhagen, Vol. 16, pp. 119-133.

Byers, B. and Goetsch, L. (1974) Duplication of spindle plaques and integration of the yeast cell cycle. *Cold Spring Harbor Symp. Quant. Biol.* Cold Spring Harbor Laboratory, Vol. XXXVIII, pp. 123-131.

Byers, B. and Goetsch, L. (1975) Behavior of spindles and spindle plaques in the cell cycle and conjugation of *Saccharomyces cerevisiae*. *J. Bacteriol.*, **124**, 511-523.

Byers, B., Shriver, K. and Goetsch, L. (1978) The role of spindle pole bodies and modified microtubule ends in the initiation of microtubule assembly in *Saccharomyces cerevisiae. J. Cell Sci.*, **30**, 331-352.

Carminati, J.L. and Stearns, T. (1997) Microtubules orient the mitotic spindle in yeast through dynein- dependent interactions with the cell cortex. *J Cell Biol*, **138**, 629-41.

Chen, X.P., Yin, H. and Huffaker, T.C. (1998) The yeast spindle pole body component Spc72p interacts with Stu2p and is required for proper microtubule assembly. *J Cell Biol*, **141**, 1169-79.

Chen, Y., Riley, D.J., Chen, P.L. and Lee, W.H. (1997a) HEC, a novel nuclear protein rich in leucine heptad repeats specifically involved in mitosis. *Mol Cell Biol*, **17**, 6049-56.

Chen, Y., Sharp, Z.D. and Lee, W.H. (1997b) HEC binds to the seventh regulatory subunit of the 26 S proteasome and modulates the proteolysis of mitotic cyclins. *J Biol Chem*, **272**, 24081-7.

Chial, H.J., Giddings, T.H., Jr., Siewert, E.A., Hoyt, M.A. and Winey, M. (1999) Altered dosage of the *Saccharomyces cerevisiae* spindle pole body duplication gene, *NDC1*, leads to aneuploidy and polyploidy. *Proc Natl Acad Sci U S A*, **96**, 10200-5.

Chial, H.J., Rout, M.P., Giddings, T.H. and Winey, M. (1998) *Saccharomyces cerevisiae* Ndc1p is a shared component of nuclear pore complexes and spindle pole bodies. *J Cell Biol*, **143**, 1789-800.

Cho, R.J., Fromont-Racine, M., Wodicka, L., Feierbach, B., Stearns, T., Legrain, P., Lockhart, D.J. and Davis, R.W. (1998) Parallel analysis of genetic selections using whole genome oligonucleotide arrays. *Proc Natl Acad Sci U S A*, **95**, 3752-7.

Chowdhury, S., Smith, K.W. and Gustin, M.C. (1992) Osmotic stress and the yeast cytoskeleton: phenotype-specific suppression of an actin mutation. *J Cell Biol*, **118**, 561-71.

Chretien, D., Buendia, B., Fuller, S.D. and Karsenti, E. (1997) Reconstruction of the centrosome cycle from cryoelectron micrographs. *J Struct Biol*, **120**, 117-33.

Christianson, T.W., Sikorski, R.S., Dante, M., Shero, J.H. and Hieter, P. (1992) Multifunctional yeast high-copy-number shuttle vectors. *Gene*, **110**, 119-22.

Ciosk, R., Zachariae, W., Michaelis, C., Shevchenko, A., Mann, M. and Nasmyth, K. (1998) An *ESP1/PDS1* complex regulates loss of sister chromatid cohesion at the metaphase to anaphase transition in yeast. *Cell*, **93**, 1067-76.

Clary, D.O., Griff, I.C. and Rothman, J.E. (1990) SNAPs, a family of NSF attachment proteins involved in intracellular membrane fusion in animals and yeast. *Cell*, **61**, 709-21.

Cohen-Fix, O., Peters, J.M., Kirschner, M.W. and Koshland, D. (1996) Anaphase initiation in *Saccharomyces cerevisiae* is controlled by the APC-dependent degradation of the anaphase inhibitor Pds1p. *Genes Dev*, **10**, 3081-93.

Conde, J. and Fink, G.R. (1976) A mutant of *Saccharomyces cerevisiae* defective for nuclear fusion. *Proc Natl Acad Sci U S A*, **73**, 3651-5.

Cooper, J.A., Buhle, E.L., Jr., Walker, S.B., Tsong, T.Y. and Pollard, T.D. (1983) Kinetic evidence for a monomer activation step in actin polymerization. *Biochemistry*, **22**, 2193-202.

Cottingham, F.R. and Hoyt, M.A. (1997) Mitotic spindle positioning in *Saccharomyces cerevisiae* is accomplished by antagonistically acting microtubule motor proteins. *J Cell Biol*, **138**, 1041-53.

Cullen, C.F., May, K.M., Hagan, I.M., Glover, D.M. and Ohkura, H. (2000) A new genetic method for isolating functionally interacting genes: high plo1(+)-dependent mutants and their suppressors define genes in mitotic and septation pathways in fission yeast. *Genetics*, **155**, 1521-34.

Danscher, G., Norgaard, J.O. and Baatrup, E. (1987) Autometallography: tissue metals demonstrated by a silver enhancement kit. *Histochemistry*, **86**, 465-9.

de Saint Phalle, B. and Sullivan, W. (1998) Spindle assembly and mitosis without centrosomes in parthenogenetic *Sciara* embryos. *J Cell Biol*, **141**, 1383-91.

DeBoer, C., Meulman, P.A., Wnuk, R.J. and Peterson, D.H. (1970) Geldanamycin, a new antibiotic. *J Antibiot (Tokyo)*, **23**, 442-7.

Demerec, M., Adelberg, E.A., Clark, A.J. and Hartman, P.E. (1966) A proposal for a uniform nomenclature in bacterial genetics. *Genetics*, **54**, 61-76.

DeZwaan, T.M., Ellingson, E., Pellman, D. and Roof, D.M. (1997) Kinesin-related *KIP3* of *Saccharomyces cerevisiae* is required for a distinct step in nuclear migration. *J Cell Biol*, **138**, 1023-40.

Dictenberg, J.B., Zimmerman, W., Sparks, C.A., Young, A., Vidair, C., Zheng, Y., Carrington, W., Fay, F.S. and Doxsey, S.J. (1998) Pericentrin and gamma-tubulin form a protein complex and are organized into a novel lattice at the centrosome. *J Cell Biol*, **141**, 163-74.

Ding, R., West, R.R., Morphew, D.M., Oakley, B.R. and McIntosh, J.R. (1997) The spindle pole body of *Schizosaccharomyces pombe* enters and leaves the nuclear envelope as the cell cycle proceeds. *Mol Biol Cell*, **8**, 1461-79.

Dirick, L., Bohm, T. and Nasmyth, K. (1995) Roles and regulation of Cln-Cdc28 kinases at the start of the cell cycle of *Saccharomyces cerevisiae*. *Embo J*, **14**, 4803-13.

Donaldson, A.D. and Kilmartin, J.V. (1996) Spc42p: a phosphorylated component of the *S. cerevisiae* spindle pole body (SPD) with an essential function during SPB duplication. *J Cell Biol*, **132**, 887-901.

Doxsey, S.J., Stein, P., Evans, L., Calarco, P.D. and Kirschner, M. (1994) Pericentrin, a highly conserved centrosome protein involved in microtubule organization. *Cell*, **76**, 639-50.

Doyle, T. and Botstein, D. (1996) Movement of yeast cortical actin cytoskeleton visualized *in vivo*. *Proc Natl Acad Sci U S A*, **93**, 3886-91.

Drubin, D.G., Jones, H.D. and Wertman, K.F. (1993) Actin structure and function: roles in mitochondrial organization and morphogenesis in budding yeast and identification of the phalloidin- binding site. *Mol Biol Cell*, **4**, 1277-94.

Dunn, T.M. and Shortle, D. (1990) Null alleles of *SAC7* suppress temperature-sensitive actin mutations in *Saccharomyces cerevisiae*. *Mol Cell Biol*, **10**, 2308-14.

Durfee, T., Becherer, K., Chen, P.L., Yeh, S.H., Yang, Y., Kilburn, A.E., Lee, W.H. and Elledge, S.J. (1993) The retinoblastoma protein associates with the protein phosphatase type 1 catalytic subunit. *Genes Dev*, **7**, 555-69.

Dutcher, S.K. and Trabuco, E.C. (1998) The *UNI3* gene is required for assembly of basal bodies of *Chlamydomonas* and encodes delta-tubulin, a new member of the tubulin superfamily. *Mol Biol Cell*, **9**, 1293-308.

Ehler, L.L., Holmes, J.A. and Dutcher, S.K. (1995) Loss of spatial control of the mitotic spindle apparatus in a *Chlamydomonas reinhardtii* mutant strain lacking basal bodies [published erratum appears in Genetics 1996 Feb;142(2):following 650]. *Genetics*, **141**, 945-60.

Elliott, S., Knop, M., Schlenstedt, G. and Schiebel, E. (1999) Spc29p is a component of the Spc110p subcomplex and is essential for spindle pole body duplication. *Proc Natl Acad Sci U S A*, **96**, 6205-10.

Engel, J., Fasold, H., Hulla, F.W., Waechter, F. and Wegner, A. (1977) The polymerization reaction of muscle actin. *Mol Cell Biochem*, **18**, 3-13.

Epstein, C.B. and Cross, F.R. (1992) CLB5: a novel B cyclin from budding yeast with a role in S phase. *Genes Dev*, **6**, 1695-706.

Erickson, H.P. and Stoffler, D. (1996) Protofilaments and rings, two conformations of the tubulin family conserved from bacterial *FtsZ* to alpha/beta and gamma tubulin. *J Cell Biol*, **135**, 5-8.

Errabolu, R., Sanders, M.A. and Salisbury, J.L. (1994) Cloning of a cDNA encoding human centrin, an EF-hand protein of centrosomes and mitotic spindle poles. *J Cell Sci*, **107**, 9-16.

Eshel, D., Urrestarazu, L.A., Vissers, S., Jauniaux, J.C., van Vliet-Reedijk, J.C., Planta, R.J. and Gibbons, I.R. (1993) Cytoplasmic dynein is required for normal nuclear segregation in yeast. *Proc Natl Acad Sci U S A*, **90**, 11172-6.

Esnault, Y., Blondel, M.O., Deshaies, R.J., Scheckman, R. and Kepes, F. (1993) The yeast *SSS1* gene is essential for secretory protein translocation and encodes a conserved protein of the endoplasmic reticulum. *Embo J*, **12**, 4083-93.

Espenshade, P., Gimeno, R.E., Holzmacher, E., Teung, P. and Kaiser, C.A. (1995) Yeast *SEC16* gene encodes a multidomain vesicle coat protein that interacts with Sec23p. *J Cell Biol*, **131**, 311-24.

Fabre, E. and Hurt, E. (1997) Yeast genetics to dissect the nuclear pore complex and nucleocytoplasmic trafficking. *Annu Rev Genet*, **31**, 277-313.

Fairbanks, G., Steck, T.L. and Wallach, D.F. (1971) Electrophoretic analysis of the major polypeptides of the human erythrocyte membrane. *Biochemistry*, **10**, 2606-17.

Fang, G., Yu, H. and Kirschner, M.W. (1998) The checkpoint protein *MAD2* and the mitotic regulator *CDC20* form a ternary complex with the anaphase-promoting complex to control anaphase initiation. *Genes Dev*, **12**, 1871-83.

Fankhauser, C. and Simanis, V. (1994) The *cdc7* protein kinase is a dosage dependent regulator of septum formation in fission yeast. *Embo J*, **13**, 3011-9.

Farkas, V., Kovarik, J., Kosinova, A. and Bauer, S. (1974) Autoradiographic study of mannan incorporation into the growing cell walls of *Saccharomyces cerevisiae*. *J Bacteriol*, **117**, 265-9.

Farr, K.A. and Hoyt, M.A. (1998) Bub1p kinase activates the *Saccharomyces cerevisiae* spindle assembly checkpoint. *Mol Cell Biol*, **18**, 2738-47.

Feldheim, D., Yoshimura, K., Admon, A. and Schekman, R. (1993) Structural and functional characterization of Sec66p, a new subunit of the polypeptide translocation apparatus in the yeast endoplasmic reticulum. *Mol Biol Cell*, **4**, 931-9.

Feldman, R.M., Correll, C.C., Kaplan, K.B. and Deshaies, R.J. (1997) A complex of Cdc4p, Skp1p, and Cdc53p/cullin catalyzes ubiquitination of the phosphorylated CDK inhibitor Sic1p. *Cell*, **91**, 221-30.

Fields, S. and Song, O. (1989) A novel genetic system to detect protein-protein interactions. *Nature*, **340**, 245-6.

Fitch, I., Dahmann, C., Surana, U., Amon, A., Nasmyth, K., Goetsch, L., Byers, B. and Futcher, B. (1992) Characterization of four B-type cyclin genes of the budding yeast *Saccharomyces cerevisiae*. *Mol Biol Cell*, **3**, 805-18.

Freeman, B.C. and Morimoto, R.I. (1996) The human cytosolic molecular chaperones hsp90, hsp70 (hsc70) and hdj-1 have distinct roles in recognition of a non-native protein and protein refolding. *Embo J*, **15**, 2969-79.

Geier, B.M., Wiech, H. and Schiebel, E. (1996) Binding of centrins and yeast calmodulin to synthetic peptides corresponding to binding sites in the spindle pole body components Karlp and Spc110p. *J Biol Chem*, **271**, 28366-74.

Geiser, J.R., Sundberg, H.A., Chang, B.H., Muller, E.G. and Davis, T.N. (1993) The essential mitotic target of calmodulin is the 110-kilodalton component of the spindle pole body in *Saccharomyces cerevisiae*. *Mol Cell Biol*, **13**, 7913-24.

Geissler, S., Pereira, G., Spang, A., Knop, M., Soues, S., Kilmartin, J. and Schiebel, E. (1996) The spindle pole body component Spc98p interacts with the gamma-tubulin- like Tub4p of *Saccharomyces cerevisiae* at the sites of microtubule attachment [published erratum appears in EMBO J 1996 Sep 16;15(18):5124]. *Embo J*, **15**, 3899-911.

Ghislain, M., Udvardy, A. and Mann, C. (1993) *S. cerevisiae* 26S protease mutants arrest cell division in G2/metaphase. *Nature*, **366**, 358-62.

Gimeno, R.E., Espenshade, P. and Kaiser, C.A. (1995) *SED4* encodes a yeast endoplasmic reticulum protein that binds Sec16p and participates in vesicle formation. *J Cell Biol*, **131**, 325-38.

Glickman, M.H., Rubin, D.M., Coux, O., Wefes, I., Pfeifer, G., Cjeka, Z., Baumeister, W., Fried, V.A. and Finley, D. (1998) A subcomplex of the proteasome regulatory particle required for ubiquitin-conjugate degradation and related to the COP9-signalosome and eIF3. *Cell*, **94**, 615-23.

Glotzer, M., Murray, A.W. and Kirschner, M.W. (1991) Cyclin is degraded by the ubiquitin pathway. *Nature*, **349**, 132-8.

Goh, P.Y. and Kilmartin, J.V. (1993) *NDC10*: a gene involved in chromosome segregation in *Saccharomyces cerevisiae*. *J Cell Biol*, **121**, 503-12.

Gordon, C.N. (1977) Chromatin behavior during the mitotic cell cycle of *S. cerevisiae*. *j. Cell Sci.*, **24**, 81.

Goshima, G. and Yanagida, M. (2000) Establishing biorientation occurs with precocious separation of the sister kinetochores, but not the arms, in the early spindle of budding yeast. *Cell*, **100**, 619-33.

Govindan, B., Bowser, R. and Novick, P. (1995) The role of Myo2, a yeast class V myosin, in vesicular transport. *J Cell Biol*, **128**, 1055-68.

Graham, T.R., Scott, P.A. and Emr, S.D. (1993) Brefeldin A reversibly blocks early but not late protein transport steps in the yeast secretory pathway. *Embo J*, **12**, 869-77.

Gray, J.V., Ogas, J.P., Kamada, Y., Stone, M., Levin, D.E. and Herskowitz, I. (1997) A role for the Pkc1 MAP kinase pathway of *Saccharomyces cerevisiae* in bud emergence and identification of a putative upstream regulator. *Embo J*, **16**, 4924-37.

Griff, I.C., Schekman, R., Rothman, J.E. and Kaiser, C.A. (1992) The yeast *SEC17* gene product is functionally equivalent to mammalian alpha-SNAP protein. *J Biol Chem*, **267**, 12106-15.

Gyuris, J., Golemis, E., Chertkov, H. and Brent, R. (1993) Cdi1, a human G1 and S phase protein phosphatase that assiciates with Cdk2. *Cell*, **75**, 791-803.

Hardwick, K.G., Weiss, E., Luca, F.C., Winey, M. and Murray, A.W. (1996) Activation of the budding yeast spindle assembly checkpoint without mitotic spindle disruption. *Science*, **273**, 953-6.

Hartwell, L.H. and Weinert, T.A. (1989) Checkpoints: controls that ensure the order of cell cycle events. *Science*, **246**, 629-34.

He, X., Asthana, S. and Sorger, P.K. (2000) Transient sister chromatid separation and elastic deformation of chromosomes during mitosis in budding yeast. *Cell*, **101**, 763-75.

Holtzman, D.A., Yang, S. and Drubin, D.G. (1993) Synthetic-lethal interactions identify two novel genes, *SLA1* and *SLA2*, that control membrane cytoskeleton assembly in *Saccharomyces cerevisiae*. *J Cell Biol*, **122**, 635-44.

Horio, T., Uzawa, S., Jung, M.K., Oakley, B.R., Tanaka, K. and Yanagida, M. (1991) The fission yeast gamma-tubulin is essential for mitosis and is localized at microtubule organizing centers. *J Cell Sci*, **99**, 693-700.

Hoyt, M.A., He, L., Loo, K.K. and Saunders, W.S. (1992) Two *Saccharomyces cerevisiae* kinesin-related gene products required for mitotic spindle assembly. *J Cell Biol*, **118**, 109-20.

Hoyt, M.A., Totis, L. and Roberts, B.T. (1991) *S. cerevisiae* genes required for cell cycle arrest in response to loss of microtubule function. *Cell*, **66**, 507-17.

Huang, B., Mengersen, A. and Lee, V.D. (1988) Molecular cloning of cDNA for caltractin, a basal body-associated Ca2+- binding protein: homology in its protein sequence with calmodulin and the yeast *CDC31* gene product. *J Cell Biol*, **107**, 133-40.

Huitorel, P. and Pantaloni, D. (1985) Bundling of microtubules by glyceraldehyde-3-phosphate dehydrogenase and its modulation by ATP. *Eur J Biochem*, **150**, 265-9.

Hwang, L.H., Lau, L.F., Smith, D.L., Mistrot, C.A., Hardwick, K.G., Hwang, E.S., Amon, A. and Murray, A.W. (1998) Budding yeast Cdc20: a target of the spindle checkpoint [see comments] [published erratum appears in Science 1998 May 29;280(5368):1331]. *Science*, **279**, 1041-4.

Hyland, K.M., Kingsbury, J., Koshland, D. and Hieter, P. (1999) Ctf19p: A novel kinetochore protein in *Saccharomyces cerevisiae* and a potential link between the kinetochore and mitotic spindle. *J Cell Biol*, **145**, 15-28.

Irie, K., Takase, M., Lee, K.S., Levin, D.E., Araki, H., Matsumoto, K. and Oshima, Y. (1993) *MKK1* and *MKK2*, which encode *Saccharomyces cerevisiae* mitogen-activated protein kinase-kinase homologs, function in the pathway mediated by protein kinase C. *Mol Cell Biol*, **13**, 3076-83.

Jackson, C.L. and Kepes, F. (1994) *BFR1*, a multicopy suppressor of brefeldin A-induced lethality, is implicated in secretion and nuclear segregation in *Saccharomyces cerevisiae*. *Genetics*, **137**, 423-37.

Jacobs, C.W., Adams, A.E., Szaniszlo, P.J. and Pringle, J.R. (1988) Functions of microtubules in the *Saccharomyces cerevisiae* cell cycle. *J Cell Biol*, **107**, 1409-26.

Jacoby, J.J., Nilius, S.M. and Heinisch, J.J. (1998) A screen for upstream components of the yeast protein kinase C signal transduction pathway identifies the product of the *SLG1* gene. *Mol Gen Genet*, **258**, 148-55.

Janke, C., Ortiz, J., Lechner, J., Shevchenko, A., Shevchenko, A., Magiera, M., Schramm, C. and Schiebel, E. (2001) The budding yeast Spc24p and Spc25p interact with Ndc80p and Nuf2p at the kinetochore and are important for kinetochore clustering and checkpoint control. *EMBO J, In press.*

Jaspersen, S.L., Charles, J.F. and Morgan, D.O. (1999) Inhibitory phosphorylation of the APC regulator Hct1 is controlled by the kinase Cdc28 and the phosphatase Cdc14. *Curr Biol*, **9**, 227-36.

Jaspersen, S.L., Charles, J.F., Tinker-Kulberg, R.L. and Morgan, D.O. (1998) A late mitotic regulatory network controlling cyclin destruction in *Saccharomyces cerevisiae*. *Mol Biol Cell*, **9**, 2803-17.

Jin, Q.W., Fuchs, J. and Loidl, J. (2000) Centromere clustering is a major determinant of yeast interphase nuclear organization. *J Cell Sci*, **113**, 1903-12.

Johnston, G.C., Prendergast, J.A. and Singer, R.A. (1991) The *Saccharomyces cerevisiae MYO2* gene encodes an essential myosin for vectorial transport of vesicles. *J Cell Biol*, **113**, 539-51.

Jones, M.H., Bachant, J.B., Castillo, A.R., Giddings, T.H., Jr. and Winey, M. (1999) Yeast Dam1p is required to maintain spindle integrity during mitosis and interacts with the Mps1p kinase. *Mol Biol Cell*, **10**, 2377-91.

Joshi, H.C. (1993) Gamma-tubulin: the hub of cellular microtubule assemblies. *Bioessays*, **15**, 637-43.

Karas, M. and Hillenkamp, F. (1988) Laser desorption ionization of proteins with molecular masses exceeding 10,000 daltons. *Anal Chem*, **60**, 2299-301.

Kelleher, J.F., Atkinson, S.J. and Pollard, T.D. (1995) Sequences, structural models, and cellular localization of the actin- related proteins Arp2 and Arp3 from *Acanthamoeba*. *J Cell Biol*, **131**, 385-97.

Kellogg, D.R., Field, C.M. and Alberts, B.M. (1994) The centrosome and cellular organization. *Annu. Rev. Biochem.*, **63**, 639-674.

Khalfan, W., Ivanovska, I. and Rose, M.D. (2000) Functional interaction between the *PKC1* pathway and *CDC31* network of SPB duplication genes. *Genetics*, **155**, 1543-59.

Kilmartin, J.V. and Adams, A.E.M. (1984) Structural rearrangements of tubulin and actin during the cell cycle of the yeast *Saccharomyces cerevisiae*. *J. Cell Biol.*, **98**, 922-933.

Kilmartin, J.V., Dyos, S.L., Kershaw, D. and Finch, J.T. (1993) A spacer protein in the *Saccharomyces cerevisiae* spindle poly body whose transcript is cell cycle-regulated. *J Cell Biol*, **123**, 1175-84.

Kilmartin, J.V. and Goh, P.Y. (1996) Spc110p: assembly properties and role in the connection of nuclear microtubules to the yeast spindle pole body. *Embo J*, **15**, 4592-602.

King, R.W., Deshaies, R.J., Peters, J.M. and Kirschner, M.W. (1996) How proteolysis drives the cell cycle. *Science*, **274**, 1652-9.

Knop, M., Pereira, G., Geissler, S., Grein, K. and Schiebel, E. (1997) The spindle pole body component Spc97p interacts with the gamma-tubulin of *Saccharomyces cerevisiae* and functions in microtubule organization and spindle pole body duplication. *Embo J*, **16**, 1550-64.

Knop, M. and Schiebel, E. (1997) Spc98p and Spc97p of the yeast gamma-tubulin complex mediate binding to the spindle pole body via their interaction with Spc110p. *Embo J*, **16**, 6985-95.

Knop, M. and Schiebel, E. (1998) Receptors determine the cellular localization of a gamma-tubulin complex and thereby the site of microtubule formation. *Embo J*, **17**, 3952-67.

Knop, M., Siegers, K., Pereira, G., Zachariae, W., Winsor, B., Nasmyth, K. and Schiebel, E. (1999) Epitope tagging of yeast genes using a PCR-based strategy: more tags and improved practical routines. *Yeast*, **15**, 963-72.

Kochanski, R.S. and Borisy, G.G. (1990) Mode of centriole duplication and distribution. *J Cell Biol*, **110**, 1599-605.

Kron, S.J. and Gow, N.A. (1995) Budding yeast morphogenesis: signalling, cytoskeleton and cell cycle. *Curr Opin Cell Biol*, **7**, 845-55.

Kubler, E. and Riezman, H. (1993) Actin and fimbrin are required for the internalization step of endocytosis in yeast. *Embo J*, **12**, 2855-62.

Kumagai, H. and Sakai, H. (1983) A porcine brain protein (35 K protein) which bundles microtubules and its identification as glyceraldehyde 3-phosphate dehydrogenase. *J Biochem (Tokyo)*, **93**, 1259-69.

Kurihara, T. and Silver, P. (1993) Suppression of a *sec63* mutation identifies a novel component of the yeast endoplasmic reticulum translocation apparatus. *Mol Biol Cell*, **4**, 919-30.

Laemmli, U.K. (1970) Cleavage of structural proteins during the assembly of the head of bacteriophage T4. *Nature*, **227**, 680-5.

Lang, B.D. and Fridovich-Keil, J.L. (2000) Scp160p, a multiple KH-domain protein, is a component of mRNP complexes in yeast. *Nucleic Acids Res*, **28**, 1576-84.

Lange, B.M., Bachi, A., Wilm, M. and Gonzalez, C. (2000) Hsp90 is a core centrosomal component and is required at different stages of the centrosome cycle in *Drosophila* and vertebrates. *Embo J*, **19**, 1252-62.

Lange, B.M.H. and Gull, K. (1996) A structural study of isolated mammalian centrioles using negative staining electron microscopy. *J Struct Biol*, **117**, 222-6.

Lechtreck, K.F., Teltenkotter, A. and Grunow, A. (1999) A 210 kDa protein is located in a membrane-microtubule linker at the distal end of mature and nascent basal bodies. *J Cell Sci*, **112**, 1633-44.

Lee, K.S., Irie, K., Gotoh, Y., Watanabe, Y., Araki, H., Nishida, E., Matsumoto, K. and Levin, D.E. (1993) A yeast mitogen-activated protein kinase homolog (Mpk1p) mediates signalling by protein kinase C. *Mol Cell Biol*, **13**, 3067-75.

Lee, K.S. and Levin, D.E. (1992) Dominant mutations in a gene encoding a putative protein kinase (BCK1) bypass the requirement for a *Saccharomyces cerevisiae* protein kinase C homolog. *Mol Cell Biol*, **12**, 172-82.

Lew, D.J. and Reed, S.I. (1993) Morphogenesis in the yeast cell cycle: regulation by Cdc28 and cyclins. *J Cell Biol*, **120**, 1305-20.

Lew, D.J. and Reed, S.I. (1995) Cell cycle control of morphogenesis in budding yeast. *Curr Opin Genet Dev*, **5**, 17-23.

Lew, D.J., Weinert, T. and Pringle, J.R. (1997) Cell cycle control in *S. cerevisiae*. In: The molecular and cellular biology of the yeast *Saccharomyces*. (edited by Pringle J.R. *et al.*). *Cold Spring Harbor Laboratory Press*.

Li, R. and Murray, A.W. (1991) Feedback control of mitosis in budding yeast [published erratum appears in Cell 1994 Oct 21;79(2):following 388]. *Cell*, **66**, 519-31.

Li, R., Zheng, Y. and Drubin, D.G. (1995) Regulation of cortical actin cytoskeleton assembly during polarized cell growth in budding yeast. *J Cell Biol*, **128**, 599-615.

Li, X. and Nicklas, R.B. (1995) Mitotic forces control a cell-cycle checkpoint. *Nature*, **373**, 630-2.

Li, X. and Nicklas, R.B. (1997) Tension-sensitive kinetochore phosphorylation and the chromosome distribution checkpoint in praying mantid spermatocytes. *J Cell Sci*, **110**, 537-45.

Li, Y.Y., Yeh, E., Hays, T. and Bloom, K. (1993) Disruption of mitotic spindle orientation in a yeast dynein mutant. *Proc Natl Acad Sci U S A*, **90**, 10096-100.

Lillie, S.H. and Brown, S.S. (1994) Immunofluorescence localization of the unconventional myosin, Myo2p, and the putative kinesin-related protein, Smy1p, to the same regions of polarized growth in *Saccharomyces cerevisiae*. *J Cell Biol*, **125**, 825-42.

Lillie, S.H. and Brown, S.S. (1998) Smy1p, a kinesin-related protein that does not require microtubules. *J Cell Biol*, **140**, 873-83.

Longtine, M.S., McKenzie, A., 3rd, Demarini, D.J., Shah, N.G., Wach, A., Brachat, A., Philippsen, P. and Pringle, J.R. (1998) Additional modules for versatile and economical PCR-based gene deletion and modification in *Saccharomyces cerevisiae*. *Yeast*, **14**, 953-61.

Lupas, A., Van Dyke, M. and Stock, J. (1991) Predicting coiled coils from protein sequences. *Science*, **252**, 1162-4.

Machesky, L.M., Atkinson, S.J., Ampe, C., Vandekerckhove, J. and Pollard, T.D. (1994) Purification of a cortical complex containing two unconventional actins from *Acanthamoeba* by affinity chromatography on profilin-agarose. *J Cell Biol*, **127**, 107-15.

Marini, N.J., Meldrum, E., Buehrer, B., Hubberstey, A.V., Stone, D.E., Traynor-Kaplan, A. and Reed, S.I. (1996) A pathway in the yeast cell division cycle linking protein kinase C (Pkc1) to activation of Cdc28 at START. *Embo J*, **15**, 3040-52.

Marschall, L.G., Jeng, R.L., Mulholland, J. and Stearns, T. (1996) Analysis of Tub4p, a yeast γ-tubulin-like protein: implications for microtubule-organizing center function. *J. Cell Biol.*, **134**, 443-454.

Martin, M.A., Osmani, S.A. and Oakley, B.R. (1997) The role of gamma-tubulin in mitotic spindle formation and cell cycle progression in *Aspergillus nidulans*. *J Cell Sci*, **110**, 623-33.

Martin, O.C., Gunawardane, R.N., Iwamatsu, A. and Zheng, Y. (1998) Xgrip109: a gamma tubulin-associated protein with an essential role in gamma tubulin ring complex (gammaTuRC) assembly and centrosome function. *J Cell Biol*, **141**, 675-87.

Mazzoni, C., Zarov, P., Rambourg, A. and Mann, C. (1993) The *SLT2* (*MPK1*) MAP kinase homolog is involved in polarized cell growth in *Saccharomyces cerevisiae*. *J Cell Biol*, **123**, 1821-33.

McDonald, H.B. and Byers, B. (1997) A proteasome cap subunit required for spindle pole body duplication in yeast. *J Cell Biol*, **137**, 539-53.

Mercer, J.A., Seperack, P.K., Strobel, M.C., Copeland, N.G. and Jenkins, N.A. (1991) Novel myosin heavy chain encoded by murine dilute coat colour locus [published erratum appears in Nature 1991 Aug 8;352(6335):547]. *Nature*, **349**, 709-13.

Michaelis, C., Ciosk, R. and Nasmyth, K. (1997) Cohesins: chromosomal proteins that prevent premature separation of sister chromatids. *Cell*, **91**, 35-45.

Middendorp, S., Kuntziger, T., Abraham, Y., Holmes, S., Bordes, N., Paintrand, M., Paoletti, A. and Bornens, M. (2000) A role for centrin 3 in centrosome reproduction. *J Cell Biol*, **148**, 405-16.

Middendorp, S., Paoletti, A., Schiebel, E. and Bornens, M. (1997) Identification of a new mammalian centrin gene, more closely related to *Saccharomyces cerevisiae CDC31* gene. *Proc Natl Acad Sci U S A*, **94**, 9141-6.

Mirzayan, C., Copeland, C.S. and Snyder, M. (1992) The *NUF1* gene encodes an essential coiled-coil related protein that is a potential component of the yeast nucleoskeleton. *J Cell Biol*, **116**, 1319-32.

Miyata, Y. and Yahara, I. (1992) The 90-kDa heat shock protein, HSP90, binds and protects casein kinase II from self-aggregation and enhances its kinase activity. *J Biol Chem*, **267**, 7042-7.

Moir, D., Stewart, S.E., Osmond, B.C. and Botstein, D. (1982) Cold-sensitive cell-division-cycle mutants of yeast: isolation, properties, and pseudoreversion studies. *Genetics*, **100**, 547-63.

Morano, K.A., Santoro, N., Koch, K.A. and Thiele, D.J. (1999) A trans-activation domain in yeast heat shock transcription factor is essential for cell cycle progression during stress. *Mol Cell Biol*, **19**, 402-11.

Morero, R.D., Vinals, A.L., Bloj, B. and Farias, R.N. (1985) Fusion of phospholipid vesicles induced by muscle glyceraldehyde-3- phosphate dehydrogenase in the absence of calcium. *Biochemistry*, **24**, 1904-9.

Morgan, D.O. (1995) Principles of CDK regulation. *Nature*, **374**, 131-134.

Moritz, M., Braunfeld, M.B., Fung, J.C., Sedat, J.W., Alberts, B.M. and Agard, D.A. (1995a) Three-dimensional structural characterization of centrosomes from early *Drosophila* embryos. *J Cell Biol*, **130**, 1149-59.

Moritz, M., Braunfeld, M.B., Sedat, J.W., Alberts, B. and Agard, D.A. (1995b) Microtubule nucleation by gamma-tubulin-containing rings in the centrosome. *Nature*, **378**, 638-40.

Moudjou, M., Bordes, N., Paintrand, M. and Bornens, M. (1996) gamma-Tubulin in mammalian cells: the centrosomal and the cytosolic forms. *J Cell Sci*, **109**, 875-87.

Mulholland, J., Preuss, D., Moon, A., Wong, A., Drubin, D. and Botstein, D. (1994) Ultrastructure of the yeast actin cytoskeleton and its association with the plasma membrane. *J Cell Biol*, **125**, 381-91.

Mullins, R.D., Heuser, J.A. and Pollard, T.D. (1998) The interaction of Arp2/3 complex with actin: nucleation, high affinity pointed end capping, and formation of branching networks of filaments. *Proc Natl Acad Sci U S A*, **95**, 6181-6.

Mumberg, D., Muller, R. and Funk, M. (1994) Regulatable promoters of *Saccharomyces cerevisiae*: comparison of transcriptional activity and their use for heterologous expression. *Nucleic Acids Res*, **22**, 5767-8.

Mumberg, D., Muller, R. and Funk, M. (1995) Yeast vectors for the controlled expression of heterologous proteins in different genetic backgrounds. *Gene*, **156**, 119-22.

Munoz-Centeno, M.C., McBratney, S., Monterrosa, A., Byers, B., Mann, C. and Winey, M. (1999) *Saccharomyces cerevisiae MPS2* encodes a membrane protein localized at the spindle pole body and the nuclear envelope. *Mol Biol Cell*, **10**, 2393-406.

Murphy, S.M., Urbani, L. and Stearns, T. (1998) The mammalian gamma-tubulin complex contains homologues of the yeast spindle pole body components Spc97p and Spc98p. *J Cell Biol*, **141**, 663-74.

Nasmyth, K. (1993) Control of the yeast cell cycle by the Cdc28 protein kinase. *Curr Opin Cell Biol*, **5**, 166-79.

Nehrbass, U., Rout, M.P., Maguire, S., Blobel, G. and Wozniak, R.W. (1996) The yeast nucleoporin Nup188p interacts genetically and physically with the core structures of the nuclear pore complex. *J Cell Biol*, **133**, 1153-62.

Newman, A.P., Graf, J., Mancini, P., Rossi, G., Lian, J.P. and Ferro-Novick, S. (1992a) *SEC22* and *SLY2* are identical. *Mol Cell Biol*, **12**, 3663-4.

Newman, A.P., Groesch, M.E. and Ferro-Novick, S. (1992b) Bos1p, a membrane protein required for ER to Golgi transport in yeast, co-purifies with the carrier vesicles and with Bet1p and the ER membrane. *Embo J*, **11**, 3609-17.

Newman, A.P., Shim, J. and Ferro-Novick, S. (1990) *BET1, BOS1*, and *SEC22* are members of a group of interacting yeast genes required for transport from the endoplasmic reticulum to the Golgi complex. *Mol Cell Biol*, **10**, 3405-14.

Newman, J.R., Wolf, E. and Kim, P.S. (2000) From the cover: A computationally directed screen identifying interacting coiled coils from *Saccharomyces cerevisiae* [In Process Citation]. *Proc Natl Acad Sci U S A*, **97**, 13203-8.

Nguyen, T., Vinh, D.B.N., Crawford, D.K. and Davis, T.N. (1998) A genetic analysis of interactions with Spc110p reveals distinct functions of Spc97p and Spc98p, components of the yeast gamma-tubulin complex. *Mol Biol Cell*, **9**, 2201-16.

Novick, P. and Botstein, D. (1985) Phenotypic analysis of temperature-sensitive yeast actin mutants. *Cell*, **40**, 405-16.

Oakley, B.R. (1992) γ-Tubulin: the microtubule organizer? *Trends Cell Biol.*, **2**, 1-5.

Oakley, C.E. and Oakley, B.R. (1989) Identification of gamma-tubulin, a new member of the tubulin superfamily encoded by mipA gene of *Aspergillus nidulans*. *Nature*, **338**, 662-4.

Osborne, M.A., Schlenstedt, G., Jinks, T. and Silver, P.A. (1994) Nuf2p, a spindle pole body-associated protein required for nuclear division in yeast. *J Cell Biol*, **125**, 853-66.

O'Toole, E.T., Winey, M. and McIntosh, J.R. (1999) High-voltage electron tomography of spindle pole bodies and early mitotic spindles in the yeast *Saccharomyces cerevisiae*. *Mol Biol Cell*, **10**, 2017-31.

Page, A.M. and Hieter, P. (1999) The anaphase-promoting complex: new subunits and regulators. *Annu Rev Biochem*, **68**, 583-609.

Paintrand, M., Moudjou, M., Delacroix, H. and Bornens, M. (1992) Centrosome organization and centriole architecture: their sensitivity to divalent cations. *J Struct Biol*, **108**, 107-28.

Palmer, R.E., Sullivan, D.S., Huffaker, T. and Koshland, D. (1992) Role of astral microtubules and actin in spindle orientation and migration in the budding yeast, *Saccharomyces cerevisiae*. *J Cell Biol*, **119**, 583-93.

Pangilinan, F. and Spencer, F. (1996) Abnormal kinetochore structure activates the spindle assembly checkpoint in budding yeast. *Mol Biol Cell*, **7**, 1195-208.

Paoletti, A., Moudjou, M., Paintrand, M., Salisbury, J.L. and Bornens, M. (1996) Most of centrin in animal cells is not centrosome-associated and centrosomal centrin is confined to the distal lumen of centrioles. *J Cell Sci*, **109**, 3089-102.

Pereira, G., Grueneberg, U., Knop, M. and Schiebel, E. (1999) Interaction of the yeast gamma-tubulin complex-binding protein Spc72p with Kar1p is essential for microtubule function during karyogamy. *Embo J*, **18**, 4180-95.

Pereira, G., Hofken, T., Grindlay, J., Manson, C. and Schiebel, E. (2000) The Bub2p spindle checkpoint links nuclear migration with mitotic exit. *Mol Cell*, **6**, 1-10.

Pereira, G., Knop, M. and Schiebel, E. (1998) Spc98p directs the yeast gamma-tubulin complex into the nucleus and is subject to cell cycle-dependent phosphorylation on the nuclear side of the spindle pole body. *Mol Biol Cell*, **9**, 775-93.

Pereira, G. and Schiebel, E. (1997) Centrosome-microtubule nucleation. *J Cell Sci*, **110**, 295-300.

Peyroche, A., Antonny, B., Robineau, S., Acker, J., Cherfils, J. and Jackson, C.L. (1999) Brefeldin A acts to stabilize an abortive ARF-GDP-Sec7 domain protein complex: involvement of specific residues of the Sec7 domain. *Mol Cell*, **3**, 275-85.

Piel, M., Meyer, P., Khodjakov, A., Rieder, C.L. and Bornens, M. (2000) The respective contributions of the mother and daughter centrioles to centrosome activity and behavior in vertebrate cells. *J Cell Biol*, **149**, 317-30.

Piggott, J.R., Rai, R. and Carter, B.L. (1982) A bifunctional gene product involved in two phases of the yeast cell cycle. *Nature*, **298**, 391-3.

Prekeris, R. and Terrian, D.M. (1997) Brain myosin V is a synaptic vesicle-associated motor protein: evidence for a Ca2+-dependent interaction with the synaptobrevin-synaptophysin complex. *J Cell Biol*, **137**, 1589-601.

Pringle, J.R. and Hartwell, L.H. (1981) The *Sacccharomyces cerevisiae* cell cycle. In *The molecular biology of the yeast Saccharomyces: Life cycle and inheritance(ed. J.N. Strathern et al.). Cold Spring Harbor Laboratory, Cold Spring Harbor, New York*, 97.

Pringle, J.R., Preston, R.A., Adams, A.E., Stearns, T., Drubin, D.G., Haarer, B.K. and Jones, E.W. (1989) Fluorescence microscopy methods for yeast. *Methods Cell Biol*, **31**, 357-435.

Provance, D.W., Jr., Wei, M., Ipe, V. and Mercer, J.A. (1996) Cultured melanocytes from dilute mutant mice exhibit dendritic morphology and altered melanosome distribution. *Proc Natl Acad Sci U S A*, **93**, 14554-8.

Ramos, P.C., Hockendorff, J., Johnson, E.S., Varshavsky, A. and Dohmen, R.J. (1998) Ump1p is required for proper maturation of the 20S proteasome and becomes its substrate upon completion of the assembly. *Cell*, **92**, 489-99.

Rattner, J.B. and Phillips, S.G. (1973) Independence of centriole formation and DNA synthesis. *J Cell Biol*, **57**, 359-72.

Read, E.B., Okamura, H.H. and Drubin, D.G. (1992) Actin- and tubulin-dependent functions during *Saccharomyces cerevisiae* mating projection formation. *Mol Biol Cell*, **3**, 429-44.

Reck-Peterson, S.L., Provance, D.W., Jr., Mooseker, M.S. and Mercer, J.A. (2000) Class V myosins. *Biochim Biophys Acta*, **1496**, 36-51.

Reed, S.I. (1980) The selection of *S. cerevisiae* mutants defective in the start event of cell division. *Genetics*, **95**, 561-77.

Reed, S.I. (1992) The role of p34 kinases in the G1 to S-phase transition. *Annu Rev Cell Biol*, **8**, 529-61.

Reiss, N., Oplatka, A., Hermon, J. and Naor, Z. (1996) Phosphatidylserine directs differential phosphorylation of actin and glyceraldehyde-3-phosphate dehydrogenase by protein kinase C: possible implications for regulation of actin polymerization. *Biochem Mol Biol Int*, **40**, 1191-200.

Reynolds, E.S. (1963) The use of lead citrate at high pH as electron-opaque stain in electron microscopy. *J. Cell Biol*, **17**, 208-12.

Richardson, H., Lew, D.J., Henze, M., Sugimoto, K. and Reed, S.I. (1992) Cyclin-B homologs in *Saccharomyces cerevisiae* function in S phase and in G2. *Genes Dev*, **6**, 2021-34.

Robbins, E., Jentzsch, G. and Micali, A. (1968) The centriole cycle in synchronized HeLa cells. *J Cell Biol*, **36**, 329-39.

Robinow, C.F. and Marak, J. (1966) A fiber apparatus in the nucleus of the yeast cell. *J Cell Biol*, **29**, 129-51.

Rodionov, V., Nadezhdina, E. and Borisy, G. (1999) Centrosomal control of microtubule dynamics. *Proc Natl Acad Sci U S A*, **96**, 115-20.

Rodriguez, J.R. and Paterson, B.M. (1990) Yeast myosin heavy chain mutant: maintenance of the cell type specific budding pattern and the normal deposition of chitin and cell wall components requires an intact myosin heavy chain gene. *Cell Motil Cytoskeleton*, **17**, 301-8.

Roof, D.M., Meluh, P.B. and Rose, M.D. (1992) Kinesin-related proteins required for assembly of the mitotic spindle. *J Cell Biol*, **118**, 95-108.

Rose, M.D. and Fink, G.R. (1987a) *KAR1*, a gene required for function of both intranuclear and extranuclear microtubules in yeast. *Cell*, **48**, 1047-60.

Rose, M.D. and Fink, G.R. (1987b) *KAR1*, a gene required for function of both intranuclear and extranuclear microtubules in yeast. *Cell*, **48**, 1047-1060.

Rout, M.P., Aitchison, J.D., Suprapto, A., Hjertaas, K., Zhao, Y. and Chait, B.T. (2000) The yeast nuclear pore complex: composition, architecture, and transport mechanism. *J Cell Biol*, **148**, 635-51.

Rout, M.P. and Kilmartin, J.V. (1990) Components of the yeast spindle and spindle pole body. *J Cell Biol*, **111**, 1913-27.

Rout, M.P. and Kilmartin, J.V. (1991) Yeast spindle pole body components. *Cold Spring Harb Symp Quant Biol*, **56**, 687-92.

Ryazanov, A.G. (1985) Glyceraldehyde-3-phosphate dehydrogenase is one of the three major RNA- binding proteins of rabbit reticulocytes. *FEBS Lett*, **192**, 131-4.

Salisbury, J.L. (1995) Centrin, centrosomes, and mitotic spindle poles. *Curr Opin Cell Biol*, **7**, 39-45.

Salisbury, J.L., Baron, A.T. and Sanders, M.A. (1988) The centrin-based cytoskeleton of *Chlamydomonas reinhardtii*: distribution in interphase and mitotic cells. *J Cell Biol*, **107**, 635-41.

Sambrook, J., Fritsch, E.F. and Maniatis, T. (1989) Molecular Cloning. *Cold Spring Harbor Laboratory Press.*

Sanders, M.A. and Salisbury, J.L. (1989) Centrin-mediated microtubule severing during flagellar excision in *Chlamydomonas reinhardtii*. *J Cell Biol*, **108**, 1751-60.

Sanders, M.A. and Salisbury, J.L. (1994) Centrin plays an essential role in microtubule severing during flagellar excision in *Chlamydomonas reinhardtii*. *J Cell Biol*, **124**, 795-805.

Sanger, F., Nicklen, S. and Coulson, A.R. (1977) DNA sequencing with chain-terminating inhibitors. *Proc Natl Acad Sci U S A*, **74**, 5463-7.

Saunders, W.S. (1999) Action at the ends of microtubules. *Curr Opin Cell Biol*, **11**, 129-33.

Schild, D., Ananthaswamy, H.N. and Mortimer, R.K. (1981) An endomitotic effect of a cell cycle mutation of *Saccharomyces cerevisiae*. *Genetics*, **97**, 551-562.

Schneider, B.L., Seufert, W., Steiner, B., Yang, Q.H. and Futcher, A.B. (1995) Use of polymerase chain reaction epitope tagging for protein tagging in *Saccharomyces cerevisiae*. *Yeast*, **11**, 1265-74.

Schramm, C., Elliott, S., Shevchenko, A. and Schiebel, E. (2000) The Bbp1p-Mps2p complex connects the SPB to the nuclear envelope and is essential for SPB duplication. *Embo J*, **19**, 421-33.

Schutz, A.R., Giddings, T.H., Jr., Steiner, E. and Winey, M. (1997) The yeast *CDC37* gene interacts with *MPS1* and is required for proper execution of spindle pole body duplication. *J Cell Biol*, **136**, 969-82.

Schutz, A.R. and Winey, M. (1998) New alleles of the yeast *MPS1* gene reveal multiple requirements in spindle pole body duplication. *Mol Biol Cell*, **9**, 759-74.

Schwob, E. and Nasmyth, K. (1993) *CLB5* and *CLB6*, a new pair of B cyclins involved in DNA replication in *Saccharomyces cerevisiae*. *Genes Dev*, **7**, 1160-75.

Seufert, W., Futcher, B. and Jentsch, S. (1995) Role of a ubiquitin-conjugating enzyme in degradation of S- and M-phase cyclins. *Nature*, **373**, 78-81.

Shah, N. and Klausner, R.D. (1993) Brefeldin A reversibly inhibits secretion in *Saccharomyces cerevisiae*. *J Biol Chem*, **268**, 5345-8.

Shortle, D., Novick, P. and Botstein, D. (1984) Construction and genetic characterization of temperature-sensitive mutant alleles of the yeast actin gene. *Proc Natl Acad Sci U S A*, **81**, 4889-93.

Shou, W., Seol, J.H., Shevchenko, A., Baskerville, C., Moazed, D., Chen, Z.W., Jang, J., Charbonneau, H. and Deshaies, R.J. (1999) Exit from mitosis is triggered by Tem1-dependent release of the protein phosphatase Cdc14 from nucleolar RENT complex. *Cell*, **97**, 233-44.

Sikorski, R.S. and Hieter, P. (1989) A system of shuttle vectors and yeast host strains designed for efficient manipulation of DNA in *Saccharomyces cerevisiae*. *Genetics*, **122**, 19-27.

Singh, R. and Green, M.R. (1993) Sequence-specific binding of transfer RNA by glyceraldehyde-3-phosphate dehydrogenase. *Science*, **259**, 365-8.

Skowyra, D., Craig, K.L., Tyers, M., Elledge, S.J. and Harper, J.W. (1997) F-box proteins are receptors that recruit phosphorylated substrates to the SCF ubiquitin-ligase complex [see comments]. *Cell*, **91**, 209-19.

Snyder, M. (1994) The spindle pole body of yeast. *Chromosoma*, **103**, 369-80.

Sobel, S.G. and Snyder, M. (1995) A highly divergent gamma-tubulin gene is essential for cell growth and proper microtubule organization in *Saccharomyces cerevisiae*. *J Cell Biol*, **131**, 1775-88.

Sohrmann, M., Schmidt, S., Hagan, I. and Simanis, V. (1998) Asymmetric segregation on spindle poles of the *Schizosaccharomyces pombe* septum-inducing protein kinase Cdc7p. *Genes Dev*, **12**, 84-94.

Songyang, Z., Blechner, S., Hoagland, N., Hoekstra, M.F., Piwnica-Worms, H. and Cantley, L.C. (1994) Use of an oriented peptide library to determine the optimal substrates of protein kinases. *Curr Biol*, **4**, 973-82.

Soues, S. and Adams, I.R. (1998) *SPC72*: a spindle pole component required for spindle orientation in the yeast *Saccharomyces cerevisiae*. *J Cell Sci*, **111**, 2809-18.

Spang, A., Courtney, I., Fackler, U., Matzner, M. and Schiebel, E. (1993) The calcium-binding protein cell division cycle 31 of *Saccharomyces cerevisiae* is a component of the half bridge of the spindle pole body. *J Cell Biol*, **123**, 405-16.

Spang, A., Courtney, I., Grein, K., Matzner, M. and Schiebel, E. (1995) The Cdc31p-binding protein Karlp is a component of the half bridge of the yeast spindle pole body. *J Cell Biol*, **128**, 863-77.

Spang, A., Geissler, S., Grein, K. and Schiebel, E. (1996b) gamma-Tubulin-like Tub4p of *Saccharomyces cerevisiae* is associated with the spindle pole body substructures that organize microtubules and is required for mitotic spindle formation. *J Cell Biol*, **134**, 429-41.

Spang, A., Grein, K. and Schiebel, E. (1996a) The spacer protein Spc110p targets calmodulin to the central plaque of the yeast spindle pole body. *J Cell Sci*, **109**, 2229-37.

Stearns, T., Evans, L. and Kirschner, M. (1991) Gamma-tubulin is a highly conserved component of the centrosome. *Cell*, **65**, 825-36.

Stempak, J.G. and Ward, R.T. (1964) An improved staining method for electron microscopy. *J Cll Biol*, **22**, 697-701.

Stepanova, L., Leng, X., Parker, S.B. and Harper, J.W. (1996) Mammalian p50Cdc37 is a protein kinase-targeting subunit of Hsp90 that binds and stabilizes Cdk4. *Genes Dev*, **10**, 1491-502.

Stirling, D.A., Rayner, T.F., Prescott, A.R. and Stark, M.J. (1996) Mutations which block the binding of calmodulin to Spc110p cause multiple mitotic defects. *J Cell Sci*, **109**, 1297-310.

Stirling, D.A., Welch, K.A. and Stark, M.J. (1994) Interaction with calmodulin is required for the function of Spc110p, an essential component of the yeast spindle pole body. *Embo J*, **13**, 4329-42.

Strambio-de-Castillia, C., Blobel, G. and Rout, M.P. (1995) Isolation and characterization of nuclear envelopes from the yeast *Saccharomyces*. *J Cell Biol*, **131**, 19-31.

Stuart, D. and Wittenberg, C. (1995) *CLN3*, not positive feedback, determines the timing of *CLN2* transcription in cycling cells. *Genes Dev*, **9**, 2780-94.

Studier, F.W. (1991) Use of bacteriophage T7 lysozyme to improve an inducible T7 expression system. *J Mol Biol*, **219**, 37-44.

Sullivan, D.S., Biggins, S. and Rose, M.D. (1998) The yeast centrin, cdc31p, and the interacting protein kinase, Kic1p, are required for cell integrity. *J Cell Biol*, **143**, 751-65.

Sun, G.H., Hirata, A., Ohya, Y. and Anraku, Y. (1992) Mutations in yeast calmodulin cause defects in spindle pole body functions and nuclear integrity. *J Cell Biol*, **119**, 1625-39.

Sundberg, H.A. and Davis, T.N. (1997) A mutational analysis identifies three functional regions of the spindle pole component Spc110p in *Saccharomyces cerevisiae*. *Mol Biol Cell*, **8**, 2575-90.

Sundberg, H.A., Goetsch, L., Byers, B. and Davis, T.N. (1996) Role of calmodulin and Spc110p interaction in the proper assembly of spindle pole body compenents. *J Cell Biol*, **133**, 111-24.

Sunkel, C.E., Gomes, R., Sampaio, P., Perdigao, J. and Gonzalez, C. (1995) Gamma-tubulin is required for the structure and function of the microtubule organizing centre in *Drosophila* neuroblasts. *Embo J*, **14**, 28-36.

Surana, U., Amon, A., Dowzer, C., McGrew, J., Byers, B. and Nasmyth, K. (1993) Destruction of the *CDC28/CLB* mitotic kinase is not required for the metaphase to anaphase transition in budding yeast. *Embo J*, **12**, 1969-78.

Surana, U., Robitsch, H., Price, C., Schuster, T., Fitch, I., Futcher, A.B. and Nasmyth, K. (1991) The role of CDC28 and cyclins during mitosis in the budding yeast *S. cerevisiae*. *Cell*, **65**, 145-61.

Sweeney, F.P., Pocklington, M.J. and Orr, E. (1991) The yeast type II myosin heavy chain: analysis of its predicted polypeptide sequence. *J Muscle Res Cell Motil*, **12**, 61-8.

Taillon, B.E., Adler, S.A., Suhan, J.P. and Jarvik, J.W. (1992) Mutational analysis of centrin: an EF-hand protein associated with three distinct contractile fibers in the basal body apparatus of *Chlamydomonas*. *J Cell Biol*, **119**, 1613-24.

Tapon, N. and Hall, A. (1997) Rho, Rac and Cdc42 GTPases regulate the organization of the actin cytoskeleton. *Curr Opin Cell Biol*, **9**, 86-92.

Tassin, A.M., Celati, C., Moudjou, M. and Bornens, M. (1998) Characterization of the human homologue of the yeast Spc98p and its association with gamma-tubulin. *J Cell Biol*, **141**, 689-701.

Theesfeld, C.L., Irazoqui, J.E., Bloom, K. and Lew, D.J. (1999) The role of actin in spindle orientation changes during the *Saccharomyces cerevisiae* cell cycle. *J Cell Biol*, **146**, 1019-32.

Thomas, J.H. and Botstein, D. (1986) A gene required for the separation of chromosomes on the spindle apparatus in yeast. *Cell*, **44**, 65-76.

Tkacz, J.S. and Lampen, J.O. (1972) Wall replication in *Saccharomyces* species: use of fluorescein- conjugated concanavalin A to reveal the site of mannan insertion. *J Gen Microbiol*, **72**, 243-7.

Tobacman, L.S. and Korn, E.D. (1983) The kinetics of actin nucleation and polymerization. *J Biol Chem*, **258**, 3207-14.

Uetz, P., Giot, L., Cagney, G., Mansfield, T.A., Judson, R.S., Knight, J.R., Lockshon, D., Narayan, V., Srinivasan, M., Pochart, P., Qureshi-Emili, A., Li, Y., Godwin, B., Conover, D., Kalbfleisch, T., Vijayadamodar, G., Yang, M., Johnston, M., Fields, S. and Rothberg, J.M. (2000) A comprehensive analysis of protein-protein interactions in *Saccharomyces cerevisiae*. *Nature*, **403**, 623-7.

Uhlmann, F. and Nasmyth, K. (1998) Cohesion between sister chromatids must be established during DNA replication. *Curr Biol*, **8**, 1095-101.

Vallen, E.A., Hiller, M.A., Scherson, T.Y. and Rose, M.D. (1992a) Separate domains of *KAR1* mediate distinct functions in mitosis and nuclear fusion. *J. Cell Biol.*, **117**, 1277-1287.

Vallen, E.A., Ho, W., Winey, M. and Rose, M.D. (1994) Genetic interactions between *CDC31* and *KAR1*, two genes required for duplication of the microtubule organizing center in *Saccharomyces cerevisiae*. *Genetics*, **137**, 407-422.

Vallen, E.A., Scherson, T.Y., Roberts, T., Van Zee, K. and Rose, M.D. (1992b) Asymetric mitotic segregation of the yeast spindle pole body. *Cell*, **69**, 505-515.

Van Aelst, L. and D'Souza-Schorey, C. (1997) Rho GTPases and signaling networks. *Genes Dev*, **11**, 2295-322.

Vaughn, K.C. and Harper, J.D. (1998) Microtubule-organizing centers and nucleating sites in land plants. *Int Rev Cytol*, **181**, 75-149.

Verna, J., Lodder, A., Lee, K., Vagts, A. and Ballester, R. (1997) A family of genes required for maintenance of cell wall integrity and for the stress response in *Saccharomyces cerevisiae*. *Proc Natl Acad Sci U S A*, **94**, 13804-9.

Visintin, R., Craig, K., Hwang, E.S., Prinz, S., Tyers, M. and Amon, A. (1998) The phosphatase Cdc14 triggers mitotic exit by reversal of Cdk- dependent phosphorylation. *Mol Cell*, **2**, 709-18.

Visintin, R., Hwang, E.S. and Amon, A. (1999) Cfi1 prevents premature exit from mitosis by anchoring Cdc14 phosphatase in the nucleolus [see comments]. *Nature*, **398**, 818-23.

Visintin, R., Prinz, S. and Amon, A. (1997) *CDC20* and *CDH1*: a family of substrate-specific activators of APC- dependent proteolysis. *Science*, **278**, 460-3.

Vogel, J.P., Lee, J.N., Kirsch, D.R., Rose, M.D. and Sztul, E.S. (1993) Brefeldin A causes a defect in secretion in *Saccharomyces cerevisiae*. *J Biol Chem*, **268**, 3040-3.

Voges, D., Zwickl, P. and Baumeister, W. (1999) The 26S proteasome: a molecular machine designed for controlled proteolysis. *Annu Rev Biochem*, **68**, 1015-68.

Volker, K.W. and Knull, H. (1997) A glycolytic enzyme binding domain on tubulin. *Arch Biochem Biophys*, **338**, 237-43.

Wach, A., Brachat, A., Alberti-Segui, C., Rebischung, C. and Philippsen, P. (1997) Heterologous *HIS3* marker and GFP reporter modules for PCR-targeting in *Saccharomyces cerevisiae*. *Yeast*, **13**, 1065-75.

Wach, A., Brachat, A., Pohlmann, R. and Philippsen, P. (1994) New heterologous modules for classical or PCR-based gene disruptions in *Saccharomyces cerevisiae*. *Yeast*, **10**, 1793-808.

Waddle, J.A., Karpova, T.S., Waterston, R.H. and Cooper, J.A. (1996) Movement of cortical actin patches in yeast. *J Cell Biol*, **132**, 861-70.

Wang, P.J. and Huffaker, T.C. (1997) Stu2p: A microtubule-binding protein that is an essential component of the yeast spindle pole body. *J Cell Biol*, **139**, 1271-80.

Wang, Y., Hu, F. and Elledge, S.J. (2000) The Bfa1/Bub2 GAP complex comprises a universal checkpoint required to prevent mitotic exit. *Curr Biol*, **10**, 1379-82.

Waters, J.C. and Salmon, E. (1997) Pathways of spindle assembly. *Curr Opin Cell Biol*, **9**, 37-43.

Watts, F.Z., Shiels, G. and Orr, E. (1987) The yeast *MYO1* gene encoding a myosin-like protein required for cell division. *Embo J*, **6**, 3499-505.

Weber, V., Wernitznig, A., Hager, G., Harata, M., Frank, P. and Wintersberger, U. (1997) Purification and nucleic-acid-binding properties of a *Saccharomyces cerevisiae* protein involved in the control of ploidy. *Eur J Biochem*, **249**, 309-17.

Weiss, E. and Winey, M. (1996) The *Saccharomyces cerevisiae* spindle pole body duplication gene *MPS1* is part of a mitotic checkpoint. *J Cell Biol*, **132**, 111-23.

Welch, M.D., DePace, A.H., Verma, S., Iwamatsu, A. and Mitchison, T.J. (1997a) The human Arp2/3 complex is composed of evolutionarily conserved subunits and is localized to cellular regions of dynamic actin filament assembly. *J Cell Biol*, **138**, 375-84.

Welch, M.D., Iwamatsu, A. and Mitchison, T.J. (1997b) Actin polymerization is induced by Arp2/3 protein complex at the surface of *Listeria monocytogenes*. *Nature*, **385**, 265-9.

West, R.R., Vaisberg, E.V., Ding, R., Nurse, P. and McIntosh, J.R. (1998) *cut11(+)*: A gene required for cell cycle-dependent spindle pole body anchoring in the nuclear envelope and bipolar spindle formation in *Schizosaccharomyces pombe*. *Mol Biol Cell*, **9**, 2839-55.

Whitesell, L., Shifrin, S.D., Schwab, G. and Neckers, L.M. (1992) Benzoquinonoid ansamycins possess selective tumoricidal activity unrelated to src kinase inhibition. *Cancer Res*, **52**, 1721-8.

Wiech, H., Buchner, J., Zimmermann, R. and Jakob, U. (1992) Hsp90 chaperones protein folding in vitro. *Nature*, **358**, 169-70.

Wiese, C. and Zheng, Y. (2000) A new function for the gamma-tubulin ring complex as a microtubule minus-end cap. *Nat Cell Biol*, **2**, 358-64.

Wigge, P.A., Jensen, O.N., Holmes, S., Soues, S., Mann, M. and Kilmartin, J.V. (1998) Analysis of the *Saccharomyces* spindle pole by matrix-assisted laser desorption/ionization (MALDI) mass spectrometry. *J Cell Biol*, **141**, 967-77.

Willems, A.R., Lanker, S., Patton, E.E., Craig, K.L., Nason, T.F., Mathias, N., Kobayashi, R., Wittenberg, C. and Tyers, M. (1996) Cdc53 targets phosphorylated G1 cyclins for degradation by the ubiquitin proteolytic pathway. *Cell*, **86**, 453-63.

Winey, M. and Byers, B. (1993) Assembly and functions of the spindle pole body in budding yeast. *Trends Genet*, **9**, 300-4.

Winey, M., Goetsch, L., Baum, P. and Byers, B. (1991) *MPS1* and *MPS2*: novel yeast genes defining distinct steps of spindle pole body duplication. *J Cell Biol*, **114**, 745-54.

Winey, M., Hoyt, M.A., Chan, C., Goetsch, L., Botstein, D. and Byers, B. (1993) *NDC1*: a nuclear periphery component required for yeast spindle pole body duplication. *J Cell Biol*, **122**, 743-51.

Wintersberger, U., Kuhne, C. and Karwan, A. (1995) Scp160p, a new yeast protein associated with the nuclear membrane and the endoplasmic reticulum, is necessary for maintenance of exact ploidy. *Yeast*, **11**, 929-44.

Winzeler, E.A., Shoemaker, D.D., Astromoff, A., Liang, H., Anderson, K., Andre, B., Bangham, R., Benito, R., Boeke, J.D., Bussey, H., Chu, A.M., Connelly, C., Davis, K., Dietrich, F., Dow, S.W., El Bakkoury, M., Foury, F., Friend, S.H., Gentalen, E., Giaever, G., Hegemann, J.H., Jones, T., Laub, M., Liao, H., Davis, R.W. and et al. (1999) Functional characterization of the *S. cerevisiae* genome by gene deletion and parallel analysis. *Science*, **285**, 901-6.

Wittenberg, C. and Reed, S.I. (1988) Control of the yeast cell cycle is associated with assembly/disassembly of the Cdc28 protein kinase complex. *Cell*, **54**, 1061-72.

Wittenberg, C., Sugimoto, K. and Reed, S.I. (1990) G1-specific cyclins of *S. cerevisiae*: cell cycle periodicity, regulation by mating pheromone, and association with the p34CDC28 protein kinase. *Cell*, **62**, 225-37.

Wooster, M.S. and Wrigglesworth, J.M. (1976) Modification of glyceraldehyde 3-phosphate dehydrogenase activity by adsorption on phospholipid vesicles. *Biochem J*, **159**, 627-31.

Wozniak, R.W., Blobel, G. and Rout, M.P. (1994) *POM152* is an integral protein of the pore membrane domain of the yeast nuclear envelope. *J Cell Biol*, **125**, 31-42.

Xu, S., Huang, H.K., Kaiser, P., Latterich, M. and Hunter, T. (2000) Phosphorylation and spindle pole body localization of the Cdc15p mitotic regulatory protein kinase in budding yeast. *Curr Biol*, **10**, 329-32.

Xue, Z., Shan, X., Sinelnikov, A. and Melese, T. (1996) Yeast mutants that produce a novel type of ascus containing asci instead of spores. *Genetics*, **144**, 979-89.

Yin, H., Pruyne, D., Huffaker, T.C. and Bretscher, A. (2000) Myosin V orientates the mitotic spindle in yeast. *Nature*, **406**, 1013-5.

Zarzov, P., Boucherie, H. and Mann, C. (1997) A yeast heat shock transcription factor (Hsf1) mutant is defective in both Hsc82/Hsp82 synthesis and spindle pole body duplication. *J Cell Sci*, **110**, 1879-91.

Zarzov, P., Mazzoni, C. and Mann, C. (1996) The *SLT2* (*MPK1*) MAP kinase is activated during periods of polarized cell growth in yeast. *Embo J*, **15**, 83-91.

Zheng, L., Chen, Y. and Lee, W.H. (1999) Hec1p, an evolutionarily conserved coiled-coil protein, modulates chromosome segregation through interaction with SMC proteins. *Mol Cell Biol*, **19**, 5417-28.

Zheng, Y., Jung, M.K. and Oakley, B.R. (1991) Gamma-tubulin is present in *Drosophila melanogaster* and *Homo sapiens* and is associated with the centrosome. *Cell*, **65**, 817-23.

Zheng, Y., Wong, M.L., Alberts, B. and Mitchison, T. (1995) Nucleation of microtubule assembly by a gamma-tubulin-containing ring complex. *Nature*, **378**, 578-83.

Zwickl, P., Voges, D. and Baumeister, W. (1999) The proteasome: a macromolecular assembly designed for controlled proteolysis. *Philos Trans R Soc Lond B Biol Sci*, **354**, 1501-11.

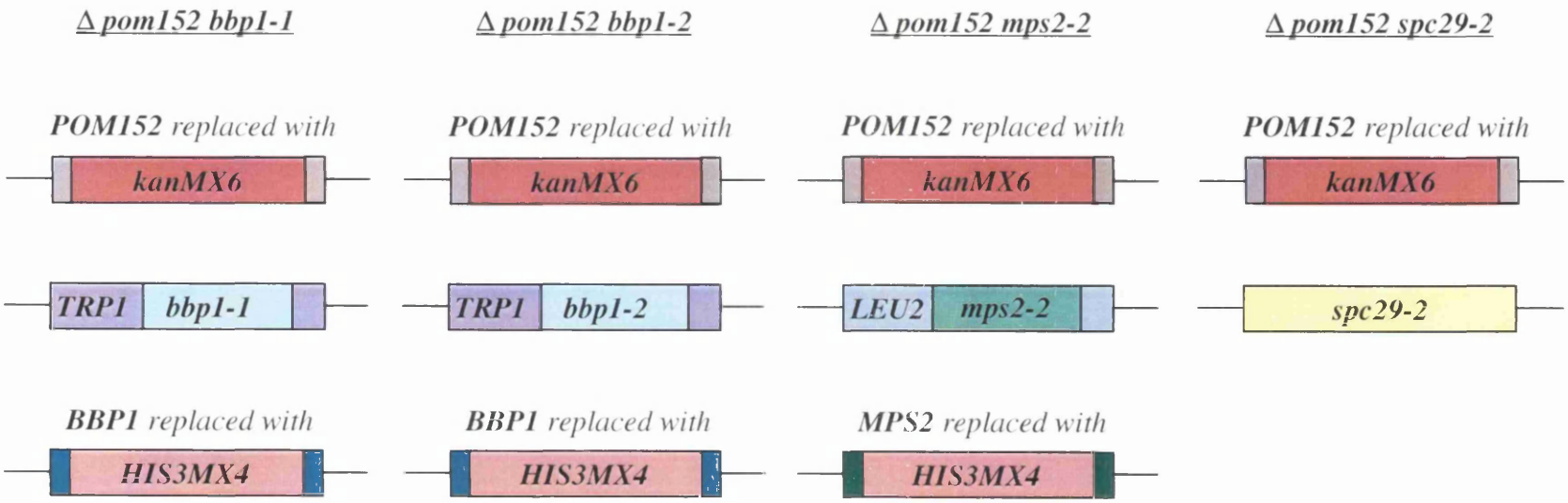

Appendix 1: Genotype of *Δpom152 bbp1-1*, *Δpom152 bbp1-2*, *Δpom152 mps2-2 and Δpom152 spc29-2 strains.*

Acknowledgements

I am thankful to Elmar Schiebel for his scientific guidance and motivation throughout my PhD. My second supervisor, Malcolm Finbow, was of great help to me with his interest in my topic and his opinions on experiments and interpretation of results.

I would like to thank Sarah Elliott my PhD ally for her friendship through three years of PhD work in R12. Furthermore, I am thankful to my colleagues Clare Simpson and Claire Manson, (my living dictionaries) for many enjoyable hours at and out of our work bay. I am also grateful to Thomas Hoefken for proof reading the thesis manuscript, which must have been a great strain to him, because he thinks Bavarians are no linguists. I appreciate the scientific assistance of my colleagues Gislene Pereira, Carsten Janke and Joan Grindley. This is also the case for Katja Siegers who explained the most difficult experiment with ease.

My special thanks go to Margaret O'Prey, Margaret Mullin, and Eion Robertson who assisted with the electron microscopy. I would like to thank Robert McFarlane and his team for the sequencing of many samples and for the synthesis of the 'exceedingly long' oligos which always worked. Furthermore, the computer team Iain White and Peter McHardy and the graphic designer Tom McGuire for their help with all computer related issues.

The MALDI-MS analyses were carried out in collaboration with Anna and Andrej Shevchenko whose work I gratefully appreciate. I would also like to thank Ivan LeMasson and Carl Mann for the collaboration on *MPS2* and *SPC24*.

I would further like to thank my parents for their support throughout my studies and my grandmother Dora Schramm who is looking forward to receiving a copy of my thesis. I am grateful to my brother Stefan Schramm who has always been a mentor for me. Furthermore, I appreciate the cheeky encouragement of Alex Coon with whom I still have to debate about the percentage problem.

Finally I am especially grateful to the Cancer Research Campaign for funding my PhD.